GEOLOGICAL SURVEY OF CANADA

OPEN FILE 2165



# Geology and mineral deposits of the Flin Flon and Thompson belts, Manitoba (Field Trip 10)

edited by

A.G. Galley
A.H. Bailes
E.C. Syme
W. Bleeker
J.J. Macek
T.M. Gordon

1991

Energy, Mines and Resources Canada    Énergie, Mines et Ressources Canada

Canada

GEOLOGICAL SURVEY OF CANADA

OPEN FILE 2165

# GEOLOGY AND MINERAL DEPOSITS OF THE FLIN FLON AND THOMPSON BELTS, MANITOBA

[FIELD TRIP 10]

BY

A.G. GALLEY[1], A.H. BAILES[2], E.C. SYME[2],
W. BLEEKER[3], J.J. MACEK[2] and T.M. GORDON[4]

8TH IAGOD SYMPOSIUM

FIELD TRIP GUIDEBOOK

1 Geological Survey of Canada, 601 Booth Street, Ottawa, Ontario, K1A 0E8

2 Manitoba Geological Services Branch, 535-330 Graham Avenue, Winnipeg, Manitoba, R3C 4E3

3 Department of Geology, University of New Brunswick, Fredericton, New Brunswick, E3B 5A3

4 Department of Geology and Geophysics, University of Calgary, Calgary, Alberta, T2N 1N4

# 8th IAGOD SYMPOSIUM

## FIELD TRIPS COMMITTEE

| | |
|---|---|
| **Chairman and Guidebook Technical Editor:** | **W.D. GOODFELLOW** |
| **Guidebook Reviewer:** | **A.R. MILLER** |
| **Field Trip Committee Members:** | **A. DOUMA**<br>**C.W. JEFFERSON**<br>**A.R. MILLER**<br>**N. PRASAD**<br>**D.G. RICHARDSON**<br>**A.L. SANGSTER**<br>**J.M. SHAW** |
| **Word Processing:** | **P. BROWN**<br>**B. GIESE** |

**TABLE OF CONTENTS**

## INTRODUCTION

The Flin Flon and Thompson belts are two distinct lithotectonic domains formed at different times and at different tectonic settings within the Early Proterozoic Trans-Hudson Orogen (THO) (Fig. 1). The differences in tectonic setting of these belts are reflected in contrasting metallogenic characteristics. The Flin Flon belt, a juvenile volcanic arc, is characterized by numerous Cu-Zn volcanogenic massive sulphide (VMS) deposits and epigenetic, mesothermal gold deposits. The Thompson belt represents a Proterozoic shelf-foredeep sequence overlying an older Archean craton (Superior Province); it contains some of the world's largest nickel deposits. The Flin Flon and Thompson belts together account for 24% of Canada's Ni production, 14% of the Co, 9% of the Cu, 5% of the Zn and 2.1% of the Au (1986 figures).

The field trip will focus on three areas of increasing metamorphic grade and deformation. In the west-central part of the Flin Flon belt are low grade (greenschist) volcanic strata containing numerous VMS deposits. At the eastern end of the Flin Flon belt, near the town of Snow Lake, are higher grade (almandine amphibolite),

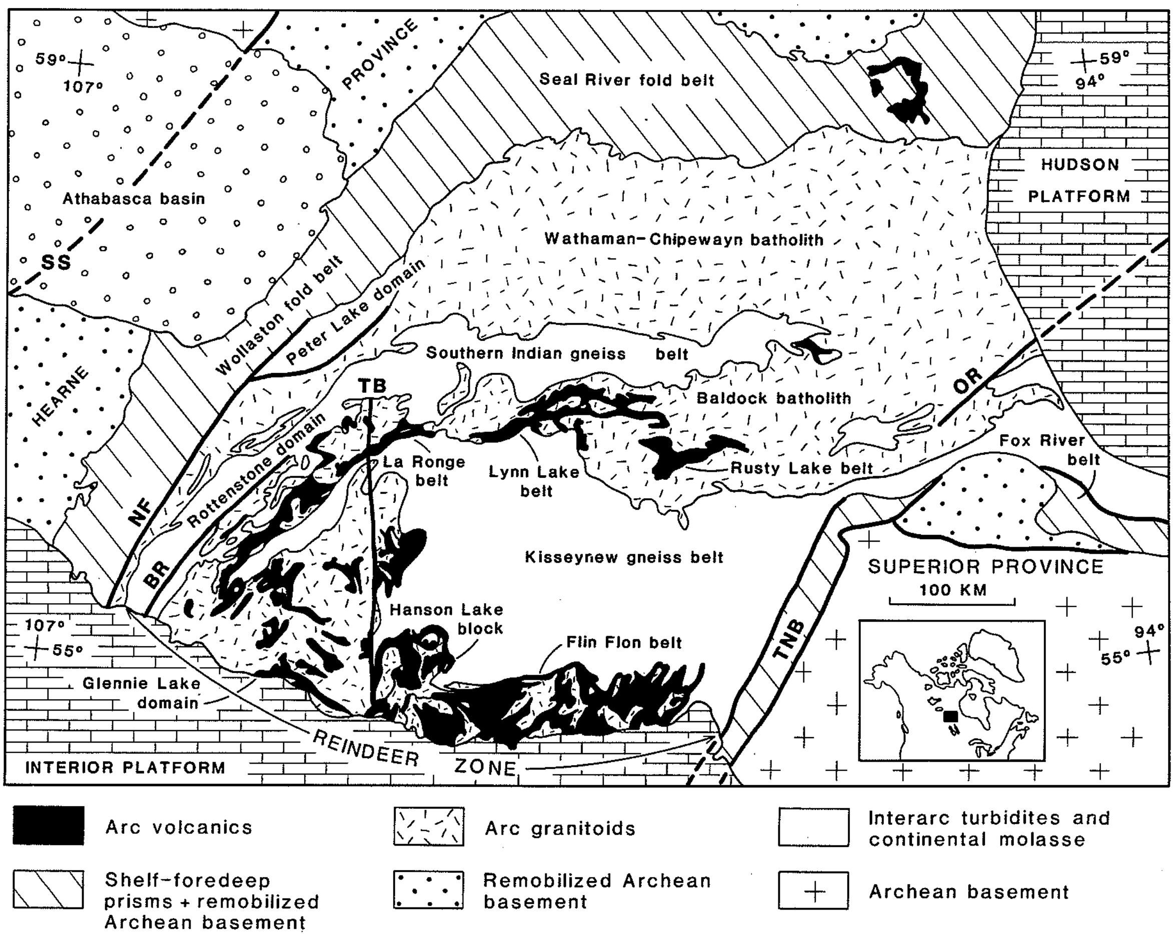


Figure 1: Tectonic domains of the Trans-Hudson Orogen (modified from Hoffman, 1988a)

strongly deformed VMS deposits and associated hydrothermally altered host volcanic rocks, plus gold deposits associated with post-fold faulting. Further east, the Churchill-Superior Boundary zone comprises high grade polydeformed paragneisses and contained nickel deposits in the Thompson area.

**Tectonic Setting of the Flin Flon and Thompson Belts**

The Early Proterozoic Trans-Hudson Orogen (THO) is a 500 km wide collisional zone sandwiched between Archean microcontinents, the Superior Province to the southeast and the Hearne-Rae Province to the northwest (Hoffman, 1988a) (Fig. 1). The orogen is a major component of a greater Early Proterozoic 'Pan American' orogenic system which includes the Wopmay, Penokean and Ketilidian orogenic belts (Fig. 2). The THO, and its remobilized Archean borders, are part of the Precambrian Shield historically known as the Churchill Province.

The orogen comprises four composite lithotectonic zones: a southeastern foreland belt (the Churchill - Superior Boundary zone, which includes the Thompson belt), an internal zone composed of juvenile Proterozoic crust (including the Flin Flon belt), an Andean-type magmatic arc batholith (Wathaman-Chipewyan) and a northwest hinterland belt (Hearne Province)(Hoffman, 1988a; Lewry, 1981). The tectonic events that took place during the orogen in the various zones are summarized in Table 1.

Deposition of clastic-carbonate shelf sequences along the two bounding Archean terranes occurred pre-1.9 Ga and represents the earliest event recognized in the Trans-Hudson Orogen. These sequences include the Wollaston Group (Lewry and Sibbald, 1980), deposited along the southeastern margin of the Hearne Province, and the Ospwagan Group (Bleeker and Macek, 1988a), deposited along the northwestern rim of the Superior Province. Along the Superior Province margin the shelf sequence is overlain by prograding clastic sedimentary strata and associated mafic igneous rocks commonly associated with the formation of a foredeep (Hoffman, 1988b). Development of the foredeep included the emplacement of mafic-ultramafic intrusions and associated nickel sulphides presently being mined in the Thompson belt. Thrusting and folding were associated with the development of south-verging nappes with infolding of Archean basement and overlying Proterozoic strata (Bleeker, in prep.)

Formation and assembly of juvenile Proterozoic crust in the internal zone (Reindeer zone; Stauffer, 1984) of THO spanned 85 Ma. Northwest directed subduction of the Reindeer zone began along its margin with the Hearne Province and caused intense thrust nappe deformation of the Wollaston Group (Bickford et al., 1990). Related island-arc volcanism began in the Lynn Lake belt at 1.91 Ga (Baldwin et al., 1987), and in the Flin Flon and La Ronge belts at 1.89 Ga (Gord n et al., 1990; Van Schmus et 1., 1987). Island arc volcanism was accompanied by the deposition of Cu-Zn VMS deposits. Late stage arc formation was typified by the deposition of volcaniclastic sediments in an intervolcanic basin (Kisseynew belt).

Continued northwest-directed subduction resulted in the intrusion of the Andean-type Wathaman-Chipewyan batholith, between 1.86 and 1.85 Ga. Uplift of the deformed and intruded arc terranes resulted in deposition of continental molasse-type sediments (including the Missi Group at Flin Flon) and intercalated subaerial volcanic rocks, between 1.85 and 1.83 Ga (Gordon et al., 1990; Delaney et al, 1988).

A major regional metamorphic event began during the waning stages of the Andean-type plutonism, reaching P-T conditions of 750°C at 5.5 Kbars within the Kisseynew belt at 1815 Ma (Gordon, 1989). Waning stages of metamorphism were accompanied by anatectic plutonism at around 1.77 Ga (Bickford et al., 1990; Bleeker, in prep.), including lithium-bearing pegmatities in the Flin Flon belt (Cerny et al., 1981)

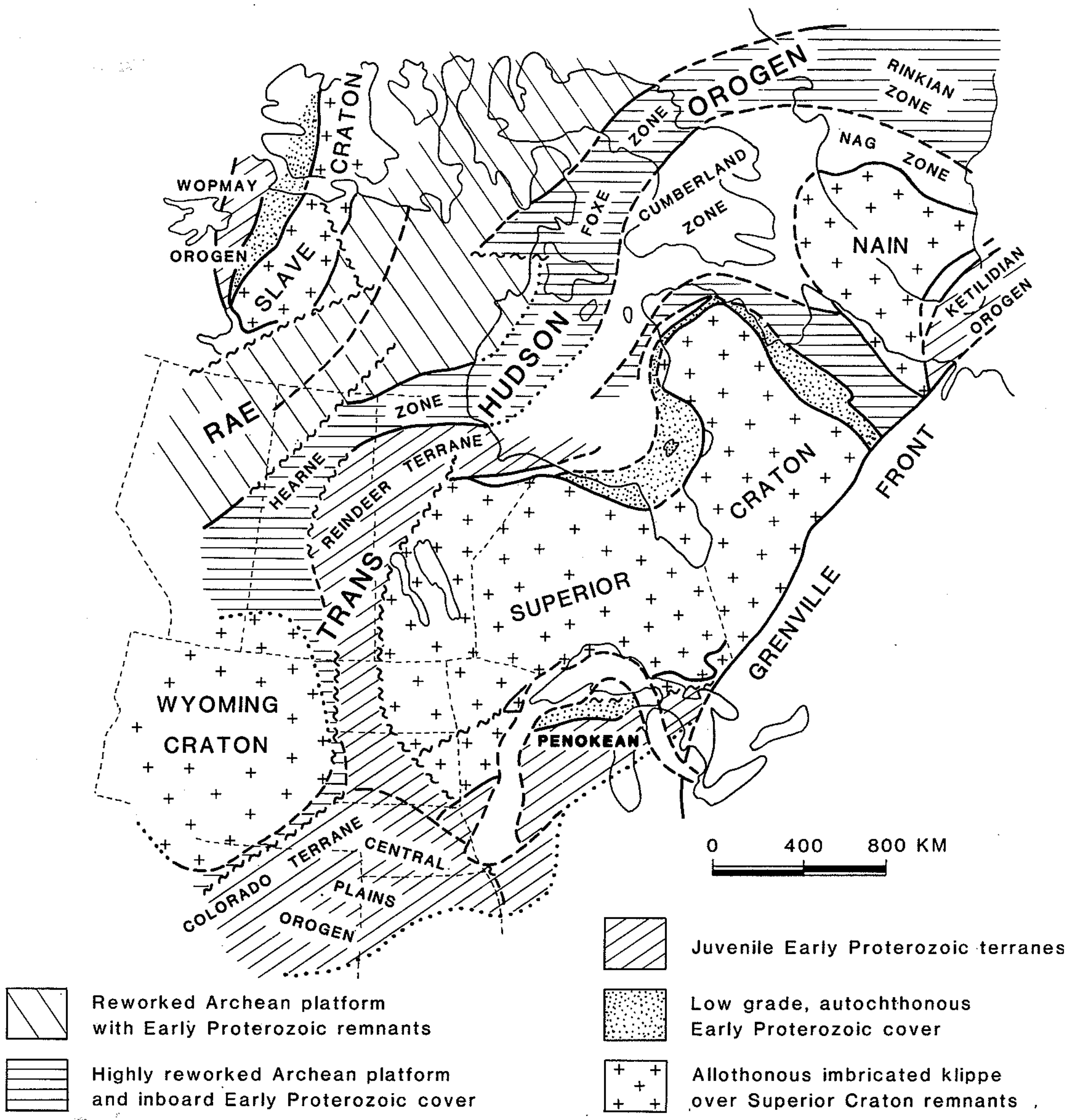


Figure 2: Precambrian tectonic components of the North American craton (modified from Hoffman, 1988a).

| TIME INTERVAL | HINTERLAND (HEARNE PROVINCE) | ANDEAN MAGMATIC ARC (WATHAMAN-CHIPEWAYN BATHOLITH) | INTERNAL ZONE (REINDEER ZONE) | FORELAND (CHURCHILL-SUPERIOR BOUDARY ZONE) |
|---|---|---|---|---|
| pre-1.9 Ga | Shelf sedimentation along margin of craton | | | Shelf sedimentation along margin of craton: Foredeep sedimentation and volcanism Emplacement of Ni-rich intrusions |
| 1.9 to 1.88 Ga | | | Island arc and oceanic rift volcan. and associated sedimentation result in island arc and interarc basin formation | $F_1$: Nappe formation<br>Thickening and stabilization of the cratonic margin. Intrusion of Molson dyke swarm and related Fox River Sill. |
| 1.88 to 1.77 Ga | NW-verging nappes infold supracrustals with underlying Archean basement | | Intr. of early kinematic tonalite and granodiorite. Volcanism in the Rusty Lake belt | |
| 1.86 to 1.84 Ga | | Intrusion of the Wathaman-Chipewayn batholith | $F_1$: Isoclinal folding and uplift of island arc assemblages with intrusion of intermediate batholiths | |
| 1.84 to 1.83 Ga | | | Continued uplift and subsequent erosion and continental molasse sedimentation infilling inter-arc Kisseynew basin. Syn-kinematic plutonism and continental volcan. | |
| 1.83 to 1.77 Ga | Rafting of the Peter Lake exotic terrane onto Hearne margin. Metamorphism of shelf-foredeep Wollaston Group | | $F_2$: South-verging thrust-nappe deform of juvenile accreted terranes. Region metamorphic event centered on the Kisseynew belt<br>$F_3$: Peak metamorphism at 1.815 Ma along with formation of NE-trending, doubly-plunging folds | $F_2$: SE-verging thrusts emplace hot Kisseynew gneisses over Thompson Nickel belt<br>$F_3$: Formation of NE-trending, doubly-plunging folds |
| post 1.77 Ga | Formation of mylonite zone between Hearne Prov. and the Wathaman-Chipewayn bath<br>Late brittle-ductile movement along domain boundaries | | Formation of NE-trending, ductile fault systems<br>Late brittle-ductile deform. along pre-existing fault zones | Formation of large-scale, dip-slip fault zones parallel to NE-trending $F_3$ folds<br>Late brittle-ductile deformation along pre-existing fault zones |

Table 1: Early Proterozoic tectonic events within the Trans-Hudson Orogen.

Throughout much of the Reindeer zone major nappe emplacement and telescoping of previously accreted juvenile crust initiated the final stages of continental collision between 1.83 and 1.80 Ga (Bickford et al., 1990, Hoffman, 1988a). This compressional event included the overthrusting of hot Kisseynew belt gneisses onto the Thompson belt (Bleeker, in prep.). Emplacment of northeast-trending folds followed nappe formation. The interference fold pattern resulted in northeast-trending, doubly plunging folds that in places are cored by remobilized Archean crust (Bickford et al., 1990 and references therein). This fold event coincided with peak metamorphism. The final deformational event took place between 1.8 and 1.7 Ga with the formation of northeast-trending, regional-scale fault systems. These include the Needle Falls Shear Zone and the Churchill-Superior Fault Zone that mark the present west and east boundaries of the Reindeer Zone (Fig. 1). The formation of epigenetic, mesothermal gold deposits is associated with this late fault event.

# FLIN FLON BELT: GENERAL GEOLOGY AND ORE DEPOSITS

## Geological Setting

The Flin Flon belt is 250 km long, with an exposed width of 32 to 48 km, and is bounded to the north by metasedimentary gneisses of the Kisseynew domain and is overlain to the south by flat-lying, Ordovician dolomitic limestones (Fig. 3). Its total width, including the area covered by Paleozoic strata, may be considerably larger (Green et al., 1985; Blair et al., 1988).

The belt is composed of an assemblage of subaqueous and subaerial volcanic rocks, synvolcanic intrusions and associated sedimentary rocks (Amisk Group), disconformably overlain by a sequence of terrestrial sedimentary and minor subaerial volcanic flows and associated high-level intrusions (Missi Group). Both rock groups are intruded by a number of intermediate to felsic, syn- to late-kinematic intrusions.

The deformational history of the Flin Flon belt includes an event of pre-Missi Group folding and uplift (Bailes and Syme, 1989). A series of folding events followed deposition of the Missi Group, the first being isoclinal east-trending folds (associated at Snow Lake with a major thrust fault) (Stauffer and Mukherjee, 1971; Bailes and Syme, 1989; Froese and Moore, 1981; Bailes, 1980). These structures were refolded by northeast to north-striking folds causing large-scale interference patterns (Froese and Moore, 1980; Bailes, 1980; Bailes and Syme, 1989). Folding was followed by the formation of a large-scale fault system that transects the belt at a high angle (Fig. 3). The fault system evolved from north-northeast striking oblique dextral to north-northwest oblique sinistral (Stauffer and Mukherjee, 1971; Syme, 1988) to northwest-northeast conjugate strike slip (Galley and Franklin, 1990). Earlier fold structures were rotated into parallelism with the northern flank of the belt; this sense of rotation suggests that late stage tectonism involved a component of dextral transpression (Sanderson and Marchini, 1984).

## Mining History

Prospecting began in the Flin Flon-Snow Lake Belt at the beginning of the 20$^{th}$ century, when prospectors travelled up the river systems northward from Prince Albert, Saskatchewan, and The Pas, Manitoba in search of gold, the first discoveries were made near Snow Lake. This resulted in the opening of Manitoba's first lode gold mine in 1914 (the Moosehorn-Ballast, Richardson and Ostry, 1987). In 1915 the first base metal discoveries were made in the Flin Flon region, and in 1917 the Mandy Mine began production as the first base-metal producer in the province. Although discovered in 1915, the Flin Flon deposit (Fig. 3) was not put into production until 1930 due to metallurgical problems. This deposit is to date exponentially the largest Zn-Cu deposit in the Belt, with production and reserves totalling 62.92 million tonnes grading 2.2%Cu, 4.1% Zn and 2.6 g/tonne gold.

The Flin Flon belt is best known for its base metal production from Cu-Zn massive sulphide deposits (Table 2); these occur in the Amisk Group and were synchronous with volcanism. To date, 19 base metal deposits have been put into production in the belt (Table 2), with an average tonnage (excluding Flin Flon) of 2.195 million tonnes, with a range in metal values from 0.5 to 7.2% Cu and 0.1 to 10% Zn.

There are numerous gold showings and deposits; most are associated with shear zones and related structures which postdate the Missi Group. Although not historically known for gold production, the Flin Flon Belt contains Canada's largest known Early Proterozoic lode gold deposit, the Nor-Acme (production and reserves at approximately 8 million tonnes

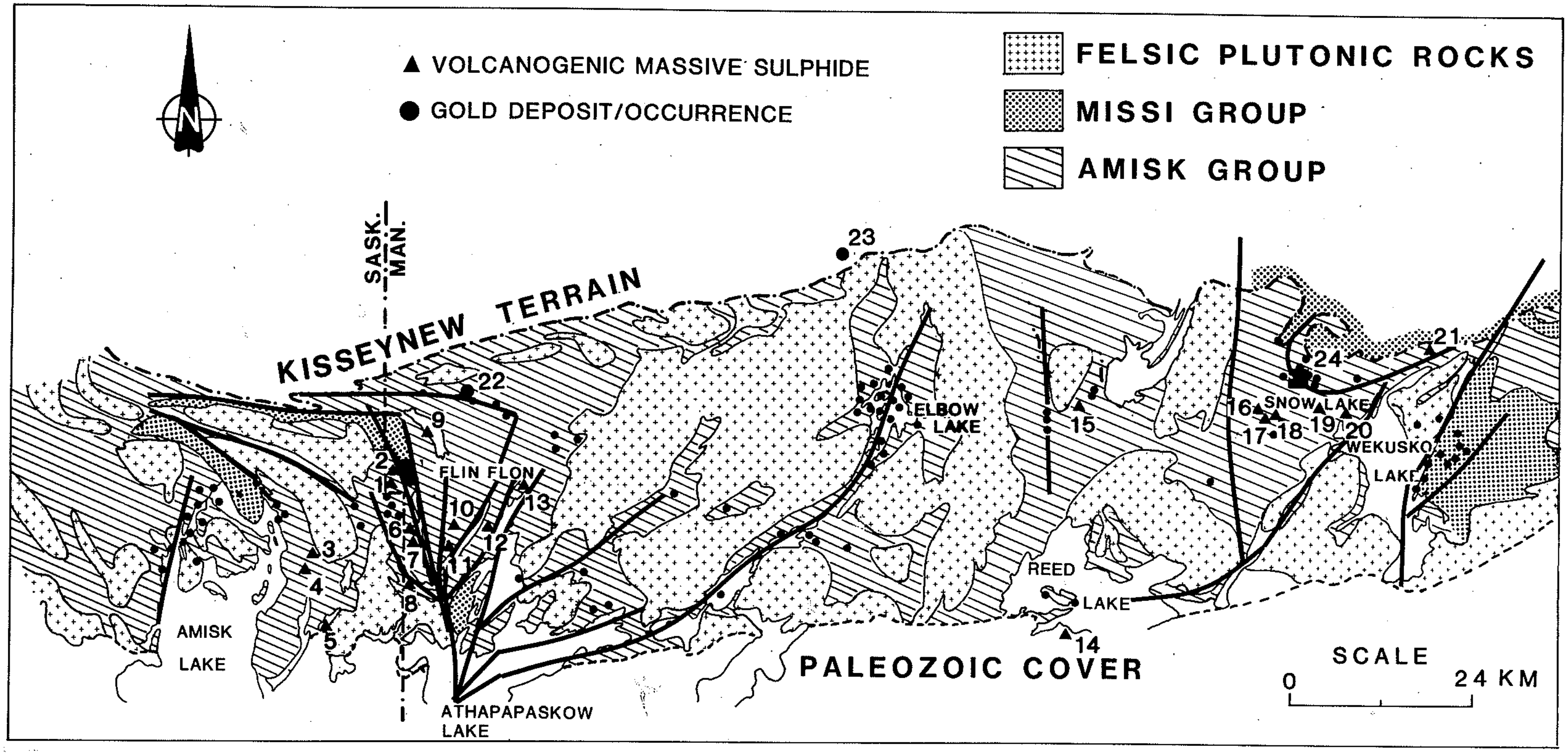


Figure 3:General geology and ore deposits of the Flin Flon belt.
Deposits (producer (P), past producer (C)): **Base Metal** 1. Flin Flon (P), 2. Callinan (P), 3. Flexar (C), 4. Birch Lake (C), 5. Coronation (C), 6. Mandy (C), 7. Schist Lake (C), 8. West Arm (C), 9. Trout Lake (P), 10. Cuprus (C), 11. White Lake (C), 12. Centennial (C), 13. North Star-Don Jon (C), 14. Spruce Point (P), 15. Dickstone (C), 16. Chisel (P), 17. Lost (C), 18. Ghost (C), 19. Anderson (C), 20. Stall-Rod (P), 21. Osborne (C). **Gold Deposits**: 22. Tartan Lake (C), 23. Puffy Lake (C), 24. Nor-Acme (C).

TABLE 2: COPPER-ZINC, NICKEL AND GOLD DEPOSITS, FLIN FLON-SNOW LAKE DISTRICT

| DEPOSIT | PRODUCTION DATES | COMMODITIES | PRODUCTION (P) + RESERVES (R) (x 000 Tonnes) | AVERAGE GRADES |
|---|---|---|---|---|
| FLIN FLON AREA | | | | |
| Flin Flon | 1930- | Cu,Zn,Au,Ag, Se,Te,Cd | 62,927 (P+R)1 | 2.2% Cu, 4.1% Zn |
| Trout Lake | 1982- | Cu,Zn,Au,Ag | 6,291 (P+R)1 | 2.0% Cu, 5.4% Zn, 1.45 g/t Au, 11.2 g/t Ag |
| Namew Lake | 1989- | Ni,Cu | 2,340 (R) | 2.4% Ni, 0.9% Cu |
| Callinan | Under development | Cu,Zn,Au,Ag | 2,619 (R) | 1.5% Cu, 4.1% Zn, 1.8 g/t Au, 21.1 g/t Ag |
| Centennial | 1977-88 | Cu,Zn,Au,Ag | 2,366 (P+R)1 | 1.5% Cu, 2.2% Zn |
| Westarm | 1978-85 | Cu,Zn,Au,Ag | 1,702 (P+R)1 | 3.7% Cu, 1.5% Zn |
| White Lake | 1972-83 | Cu,Zn,Au,Ag | 850 (P)1 | 2.0% Cu, 4.8% Zn |
| Schist Lake | 1950-76 | Cu,Zn,Au,Ag | 1,871 (P) | 4.3% Cu, 7.3% Zn |
| North Star | 1945-58 | Cu,Zn | 242 (P) | 6.1% Cu |
| Don Jon | 1955-57 | Cu,Zn | 79 (P) | 3.1% Cu |
| Cuprus | 1948-54 | Cu,Zn,Au,Ag | 462 (P) | 3.3% Cu, 6.4% Zn |
| Mandy | 1916-19<br>1943-44 | Cu,Zn,Au,Ag | 23 (P)<br>102 (P) | 20.2% Cu<br>5.6% Cu, 14.0% Zn |
| Big Island | Drilling 1989 | Zn,Cu,Au,Ag | 180 (R) | economic grades |
| Hudvam | Drilling 1989, Decline | Cu,Zn,Au,Ag | 612 (R) | 1.5% Cu, 1.9% Zn, 4.0 g/t Au, 14.1 g/t Ag |
| Pine Bay | Inactive | Cu | 1,361 (R) | 1.3% Cu |
| Tartan | 1987-89 | Au | 544 (P+R) | 13.0 g/t Au |

| DEPOSIT | PRODUCTION DATES | COMMODITIES | PRODUCTION (P) + RESERVES (R) (x 000 Tonnes) | AVERAGE GRADES |
|---|---|---|---|---|
| Puffy Lake | 1987-89 | Au | 603 (P+R) | 6.5 g/t Au |
| Nokomis Lake | Drilling 1986 | Au | 91 (R) | 10.3 g/t Au |
| Laguna | 1920, 1924-25, 1936-40 | Au | 98 (P) | 17.7 g/t Au |
| Gurney | 1937-39 | Au,Ag | 92 (P) | 8.5 g/t Au, 24.2 g/t Ag |
| SNOW LAKE-REED LAKE AREA | | | | |
| Chisel Lake | 1960- | Zn,Pb,Cu,Au, Ag | 7,490 (P+R)1 | 0.5% Cu, 10.9% Zn |
| Stall Lake | 1964- | Cu,Zn,Au,Ag | 6,513 (P+R)1 | 4.4% Cu, 0.5% Zn |
| Anderson Lake | 1970- | Cu,Zn,Au,Ag | 3,354 (P+R)1 | 3.4% Cu, 0.1% Zn |
| Spruce Point | 1982- | Cu,Zn,Au,Ag | 1,763 (P+R)1 | 2.7% Cu, 4.3% Zn |
| Rod No. 2 | 1984- | Cu,Zn,Au,Ag | 688 (P+R)1 | 7.2% Cu, 3.0% Zn |
| Chisel North | Under development | Zn,Cu,Au,Ag | 2,457 (R) | 0.3% Cu, 9% Zn |
| Ghost/Lost Lake | 1972-88 | Zn,Pb,Cu,Au | 646 (P+R)1 | 1.3% Cu, 8.5% Zn |
| Osborne Lake | 1968-85 | Cu,Zn,Au,Ag | 3,380 (P+R)1 | 3.1% Cu, 1.5% Zn |
| Dickstone | 1970-75 | Cu,Zn,Au,Ag | 1,083 (P+R) | 2.4% Cu, 3.4% Zn |
| Rod No. 1 | 1962-64 | Cu,Zn | 23 (P) | 5.0% Cu, 4.5% Zn |
| Silvia Zone | Drilling 1985 | Cu,Zn | 907 (R) | 2.4% Cu, 0.8% Zn |
| Morgan Lake | Drilling 1985 | Cu,Zn | | |
| Farewell Lake | Inactive | Cu | 257 (R) | 2.0% Cu |

| DEPOSIT | PRODUCTION DATES | COMMODITIES | PRODUCTION (P) + RESERVES (R) (x 000 Tonnes) | AVERAGE GRADES |
|---|---|---|---|---|
| Copper Man | Inactive | Cu,Zn | 221 (R) | 2.6% Cu, 4.5% Zn |
| Rail Lake | Inactive | Cu,Zn | 295 (R) | 3.0% Cu, 0.7% Zn |
| Wim | Inactive | Cu | 989 (R) | 2.9% Cu |
| Reed Lake | Inactive | Cu | 1,361 (R) | 1.3% Cu |
| Ferro | Drilling 1988 | Au | 65 (R) | 12.48 g/t Au |
| Nor-Acme | 1949-58 Drilling 1988 | Au,Ag | 4,893 (P) 2,457 (R) | 3.9 g/t Au, 0.32 g/t Ag 4.7 g/t Au |
| Squall Lake | Drilling 1986 | Au | 680 (R) | 3.43 g/t Au |
| Main Zone Snow Lake Mines | Drilling 1985 | Au | 454 (R) | 10.28 g/t Au |

1 Production and Reserves figures as of Dec. 31, 1984

Sources of information: Fogwill (1983), Esposito (1986), Hosain (1988).

grading 4.6 g/tonne Au) (Nor-Acme Gold Mines Ltd. Annual Report, 1987) (Fig. 3). The largest source of gold in the belt has been the VMS deposits, with the Flin Flon deposit alone having produced over 163 tonnes. Since 1984 two new lode gold deposits came into production (Puffy and Tartan Lake mines, Table 2), but both have since been closed.

Disseminated Cu-Mo sulphide showings are known from a number of porphyritic felsic plutons (Baldwin, 1980) and lithium-bearing pegmatites are present in the Wekusko Lake pegmatite field (Cerny et al., 1981). In 1984, nickel was discovered beneath the Paleozoic cover at Namew Lake, 60 km south of Flin Flon.

Total mineral production in the Flin Flon belt exceeds that in any other greenstone belt in Manitoba, and it is one of the more productive Precambrian mineral districts in Canada.

# Flin Flon Area: General Geology and Ore Deposits

## Geological Setting

### Introduction

Precambrian rocks in the Flin Flon region comprise an Early Proterozoic island arc assemblage (Amisk Group), zoned or polyphase calc-alkaline plutons, and an unconformably overlying sequence of terrestrial alluvial sediments (Missi Group). U/Pb zircon age determinations indicate that these rocks were emplaced during a 60 Ma period, with the Amisk Group approximately 1886 Ma, most plutons about 1850 Ma and the Missi Group 1832 Ma (Gordon et al. 1990). The rocks underwent polyphase deformation, and attained peak metamorphic conditions at about 1815 Ma (Gordon et al., 1990).

Previous mapping in this area was conducted at a scale of 1 inch to 1 mile by Tanton (1941a, b), Bateman and Harrison (1945), Byres et al. (1965), and Buckham (1944). More detailed mapping in the vicinity of Flin Flon was carried out by Stockwell (1960) at a scale of 1 inch to 1000 feet. Recent 1:20 000 mapping

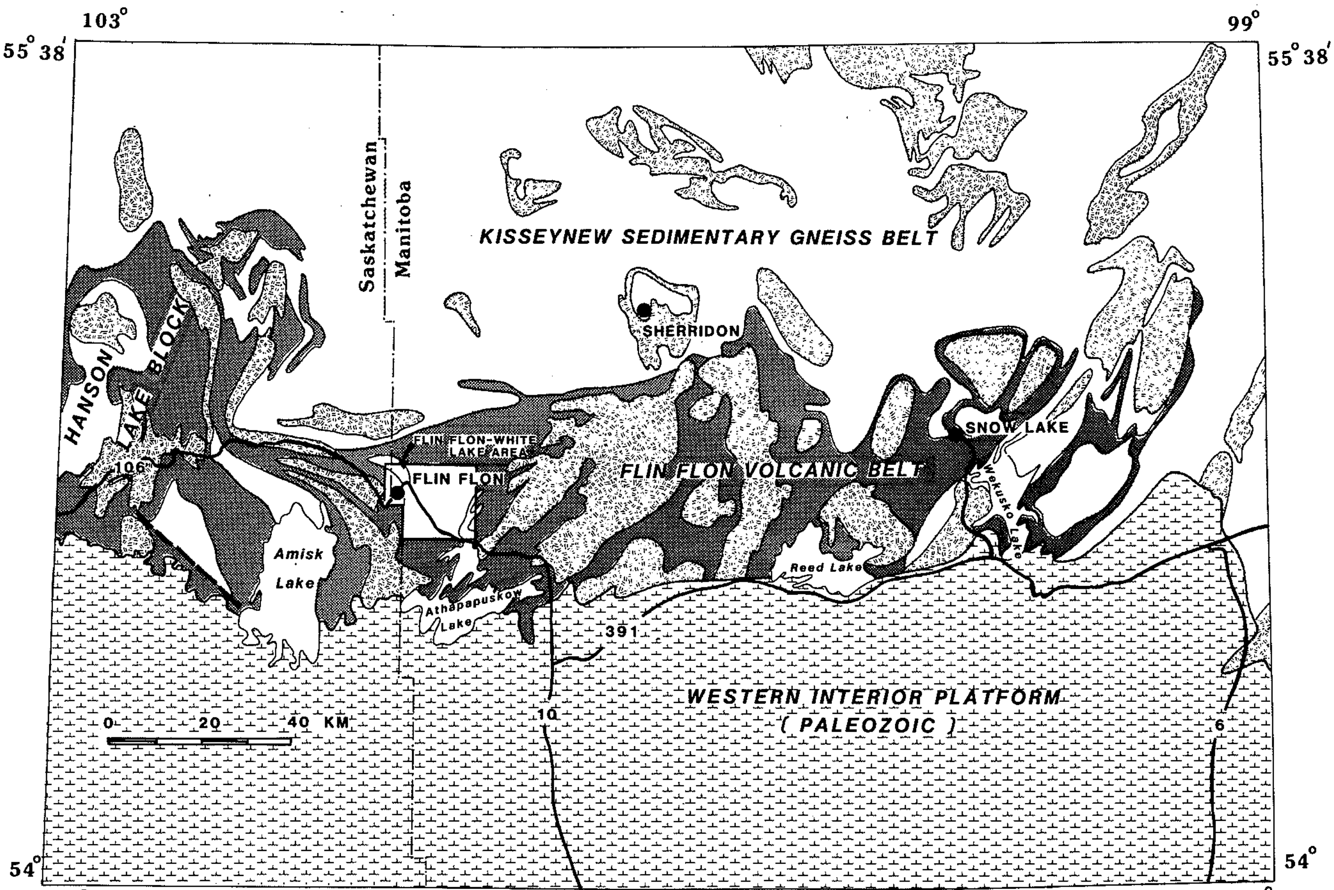


Figure 4: Location map of the Flin Flon - White Lake area on a generalized geological map of north central Manitoba and Saskatchewan. Legend: dark - metavolcanic rocks; light dots - sedimentary rocks, paragneiss and orthogneiss; hachures - granitic plutons.

in the Flin Flon-White Lake area (Fig. 4) resulted in a detailed subdivision of the Amisk Group and definition of the stratigraphic position of volcanogenic massive sulphide deposits (Bailes and Syme, 1989). Mapping continues in the Flin Flon region (Athapapuskow Lake: Syme, 1985-88; Tartan Lake: Gilbert, 1986-89; Creighton: Thomas, 1989).

**Amisk Group**

The Amisk Group consists of a wide variety of volcanic lithologies, comprising a number of distinct stratigraphic sequences separated by large-scale late faults. Most of the rocks were deposited in a shallow to moderately deep marine environment, but some of the pyroclastic rocks are interpreted to have been erupted subaerially and deposited under water.

In the Flin Flon - Athapapuskow region the Amisk Group can be subdivided into four lithologic subgroups which represent different tectonic assemblages in the former arc (Syme, 1988, 1990; Fig. 5):

1. Most of the Amisk Group occurs in a variety of thick, heterolithologic, complex stratigraphic packages dominated by subaqueous mafic volcanic rocks with classic oceanic island arc tholeiite geochemical characteristics. Basalts in this group have high LIL element (eg. Rb, Ba, K, Sr, Th) contents, low HFS element (eg. Ti, P, Hf, Zr) contents, and very low Ni and Cr contents. Volcanism was essentially bimodal, with rare intercalated rhyolite flows.

2. Athapapuskow basalts in the southern part of the area (Fig. 5) form a thick sequence of predominantly massive sheetflows, with possible back-arc geochemical characteristics. These basalts are much more magnesian than the arc tholeiites, and have higher HFS element, Ni and Cr contents. No rhyolites occur in the portion of this unit mapped to date. The distinctive high aeromagnetic signature of the Athapapuskow subgroup extends 50 km northeast to southern Elbow Lake.

3. Millwater basalts (Fig. 5) occur as thick pillowed flows lithologically and magnetically very distinct from Athapapuskow basalt. Millwater basalts are geochemically intermediate between the island arc tholeiites and back-arc basalts.

4. A small package of coarse volcaniclastic rocks containing shoshonite boulders occurs in a fault-bounded panel on Schist Lake (Fig. 5). These rocks are significant because they record a mature stage of arc development.

The areal distribution of basalt types in the western Flin Flon belt appears to exert a fundamental control on the distribution of contained volcanogenic massive sulphide deposits. To date, all volcanogenic massive sulphide deposits in the Manitoba portion of the Flin Flon belt occur in the arc tholeiite subgroup (1, above), invariably associated with the infrequent rhyolite flows in the succession. No significant massive sulphides occur between Athapapuskow and Elbow Lakes, in that portion of the belt underlain by Athapapuskow basalt.

In the Flin Flon-White Lake area (Bailes and Syme, 1989; Fig. 4 and 6) the Amisk Group is dominated by arc tholeiite basalt (45-53% $SiO_2$) and basaltic andesite (53-57% $SiO_2$) subaqueous flows and related breccias. Rhyolite (70-80% $SiO_2$) flows occur as sporadic, discrete bodies of two morphologic types, massive flows with associated breccia and composite types with massive lobes in a microbreccia matrix. Mafic volcaniclastic rocks vary widely in grain/clast size, bedding characteristics, phenocryst population, and texture,; most were deposited from subaqueous density currents. Intermediate volcaniclastic rocks (57-62% $SiO_2$) occur in only in the Bear Lake block (Fig. 6); intermediate (andesite) flows are very rare. Minor rock types include fractionated ferrobasalt, felsic volcaniclastic rocks, volcanic conglomerate, greywacke-siltstone-mudstone, oxide facies iron formation, and carbonate-rich sedimentary rocks. Narrow units of

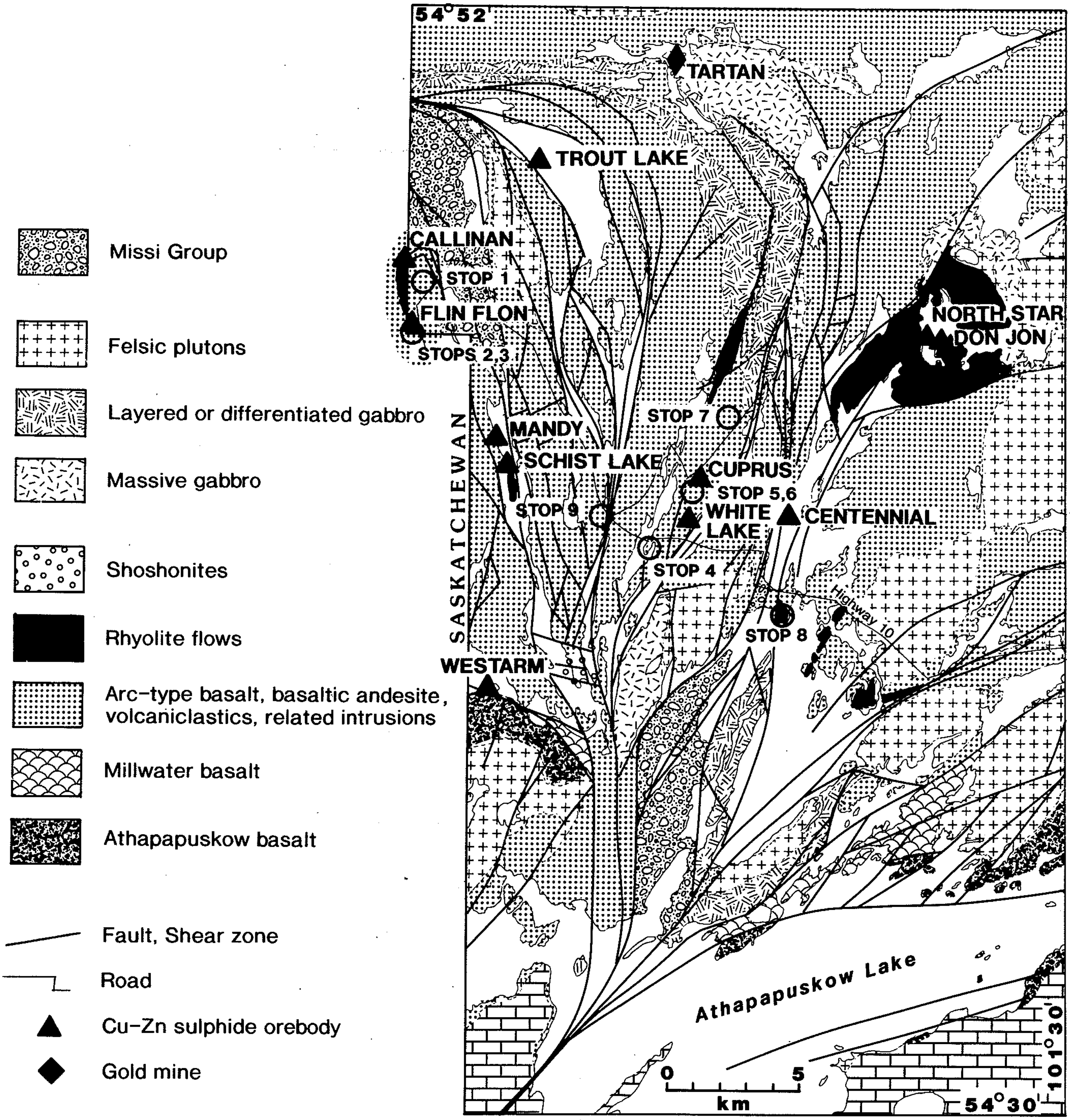


Figure 5: Simplified geology of the Flin Flon - Athapapuskow area, showing the distribution of the 4 major lithotectonic members of the Amisk Group, massive sulphide and gold mines, and Stop locations. Geology modified from Syme (1988), Bailes and Syme (1989), Gilbert (1989), and Bateman and Harrison (1945).

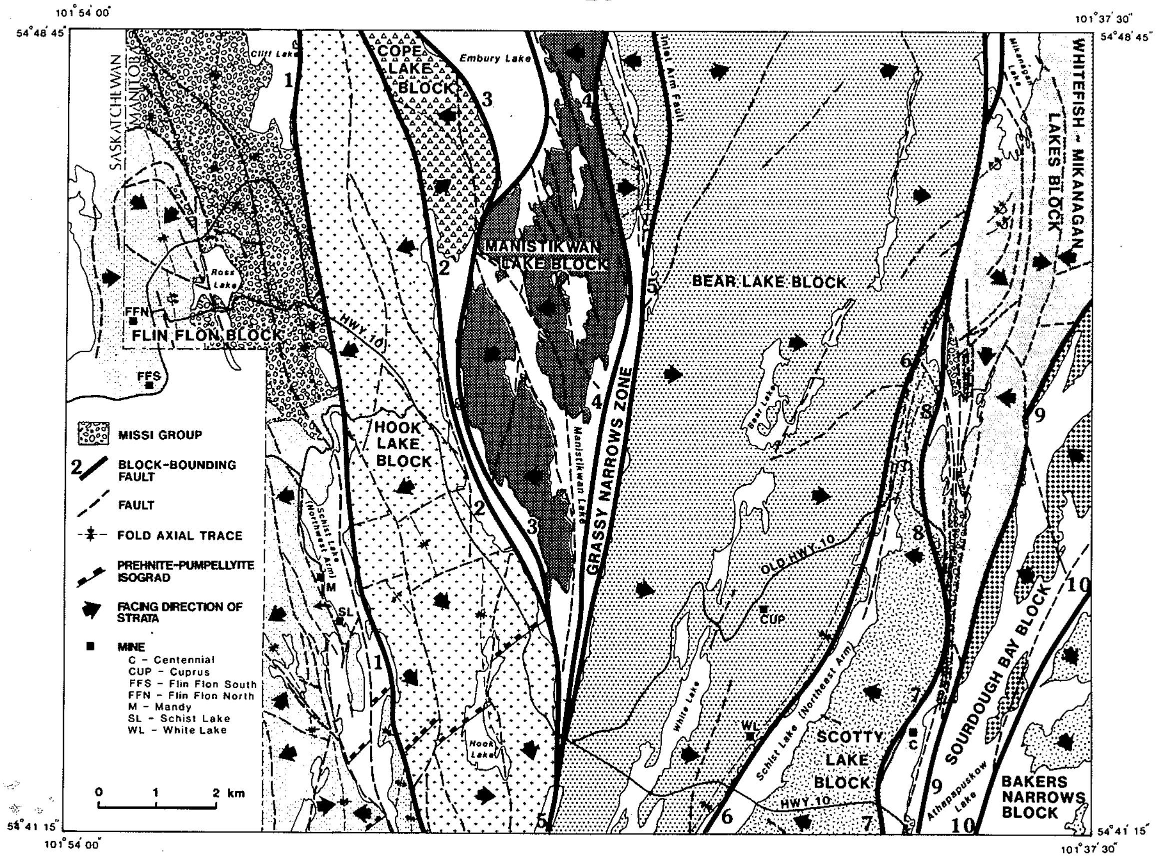


Figure 6: Structural blocks, major faults and folds, and metamorphic isograds in the Flin Flon - White Lake area. From Bailes and Syme (1989).

cherty graphite and pyrite-pyrrhotite-rich sediments are rarely exposed but can be traced for considerable distances as electromagnetic anomalies.

The Hook Lake fault block (Fig. 6) contains the thickest reconstructed section in the Flin Flon area, comprising about 7.5 km of mafic flows, related breccias, and subordinate tuff (Bailes and Syme, 1989). Inasmuch as each of the 10 fault-bounded blocks contains a unique stratigraphic sequence not repeated in other blocks, the total thickness of the Amisk Group is sure to be greater than 7.5 km.

**Missi Group**

The Missi Group is the youngest supracrustal succession in the Flin Flon belt. Volcanic rocks within the Missi at Wekusko Lake (Snow Lake area) have a U-Pb zircon age of 1832 Ma (Gordon et al., 1990).

The Missi Group is more than 1900 m thick at Flin Flon and consists of metamorphosed sandstone, pebbly sandstone and polymictic conglomerate that lies with profound angular unconformity on previously folded Amisk Group rocks and contained intrusions (Bailes and Syme, 1989). At least 2.5 - 3 km of Amisk section is truncated at the basal Missi unconformity west and south of Ross Lake. A hematiferous weathered zone (paleosol) several metres thick is developed in Amisk volcanic and intrusive rocks at all exposed, unfaulted contacts with the Missi. The paleosol is characterized by a distinctive spheroidal weathering defined by concentric bands of reddish-purple to black hematite.

On Athapapuskow Lake more than 1900 m of Missi Group rocks occur in a fault-bounded block (Fig. 5; Syme, 1987). The Missi section is comparable in thickness to that at

Flin Flon, but represents a significantly different stratigraphic sequence, dominated by coarse clastics with abundant detritus derived from the hematiferous Amisk Group paleosol. The entire section constitutes a more proximal assemblage than that at Flin Flon.

Missi Group rocks contain primary structures such as trough cross-bedding, pebble lags, heavy mineral placers, conglomerate lenses and multiple scours that are consistent with deposition by fluvial processes, probably within a subaerial alluvial fan. Clasts in the conglomerate include abundant Amisk Group mafic and felsic volcanic rocks, fine- to medium-grained mafic to felsic high level intrusive rocks, and minor medium to coarse grained granitoid rocks (predominantly tonalite), quartz, jasper, iron formation, chert and epidosite. Intraformational sandstone clasts form a significant part of conglomerates in the upper part of the Group at Flin Flon. Detrital quartz in conglomerate and sandstone was derived from quartz veins and granitoid plutons; detrital feldspar is altered, Fe-stained and derived mainly from plutonic rocks. Accessory heavy minerals include specular hematite, zircon, epidote, allanite and tourmaline.

Geologic relationships clearly indicate that prior to deposition of the Missi Group, Amisk volcanic rocks were folded, intruded by granitoid plutons and deeply weathered in a subaerial environment. A source area composed of these rock types is consistent with the provenance of the clastic material in the Missi. Selective concentration of mechanically and chemically stable components such as vein quartz, chert, iron formation and jasper explains their abundance out of proportion to their abundance in the exposed Amisk Group.

**Intrusive Rocks**

Amisk Group rocks in the Flin Flon-White Lake area are cut by a wide variety of intrusive rocks that are not present in the unconformably overlying Missi Group. Some of the intrusions are syn-Amisk Group, some were emplaced in folded Amisk rocks and thus postdate volcanism, and some occur as isolated intrusions whose age relative to Amisk volcanism and the Missi Group are unknown. Cross-cutting relationships providing relative ages between different intrusions are not common; consequently it is not possible to determine the chronological order of all intrusions.

There is limited direct stratigraphic evidence for pre-Missi, post-Amisk felsic plutonism. At one locality 4 km northwest of Flin Flon there is an unconformity between the Missi Group and an underlying heterogeneous granitic complex. Indirect evidence for pre-Missi plutonism includes the occurrence of granitoid clasts in the Missi and plutonic provenance of many framework quartz and feldspar grains in Missi sandstones. A substantial volume of granitic rock must have been exposed to provide detritus forming the 1900+ m of quartzofeldspathic Missi arenites. One of the ovoid granodiorite plutons emplaced in Amisk Group rocks at Athapapuskow Lake has a zircon date of 1847 Ma (Gordon et al., 1990), consistent with the interpretation that most of the plutons shown on figure 5 are pre-Missi.

Intrusions emplaced in the Amisk Group include a layered ultramafic body (West Arm of Athapapuskow Lake), a layered gabbro - anorthosite - pyroxenite complex (Limestone Narrows), and ovoid calc-alkaline plutons ranging in composition from gabbro to granodiorite. Most plutons have a fairly simple internal zoning, with the most felsic phases occurring in the cores; one pluton has a metaluminous margin and peraluminous core. Another pluton (at Neso Lake) is complexly zoned; trace element compositions of the various phases in the Neso Lake pluton parallel Amisk Group shoshonite compositions, suggesting that the pluton, like the shoshonites, may represent late arc magmatism.

The Flin Flon-White Lake area contains four major differentiated gabbroic intrusions which, despite differences in detail, share a number of important characteristics. These intrusions are medium to coarse grained and have prominent compositional zoning (gabbronorite - gabbro - ferrogabbro - quartz ferrodiorite - micrographic leucotonalite). They display strong Fe-enrichment and are clearly tholeiitic. The intrusions comprise the largest mafic bodies in the area, with the largest, the Mikanagan Lake Sill, 1.2 km thick and over 15 km long. Similar large, compositionally zoned tholeiitic sills are prominent throughout the entire Flin Flon metavolcanic belt, and assuming a similar age for all they collectively represent a major magmatic episode in the development of the belt.

Porphyritic felsic intrusions in the Flin Flon-White Lake area include the body east of Cliff Lake and the intrusion north of Whitefish Lake. Both have associated Cu-Mo mineralization as minor disseminations and fracture fillings (Baldwin, 1980), and both are characterized by strongly xenolithic margins and abundant dykes in adjacent, altered host rocks. The Cliff Lake intrusion is synvolcanic (Gordon et al., 1990) whereas the Whitefish Lake body is probably post-Missi (Bailes and Syme, 1989).

The Boundary intrusions, so named because of their proximity to the Manitoba - Saskatchewan boundary, include a distinctly heterogeneous group of late, post-Missi dykes and elongate intrusions which occur in a north northwest-trending zone centered on Flin Flon. They comprise three compositionally distinct, sequentially emplaced groups: meladiorite (oldest), felsic, and wehrlite - olivine gabbro (youngest) (Syme and Forester, 1977). Several phases may be seen together on a single small exposure, and they are commonly charged with xenoliths of earlier Boundary types and Amisk Group rocks. Foliation and lineation in the meladiorites indicate that they were emplaced before the cessation of tectonic activity.

The youngest intrusion in the Flin Flon area is the Boot Lake - Phantom Lake intrusive complex (Galley and Franklin, 1989; Kaminis granite of Stockwell, 1960). This late synkenematic complex intrudes the Boundary intrusions; its felsic core has a U/Pb zircon date of about 1820 Ma (MacQuarrie, 1980).

**Folds**

There are 5 phases of folding recognized in the area (P1 to P5). These include one phase of pre-Missi folding and four phases that postdate the Missi Group.

F1 folds occur only in the Amisk Group and are overprinted by S3 schistosity, which locally crosses F1 axial planes at a high angle. Prior to deposition of the Missi Group the tightly folded Amisk rocks were tilted and deeply eroded; west of Ross Lake between 2.5 and 3 km of Amisk section is truncated at this unconformity.

F2 folds occur only in the Missi Group, as approximately east-trending structures (described by Stauffer and Mukherjee, 1971). The folds do not have an axial plane schistosity and have no expression in the Amisk Group. They are overprinted by S4 axial planar schistosity.

The third phase of folding (P3) resulted in the development of major north- and northeast-trending folds in the Amisk Group. All of these folds are characterized by a moderate to strong axial planar schistosity that remains parallel to the axial planes regardless of variation in the attitudes of the axial planes. One of these folds clearly refolds an F1 structure south of Flin Flon.

North-trending folds developed during P4 have a strong axial planar schistosity (S4) and lineation in the Missi Group (Stauffer and Mukherjee, 1971). Interference of F2 folds with subsequent F4 folds resulted in basin structures in the Missi; these structures are prominent east and north of Ross Lake and are responsible for the small arcuate Missi outlier west of Channing. At Hidden Lake an S4 schistosity overprints a stronger S3 present in Amisk Group rocks. The dominant Missi fabric is interpreted to be S4 whereas in the Amisk Group it is S3.

The northeast-trending F5 Embury Lake antiform is a large structure which causes bedding and P4 structures to swing to the west, north of the Flin Flon area. It has no well developed axial planar schistosity.

**Faults**

Faults dominate the structural fabric of the Flin Flon-White Lake area. Two groups of faults are recognized, those that bound major stratigraphic blocks and those that occur within the blocks (Bailes and Syme, 1989). Stratigraphic correlations cannot be made across block-bounding faults whereas either correlation or similarity of sequences can be observed across internal faults. In other respects (e.g. physical expression, age) the block-bounding and internal faults are indistinguishable. Where dips of faults have been observed they are invariably steep. Many faults are not simple isolated structures, but tend to splay or occur in clusters, resulting in numerous lens-shaped fault-bounded domains of all sizes (Fig. 5).

A set of northeast-trending dextral faults and shear zones, some up to 1 km wide, dominate the eastern half of the area (Fig. 5). Faults in the western half of the area trend north northeast to north northwest, are dominantly sinistral, and offset metamorphic isograds. All major faults in the region appear to be rooted in a large-scale structure trending southwest from western Athapapuskow Lake (Fig. 5; Syme, 1988); this structure has also been identified in the sub-Paleozoic as a linear which truncates large magnetic domains in the Precambrian (Blair et al., 1988).

The age of every fault cannot be precisely established. With the exception of early faults folded by P3 structures most faults appear to have initiated during the P5 deformation event. Evidence for P5 faulting includes offset of P4 metamorphic isograds, fault offsets in most intrusions (including one pluton dated at 1847 Ma; Gordon et al., 1990), offset of F3 and F4 folds and truncation of S3 and S4 schistosity. Faults were initiated at different times during P5 folding, and as a result display different degrees of flexure about the F5 Embury Lake antiform, consistent with the findings of Stauffer and Mukherjee (1971).
The implications of the fault-block style of deformation are far-reaching. Each block has a more or less intact, definable stratigraphy that is unique to that block alone: correlation of sequences or individual units across block-bounding faults is impossible. Consequently a comprehensive, composite or regional Amisk Group stratigraphy cannot be determined.

**Metamorphism**

Regional metamorphism in the Flin Flon belt increases in grade towards the Kisseynew metasedimentary gneiss belt (Bailes and McRitchie, 1978; Harrison, 1951). In the Flin Flon-White Lake area, metamorphic grade increases from subgreenschist (prehnite-pumpellyite) at Hook Lake (Fig. 6) to middle greenschist (biotite) at Ross Lake. Primary textures and some igneous minerals are commonly well preserved in the subgreenschist zone. In the greenschist zone primary minerals are generally absent and primary textures, although locally well preserved, are commonly obscured due to recrystallization. Lower greenschist mineral assemblages are characterized by chlorite, tremolite-actinolite, epidote, albite, sericite and quartz. Stilpnomelane is common in iron-rich rocks.

Regional metamorphism is superimposed on earlier contact metamorphic aureoles which occur around every major felsic pluton. The aureoles are up to 1 km wide and are manifested in the field by a black-weathering, unfoliated, hornfels-like appearance in which primary structures are generally preserved. Hornblende is the dominant amphibole in contact aureoles, locally overprinted by chlorite-actinolite developed during the subsequent regional metamorphism.

The age of regional metamorphism in the Flin Flon area is probably equivalent to the age of metamorphism in the Kisseynew belt, approximately 1815 Ma (Gordon et al., 1990). This metamorphism postdates the deposition of the Missi Group and all intrusions., and took place with the development of schistosity during P3 and P4. Metamorphic zones are offset by faults developed during P5. In higher grade areas to the north of Flin Flon, retrograde lower greenschist mineral assemblages are reported in P5 fault zones (Stauffer and Mukherjee, 1971; Byers et al., 1965).

## Base Metal Deposits

### Introduction

Base metal deposits in the Flin Flon area (Fig. 5) are volcanogenic stratabound massive sulphide (VMS) bodies (Sangster, 1972). Two types are recognized: proximal deposits with a spatially associated alteration zone (Flin Flon, Schist Lake, Mandy, Centennial, Trout Lake) and distal deposits which lack any recognized associated alteration zone (White Lake, Cuprus, possibly Westarm). Proximal deposits are hosted by coarse felsic fragmental rocks whereas distal deposits are hosted by fine grained graphitic mudstones.

The purpose of the Flin Flon portion of the field trip is to contrast these two associations, by examining the stratigraphy and host rocks of Flin Flon Mine and the Cuprus-White Lake zone.

### Deposit Summaries

Flin Flon Mine is the largest VMS deposit (almost 63 million tonnes) in the Flin Flon volcanic belt, an order of magnitude larger than the next largest deposit (Table 2). The host rock for the ore is a rhyolite flow and flow breccia that has traditionally been called "quartz porphyry"; it contains euhedral to subhedral corroded quartz and euhedral plagioclase phenocrysts. This unit is up to 150 m thick and is underlain to the west by mafic flows and breccias (South Main basalt) and is overlain to the east by porphyritic, pillowed mafic flows (Hidden Lake basalt). The orebody includes both massive and disseminated sulphides and shows metal zoning from a Cu-rich base to a Zn-rich top. There is an extensive footwall alteration zone consisting of dominantly chlorite with lesser amounts of sericite, talc and carbonate. These altered rocks contain relict amygdales and quartz phenocrysts showing they were originally mafic volcanics and "quartz porphyry". According to Koo and Mossman (1975) the alteration resulted in depletion in $SiO_2$, $K_2O$ and $Na_2O$ and enrichment in MgO, CaO, $CO_2$ and $H_2O$ within the alteration zone.

Schist Lake and Mandy deposits are located 5 km southeast of Flin Flon. Neither mine is presently producing; past production totalled approximately 2 million tonnes. These deposits consist of several ore lenses that occur within the same stratigraphic interval. Host rocks for the deposits are sericite-carbonate schists derived from heterolithologic felsic volcanic breccias; the rocks occur within a fault-bounded panel; stratigraphic relationships with other deposits are unknown. The orebodies are zoned with Cu-rich base and Zn-rich tops (Howkins and Martin, 1970). A chloritic alteration zone underlies the Schist Lake orebody; on surface exposures it consists of an anastomosing stockwork of greenish-black chlorite within the felsic volcaniclastics. Minor Cu values are associated with this alteration. Additional alteration features in the felsic volcaniclastic host sequence include patchy silicification, carbonatization and pyritization.

Trout Lake deposit occurs beneath Embury Lake, 8 km northeast of Flin Flon. This mine is currently producing and has combined production and reserves totalling approximately 6.5 million tonnes. The deposit consists of massive and stringer sulphides, and is hosted by sericitized quartz-phyric rhyolite within a sequence of fine grained argillite, greywacke and minor mafic flows (Ko, 1986). The deposit consists of two main zones, each containing a number of stacked en-echelon concordant massive sulphide lenses underlain by stringer sulphides. Each lens is underlain by a chloritic alteration zone. Original stratigraphic relationships between sulphide lenses and their wall rocks are unclear due to the presence of extensive P5 faulting.

Centennial deposit subcrops under about 50 m of water and overburden some 400 m from the west shore of Athapapuskow Lake, about 1.5 km north of the Flin Flon airport at Bakers Narrows. It contained approximately 2.3 million tonnes of ore. The deposit as described by Provins (1980) is a long tabular sheet with a near vertical pitch, enclosed within a unit of quartz-phyric felsic pyroclastic rocks. The felsic pyroclastics are overlain to the west by 30 m of pyritic argillite and 50 m of felsic lapilli tuff and flow breccias. The orebody is a single sulphide lens consisting of alternating beds of sulphide and siliceous gangue; it is zoned with a Cu-rich base, a pyrite-rich core and a Zn-rich top. A pipe-like alteration zone underlies the deposit; chloritic schists directly underlie the ore zone and a more subtle geochemical halo defined by anomalous element distributions outlines a much larger zone (Provins, 1980).

White Lake and Cuprus Cu-Zn deposits occur 11 km southeast of Flin Flon. They produced about 1.3 million tonnes, and both mines are now closed. The orebodies consist of a complex series of elongate lenses that plunge northwards, parallel to a major F3 fold structure. Both the White Lake and Cuprus deposits are interpreted to occur within a single 25 m thick statigraphic interval consisting of graphitic mudstone, siliceous argillite and minor chert. The mineralized unit is underlain by andesitic lapilli tuff and overlain by ferrobasalt flows. It cannot be traced directly between White Lake and Cuprus either on surface or by EM surveys due to the presence of a series of slightly discordant gabbro sills which offset stratigraphy. Neither White Lake nor Cuprus have a recognized alteration zone apart from some minor alteration a few metres thick in one locality south of Cuprus Mine.

Westarm deposit subcrops under the West Arm of Schist Lake, 14 km south of Flin Flon. Little is known about the setting of this deposit because the immediate host rocks are not exposed and the deposit is separated from the nearby mainland by a block-bounding fault. The massive sulphides are hosted by fine grained Amisk sedimentary rocks, and are underlain by carbonatized mafic flows and breccias.

**Controls on Base Metal Mineralization**

Stratigraphic mapping and whole-rock geochemistry have resulted in a number of empirical observations regarding VMS deposits in the western Flin Flon belt (Bailes and Syme, 1989; Syme, 1987, 1988):

1) All economic deposits lie within that portion of the Flin Flon belt underlain by Amisk Group rocks with island arc tholeiite geochemistry; none to date have been found in the more magnesian (back-arc?) Athapapuskow basalts which trend northeast through Athapapuskow and Cranberry lakes.

2) All massive sulphides are associated with felsic flows or felsic volcaniclastic rocks. In some the association is direct, as at Flin Flon, Centennial and Trout Lake mines. In others, like Cuprus-White Lake, rhyolite occurs not with the sulphides but at the identical stratigraphic interval.

3) Detailed stratigraphic mapping of volcanic facies indicates that the deposits for which we have the best information occur in topographic lows: at Flin Flon this was in a mafic, coarse clastic basin probably of limited size, whereas for Cuprus-White Lake the sulphides occur in sedimentary sub-basins within a much larger basinal structure probably representing a summit caldera.

4) Synvolcanic faults may have served to focus the discharge of

hydrothermal fluids; there is indirect evidence of this in an exposed unconformity in the footwall of Flin Flon Mine.

5) The stratigraphic interval containing VMS deposits commonly represents a hiatus in basaltic volcanism, and in some instances indicates a change from explosive to effusive volcanism. In the case of the Cuprus - White Lake deposits the mineralized interval is overlain by highly fractionated, iron-rich basalts.

## Flin Flon Area: Stop Descriptions

### STOP 1: HIDDEN LAKE BASALT

The purpose of this stop is to demonstrate the state of preservation and metamorphic grade of typical Amisk Group rocks, prior to proceeding to the footwall of Flin Flon Mine where alteration is more pronounced. Several outcrops will be examined in the Hidden Lake area, north of the Flin Flon perimeter highway. Outcrops are large and completely vegetation free, facilitating observation of a variety of primary volcanological features as well as the effects of folding and faulting.

Most Hidden Lake basalt flows (Unit 2a in Bailes and Syme, 1989) are pillowed; pillow fragment breccia, interflow tuff, interflow sediments and pyroclastic rocks are virtually absent. The "typical" flow organization observed in Amisk Group mafic flows (Fig. 7) is only rarely displayed by Hidden Lake basalt; consequently it is often difficult to determine flow contacts and measure flow thickness.

The pillowed flows commonly show irregular transitions from pillowed lava to amoeboid pillow breccia. Amoeboid pillows have highly involuted shapes that bud from the top of the massive or pillowed division of a flow (Fig. 7). Amoeboid pillows are complex, interconnected bodies up to 1 m long, elongate parallel to flow contacts. They have complete selvages and commonly contain spherical, quartz-filled amygdales. Amoeboid pillows are rarely in mutual contact and are contained in a matrix of recrystallized hyaloclastite. The hyaloclastite is composed mainly of brownish selvage fragments, light buff to light green epidotized granules, rusty chocolate-brown granules, and intergranular chlorite, quartz and epidote. In the past these breccias have been misidentified as pyroclastic rocks ("mafic agglomerate"); in mapping mafic piles it is important to recognize that they are the flow-top facies of massive, compound and pillowed flows (Fig. 7).

Flow contacts are in some instances identified by changes in phenocryst content or significant changes in colour. Folding of flow contacts and repetition or omission of section through faulting also introduce complications that serve to obscure flow contacts.

Concentrically banded lava tubes, up to 2.5 m in diameter by several tens of metres long, commonly occur in this unit more than in any other major mafic pile in the area; one particularly good example is exposed in cross section at the east end of Hidden Lake. Synvolcanic dykes with banded margins are also common. The banding in both lava tubes and dykes is interpreted to be the result of passage of multiple pulses of magma through the structures.

All rocks in the Hidden lake area display deformation features associated with the F3 Hidden Lake synform. The dominant style of deformation is constriction: rodded pillows plunge about 30 degrees to the southeast, parallel to the axis of the synform. Pillows viewed down plunge most closely approximate their primary morphology. Other deformation features include development of minor F3 folds in pillow selvages and inter-pillow laminated tuff, and larger scale tight F3 folds in flow contacts. Locally there is an S4 foliation superimposed on the dominant S3 axial planar foliation.

### STOPS 2 AND 3: Footwall and hangingwall rocks adjacent to the Flin Flon massive sulphide deposit

#### Introduction

Flin Flon Mine is the largest VMS deposit (63 million tonnes of 2.2% Cu, 4.1% Zn and 2.6 g/tonne Au) in the Flin Flon volcanic belt, an order of magnitude larger than the next largest deposit (Table 2). The deposit was discovered by prospectors in 1915. First production from the Flin Flon Mine was in 1930; peak

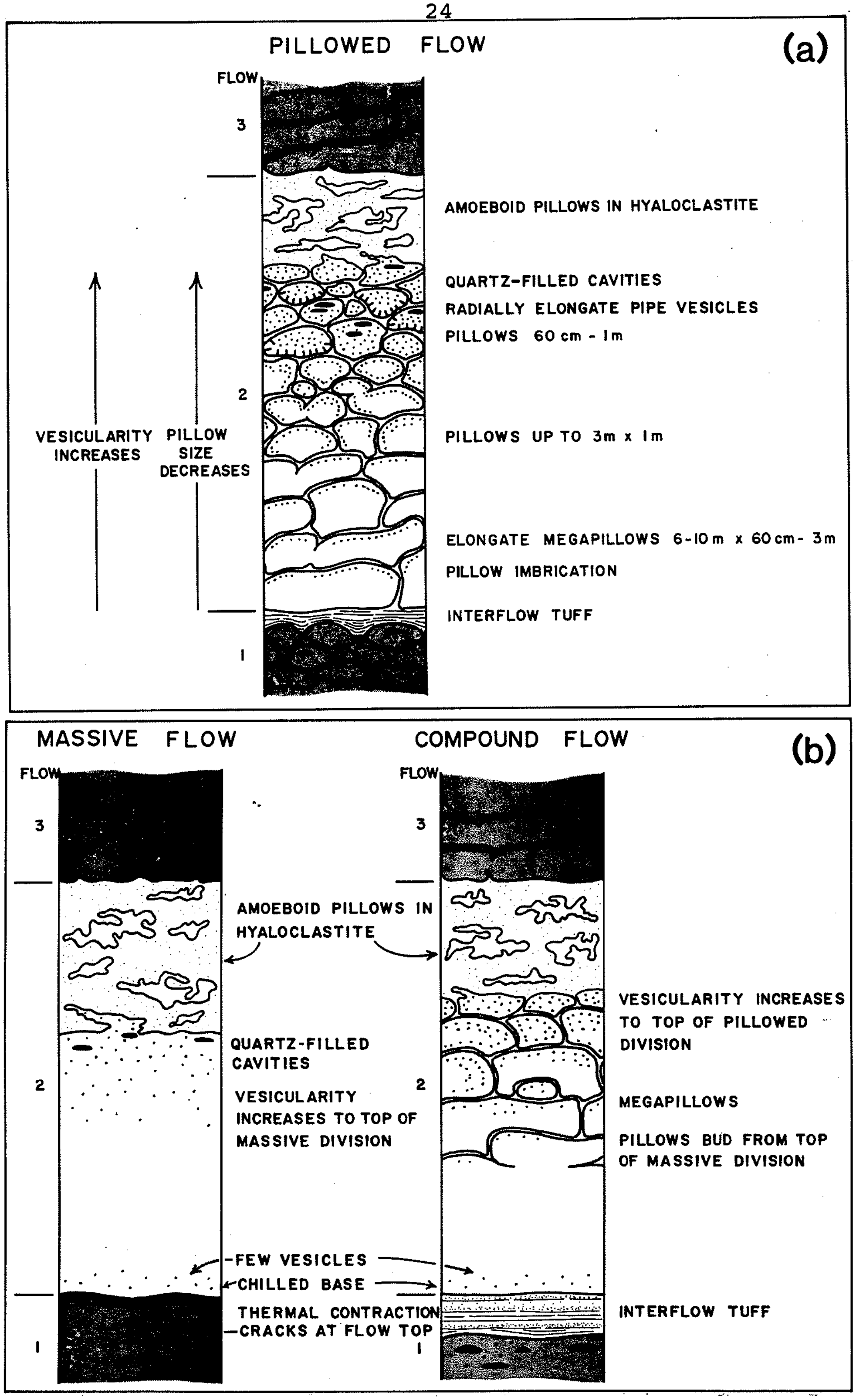


Figure 7: Typical features in (a) pillowed and (b) massive and compound basalt and basaltic andesite flows in the Flin Flon region. Numbers beside columns refer to individual flows. From Bailes and Syme (1989).

production was reached in 1943. Production after 1976 has been mainly from pillars and remnants.

The Flin Flon sulphide orebody is predominantly massive with chalcopyrite concentrated near the base and sphalerite, sometimes banded with pyrite, more common toward the hanging wall. Disseminated chalcopyrite and pyrite occur in the altered footwall rocks and formed approximately 30% of the ore mined. Six ore zones strike 330° and dip 70° east for 1650 m down plunge. The zones average of 270 m long, 21 m thick and 450 m in vertical extent.

The Callinan Cu-Zn deposit, approximately 2 km north of the Flin Flon deposit, occurs at the same stratigraphic level as the Flin Flon orebody (Fig. 5B). Exploration began in 1927 with Cu-Zn mineralization identified in 1938 (Byers et al., 1965). Recent drilling by HBMS has outlined a deposit of 2.4 million tonnes of 1.5% Cu, 4.1% Zn, 1.8 g/tonne Au and 21.1 g/tonne Ag (Table 2).

The stratigraphic package containing the deposit will be examined in two separate localities: the first is approximately 300 m northwest of the smelter and the second is in the vicinity of South Main shaft (Fig. 8). Although the rocks are folded, faulted and cut by a variety of dioritic intrusions, well preserved primary structures and map-scale facies relationships permit interpretation of the physical

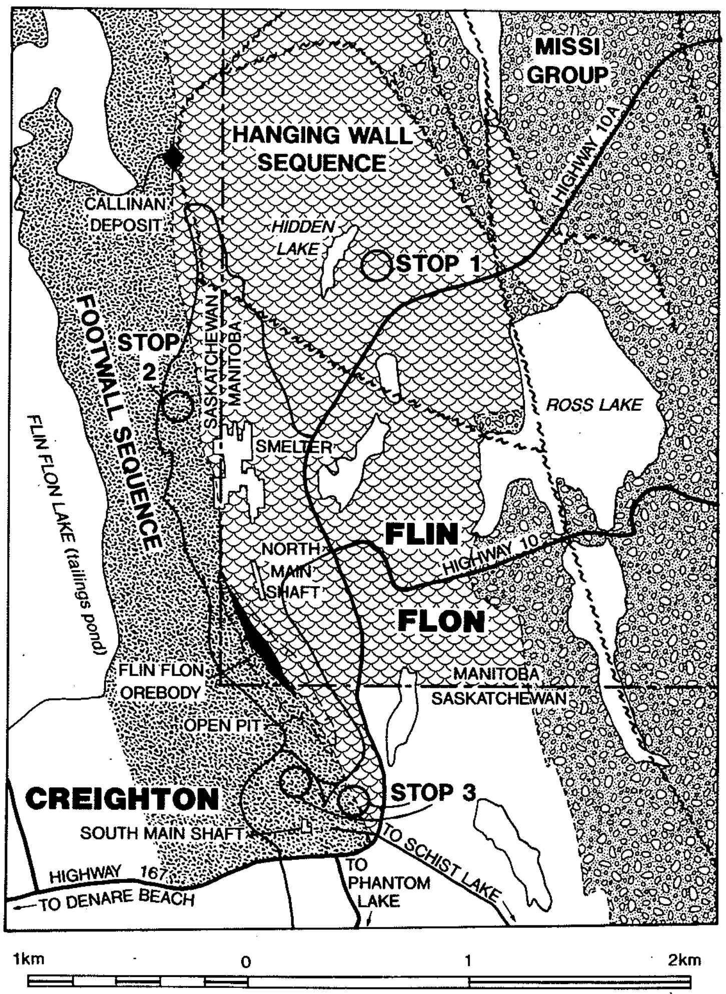


Figure 8: Location map for STOPS 1, 2, and 3, showing distribution of footwall and hanging wall rocks of the Flin Flon and Callinan deposits.

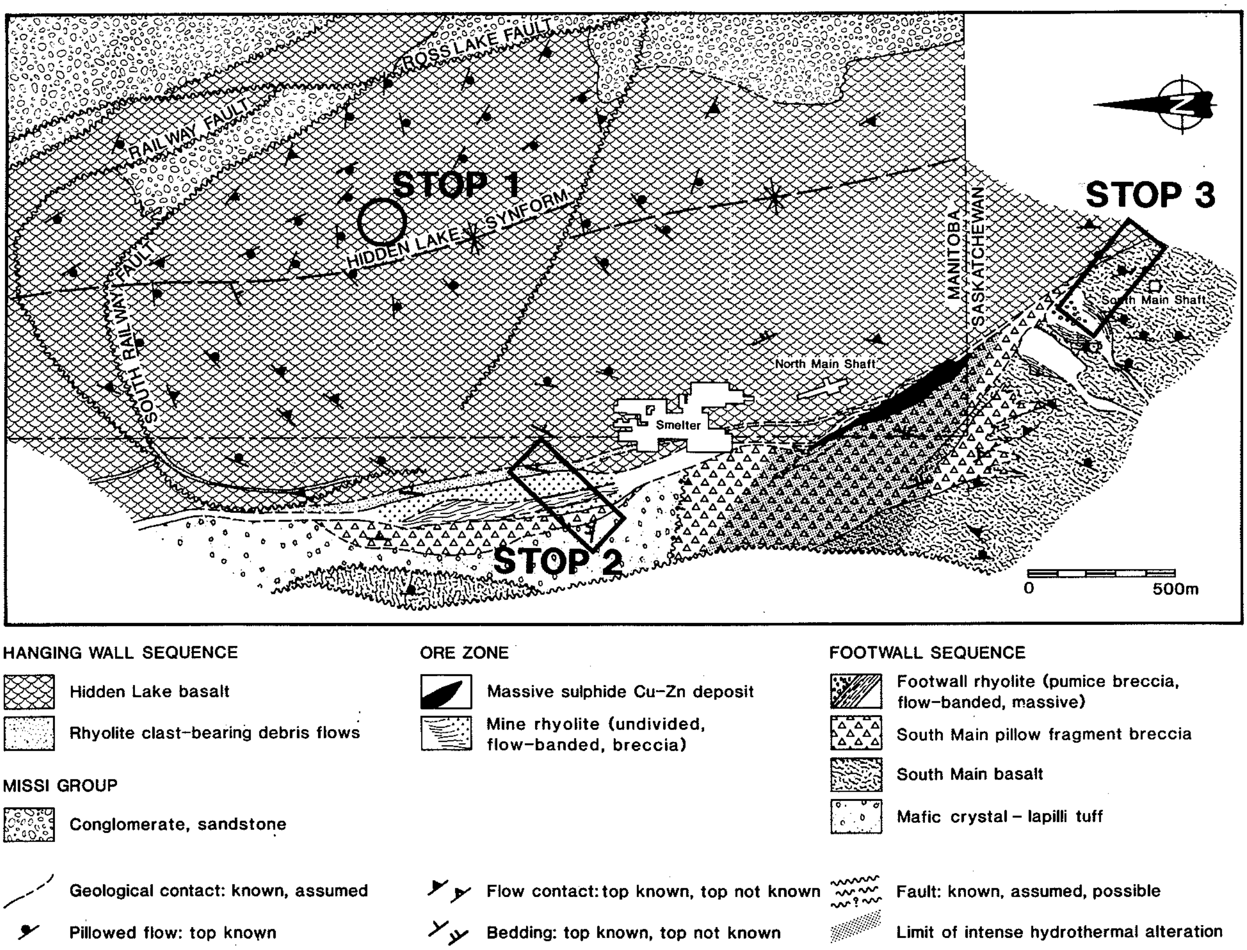


Figure 9: Simplified geology of the Flin Flon mine area. Minor faults and all intrusions have been omitted to clarify relationships between volcanic units. From Bailes and Syme (1989).

environment of deposition of the various rock units.

**General Setting**

Flin Flon mine is a classic proximal VMS deposit (Franklin et al., 1981), hosted by felsic volcanic rocks and underlain by a discordant zone of chloritic alteration.

South Main pillowed basalt flows and pillow fragment breccias form the immediate footwall to the Flin Flon deposit (Fig. 9). A lateral facies change from pillowed flows at South Main shaft, northwards into a thick sequence of now altered pillow fragment breccias underlying the orebody, indicates that the source area for this mafic pile lay to the south of South Main shaft. The breccias presumably accumulated on the flank of a subaqueous basalt volcano or in a basin adjacent to the volcano. It is within this topographic low that the orebody was deposited. The uppermost part of the South Main basalt shows evidence of relatively shallow water emplacement, including the abundance and large size of amygdales and the local profusion of radial pipe vesicles.

The Flin Flon massive sulphide orebody was deposited during a hiatus in basaltic volcanism. During this hiatus volcanic activity shifted to intrusion of high level rhyolite domes, extrusion of the Mine rhyolite flow, and development of a large-scale hydrothermal convection system which altered the footwall basaltic sequence and led to the deposition of the stratiform volcanogenic Flin Flon orebody contemporaneous with the Mine rhyolite. An unconformity exposed in footwall rocks may be one expression of a synvolcanic fault which may have acted as a focus for hydrothermal discharge. Bedded volcaniclastic rocks which overlie the Mine rhyolite (Fig. 9 and 10) and orebody represent the final depositional unit accumulated during the hiatus in basaltic volcanism.

The Hidden Lake basalt sequence, more than 3.3 km thick, represents the resumption of basaltic volcanism following deposition of the Flin Flon orebody (Fig. 9). These rocks are chemically and petrographically different from the underlying South Main basalt, and do not show evidence of hydrothermal alteration. At South Main shaft they directly overlie South Main basalt whereas to the north of the smelter there are 180 m of Mine rhyolite and volcaniclastic rocks between the two basalt units. Hidden Lake basalt may have been extruded in relatively shallow water, evidenced by abundant amygdales up to 1 cm in diameter. Flow morphology (dominated by thick amalgamated flow units) and the scarcity of intercalated sedimentary rocks suggest rapid accumulation of this mafic pile.

**STOP 2: NORTHWEST OF HBMS SMELTER COMPLEX**

At this locality (Fig. 9 and 10) are some of the best exposures of the immediate mine stratigraphy. The various units comprising the footwall rocks, Mine rhyolite and overlying volcaniclastics will be examined. Evidence for an angular unconformity in the footwall sequence will also be shown.

**Plagioclase-phyric mafic volcaniclastic rocks**

The local stratigraphic sequence (Fig. 10) begins with a bedded unit of yellow-buff weathering, altered, plagioclase-phyric mafic volcaniclastic rocks comprising interbedded plagioclase-rich tuff and heterolithologic breccia. The tuff contains up to 50% plagioclase crystals (1 - 10 mm), contained in mafic fragments up to 3 cm across; outlines of the fragments are poorly defined due to recrystallization. Heterolithologic breccia is composed of variably amygdaloidal fragments 2 mm - 10 cm long. Beds are thick and contacts with tuff are abruptly gradational over a few centimetres. The breccia beds are poorly sorted, fragment-supported, and vary with respect to abundance of plagioclase phenocrysts and size of fragments. Fragment types include coarsely plagioclase-phyric, sparsely plagioclase-phyric and silicified, densely quartz-amygdaloidal types with few, if any, phenocrysts.

An angular unconformity between yellowish-weathering tuff and the overlying, green-weathering pillow fragment breccia is exposed on two outcrops. The unconformity surface is sharp, unfaulted and truncates bedding in the tuff at a high angle (Fig. 10). Thin (1 m) mafic sills in the bedded tuff and breccia are also clearly truncated at the unconformity (Fig. 10); the dykes have chilled margins and amygdaloidal cores. Unconformities in volcanic terrains should not be uncommon but this is the only well-documented example in the Flin Flon-White Lake area. Its position in the immediate footwall of the orebody may be more than coincidence; the unconformity may represent a period of synvolcanic faulting contemporaneous with the period of massive sulphide deposition. A synvolcanic fault in this location may have served to focus the discharge of metal-bearing hydrothermal solutions, resulting in the deposition of the Flin Flon orebody.

**Pillow fragment breccia**

Pillow fragment breccia forms a 400 m thick unit directly underlying the Flin Flon orebody (Fig. 9, 10). North of the orebody the breccia underlies the Mine rhyolite. South of the orebody there is a lateral gradation into the South Main pillowed basalt flows through a transition zone of intercalated amoeboid pillow breccia, pillow fragment breccia, and subordinate thin pillowed flows.

Petrographically, fragments in the pillow fragment breccia are identical to South Main basalt, clearly indicating that these units are facies equivalents.

The breccias are dark green weathering, monolithologic, poorly sorted, clast supported and massive, without recognizable bedding contacts. Where best preserved (northwest of the smelter complex) fragments (1 mm - 40 cm) are subangular to rounded, equant, and variably amygdaloidal. Range in amygdale size and abundance is identical to those in the South Main basalt. Matrix of the breccia is a mosaic of epidote, actinolite, chlorite and feldspar which has overprinted small basalt granules. Stratigraphically beneath the Flin Flon orebody the breccias are variably altered (Fig. 9). In "least altered" varieties the matrix is chlorite-rich and fragments vary from relatively unaltered to partially silicified or epidotized. With increasing intensity of alteration the fragments also are strongly chloritized. Other forms of alteration include epidotization and local strong sericitization accompanied by 5 - 20% disseminated pyrite. Surface exposure within the alteration zone is very poor; the most detailed information comes from studies conducted in mine workings (eg. Koo and Mossman, 1975).

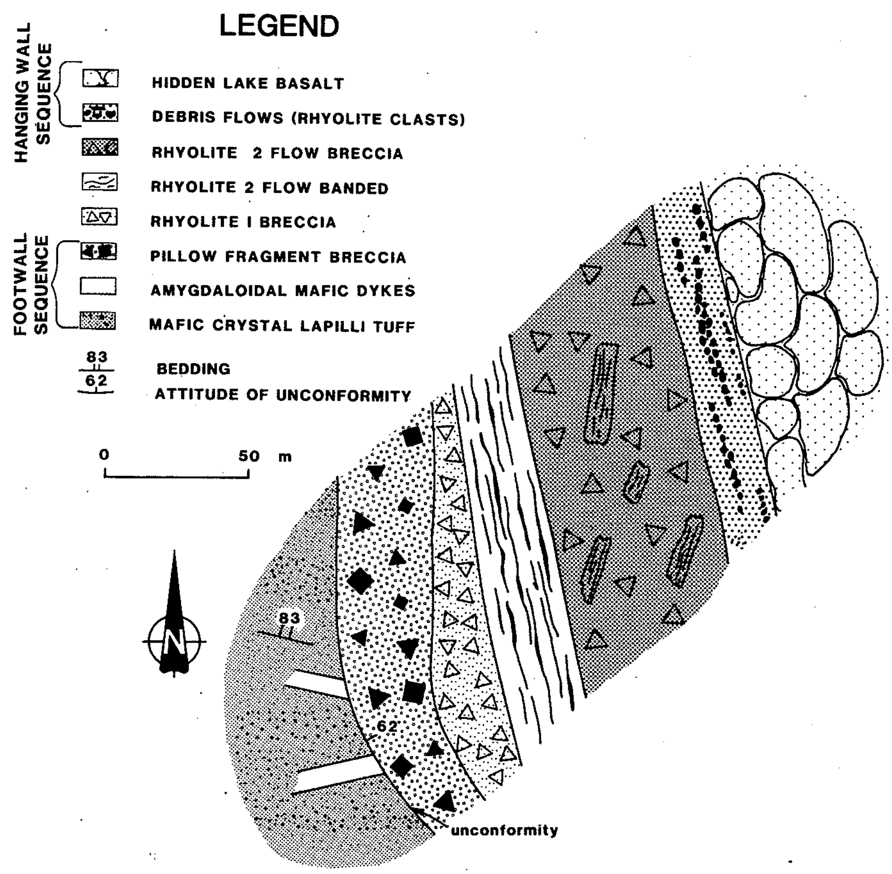


Figure 10: Schematic illustration depicting the stratigraphic sequence northwest of the HBMS smelter, through the stratigraphic footwall and hanging wall of the Flin Flon orebody. Section tops to the east. Unconformity at the base of the pillow fragment breccia truncates bedding and mafic dykes in the underlying mafic crystal lapilli tuff. From Bailes and Syme (1989).

**Mine rhyolite**

A porphyritic, light yellow weathering rhyolite flow composed of two distinct phases overlies the pillow fragment breccia (Fig. 9 and 10) and hosts the Flin Flon orebody (Price, 1977; Koo and Mossman, 1975). The rhyolite has been traced on surface, in underground workings, and in exploration drilling for approximately 3 km. It is a maximum of 150 m thick northwest of the smelter complex and thins to both north and south (Fig. 9).

The basal portion of the rhyolite is 30 m thick and contains 1 - 2% euhedral quartz phenocrysts (0.4 - 1.2 mm) and 4% euhedral tabular plagioclase phenocrysts (0.4 - 2 mm). This part of the flow is a breccia composed of angular to subrounded rhyolite fragments (1 mm - 20 cm) closely packed in a lighter yellow, more chloritic rhyolite matrix.

The main phase of the Mine rhyolite flow contains 3 - 4% lavender, euhedral quartz phenocrysts (0.2 - 2.5 mm) and 7% euhedral tabular plagioclase phenocrysts (0.2 - 1.2 mm). It is readily distinguished on outcrop from the basal phase by the presence of quartz phenocrysts 2 mm or more in diameter. The main phase has two components; a lower zone of massive rhyolite and an upper unit of rhyolite flow breccia (Fig. 10). The massive rhyolite is a maximum of about 43 m thick. It is flow banded, with alternating dark greyish-yellow and yellow bands 1 mm - 1 m wide. The groundmass is a recrystallized mosaic of quartz, feldspar, chlorite, magnetite, biotite and carbonate; mafic minerals comprise only 3% of the rock. Variation in groundmass grain size occurs between adjacent flow bands.

The upper rhyolite flow breccia (Fig. 10) contains exactly the same phenocryst population as the massive rhyolite. The breccia contains tabular slabs of flow banded rhyolite ranging up to 1.9 m long by 20 cm wide. These flow banded slabs comprise 5 - 20% of the breccia and have a more or less consistent attitude, striking 190° and dipping 55° to 60° west. The slabs are in a rhyolite breccia "matrix" composed of angular to subangular rhyolite fragments (to 10 cm) in a dark grey rhyolite matrix.

The top of the Mine rhyolite is a gossaned, foliated breccia in which the fragments are less abundant than in the main portion of the flow. This suggests that the contact with the overlying rhyolite clast-bearing Railway volcaniclastic rocks is gradational.

Koo and Mossman (1975) have observed that the orebodies of the Flin Flon massive Cu-Zn sulphide deposit occur within, as well as directly above or below, the Mine rhyolite. Within the mine they outlined a chloritic alteration zone 2000 m x 1000 m x 200 m which transects the underlying pillow fragment breccia and Mine rhyolite, and terminates against Hidden Lake basalt in the stratigraphic hanging wall.

**Railway volcaniclastic rocks**

Bedded volcaniclastic rocks with abundant rhyolite fragments comprise a 35 m thick unit which overlies the Mine rhyolite (Fig. 9 and 10). These rocks also directly overlie the Flin Flon orebody according to Stockwell (1960).

Beds are well defined, 10 cm - 1 m thick, parallel sided to lenticular, and are defined by grain size differences in sandy beds and by variable fragment abundance in coarser beds. Some lenticular beds are clearly scours that cut underlying beds. Size grading, either normal or reverse to normal type, occurs in some beds.

In coarse beds the predominant fragment type is a yellow weathering porphyritic rhyolite corresponding to the upper phase of the Mine rhyolite. These rhyolite fragments are 1 mm - 18 cm long and are crudely lenticular in shape, with long axes parallel to bedding. A subsidiary fragment type is sparsely plagioclase-phyric, amygdaloidal basalt containing 1% stubby euhedral plagioclase phenocrysts. The rhyolite and basalt fragments are contained in, and supported by, a matrix composed of poorly defined rock fragments, plagioclase, quartz and pyroxene (pseudomorph) crystals and crystal fragments, and a fine grained mixture of epidote, chlorite, actinolite, biotite and pyrite.

Fine-grained, recrystallized sandy interbeds are similar in composition to the matrix of breccia beds; detrital quartz and plagioclase (to 0.25 mm) are present but fine grained mafic minerals predominate.

**STOP 3: SOUTH MAIN SHAFT**

At this locality the felsic host rocks of the orebody are absent, and the stratigraphic footwall and hanging wall basalt sequences are in direct contact. The characteristic features of the two basalt units will be examined, and the primary structures in two rhyolite domes emplaced in the footwall basalt can be observed.

**South Main basalt**

This major unit of basalt underlies the Flin Flon ore deposit. It is at least 700 m thick, extending an unknown distance west, into Saskatchewan. Most of the mapped portion of this basalt lies within the hydrothermal alteration zone associated with the Flin Flon deposit. It is best preserved and least altered in the large outcrop at South Main shaft (Fig. 9).

South Main basalt normally weathers dark green to brownish green, but is dark rusty brown to dull green where altered. Flows are pillowed, commonly with a substantial proportion of amoeboid pillow breccia. Pillows vary in size from less than 1 m to 3 m across, and have 5 mm thick rusty brown weathering selvages. Amygdales are filled with quartz and epidote; they are commonly 1 - 5 mm in diameter but attain a maximum of 2 cm. In some flows there is a bimodal amygdale size distribution, with abundant 0.5 - 1 mm amygdales and sporadic 3 - 7 mm amygdales. Radial pipe vesicles in the margins of pillows are up to 8 cm long by 8 mm in diameter.

South Main basalt appears to be aphyric in hand specimen, but in fact contains 2 - 3% pyroxene microphenocrysts (0.2 - 0.8 mm) pseudomorphed by actinolite. The pyroxene microphenocrysts commonly occur in clumps of crystals (glomerocrysts) up to 1 mm across. The groundmass is composed of elongate plagioclase laths (up to 0.4 mm long) and abundant dark green actinolite, chlorite, epidote and local leucoxene or magnetite.

Alteration of the basalt takes a variety of forms but most commonly comprises intense epidotization, accompanied by local zones of chloritization and sericitization. Epidotized pillows have yellow epidosite domains in pillow cores and dark green chloritic margins. Some pillows are thoroughly epidotized. Local zones of "bleaching" due to introduction of silica, and gossaned zones characterized by anastomosing chlorite-pyrite-filled fractures, are also present. Within the mine workings the alteration zone is characterized by abundant dark green chlorite, which occurs in the overlying Mine rhyolite as well as the South Main basalt. This intense chloritization is not exposed at surface.

The top of the South Main basalt is exposed 250 m northeast of South Main shaft. There, a recessive, poorly exposed zone 10 - 20 m wide consists of gossaned, chloritic basalt with disseminated and fracture-filling pyrite. It is directly overlain by unaltered, unmineralized, plagioclase-phyric basalt belonging to the Hidden Lake basalt sequence. This gossan zone is interpreted to be laterally equivalent to the Flin Flon ore zone (Fig. 9).

**South Main rhyolite domes**

Two rhyolite bodies, which cut across flow contacts in the South Mine basalt, are interpreted as small rhyolite domes. The domes have bulbous upper portions, up to 150 m across, connected to feeder dykes less than 45 m thick. The feeder dykes contain xenoliths of South Main basalt.

The bulbous portions of the domes contain a number of primary structures including well defined flow banding (parallel to the margins of the domes), clasts of long-tube pumice, pumice breccia in the top of one dome, and rhyolite breccia alternating with flow banded rhyolite. These structures are all consistent with the interpretation of the rhyolite bodies as high-level intrusive domes (e.g. Fink and Pollard, 1983).

The rhyolite domes are composed of at least four separate phases, as defined by variation in phenocryst population. Quartz phenocrysts are commonly euhedral but are embayed or corroded in some phases. Plagioclase phenocrysts vary from euhedral elongate tablets to stubby crystals and glomerocrysts. The groundmass consists of a fine grained recrystallized mosaic of quartz and feldspar, sericite, carbonate and less than 5% chlorite and epidote. Zircon is an accessory mineral in some samples.

At South Main shaft the south rhyolite dome is cut by a spectacular intrusion breccia cored by a dyke of Boundary meladiorite. Fragments in the breccia include basalt, rhyolite and diorite; the age is post-Missi as the Boundary intrusions are observed to cut the Missi Group.

**Hidden Lake basalt**

Hidden Lake basalt conformably overlies South Main basalt at South Main shaft (Fig. 9). It is readily distinguished from South Main basalt by its distinctive buff weathering colour, absence of pipe vesicles, absence of hydrothermal alteration, abundance of plagioclase phenocrysts, and lower specific gravity. To the north, Hidden Lake basalt overlies the Railway volcaniclastic rocks; the contact is not observed. The entire Hidden Lake sequence is over 3.3 km thick.

This is the same unit that was examined at STOP 1, north of the perimeter highway. Pillows here range in size from less than 1 m to megapillows several metres in long dimension. Selvages range in thickness from 2 - 10 mm and weather rusty brown. Amygdales vary in size and abundance between and within flows; they are commonly 1 - 5 mm in diameter but are up to 2 cm across. They comprise 5 - 35% of pillows and may be concentrated either in pillow cores or pillow margins. There is no systematic stratigraphic change in amygdale abundance.

Hidden Lake basalt is commonly plagioclase-phyric and glomerophyric, although the abundance and size of phenocrysts varies considerably: maximum phenocryst size throughout the sequence ranges from 1.5 mm to 8 mm. Phenocryst abundance ranges from 5% to 25% between flows. Groundmass (in best preserved samples) consists of plagioclase microlites (0.1 - 0.4 mm) with interstitial chlorite, actinolite, epidote and minor biotite.

**STOPS 4 TO 7: Cuprus-White Lake deposits**

**Introduction**

The Cuprus and White Lake deposits, 11 km southeast of Flin Flon (Fig. 11), produced a total of about 1.3 million tonnes of ore averaging 2.3% Cu and 5.3% Zn. Initial prospecting on the showings that would become the orebodies began in 1919. Cuprus Mine was brought into operation in 1948 and peak production occurred in 1953; by 1954 the orebody was exhausted. Production began at White Lake Mine in 1972 and the mine closed in 1982.

White Lake and Cuprus deposits are interpreted to occur within a single 25 m thick interval consisting of graphitic mudstone, siliceous mudstone and minor chert. Both deposits are stratiform, lensoid, and strongly folded along with the enclosing sedimentary rocks. In White Lake Mine the north northeast plunge of ore lenses shallows with depth from 35-40o at surface to 23o at the 2110 foot level (Provins, pers. comm. 1981), parallel to the axis of the F3 Northeast Arm syncline. The White Lake orebody is associated with

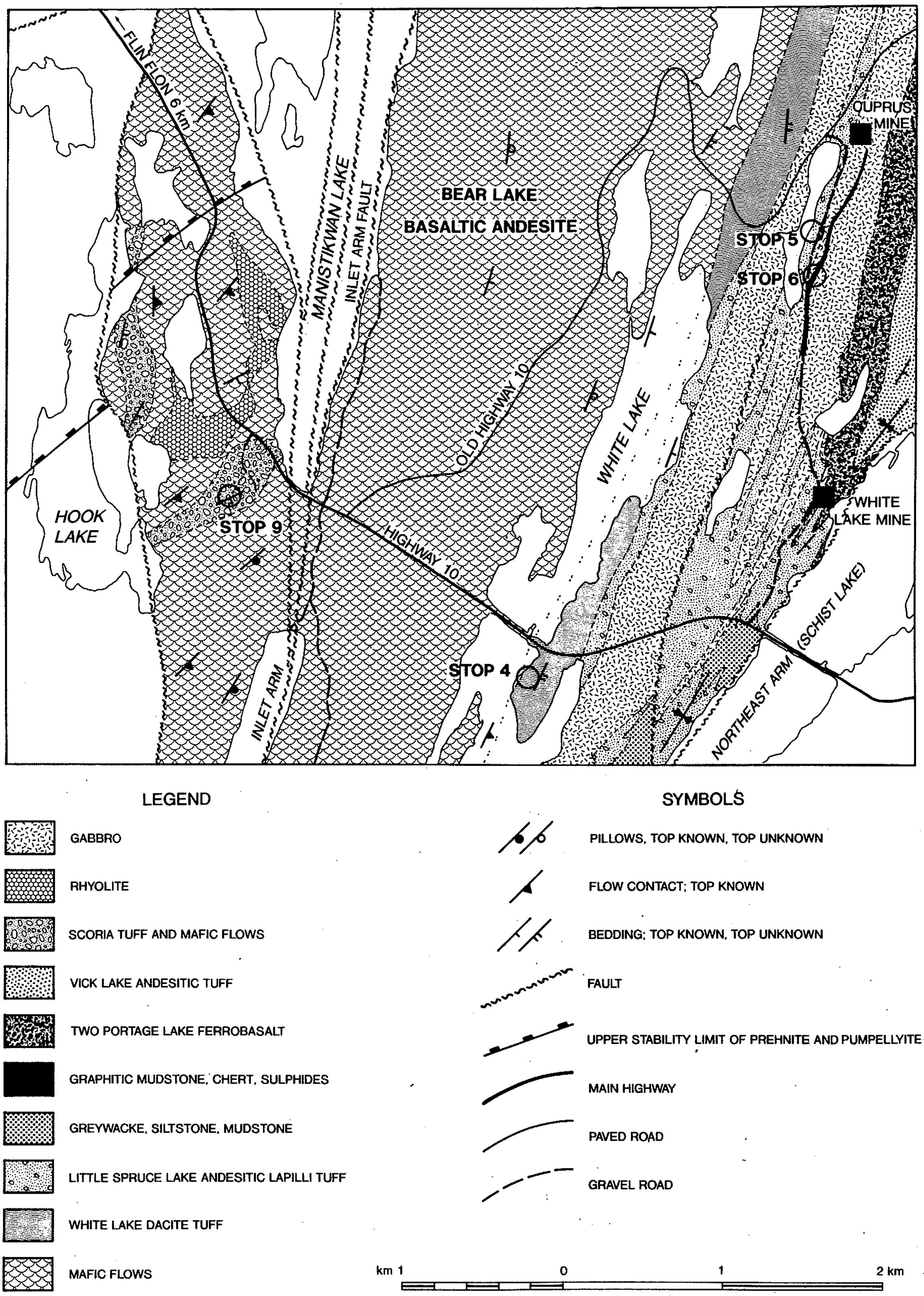


Figure 11: Simplified geological map of the area between Hook Lake and Northeast Arm, showing the location of Cuprus and White Lake mines and STOPS 4,5,6 and 8. The Bear Lake block (see Fig. 6) lies between the Inlet Arm fault and Northeast Arm. South and east of Hook Lake the rocks are in subgreenschist facies, and contain sporadic prehnite and pumpellyite.

graphitic argillite, which completely encloses the massive sulphides at depth. Neither the Cuprus or White Lake deposits have extensive footwall alteration zones, and can be considered as distal VMS deposits. Mineralogic banding (chalcopyrite - sphalerite - pyrrhotite) occurs within the White Lake deposit; these define repetitive Cu-rich and Zn-rich cycles but Cu content is highest in the base of the deposit.

**General setting**

Despite the fact that thick gabbro sills transect the stratigraphy in the immediate vicinity of the mines, the stratigraphic setting of both deposits can be well defined within the Bear Lake fault block (Bailes and Syme, 1989; Fig. 6 and 12).

Bear Lake basaltic andesite forms the base of the succession, and represents a shoaling subaqueous volcano at least 3.3 km thick. Flow directions in this unit are uniformly to the north. The basaltic andesite volcano is overlain by more than 1650 m of basin-filling volcaniclastic rocks, suggesting that a large summit caldera formed in the final stages of Bear Lake volcanism.

The cessation of mafic volcanism was abruptly followed by eruption of the Solodiuk Lake subaqueous rhyolite flow, probably at the caldera margin. Contemporaneous with the rhyolite, the southward-deepening basin filled with a succession of volcaniclastic rocks. These include: 1) a proximal heterolithologic breccia derived in part from the rhyolite, 2) White Lake dacite tuff and reworked tuff derived in large part from pyroclastic components of rhyolitic volcanism, and 3) redeposited andesitic lapilli tuff. The units are wedge-shaped and thicken to the south, defining the basin structure.

The period of rhyolite volcanism and deposition of volcaniclastic rocks ended in a period of volcanic quiescence, during which graphitic pelagic mudstones, cherts and stratabound massive sulphides were deposited, very likely in sub-basins within the larger basinal structure. There is no alteration zone in the footwall of the deposits. Although the orebodies are emplaced in sediments, they are clearly at exactly the same stratigraphic level as the Solodiuk Lake rhyolite (Fig. 12).

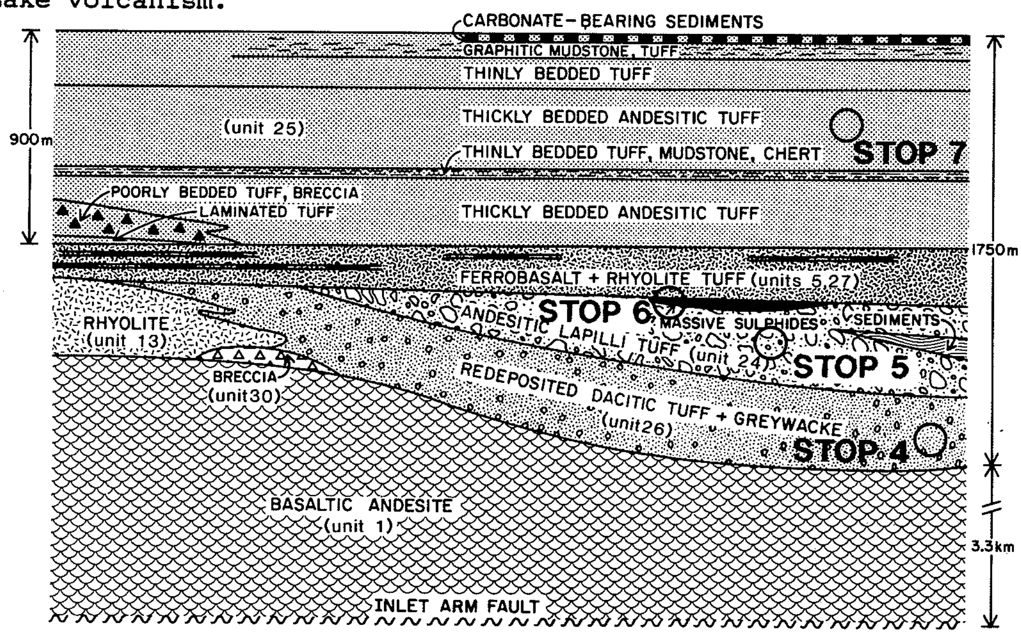


Figure 12: Schematic diagram showing the main stratigraphic elements of the Bear Lake Block, plus STOP locations. Unit numbers refer to those on the 1:20 000 geological map (Bailes and Syme, 1989). The horizontal scale on this diagram represents about 10 km; north is to the left. From Bailes and Syme (1989).

Following deposition of the sulphides, the entire basin-fill sequence was covered by a highly distinctive unit: Two Portage Lake ferrobasalt and intercalated rhyolite crystal tuff. This bimodal unit is very distinctive in both lithology and geochemistry.

The Bear Lake succession is topped by more than 900 m of andesitic tuffs with turbidite bedforms. These rocks appear to occupy a very large, deep basin probably unrelated to the previous caldera basin.

Four short stops will be made through some of the units which make up the Bear Lake stratigaphic sequence. None of the first three exposures are exceptional; the rocks have undergone a significant amount of strain and primary structures are not as well preserved as elsewhere in the area. The purpose is to compare and contrast the volcaniclastic rocks which underlie, host and overlie the deposits.

**STOP 4: WHITE LAKE DACITE TUFF**

A heterolithologic unit comprising rocks of dacitic bulk composition conformably overlies Bear Lake basaltic andesite (Fig. 11 and 12). The dacitic sequence forms a southward-thickening, wedge-shaped deposit with a maximum thickness of 300 m at White Lake.

The dacitic unit has four distinct members; these are locally interlayered and are laterally equivalent. The members form a series of wedge-shaped units including: 1) dacite tuff with weakly defined layering, 2) dacite tuff and tuff breccia characterized by abundant pumice blocks, 3) reworked dacite tuff and greywacke, and 4) dacite tuff with subtle bedding and sporadic pumice clasts.

At this location member 1 (above) is exposed; the tuff directly overlies Bear Lake basaltic andesite flows, which are exposed at the base of the cliff that forms the western margin of this outcrop (Fig. 11).

The tuff generally lacks distinct bedding and internal structures. A subtle bedding is defined by variation in the abundance and size of small quartz grains (0.25 - 1.0 mm). Sharp bedding plane contacts between quartz-rich and quartz-poor material occur locally. Epidotized, densely vesicular lapilli occur throughout the tuff and locally comprise up to 30% of some beds. Strongly flattened, dark chocolate brown mafic fragments up to 25 cm in length occur in some zones.

Although the tuff appears monotonous, there is a vague heterogeneity on a 50 cm to 2 m scale. These units (beds or sets of beds) are defined by the abundance of epidotized lapilli, abundance and size of quartz, and weathering colour. Plagioclase-crystal-bearing tuff is interlayered on a scale of 1 to 2 m with the quartz-bearing tuff on the eastern of the outcrop.

Structural features to observe include kink bands and brecciated kink bands; these late features are superimposed on the S3 schistosity.

**STOP 5: ANDESITE LAPILLI TUFF IN THE STRATIGRAPHIC FOOTWALL OF CUPRUS MINE**

An east-facing, wedge-shaped unit of andesitic lapilli tuff overlies the dacite tuff observed at the previous stop (Fig. 11 and 12). The Cuprus-White Lake mine zone occurs in a 25 m thick formation of graphitic mudstone and minor chert that directly overlies these andesitic rocks. A sub-concordant gabbro sill 60 m thick separates the Cuprus Mine zone (STOP 6) from footwall andesite tuff (STOP 5) (Fig. 11).

Rocks with andesite bulk composition are extremely rare in the Flin Flon region. Andesite flows are virtually nonexistent, and there are only two volcaniclastic units with andesitic bulk composition: this unit and Vick Lake tuff (STOP 7).

On this outcrop the lapilli tuffs are crudely stratified, with bed contacts defined by interbeds of fine-grained tuff. In general, however, bed organization is poor and bedding plane contacts are absent.

The tuff is poorly sorted, oligomictic, and composed of vesicular, plagioclase-phyric fragments which range in size from granules to 10 by 50 cm. The fragments are replaced by epidote and quartz and are tectonically flattened into lenticular forms within the plane of foliation (S3). The degree of flattening is variable. The matrix has a granular texture resulting from a high proportion of fragments and plagioclase crystals smaller than 2 mm. Locally there appears to be more than one fragment type, but this is probably a result of varying degrees of silicification; in some fragments there is almost a complete replacement by very fine grained quartz.

**STOP 6: CUPRUS MINE ZONE**

At this location the unit of sedimentary rocks which hosts the Cuprus Mine zone is 15 m wide, bounded on the east and west by gabbro sills; the western sill partly truncates the sediments in the outcrop 20 m north. The maximum stratigraphic separation from the lapilli tuff examined at STOP 5 is 10 m.

The sedimentary rocks, which strike north and top east, are exposed in a series of small exploration pits. They are composed of two poorly defined subunits; a lower zone of laminated graphitic mudstone with sulphide layers and minor chert laminae, and an upper zone of siliceous argillite-chert-sulphide. Minor folds are common, and are similar to those in the highly folded Cuprus orebody.

Several metres south of the exploration pits, across a narrow east-trending sinistral fault, a small exposure of altered andesite lapilli tuff directly underlies the sulphide-bearing sedimentary formation. The altered rocks are exposed for a width of 5 m. The fragmental nature of the tuff is still apparent in this exposure but its chemical composition is significantly different from the unaltered tuff at STOP 5; it contains high contents of MgO (9.91%) and $FeO^T$ (15.89%), and low contents of $Na_2O$ (0.05%) and CaO (1.81%).

**STOP 7: VICK LAKE ANDESITIC TUFF**

This stop emphasizes the primary structures in a fine-grained subaqueous pyroclastic unit with turbidite bedforms, interpreted to have been deposited in a deep basinal environment. The pyroclastic sequence is 900 m thick, conformably overlies ferrobasalt (Fig. 12) and underlies poorly exposed dacitic flows and mixed pyroclastics. These rocks contrast sharply with the coarser, poorly bedded caldera-fill volcaniclastics (STOPS 5 and 6).

**General features**

The sequence is broadly upward fining and is interlayered in the top 100 m with locally pyritic graphitic mudstones. The basal 250 m is characterized by abundant thick beds containing large pumice fragments. A 50 m thick subunit of thin-bedded mudstone and chert, occurring approximately a quarter of the way up the section, is the only non-pyroclastic unit in the sequence (with the exception of the mudstones in the upper 100 m). The absence of significant interbeds derived from "background" sedimentation indicates rapid deposition of the pyroclastic sequence.

Areas of good preservation include Two Portage Lake and portions of the area traversed by old Highway 10. Further south a strong foliation accompanied by metamorphic recrystallization obliterates the fine-scale features in these rocks (Fig. 13).

The tuff is composed of shards, pumice, plagioclase crystals and crystal fragments, brown "vitric" microclasts, microlitic lithics, amphibole crystals and crystal fragments, and a fine grained recrystallized matrix:

1) Shards are 0.05 - 0.4 mm across, and are generally smaller than 0.2 mm. They have equant to tabular shapes; boundaries are defined by a combination of straight to conchoidal fracture surfaces and vesicle walls (Fig. 14). Fracture surfaces commonly

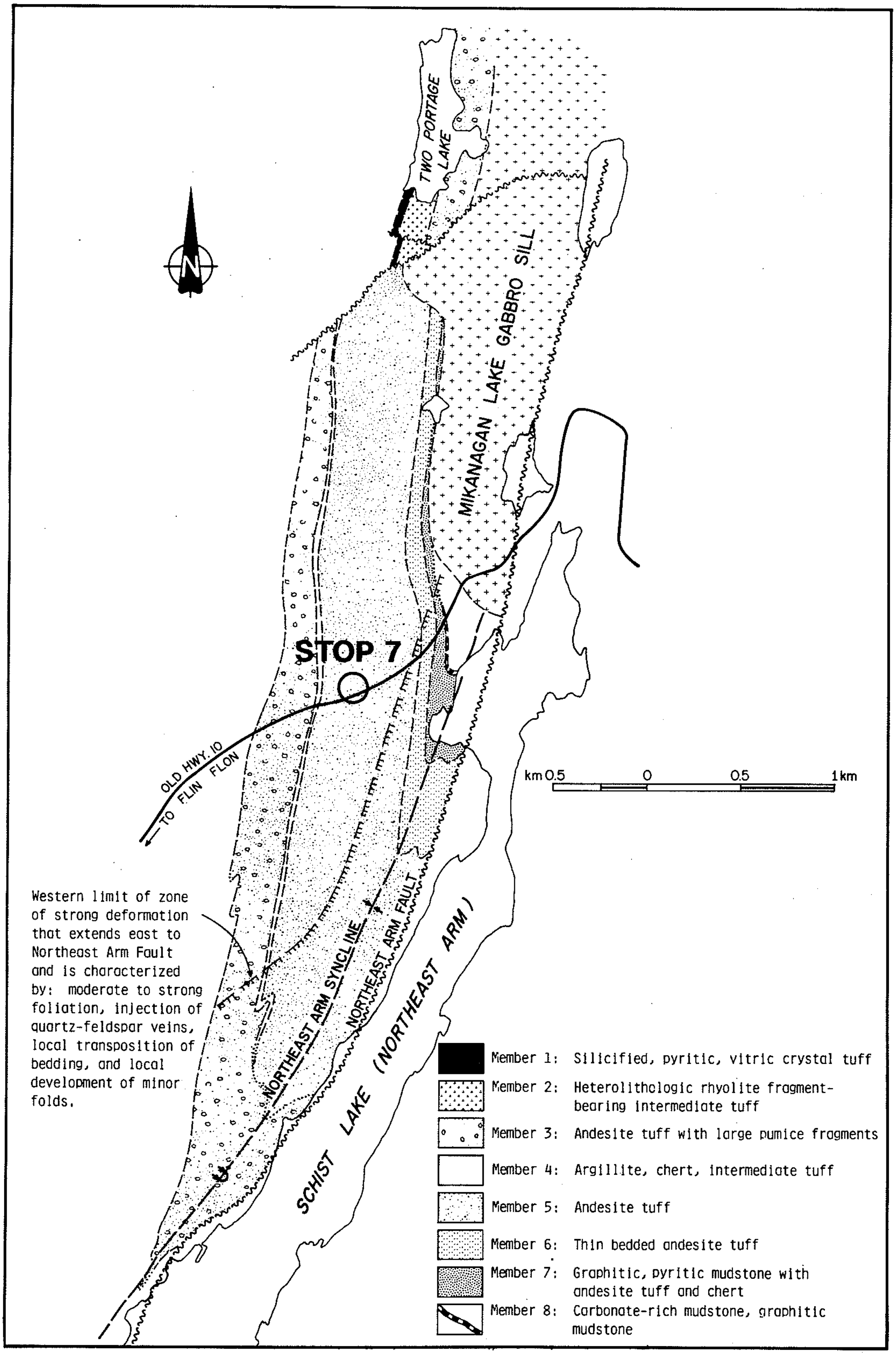


**Figure 13: Distribution of stratigraphic members in Vick Lake andesitic tuff, showing location of STOP 7. East of the toothed line primary structures are less well preserved. From Bailes and Syme (1989).**

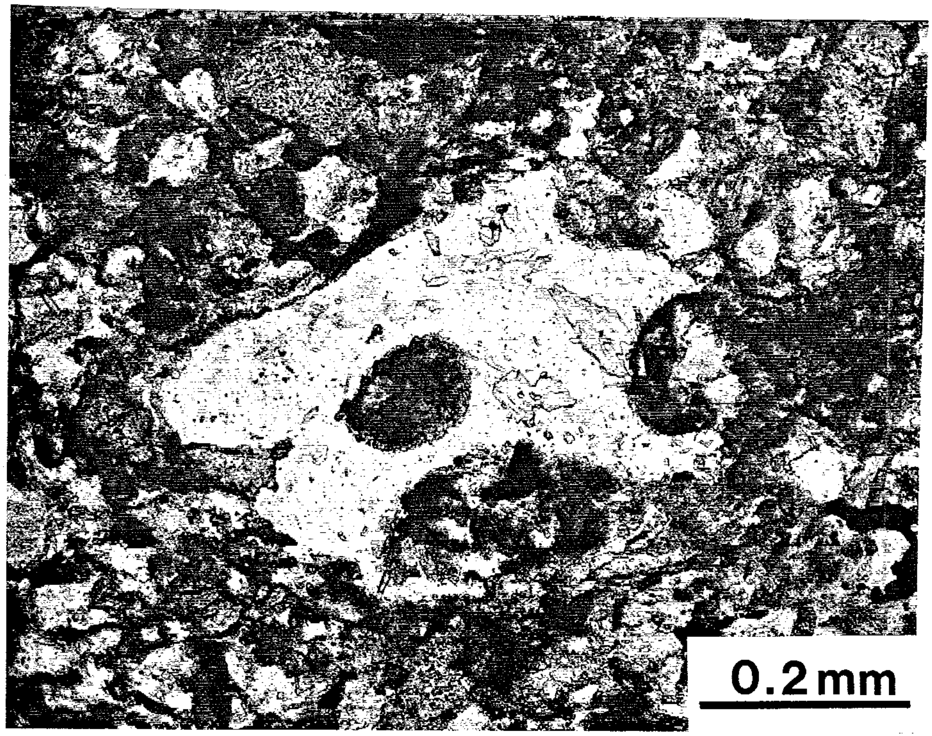


Figure 14: Photomicrograph of large shard in Vick Lake andesitic tuff. Conchoidal boundaries cut through vesicles. Smaller shards occur in the matrix. Plane polarized light. From Bailes and Syme (1989).

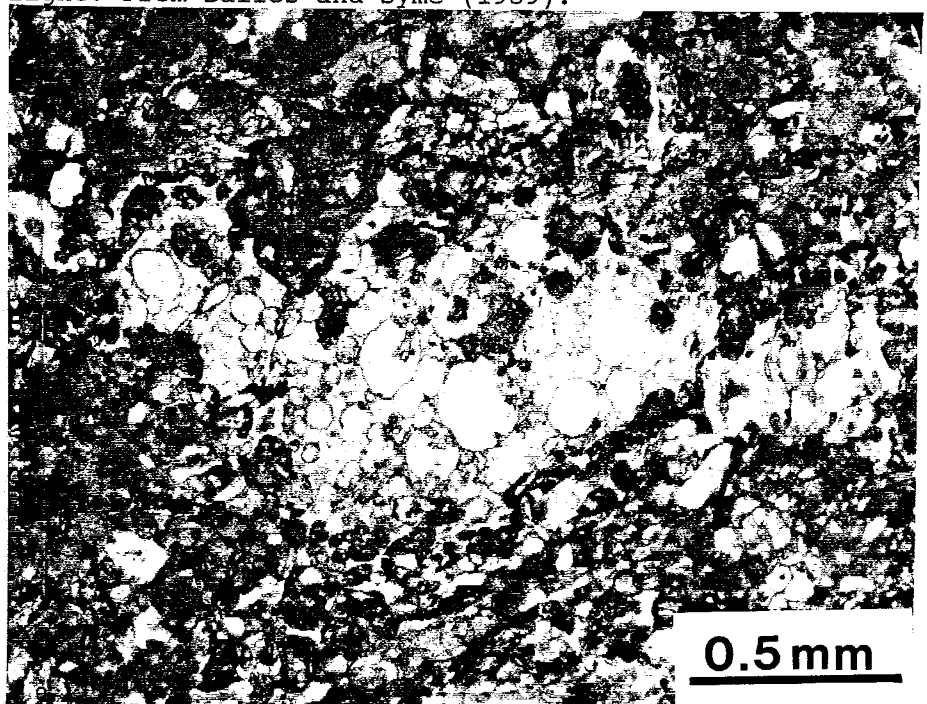


Figure 15: Photomicrograph of pumice fragment in Vick Lake andesitic tuff. Vesicles are filled with quartz and albite and are separated by septa composed of very fine grained secondary chlorite and epidote. Plane polarized light. From Bailes and Syme (1989).

cut through vesicles at grain boundaries. Some particles are completely controlled by vesicle walls but these are generally small and appear to be shreds of pumice. The shards are aphyric and non-vesicular to weakly vesicular. Vesicles are generally less than 0.05 mm across, and are round, oval or tube-shaped, and filled with very fine grained epidote, chlorite, feldspar or quartz. Shards are recrystallized and replaced by a mixture of albite, subordinate quartz, and a dusting of epidote, chlorite and sericite.

2) Pumice in the ash-sized matrix of most beds is 0.4 - 6 mm. As observed in outcrop it is typically less than 3 cm long but can be up to 30 cm in maximum dimension in some pumice-rich beds. The shape of pumice granules and blocks is variable and ranges from oval, equant to irregular. Vesicularity ranges from 50 to 80%; vesicles are round, oval or tube-shaped, less than 0.4 mm in diameter (Fig. 15). Pumice fragments contain plagioclase phenocrysts similar in size and shape to complete crystals in the matrix. Pumice is replaced by a polygranular mosaic of feldspar and quartz, similar to shards. Very fine grained chlorite and epidote outline vesicle walls.

3) Tabular euhedral plagioclase crystals and angular to subangular crystal fragments comprise approximately 15 - 40% of tuff beds; they range from 0.1 to 2 mm in size. Normal size and abundance grading of plagioclase is typical in most beds. Best preserved crystals are monocrystalline, albite-twinned, slightly turbid, with patchy replacement by green chlorite, epidote, carbonate and sericite.

4) Tan-brown microclasts up to 2 mm, but generally less than 1 mm across, are common in the lower parts of graded beds where they comprise up to 15% of the tuff. Shapes vary from subrounded to subangular but larger granules may have ragged margins, a few vesicles and irregular amoeboid shapes. They are aphyric or plagioclase-phyric; large phenocrysts are typically broken at clast margins. The groundmass is composed of very fine grained, brownish, semi-opaque material (largely epidote) with or without randomly oriented acicular plagioclase microlites (0.05 - 0.1 mm). Some granules contain a few small (0.08 mm) round to tube-shaped vesicles. These clasts are interpreted as juvenile glass fragments, bounded largely by conchoidal fracture surfaces, with shapes subsequently smoothed by abrasion.

5) Microlitic lithics are shades of grey in colour and contain abundant lath-shaped plagioclase microlites (0.05 - 0.1 mm) in felted to pilotaxitic texture. They are subrounded, non-vesicular to weakly vesicular, and are generally less than 0.5 mm across. Some contain stubby plagioclase phenocrysts 0.1 - 0.25 mm long. These microclasts are interpreted as accidental lithics.

6) Broken euhedral prisms of magmatic hornblende comprise 0 - 3% of tuff and are typically concentrated in the bases of beds. Some are unaltered, strongly pleochroic (yellow green to deep olive green) crystals; others are variably altered to tremolite-actinolite.

7) In rocks with best preservation the matrix between shards consists of a very fine grained mixture of brown epidote with subordinate feldspar, tremolite-actinolite or chlorite, quartz and sphene. In more recrystallized and foliated rocks the secondary assemblage completely overprints shards and microclasts. In highly recrystallized tuff even the pumice fragments are obliterated.

Tuff beds range in thickness from 30 cm to 18 m and average 1 m. The beds have a Bouma-type internal zonation comprising one or more of the following: a graded "A" division; parallel laminated "B" division; ripple laminated "C" division; parallel laminated "D" division; and very fine grained structureless "E" division. Most of the beds are AB(E) types. Pumice strata, both continuous and discontinuous layers 5 mm to 20 cm thick, occur in the upper part of the "A" division, and rarely in the "B" division (Fig. 16). Grading, defined by the upward decrease in

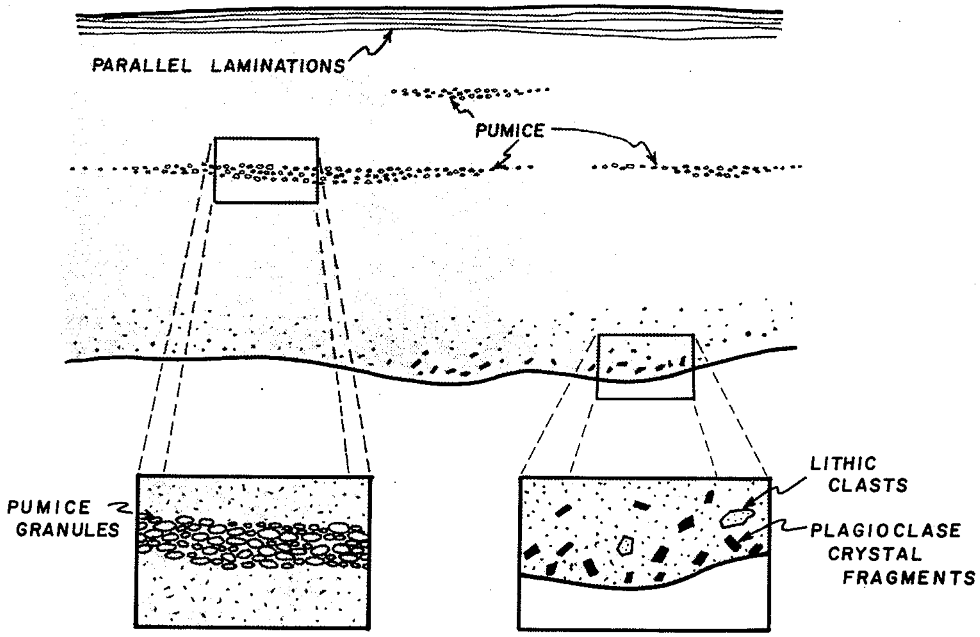


Figure 16: Schematic diagram of typical Vick Lake tuff AB bed, showing concentration of lithic granules and plagioclase crystal fragments at base of bed and the lensoid nature of narrow pumice-rich internal layers. From Bailes and Syme (1989).

size of plagioclase crystal fragments, is continuous across the pumice strata.

The tuff is andesitic in composition (56.3% $SiO_2$, average of six analyses calculated volatile-free) and is characterized by high contents of $K_2O$, $Na_2O$ and $Al_2O_3$. It also has elevated $P_2O_5$ and $TiO_2$. The LIL elements, which are all in relatively high concentrations in this unit, were mobile during seafloor alteration and metamorphism. Limited data from this unit (serial samples through three beds in the lower, middle and upper part of the sequence) indicate that all of the tuff is similarly characterized by high LIL element, $P_2O_5$ and $TiO_2$ concentrations. This compositional homogeneity suggests that the abundance of these elements approximates primary values. If this is true, the andesitic magma approached an alkalic character and the unit is better termed trachyandesite.

**Interpretation**

The local exceptional state of preservation and well-defined stratigraphic setting of the Vick Lake andesitic tuff permit important constraints to be placed on any model for the origin of this unit. These constraints include:

1) The unit was deposited upon a subaqueous lava plain (Two Portage Lake ferrobasalt).

2) The thickness of the Vick Lake tuff (900 m) indicates deposition in a large, deep basin.

3) Ash morphology, with shard boundaries controlled largely by fracture surfaces, indicates an eruptive style which was dominated by a phreatomagmatic component (cf. Heiken, 1972; Heinrichs, 1984). This type of eruption can occur only in relatively shallow water or subaerial conditions.

4) The presence and abundance of pumice, in ash to block-size fractions, indicates that eruptions also had plinian components, again emphasizing a very shallow water or subaerial environment.

5) Bouma organization of beds indicates that the pyroclastic material was deposited from turbulent subaqueous density currents.

6) The absence of welding is consistent with both a

phreatomagmatic eruption mechanism and deposition from subaqueous density currents.

7) The absence of interbeds of extraneous sedimentary or volcanic material indicates that the eruptions were closely spaced in time.

8) The general upward fining of the sequence, and gradual increase and ultimate dominance of pelagic sedimentary components in the upper 180 m of the unit indicates a gradual cessation of pyroclastic volcanism, with eruptions becoming more widely spaced and smaller in volume of ejected material.

9) The presence of thick beds (up to 19 m) indicates proximity to source vents.

10) The presence of primary amphibole phenocrysts and near alkalic bulk compositions is consistent with high volatile contents in the magma, and explosive eruption styles.

11) The absence of exotic clasts or particles in the tuff beds indicates that there was virtually no mixing of the pyroclastic material with foreign detritus.

A model which is consistent with the above constraints (Fig. 17) is similar to that proposed by Heinrichs (1984) for an Archean volcaniclastic turbidite deposit. Shallow water or subaerial phreatomagmatic and plinian eruptions produced ash, pumice and crystal fragments which entered the water column from base surges, pyroclastic flows(?) and fallout. The absence of exotic fragments suggests immediate

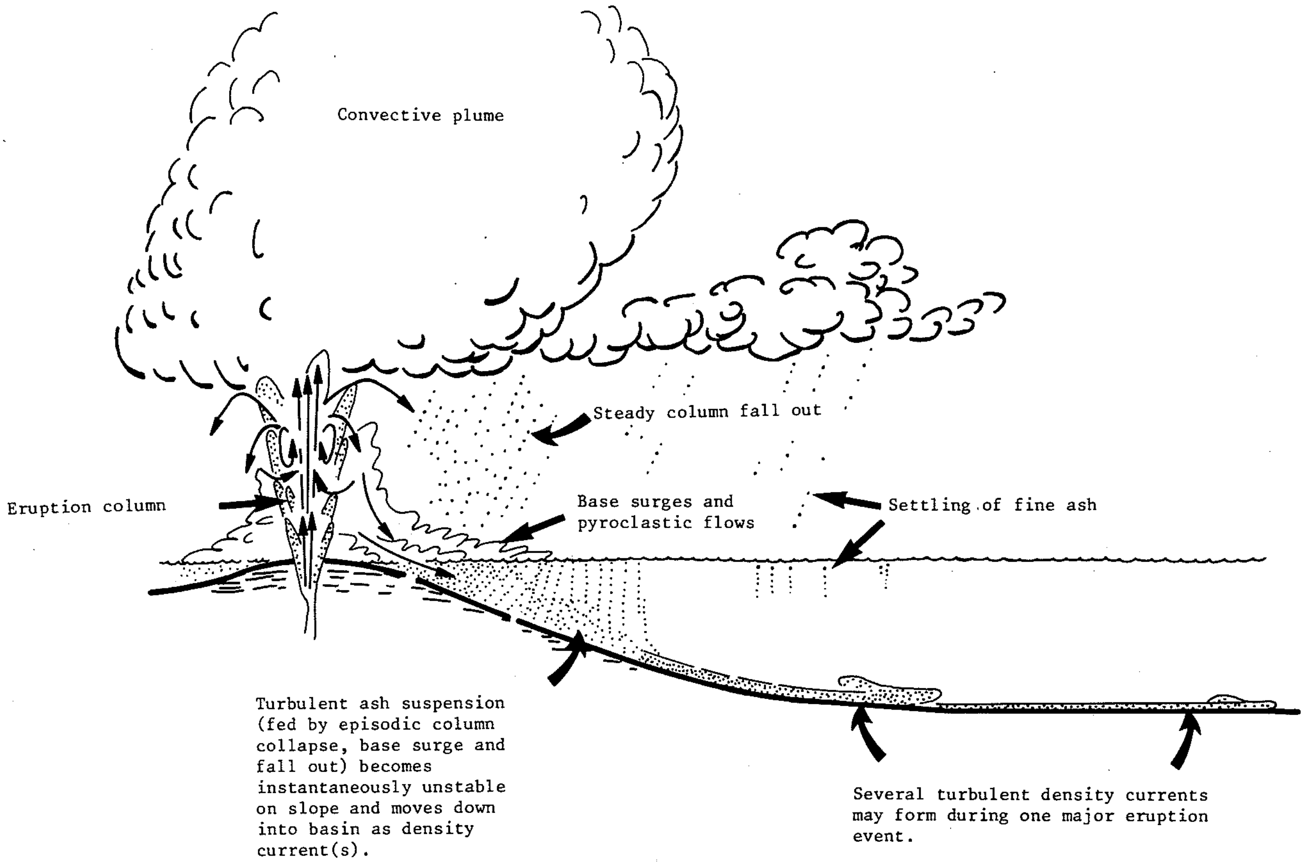


**Figure 17: Model for eruptive mechanism and depositional environment of Vick Lake andesitic tuff. Diagram from Bailes and Syme (1989), after Heinrichs (1984).**

gravity flow transport of these pyroclastic materials from the flanks of the subaqueous portion of the cone into the adjacent deeper water basin. Similarly the gravity flows are not considered to have been initiated as lahars, mudflows, landslides nor subaqueous slumps of more or less consolidated material. In this model a number of individual beds may have been deposited during a single eruption event. The entire deposit represents a large number of eruption events relatively closely spaced in time; the white, very fine grained tuff E division layers probably represent settling of the finest ash through the water column between eruptions. Rare sedimentary units represent longer quiescent periods during which pelagic shales and cherts were also deposited. As the andesitic pyroclastic volcanism waned, increasing proportions of pelagic graphitic shales were deposited between eruptions.

At the outcrop to be examined, a series of thin beds shows features typical of the entire unit:

a) erosional features: Shallow scours with high width to depth ratios occur at the base of many beds.

b) flame structures: Many flames show apparent opposing transport directions and are exceptionally long. One interpretation of these unusual structures is that the transport direction is approximately perpendicular to the outcrop surface.

c) grading: Grading, defined by an upward decrease in size of plagioclase crystal fragments, is continuous from base to top of beds. Note that the grading is continuous across the pumice granule strata, indicating that the pumice layers are integral parts of the beds and do not represent separate depositional events.

d) pumice strata: Pumice-rich strata occur within the graded A division of many beds. These strata vary from 1 mm to 5 cm in width and are composed of pumice granules up to 1 cm in maximum dimension. Primary vesicularity (less than 0.5 mm) in the pumice granules is barely visible in some of the larger fragments. The thinner pumice strata are discontinuous along strike; thicker pumice strata (5 cm) are continuous along strike for at least 5 m and show only minor variations in thickness.

e) parallel laminations: Weakly laminated tuff forms the topmost B division of many beds.

**STOP 8: RHYOLITE FLOWS, BAKERS NARROWS CAMPGROUND.**

Two morphologic types of rhyolite flow occur in the Amisk Group. The first, exemplified by Flin Flon Mine rhyolite (STOP 2), is massive, commonly flow banded, with a flow top autoclastic breccia composed of rhyolite slabs in a granular felsic matrix. The second type is more common, and is composed of massive rhyolite lobes in a matrix of felsic microbreccia/hyaloclastite. This second type is identical to rhyolite flows described from the Archean (de Rosen-Spence et al., 1980) and Cenozoic (Furnes et al., 1980).

Solodiuk Lake rhyolite, stratigraphically associated with massive sulphides at Cuprus and White Lake (Fig. 12), is a lobe-and-microbreccia flow sequence. Because Solodiuk Lake rhyolite is inaccessible, a morphologically similar rhyolite flow at Bakers Narrows will be examined to complete the tour of the stratigraphic package hosting the massive sulphides.

STOP 8 consists of two separate outcrops in Bakers Narrows Provincial Recreation Park, located off Highway 10, 2 km east of Flin Flon airport. The Campground rhyolite is more than 420 m thick, comprising a core of massive aphyric rhyolite, and basal and upper zones of massive rhyolite lobes in rhyolite microbreccia matrix (Syme, 1988). At the first outcrop to be examined, both lobes and microbreccia are well exposed. Lobes of massive white rhyolite are centimetres to metres thick, elongate, irregular, with flow-banded margins and, locally, rinds that have partially to completely spalled into the microbreccia matrix. Contacts with microbreccia are dominated by irregularities, brecciation of lobe margins, and bifurcation of larger lobes into smaller lobes. The microbreccia is darker weathering, fine grained, moderately foliated and felsic in composition. Well defined pumice clasts are preserved in some portions of the microbreccia, and small lithic rhyolite clasts and granules are widespread. Spherulites up to 1 cm in diameter have developed locally where the formerly glassy microbreccia devitrified; generally these spherulitic zones are spatially associated with massive rhyolite lobes.

On the second outcrop, a large lobe of massive white rhyolite contains well-defined flow bands. The bands are <1 - 4 cm thick, parallel to the margin of the lobe and the contact with darker weathering, fine grained, felsic hyaloclastite.

The Campground (and Solodiuk Lake) rhyolite contains many of the structures and relationships described by Furnes et al.(1980) in a Cenozoic subglacial (subaqueous) rhyolite complex in Iceland. The Icelandic microbreccia comprises two phases also found in the Campground rhyolite. The first is pumiceous and is considered by Furnes et al. (1980) to have been produced by violent magmatic explosive events. The second phase is composed of obsidian and lithic rhyolite granules derived directly from break-up of rhyolite lava by a continuous process of construction and destruction (by quenching and thermal fragmentation) of massive lobes.

**STOP 9: SCORIA-RICH MAFIC TUFF, HOOK LAKE BLOCK**

This stop will emphasize the components and bedforms of a pyroclastic unit quite different from Vick Lake andesitic tuff (STOP 7). The mafic tuff and breccia at this location has characteristics indicating that the pyroclastic material was erupted in a subaerial or very shallow water environment, and deposited in a subaqueous environment. Vick Lake tuff, with ubiquitous turbidite bedforms, was deposited in a deep basin. This unit was probably deposited in much shallower water, very close to the source vent.

The rocks to be examined are part of a distinctive, 300 m thick unit comprising intercalated pillowed basalt flows, scoria tuff and pillow fragment breccia (Fig. 11). This area lies within the subgreenschist (prehnite-pumpellyite) zone of metamorphism and the rocks are unfoliated; consequently structures and textures are exceptionally well preserved. The pyroclastic rocks and excellent state of preservation are typical of a much thicker (3 km) multicomponent pyroclastic sequence exposed to the south (Syme, 1988).

In the area of most continuous exposure (Fig. 18), located 520 m east of the south end of Manistikwan Lake (Fig. 11), this unit comprises 50% flows, 30% scoriaceous tuff and 20% pillow fragment breccia. The pillowed flows are 2 - 40 m thick, and contain 5 - 30% plagiolase phenocrysts and 1 - 5% pyroxene phenocrysts (Fig. 18). Some flows abruptly terminate in the exposed section. Pillow fragment breccia is directly associated with two of the flows; amoeboid pillow breccia is absent. Amygdales range in size up to 6 mm but vary in size and abundance between flows and between pillows in a single flow. Pillow fragment breccia beds are 3 - 5 m thick, contain fragments to 20 cm, and include both monolithologic and heterolithologic types. Monolithologic breccias can in some instances be shown to contain fragments identical to the directly underlying basalt flow. Breccia beds have fragment-supported bases and matrix-rich tops but do not display normal size grading.

The distinctive component of this unit is scoria-rich tuff and lapilli tuff. Scoria tuff beds (15 cm - 13.4 m) are typically less than 5 m thick. Beds less than 1 m thick display normal grading with respect to plagioclase crystal size. They are A and, less commonly, AB types, and have basal scours. Beds thicker than 1 m are commonly reverse to normally graded with respect to plagioclase crystal size (Fig. 19). They include

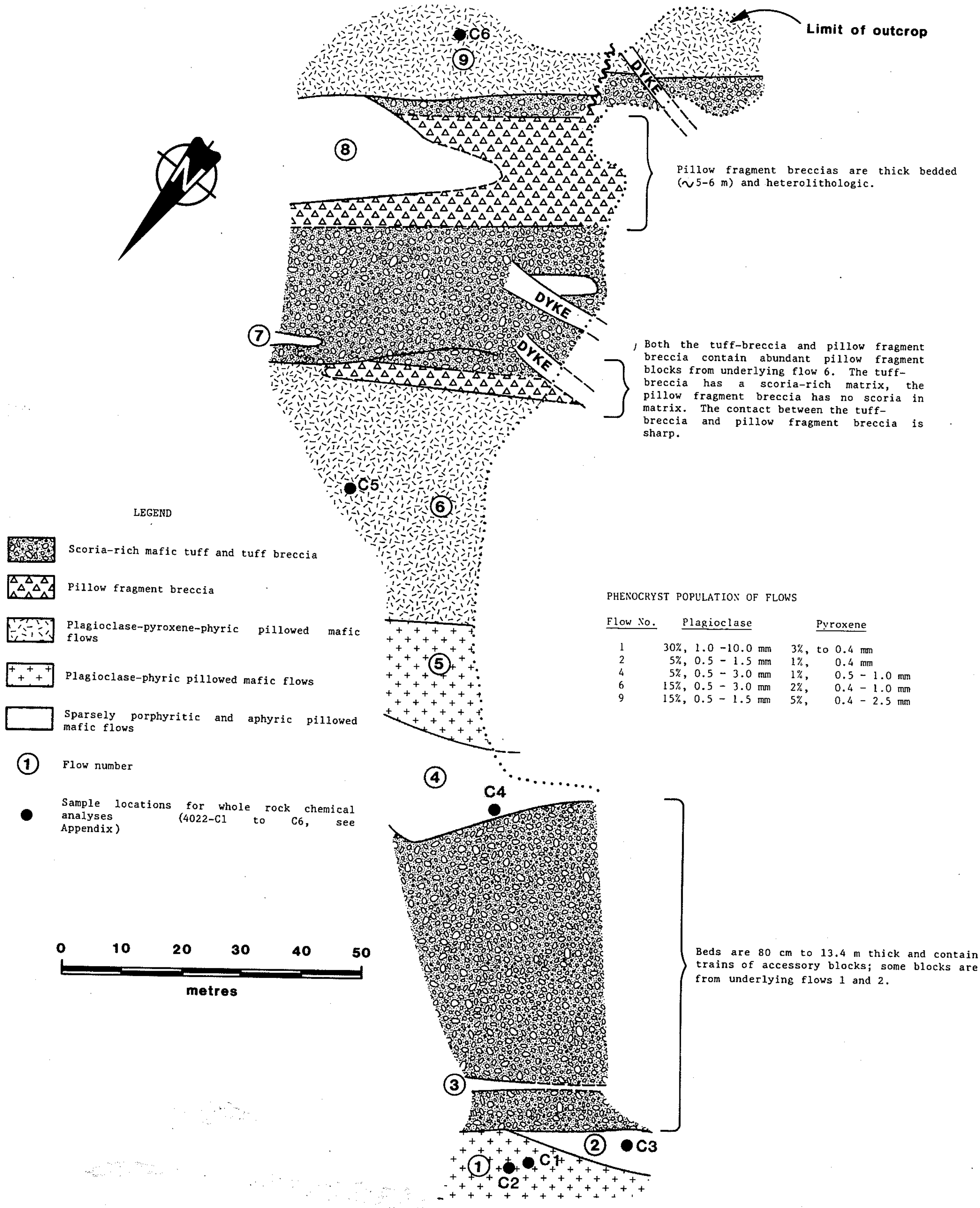


PHENOCRYST POPULATION OF FLOWS

| Flow No. | Plagioclase | Pyroxene |
|---|---|---|
| 1 | 30%, 1.0 -10.0 mm | 3%, to 0.4 mm |
| 2 | 5%, 0.5 - 1.5 mm | 1%, 0.4 mm |
| 4 | 5%, 0.5 - 3.0 mm | 1%, 0.5 - 1.0 mm |
| 6 | 15%, 0.5 - 3.0 mm | 2%, 0.4 - 1.0 mm |
| 9 | 15%, 0.5 - 1.5 mm | 5%, 0.4 - 2.5 mm |

**Figure 18: Stratigraphic sequence in the area of STOP 9, Hook Lake Block. Geology modified from Corkery (pers. comm., 1983). From Bailes and Syme (1989).**

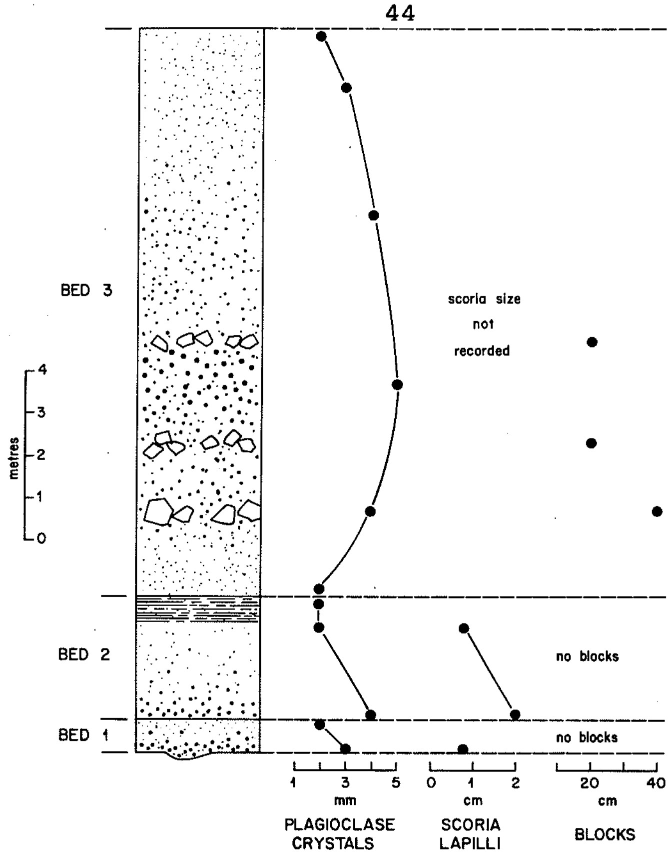


Figure 19: Grading displayed by three scoria tuff beds, STOP 9. Maximum sizes of plagioclase crystals, scoria lapilli, and accessory blocks are shown. Bed 1 is normally graded A type, bed 2 is normally graded AB type, and bed 3 is reverse to normally graded with three crude layers of blocks. The latter are accessory fragments derived from pillowed flows lower in the sequence. From Bailes and Syme (1989).

A and AB types, and in some instances contain "trains" of accessory blocks (Fig. 19). The occurrence of scoria in Bouma-zoned beds intercalated with pillowed basalt indicates the pyroclastic material was transported and deposited by subaqueous density currents.

Scoria particles range in size from about 1 mm to 6 cm. The primary vesicularity and grain shapes of scoria are well preserved (Fig. 20). Scoria grains are framework supported with vesicles and inter-particle voids filled predominantly with carbonate.

The shapes of scoria particles are controlled by a combination of vesicle walls, fracture surfaces, and chilled droplet margins (Fig. 20). Vesicle-controlled margins are highly scalloped where vesicles are large, and less scalloped where vesicles are small. Fractures at particle margins are of two types: short fractures occur at points of weakness between adjacent vesicles and longer, planar fractures cut through several vesicles. Droplet margins are smooth or wrinkled and display no scalloping or fracture surfaces. Tiny vesicles (less than 0.1 mm) occur to outermost parts of droplet margins. The particles are interpreted to have been produced during explosive subaerial magmatic eruptions, probably on a small volcanic island. During eruptions, rapidly vesiculating magma droplets in the eruption column were probably fragmented by internal gas pressure. Many of these hot vesiculated fragments may have been subsequently broken by thermal shock on contact with seawater.

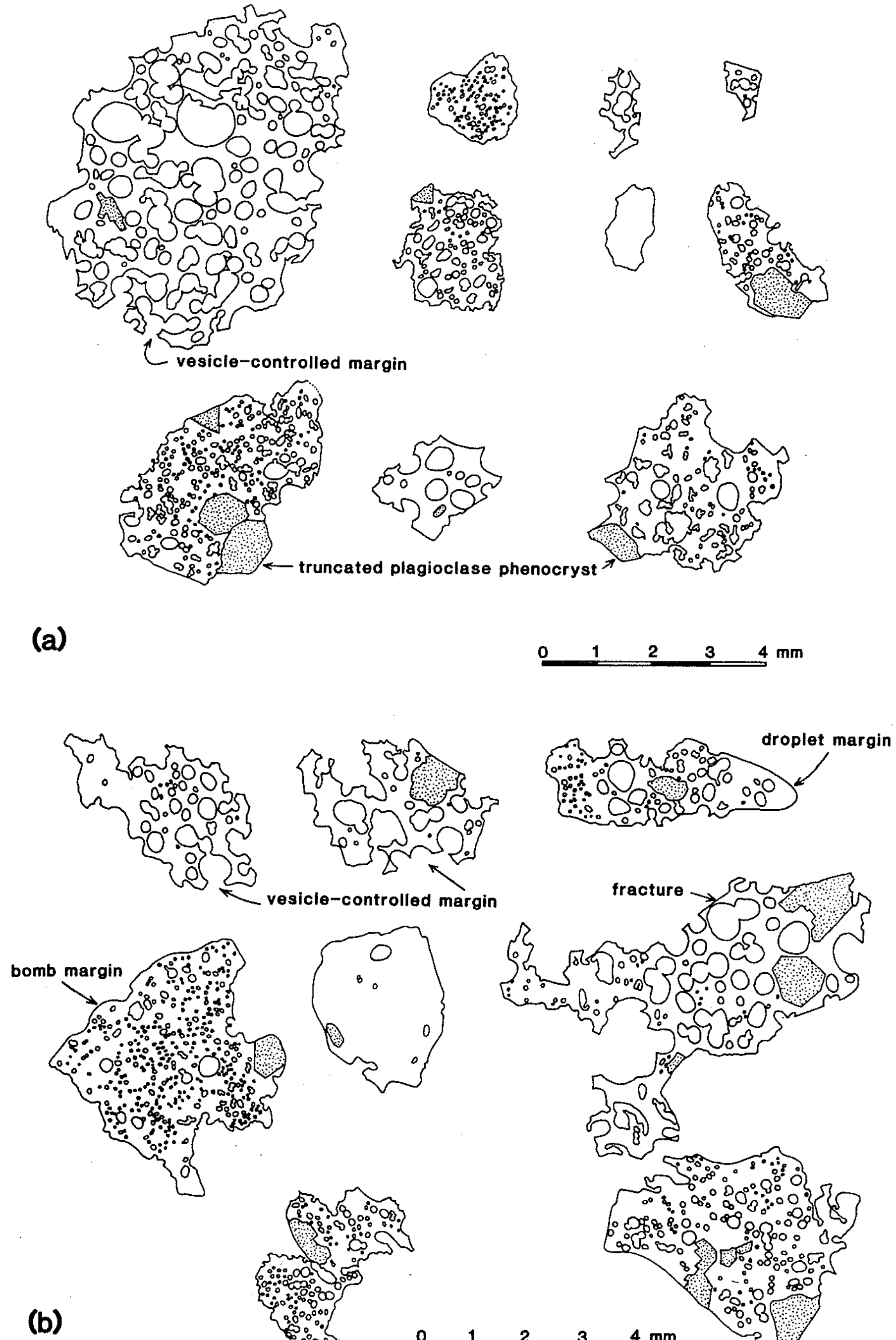


Figure 20: Tracings of scoria particles in scoria-rich mafic tuff, Stop 9. Scoria particles have predominantly vesicle-controlled margins; some are partly bounded by fractures or chilled droplet margins. (a) from 6 m above base of bed 3, Fig. 16. (b) from 1.5 m above base of bed 2, Fig. 16. From Bailes and Syme (1989).

The accessory blocks (Fig. 19) are interpreted to be ballistic fragments. Individual blocks are angular, up to 40 cm across, and are fragments of amygdaloidal pillowed basalt that can be precisely matched to specific flows lower in the sequence. The blocks commonly occur in discontinuous "trains" (1 block thick) and as isolated fragments; both "trains" and isolated blocks can occur at any level within a tuff bed (e.g. Fig. 19). Blocks also occur in thin beds where, in some instances, they have depressed bedding contacts or laminae. The blocks are much larger and denser than the matrix scoria and were clearly not in hydraulic equilibrium with the density current that deposited the scoria. Evidence indicates that the ballistic fragments were incorporated into the scoria density flows as the density flows were in the process of being deposited. The accessory blocks may have been torn from vent walls by periodic phreatic explosions which punctuated the dominantly magmatic eruptions.

At this Stop a line has been flagged which lies within and adjacent to the area shown on figure 18. The flagged line begins at pillowed flow 1 and terminates in the pillow fragment breccia associated with pillowed flow 8. Features to be observed include bedforms and texture of scoria tuff, accessory blocks in the tuff (compare the textures in these blocks to the pillowed flows low in the sequence), variation in pillowed flow type, and characteristics of pillow fragment breccia (compare with scoria tuff).

# Snow Lake Area: General geology and Ore Deposits

## Geological Setting

### Introduction

General geology of the portion of the Snow Lake area to be examined during this field trip is shown on figure 21. Descriptions of geology of this area are given by Harrison (1949), Russell (1957), Froese and Moore (1980), Walford and Franklin (1982), Bailes (1987, 1988) and Bailes and Galley (1989). The Amisk Group in this area differs from that at Flin Flon in that it contains substantial thicknesses of felsic volcanic rocks, large portions are hydrothermally altered, synvolcanic tonalite plutons are common, and it includes a thick sequence of volcanogenic greywacke turbidites. The greywackes are stratigraphically equivalent to more highly metamorphosed paragneisses of the Kisseynew belt (Froese and Moore, 1980; Bailes, 1980). The Missi Group is similar to that at Flin Flon, but east of Wekusko Lake it also includes subaerial and subaqueous volcanic rocks including some felsic welded ash flows (Gordon and Gall, 1982). The supracrustal rocks at Snow Lake have been isoclinally folded and subsequently refolded about the northeast-trending Threehouse syncline. Metamorphic grade is higher than at Flin Flon and ranges from lower to upper almandine-amphibolite facies. Late north-trending faults postdate folding and regional metamorphism and offset fold axial traces and east-trending metamorphic reaction isograds.

### Amisk Group

Between the Berry Creek fault and the McLeod Road Thrust (Fig. 21), the Amisk Group comprises approximately 6 km of north-facing, subaqueously-deposited rocks, broadly folded by the northeast-trending Threehouse syncline and related folds. South facing strata are restricted to a fault-bounded slice in the vicinity of the Linda deposit and to the north limb of the NW-trending Ghost Lake syncline. Approximately 1 km of Amisk Group rocks occur north of the McLeod Road Thrust; their stratigraphic position relative to Amisk rocks south of the fault is not known.

The Amisk Group between the Berry Creek fault and the McLeod Road Thrust contains six main subdivisions (Fig. 22). The first, and lowermost, consists of over 3 km of pillowed aphyric to sparsely porphyritic basalt, basaltic andesite and andesite flows (e.g. Welch Lake basalt), within which there are local domes of aphyric to sparsely quartz phyric rhyolite (e.g. Daly Lake rhyolite). Overlying the mafic platform is a diverse suite of volcanic rocks that includes thick bedded felsic and mafic heterolithologic breccia (e.g. Stroud Lake felsic breccia, Lower Mine Felsics and Edwards Lake mafic heterolithologic mafic breccia), and subaqueously deposited felsic and porphyritic mafic flows (e.g. Snell Lake basalt). This second group of rocks is in turn overlain by up to 1 km of mafic to felsic volcanic flows characterized by high incompatible element and elevated light REE abundances, combined with low Ni and Cr and elevated Th and U (e.g. Moore-Powderhouse-Ghost sequence). The fourth subdivision consists of mafic tuff, lapilli tuff, tuff breccia and related porphyritic basalt flows (e.g. Chisel basin mafic tuff, Threehouse basalt). These latter rocks are important in that they form the stratigraphic hanging wall to most of the major base metal deposits in the Snow Lake area, and they also do not display the ubiquitous hydrothermal alteration characteristic of stratigraphically underlying rocks. North of Anderson Lake the Chisel basin-Threehouse sequence is overlain by a fifth group of rocks consisting of aphyric basalt flows and felsic breccias. The sixth subdivision consists of volcaniclastic greywacke-mudstone turbidites that are truncated to the north by the McLeod Road Thrust. Bailes (1980) concluded that the greywacke-mudstone sequence, termed the File Lake formation, was

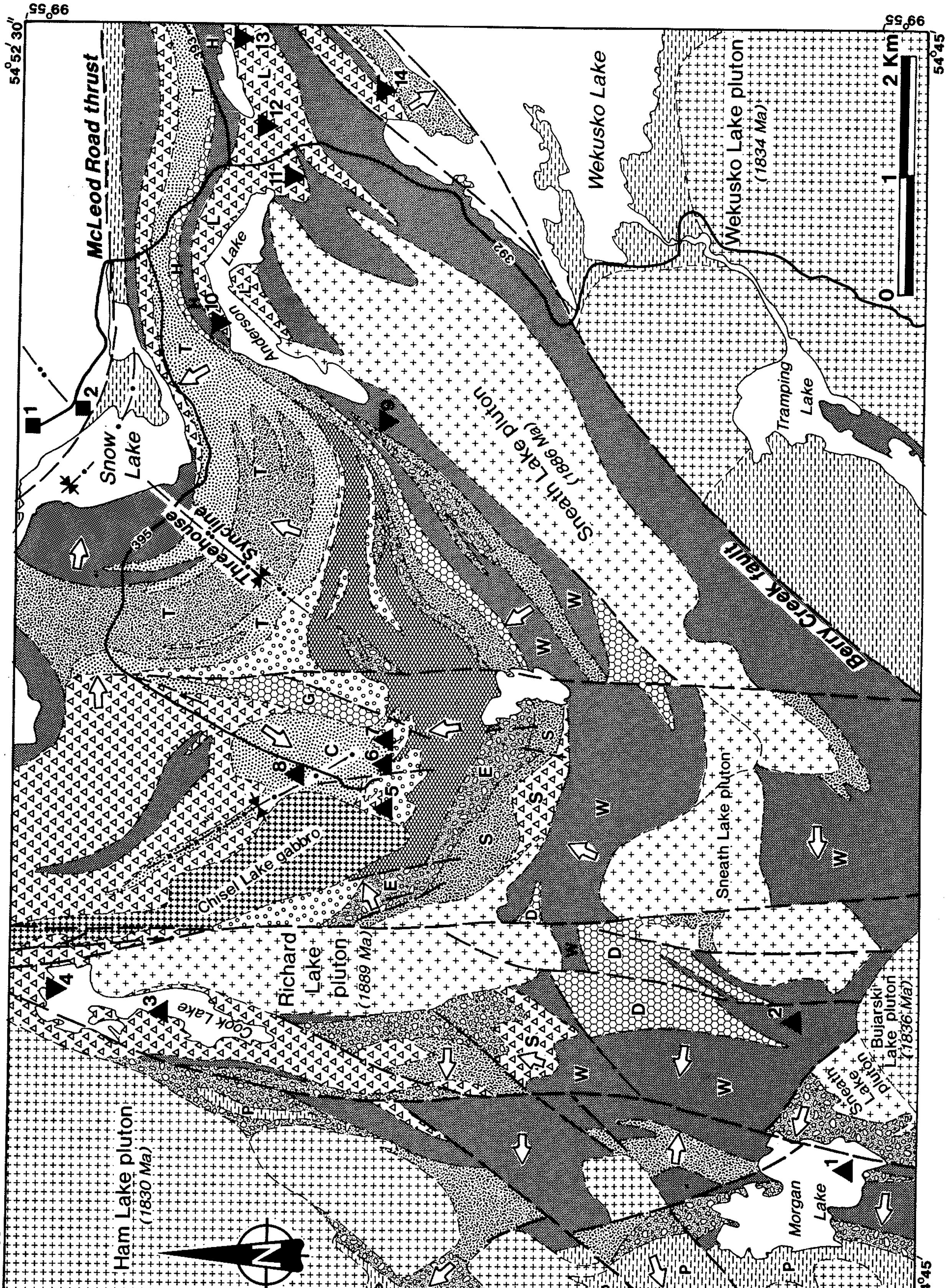

McLeod Road thrust
Snow Lake
Threehouse Syncline
Anderson Lake
Sneath Lake pluton
(1886 Ma)
Berry Creek fault
Wekusko Lake
Wekusko Lake pluton
(1834 Ma)
Tramping Lake
Chisel Lake gabbro
Richard Lake pluton
(1889 Ma)
Cook Lake
Ham Lake pluton
(1830 Ma)
Morgan Lake
Sneath Lake pluton
Bujarski Lake pluton
(1836 Ma)
N
0
1
2 Km
54°52'30"
99°55'
54°45'
100°15'

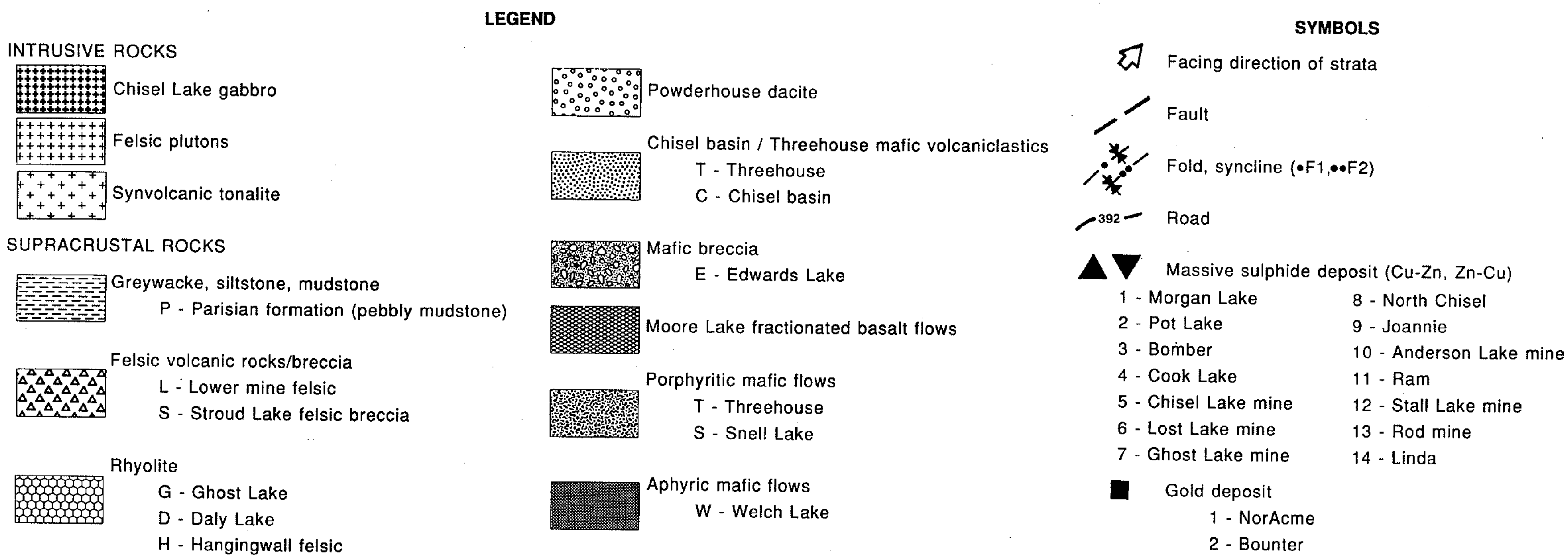


Figure 21: General geology of the Snow Lake area (after Harrison, 1949; Hutcheon, 1977; Froese and Moore, 1977; Walford and Franklin, 1982; Trembath, 1986; Bailes, 1989; Zaleski, 1989)

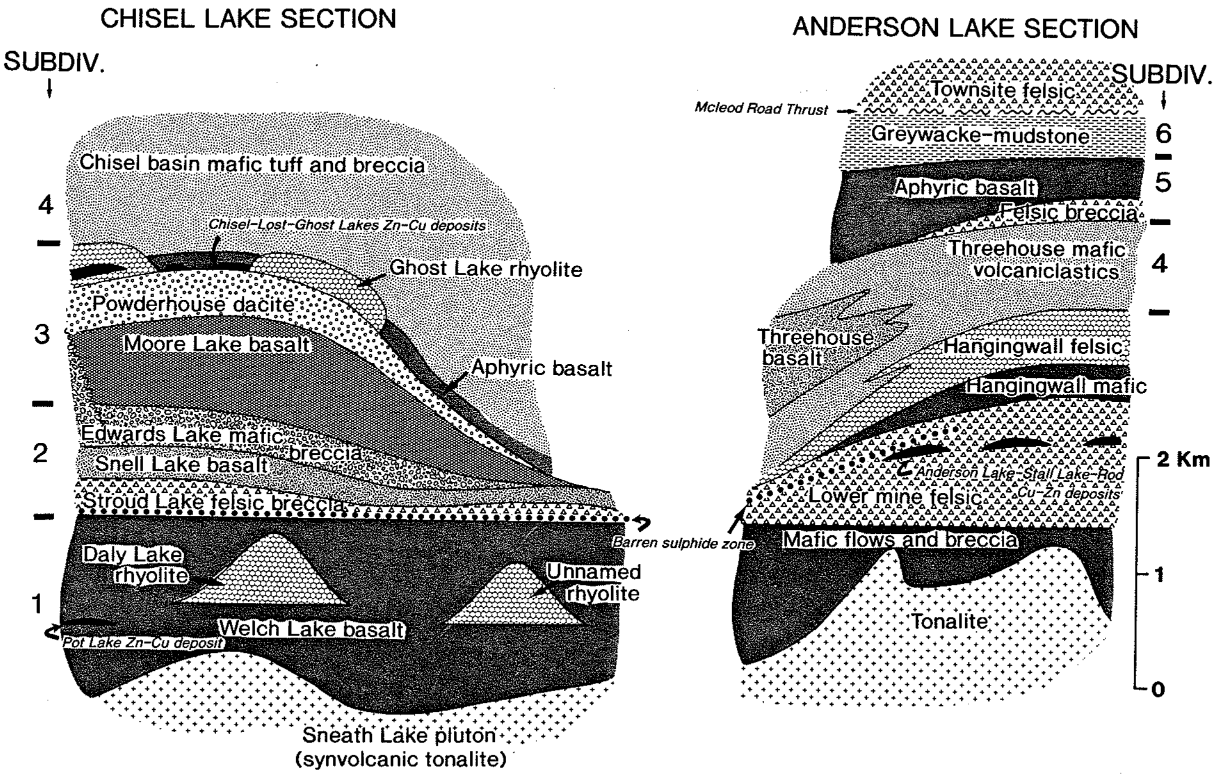


Figure 22: Schematic composite stratigraphic section, Snow Lake area. Chisel Lake section is from Bailes and Galley (1989) and Anderson Lake section is slightly modified from Walford and Franklin (1982). Anderson Lake unit thicknesses are exaggerated to compensate for greater tectonic flattening of units at Anderson Lake relative to those at Chisel Lake

part of a submarine dispersal system that is composed mainly of unconsolidated felsic volcanic detritus eroded from Flin Flon belt volcanoes.

Detailed mapping of the Amisk group is available in the vicinity of the major base metal mines at Chisel Lake (Williams, 1966; Walford and Ziehlke, 1972 and 1982, unpublished H.B.E.D. mapping; Skirrow, 1987; Skirrow and Franklin, 1989; Bailes and Galley, 1989) and at Anderson Lake (Hutcheon, 1977; Walford and Franklin, 1982; Trembath, 1986; Zaleski, 1989). Stratigraphic subdivision of the Amisk Group in these two localities is covered more fully with the descriptions of base metal deposits and their host rocks.

**Missi Group**

The Missi Group in the Snow Lake area is a monotonous sequence of metamorphosed lithic arenites (Froese and Moore, 1980). Conglomerate, although characteristic of the Missi Group in the Flin Flon area, is notably lacking in the Snow Lake area. East of Wekusko Lake conglomerate does occur, as well as trough cross-bedded fluviatile sandstones.

Missi volcanic rocks are not present near Snow Lake but form a substantial part of the Missi Group east of Wekusko Lake. These felsic volcanic rocks have a U-Pb zircon age of 1832 +/-2 Ma (Gordon et al., 1990). Within experimental error, this is coeval with several post-Amisk intrusions in the Snow Lake area. An Amisk Group rhyolite crystal tuff from the Flin Flon area gives a U-Pb zircon age of 1886 ± 2 Ma suggesting that there is a considerable time gap between deposition of the Amisk and Missi Groups.

**Intrusive Rocks**

Amisk Group volcanic rocks are cut by a wide variety of dykes, sills and small intrusions that are not present in the turbiditic greywacke suite at the top of the Amisk Group nor in the overlying Missi Group. Most of these smaller intrusions are considered to be synvolcanic; this is supported by geochemical similarity of some intrusions with stratigraphically overlying extrusive equivalents and by absence of many of these intrusions in younger volcanic sequences.

The Amisk Group is also cut by a variety of felsic plutons ranging from synvolcanic tonalite to post-tectonic granite (Fig. 21). There are two major synvolcanic tonalite plutons, the Sneath Lake and Richard Lake plutons. Sneath Lake tonalite is a broadly folded semiconformable body 1.5 km wide and over 14 km long. It has a U-Pb zircon age of 1886 +17/-9 Ma (Bailes et al., 1990). The pluton stratigraphically underlies the major base metal sulphide deposits of the Snow Lake area (Fig. 21 and 22) and is considered by Walford and Franklin (1982) and Bailes (1986) to be the "heat engine" which drove the hydrothermal system producing sulphide deposits and associated alteration. The intrusion is a multi-component body, composed largely of equigranular tonalite but locally of coarsely quartz-phyric varieties. Much of the intrusion is altered, largely through the addition of Fe and Mg along fractures in a rectlinear grid pattern but also by Fe and Mg addition along irregular anastomosing alteration veinlets (Bailes, 1986; Trembath, 1986). South and west of Anderson Lake the intrusion has hydrothermal alteration with minor pyrite and chalcopyrite in microfractures (Walford and Franklin, 1982).

The synvolcanic Richard Lake tonalite is 1.7 by 7.3 km in size and cuts across 3 km of Amisk Group stratigraphy and across a series of hydrothermal alteration zones. A sample from the pluton has a U-Pb zircon age of 1889 +8/-6 Ma, and is therefore considered syn-Amisk (Bailes et al., 1988). The pluton is composed of quartz megacrystic and equigranular tonalite similar to the Sneath Lake tonalite but the two plutons are chemically distinct and are not co-magmatic (Bailes et al., 1988). The Richard Lake pluton is locally cut by zones of Fe-Mg metasomatism but the general level of alteration is significantly lower than that displayed by the Sneath Lake pluton.

Post-Amisk granitic plutons do not contain the distinctive hydrothermal alteration displayed by the synvolcanic tonalite intrusions and are generally much less foliated and deformed. Some of these intrusions are probably coeval with Missi volcanism (Gordon et al., 1987) whereas others are likely late- to post-tectonic (Cerny et al., 1981).

An 1800 by 4500 m tear-shaped differentiated mafic intrusion (Chisel Lake gabbro) cuts the Chisel Lake orebody (Fig. 21). This intrusion is zoned from peridotite at the margin to diorite at the centre. It is a funnel-shaped body which tapers at depth. It is considered to postdate regional metamorphism and to be late tectonic (Ayres and Young, 1989).

**Structure**

The structure of the Snow Lake area is dominated by two folding events (Froese and Moore, 1980). The earliest fold phase resulted in isoclinal structures with a prominent axial plane schistosity. The second fold phase is represented by the shallow northeast-plunging Threehouse syncline. A second schistosity is developed axial planar to this fold, and a prominent linear fabric defined by deformed clasts and elongate minerals plunges parallel to its axis.

**Metamorphism**

Metamorphism began during the early fold phase, continued through the second fold phase, and reached a thermal peak after most of the second phase of deformation had occurred (Froese and Moore, 1980). It occurred after deposition of the Missi Group (1832 +/-2 Ma) and continued to approximately 1800 Ma (Gordon et al., 1990). The P-T conditions of the peak metamorphic event are estimated by Froese and Moore (1980) to be approximately 5 kb and 550-650°C; garnet-biotite geothermometry of an Anderson mine area sample by Trembath (1986) gives a temperature of 530° ± 10°C. Sphalerite geobarometry combined with an analysis of stable metamorphic mineral phases for samples from the Linda deposit by Zaleski (1989) gives 5 kb pressure and 550°C temperature for the peak metamorphism. Despite high grade metamorphism, primary features, such as bedding, pillows, amygdales, etc., are preserved. Sulphide ores and their associated hydrothermal alteration zones, however, show a spectacular coarsening of grain size relative to those at Flin Flon. Large crystals of kyanite, staurolite, garnet, cordierite, anthophyllite, plagioclase, biotite and muscovite are prominent making this a classic area for studying effects of metamorphism on footwall alteration zones.

## Base Metal Deposits

**Introduction**

Snow Lake area contains six producing and past-producing base metal mines, and several undeveloped or partially developed deposits (Fig. 21). Most have closely associated footwall hydrothermal alteration zones and are thus proximal volcanogenic massive sulphide (VMS) deposits. The deposits occur at several levels within the over 6 km thick Amisk section and thus here, as at Flin Flon, there was more than one mineralizing event. The Pot Lake Zn-Cu deposit is associated with the Daly Lake rhyolite flows within the Welch Lake subaqueous basalt flows in the lower part of the Amisk section (Fig. 21 and 22) whereas the Stall, Rod, Ram, Linda and Anderson Cu-Zn deposits are associated with the Lower Mine felsic volcanic rocks in the central part of the Amisk section (Fig. 22). The Chisel, Ghost, Lost and North Chisel Zn-Cu deposits occur slightly higher in the section at the base of the Chisel basin/Threehouse mafic tuff-lapilli tuff unit and are associated with rhyolite flows that are part of a distinctive mafic to felsic fractionated cycle (Moore-Powderhouse-Ghost sequence, Fig. 22). Lead isotope data on the Anderson-Stall-Rod Cu-Zn and the Chisel-Ghost-Lost-North Chisel Zn-Cu sulphide deposits indicates a separate metal source for these two mineralizing events (Walford and Franklin, 1982).

**Controls on Base Metal Deposits**

Mafic volcanic rocks in the Snow Lake area display arc tholeiite chemistry and are similar to basalt and basaltic andesite sequences that host base metal deposits at Flin Flon (Syme, 1990). Both the Snow Lake and Flin Flon mafic lavas are enriched in LIL (light ion lithophile) elements and moderately to strongly depleted in HFS (high field strength) elements, a feature characteristic of subduction related magmas (Saunders et al., 1980; Gill, 1981; Tarney et al., 1981). The base metal deposits also share a number of stratigraphic associations in common with other Flin Flon belt base metal deposits:

1) they are spatially associated with fractionated ferrobasalts similar to those associated with the Cuprus Lake and White Lake base metal deposits of the Flin Flon area;

2) they are at the same stratigraphic position as major felsic complexes, an association they share with almost all significant base metal deposits in Flin Flon belt (Bailes and Syme, 1989), as well as those in many major Precambrian base metal camps (Franklin et al., 1981);

3) they are associated with discordant zones of alteration that are generally considered to be sited on synvolcanic faults (Walford and Franklin, 1982; Zaleski, 1989).

**Alteration**

One of the features that distinguishes base metal deposits in the Snow Lake area from those of the Flin Flon area is the much greater volume of hydrothermally altered rocks in their stratigraphic footwall. Bailes (1987) estimates that between 10 and 20 percent by volume of all footwall supracrustal rocks and synvolcanic tonalite plutons are altered; this represents approximately 30 square kilometres of footwall rocks that have recognizable alteration. The alteration includes Fe-Mg metasomatism, silicification/albitization, and minor epidotization and pyritization. Alteration occurs in small discordant zones ("pipes") directly below massive sulphide deposits and in larger regionally disposed semiconformable zones. The general character of these two types of alteration zones is briefly discussed below, with more details given elsewhere for those deposits that are to be examined during the field trip.

Discordant "pipe-like" zones of alteration are reported beneath the Chisel Lake Zn-Cu deposit (Galley and Bailes,1989; Bailes and Galley, 1989), the Anderson Lake Cu-Zn deposit (Walford and Franklin, 1982: Trembath, 1986), the Stall Cu-Zn deposit (Studer, 1982), the Rod Cu-Zn deposit (Coats et al., 1970) and the Linda Cu-Zn deposit (Zaleski, 1989). The alteration pipes are characterized by chloritized cores and sericitized peripheries, a feature typical of alteration pipes beneath many volcanogenic massive sulphide deposits (Lydon, 1984). The pipes in the Snow Lake area tend to be a few hundred metres wide, short (less than 1 km), and merge at depth with the semiconformable zones of alteration (Walford and Franklin, 1982; Bailes and Galley, 1989; Zaleski, 1989).

Semiconformable zones of alteration occur in several discrete strata-parallel domains 0.5 to 3 km below the base metal sulphide deposits (Bailes and Galley, 1989). They do not occur in the Chisel basin mafic tuff/lapilli tuff or in the Threehouse basalt that overlie the sulphide deposits, nor have they been observed in strata that underlie the synvolcanic Sneath Lake pluton. The zones vary from 300 to 700 m in width and are up to 12 km in strike length. Most semiconformable alteration consists of silicification/albitization (hereafter referred to simply as silicification) and diffuse Fe-Mg metasomatism. Some semiconformable zones display lateral variation, changing from silicification to Fe-Mg metasomatism with proximity to disconformable "pipe-like" alteration zones and associated sulphide deposits. The semiconformable zones of alteration tend to be restricted to individual formations and to not significantly effect overlying and underlying formations suggesting that hydrothermal fluid flow was conformable.

**Genetic model**

Recent models for formation of volcanogenic massive sulphide deposits attempt to account for four aspects in the development of a hydrothermal system: generation of the metal-bearing fluid, transport of metals to a site of deposition (such as the sea floor), deposition of sulphides on or immediately below this surface (Sangster,1972; Franklin et al., 1981; Lydon, 1984, 1988; Rona, 1988), and localization of fluid flow and subsequent sulphide deposition by synvolcanic structures (Kappel and Franklin, 1989; Watkins and Gibson, 1990). The least understood aspect is the nature of the deep hydrothermal system beneath the deposits where the generation of metal-forming fluids occurs. Understanding of this latter process is limited to a few examples of fossil systems which display alteration (fluid-rock interaction) at this level (eg. MacGeehan, 1978; Gibson et al, 1983; Morton and Franklin, 1987; Skirrow and Franklin, 1989), and observations and inferences from active geothermal systems (e.g. Mottl, 1983; Franklin, 1986). One objective of this field trip is to examine the deeper parts of a large paleo-hydrothermal system in the Snow Lake area with a view to illustrating the relationship of alteration in this portion of the hydrothermal system to the mineralizing process.

The large-scale hydrothermal system and attendant alteration is generally considered to have been driven by heat from synvolcanic tonalite intrusions such as the Sneath Lake and Richard Lake plutons (Walford and Franklin, 1982; Bailes et al., 1987). U-Pb ages of 1889 +8/-6 Ma for the Richard Lake tonalite and 1886 +17/-9 for the Sneath Lake tonalite (Bailes et al., 1990), comparable to a U-Pb age of 1886 +/-2 Ma on an Amisk Group rhyolite tuff (Syme et al, 1987) from Flin Flon, are consistent with this interpretation. The absence of substantive hydrothermal alteration in volcanic rocks overlying base metal sulphide zones in the Chisel Lake and Anderson Lake areas supports a synvolcanic age for the alteration. Similarly the absence of alteration in supracrustal rocks that underlie the Sneath Lake pluton supports the tonalite plutons as having been the "heat engine" that drove the hydrothermal system.

Skirrow (1987) has speculated that silicification, the dominant alteration type in semiconformable (deeper level) portions of the fossil hydrothermal system, may be the source for metals deposited by hydrothermal fluids higher in the system, and further speculated that silicification may have a fairly direct link to deposition of volcanogenic base metal deposits.

## Gold Deposits

### Introduction

Most of the gold mineralization in the Snow Lake region is hosted by VMS deposits and fault-controlled, mesothermal vein systems. Gold is an important byproduct of base-metal mining, with the six producing and past-producing Zn-Cu deposits containing an average of 1.29 g/t Au. The Chisel Lake Zn-Cu deposit averages 2.53 g/t Au (Hudson's Bay Mining and Smelting Co. Ltd. records). These gold concentrations are similar to those recorded in Phanerozoic Zn-Cu-Pb deposits and higher than the average for Archean Cu-Zn deposits (Hannington and Scott, 1990 and references therein). The distribution of gold within the Snow Lake VMS deposits with respect to metal zonation and deposit morphology has been obscured by subsequent deformation, with the gold presently being controlled, in large part, by syn-kinematic structures.

### Structurally Controlled Gold Occurrences

Detailed descriptions of lode gold occurrences are given by Wright (1931), Ebbutt (1941), Harrison, (1949), Russell (1957), Galley et al. (1986) and Fedikow et al.(1989). Most of the major vein-hosted, lode gold deposits are hosted by Amisk Group volcanic rocks. The Squall Lake deposit is the exception, being hosted by mafic igneous rocks interlayered with Missi Group arenite (Harrison, 1949). The Nor-Acme deposit and three other major occurrences (Bounter, Boundary and Main Zone) all lie within 500 m of the surface expression of the McLeod Road Fault and the structurally underlying Amisk greywacke unit (Fig. 23 and 24). The McLeod Road Fault is one of a series of D1 thrust faults that were reactivated after D2 folding and peak metamorphism. The actinolite-biotite-ferroan dolomite assemblage that typifies the fault zone cross-cuts a hornblende-andesine-magnetite assemblage characteristic of the metamorphosed mafic rocks. Within the hangingwall of the McLeod Road Fault the gold occurrences are hosted by a series of smaller faults that either splay from, or are truncated by, the thrust fault. The larger gold zones are localized within the faults where these structures intersect the hinges of D1 folds at a high angle, usually at the contact between lithologies of contrasting competency.

The gold zones are within fault-parallel, 1 to 30 m wide vein breccias in which strongly altered and mineralized wallrock fragments are suspended within a quartz-albite-iron carbonate matrix. Wallrocks within 20 to 100 cm of the veins are strongly foliated and commonly mineralized. Vein-hosted wallrock fragments close to the vein margins

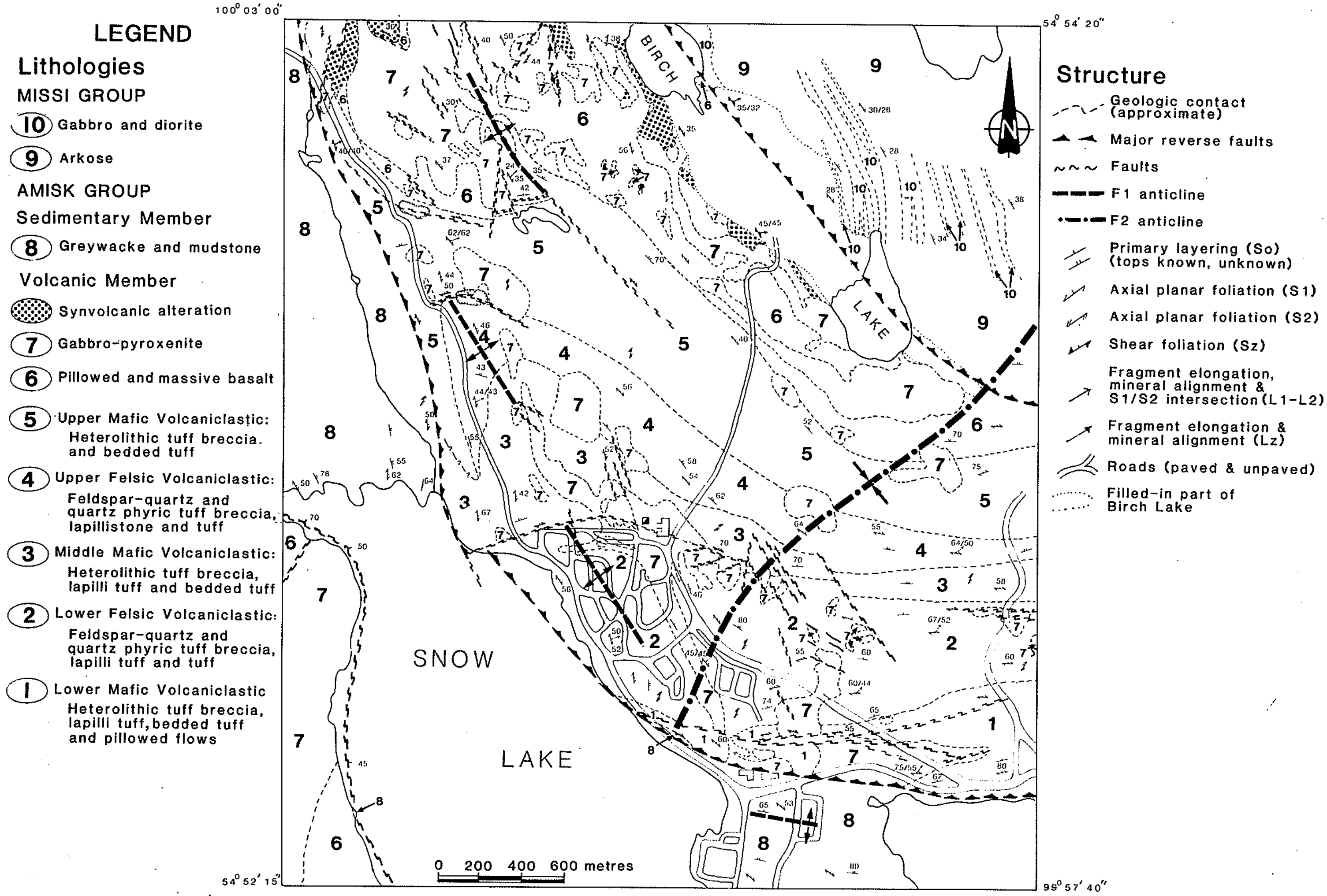


Figure 23: Geology of the Snow Lake area

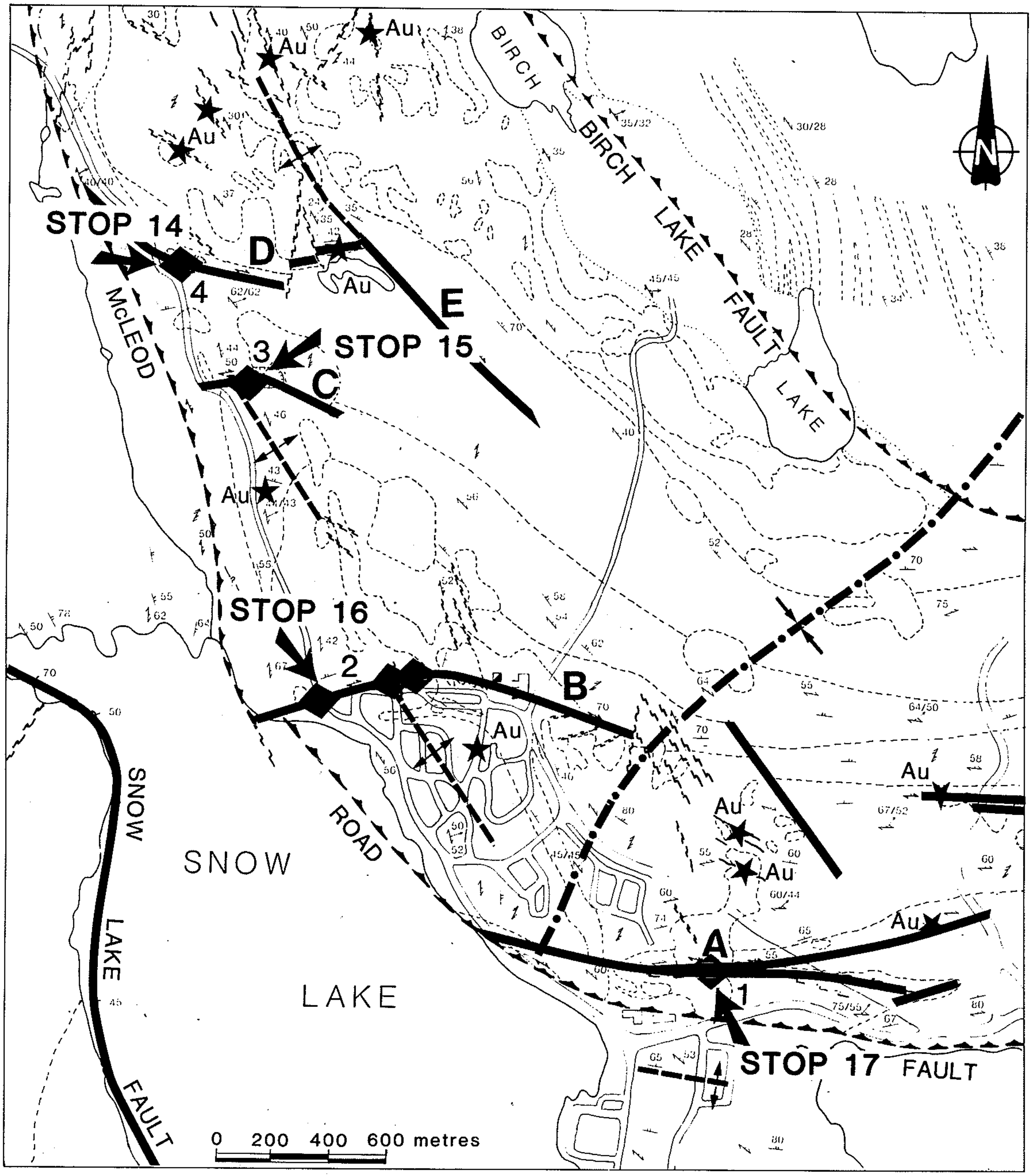


GOLD DEPOSITS & OCCURRENCES

1. Bounter Zone
2. Nor-Acme Mine
3. Boundary zone
4. Main zone

★ Gold occurrences

STRUCTURAL SYMBOLS

Reverse Faults

A. Bounter Fault
B. Howe Sound Fault
C. Boundary Fault
D. Main Zone Fault
E. Median Fault

F1 fold axis

F2 fold axis

Foliations

S1 S2 Sz

Lineations

L1-L2 Lz

Figure 24: Structures and gold occurrences in the Snow Lake area

are deformed, with flattening and transposition giving the vein margin a banded appearance.

The principal sulphide mineral in the gold zones is arsenopyrite; it occurs as fine-grained asicular crystals averaging 1 to 5% of the rock volume. Microscopic examination indicates that 80% of the gold is present as irregular blebs to 20 microns, and is spatially associated with the arsenopyrite. Arsenopyrite crystals are commonly brecciated in-situ by late-stage cataclasism. The carbonate-filled fractures associated with this late-stage, brittle deformation sometimes contain fine-grained gold (Harrison, 1949; Galley et al., 1986). Minor sphalerite and pyrite and pyrrhotite are also present.

Gold zones plunge moderately to the northeast along the fault planes, parallel to the plunge of the regional D2 L-S fabric. The latest period of motion recorded in the fault zones is dip-slip, with a sinistral component, parallel to the plunge of the gold zones. The fault-parallel veins are commonly boudinaged, and secondary veins at a large angle to the main veins are typically buckled, with fold axes plunging parallel to the direction of fault movement.

**Alteration**

Alteration associated with gold mineralization is commonly restricted to the sheared host rocks. One exception is the Nor-Acme deposit, where alteration centered on the host fault extends over 100 m beyond the sheared fault margin. Alteration assemblages in the auriferous faults overprint the regional, lower almandine-amphibolite facies metamorphic mineral assemblages. Different intensities of alteration are represented by the appearance and disappearance of various minerals (Fig. 25a). The resultant assemblages are interpreted to be chemical fronts that originated in the core of the auriferous faults. These fronts are characterized by an increase in potassium, sodium, sulphur, $CO_2$, $H_2O$, boron, tungsten, silver and gold. There is a progressive drop-off in anomalous element concentrations away from the ore zone, with the widest haloes represented by high $H_2O$ and then $CO_2$ (Fig. 25b). At the Nor-Acme deposit there is a well-defined alteration halo that includes the following mineral changes with increased proximity to the mineralized zone:

1. Titanomagnetite --> titanite --> ilmenite --> rutile*

2. Andesine --> andesine-oligoclase --> oligoclase --> albite*

3. Hornblende --> actinolite --> biotite --> chlorite --> sericite*

4. Calcite --> ferroan dolomite --> ankerite*

5. Pyrrhotite --> arsenopyrite-pyrrhotite --> arsenopyrite-pyrite*

* mineral present within the breccia veins

The progressive change in the carbonate species from the prograde metamorphic mineral assemblages through to the core of the gold zones can be observed clearly with the use of a carbonate stain (1 gm Alizarin Red S, 5 gm potassium ferrocyanide, 2 ml 12M HCl; made up to one litre with distilled $H_2O$). The change from calcite to ferroan dolomite and ankerite is typified by a change in the colour of the stained carbonate from red through blue to deep blue.

**Age of Gold Mineralization**

Gold occurrences in the Snow Lake region display features that are typical of epigenetic, mesothermal vein deposits of the Canadian Shield as described by Colvine et al. (1984), Roberts, (1987), Poulsen and Robert (1989). Age relationships between the auriferous faults and other major structures in the Snow Lake area dictate that mineralization took place late in the thermotectonic history of the greestone belt.

Auriferous faults cross-cut all lithologies and offset the hinges of D1 isoclinal folds. They are typified by an upper greenschist

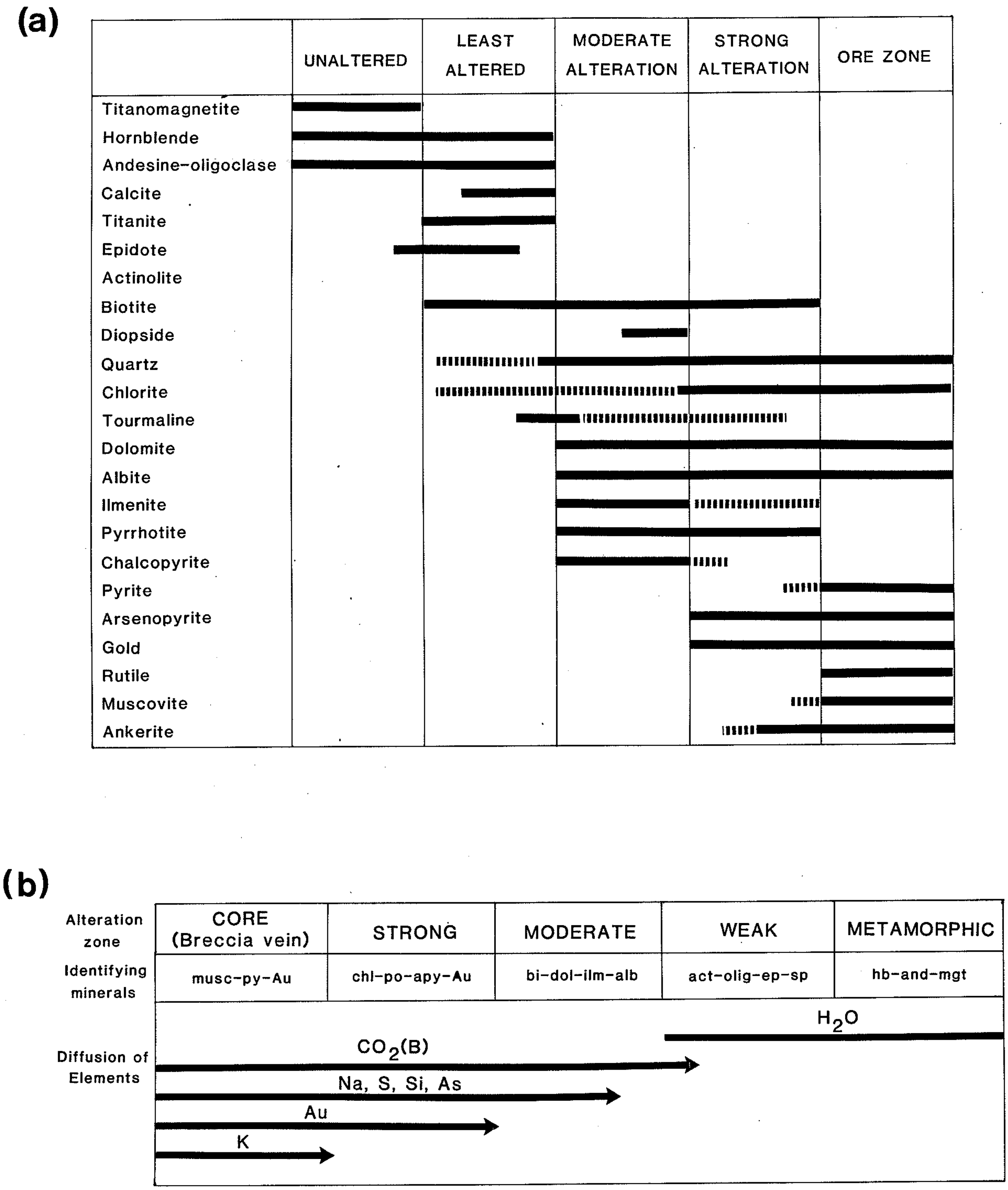


Figure 25: Alteration zonation associated with gold mineralization: a) Mineralogical distribution with alteration zones associated with the Nor-Acme deposit, and b) Element addition during alteration of the wallrocks to the Nor-Acme deposit.

facies mineral assemblage of acinolite-biotite-chlorite-ferroan dolomite that clearly overprints the lower almandine-amphibolite facies regional mineral assemblages. As peak metamorphism is temporally associated with D2 folding (Froese and Moore, 1980; Zaleski, 1989, Bailes and Galley, 1989) this would suggest that the latest phase of movement along these faults was post-D2.

The eastern part of the Flin Flon belt is characterized by a series of northeast-striking faults that parallel, but offset the axes of D2 folds. Movement along these structures was dominantly reverse, dip-slip, with a component of dextral movement, and they are characterized by greenschist facies mineral assemblages (Bailes, 1985, Frarey, 1948). Since the auriferous faults have a similar reverse, dip-slip movement and associated greenschist facies mineral assemblages, it is possible that they may be related to this period of regional faulting. From the calculated PT path for regional metamorphism (Zaleski, 1989), and taking into account the higher fluid pressure within the faults, Snow Lake rocks would likely have crossed the greenschist-amphibolite ($500-550^{o}$ at 4Kb) transition between 1.8 and 1.75 Ga.

The mechanism responsible for the creation of the late fault system and associated gold mineralization may be determined from the associated kinematic features. The fault-hosted vein occurrences have a common characteristic in which all linear features are parallel, and plunge moderately to the northeast. This includes fragment elongation and mineral orientation within the fault zone, axes of buckled veins that dip and plunge northeast, slickensides along vein margins and the plunge of the gold zones. This strong prolate strain fabric is indicative of a stress regime in which there is both shortening and translation. This can involve either combined thrusting and wrenching (Brun and Burg, 1982) or transpression (Sanderson and Marchini, 1984). Hoffman (1988a) has suggested that the formation of the late fold-fault features throughout the Trans-Hudson Orogen was the result of transpression during the oblique collision of the Archean Superior and Hearne microcontinents.

## Snow Lake Area: Stop Descriptions

### STOPS 1 TO 8: Alteration underlying the Chisel-Lost-Ghost-North Chisel Zn-Cu base metal zone

### Introduction

Hydrothermally altered rocks in the stratigraphic footwall of the Chisel Lake, Lost Lake, Ghost Lake and North Chisel Zn-Cu deposits will be examined during this part of the trip. This will be followed by a tour of the massive Zn-Cu sulphide deposit in the Chisel Mine open pit. Descriptions for Stops 1 to 3 were prepared by Roger Skirrow for an earlier field trip guidebook (Bailes et. al, 1987) and have been incorporated in this guidebook with only minor changes.

The Chisel-Lost-Ghost-North Chisel Zn-Cu deposits occur near the top of an over 5 km, mainly north facing, intact section of Amisk Group volcanic rocks (Table 3, Fig. 26 and 28a). The deposits occur within and along strike from the Ghost Lake rhyolite, and are overlain by mafic tuff and tuff breccia of the Chisel basin formation. Rocks underlying the deposit are extensively altered for several thousand metres below the Zn-Cu sulphide-bearing zone. No significant alteration is present in the overlying Chisel basin mafic tuff and tuff breccia, indicating that the hydrothermal system responsible for deposition of base metals and for the alteration was largely shut down prior to deposition of the Chisel basin formation.

Bailes and Galley (1989) have identified alteration at four stratigraphic positions below the Chisel-Lost-Ghost-North Chisel Zn-Cu base metal zone (Fig. 27 and 28b); the alteration zones from lowest to highest stratigraphic position are briefly described below:

a) Welch zone: This semiconformable zone of alteration, 3 km stratigraphically below the Chisel-Lost-Ghost deposits, selectively affects the upper 500 m of the over 3 km thick Welch Lake basalt sequence. The Welch zone displays mainly silicification and can be traced for over 12 km along strike. To the east it may correlate with a semiconformable zone of Fe-Mg metasomatism that underlies the Anderson Lake area Cu-Zn massive sulphide deposits.

b) Edwards zone: This 300 to 600 m thick semiconformable zone of alteration is located within volcaniclastic rocks of the Edwards Lake formation, 1 to 2 km below the Zn-Cu sulphide deposits. The primary permeability of the Edwards Lake formation is thought to have played a significant role in focussing hydrothermal fluid flow and resultant alteration. Silicification is the major alteration type in this zone.

c) Moore zone: This 50 to 300 m wide semiconformable zone of alteration 500 to 700 m below the Chisel-Lost-Ghost deposits is localized in pillowed basalts of the Moore Lake formation. It can be traced for over 6 km along strike to the east and is truncated to the west by the Chisel Lake pluton. The eastern 3 km of the zone is characterized by silicification whereas the western portion is characterized by the presence of abundant coarse actinolite and local sericitization and pyritization.

d) Chisel "pipe": This zone of alteration is discordant and immediately underlies the Chisel Lake Zn-Cu deposit. It can be divided into a number of mineral assemblages that define a classic alteration pipe of the type described by Lydon (1984) in which there are potassic-, Fe-Mg-, Al-, and Mg-rich zones (Galley and Bailes, 1989). The Chisel pipe may connect at depth with the semiconformable Moore zone.

Geochemical study of silicification in the semiconformable Edwards zone by Skirrow (1987) indicates that Fe, Mg, Zn, and other elements were leached during silicification. Skirrow further suggested that these elements then moved up through this semiconformable alteration system to be deposited in the Chisel pipe and sulphide deposit. Although it now appears as if the

**TABLE 3**

**STRATIGRAPHY OF THE CHISEL LAKE SECTION**

| Thickness (metres) | Unit No. (Figure 26) | Lithology (Names of units are informal) |
|---|---|---|
| 400 | 11 | **Chisel basin mafic tuff, tuff breccia, lapilli tuff and wacke**, minor pillowed porphyritic basalt flows; well stratified with turbidite bedforms and local accretionary lapilli |
| 0-30 | | **Massive Zn-Cu sulphides** (Chisel- Lost-Ghost zone) |
| 0-300 | 10 | **Ghost Lake aphyric and sparsely quartz- and plagioclase-phyric rhyolite flows** |
| 0-100 | 9 | **Aphyric basalt flows**, mainly massive |
| 50-300 | 8,8a | **Powderhouse plagioclase-phyric dacite tuff and lapilli tuff**, minor stratified heterolithic breccia and wacke |
| 250-600 | 7 | **Moore Lake basalt and basaltic andesite flows and amoeboid pillow breccia**, characterized by high vesicularity and radial pipe vesicles; includes minor plagioclase-phyric mafic flows and intercalated monolithologic and heterolithologic mafic breccia |
| 0-150 | 6 | **Caboose andesite**, mainly massive flows |
| 300 | 5 | **Edwards Lake heterolithologic volcanic wacke**, minor intercalated mafic wacke; stratified with 1 to more than 35 m thick beds; includes mafic and felsic debris with mafic detritus more prominent |
| 0-300 | 5a | **Edwards Lake mafic volcanic wacke** and minor breccia |
| 200-700 | 4 | **Snell Lake plagioclase- and plagioclase-pyroxene-phyric massivé and pillowed basalt and basaltic andesite flows**; flows are up to 100 m thick |
| 100-400 | 3,3a | **Stroud Lake stratified heterolithic and monolithic felsic breccia and wacke** with intercalated units of intermediate to mafic greywacke, siltstone and mudstone, local strong gossan zones |
| 0-750* | 2 | **Daly Lake quartz-phyric, quartz- plagioclase-phyric and aphyric subaqueous rhyolite flows**, minor breccia |
| 3300* | 1 | **Welch Lake aphyric and sparsely pyroxene-phyric massive and pillowed basalt, basaltic andesite and andesite flows**, minor strongly porphyritic flows |

Edwards zone is not physically connected, at least in surface exposures, to the Chisel pipe (Fig. 27), the concept, that metals leached from semiconformable zones is related to the mineralizing process, is still viable.

Most of the field trip stops in semiconformable alteration are in the Edwards zone as it is best exposed and most accessible. Footwall alteration directly beneath the Chisel Lake deposit will be examined in the Chisel Mine open pit.

**STOP 1: SILICIFIED AND EPIDOTIZED PILLOWED AND MASSIVE MAFIC FLOWS IN THE WELCH SEMICONFORMABLE ALTERATION ZONE.**

This stop is located in the predominantly aphyric pillowed mafic flow sequence that forms the base of the Chisel Lake section (Fig. 26, 27 and 28). The stop description is based on work by Skirrow (1987), who studied silicification in these flows as part of his M.Sc. thesis at Carleton University.

At this stop the flows are locally strongly silicified and affected by patchy epidotization. The lowermost exposed flow (LOCATION 1) is an intensely silicified, plagioclase-phyric, pillowed basaltic andesite to andesite. It is overlain by a narrow heterolithologic clast-supported breccia unit (LOCATION 2) which is in turn overlain by a sequence of silicified and epidotized aphyric pillowed and massive basaltic andesite flows (LOCATIONS 3 and 4).

Alteration exposed at this stop is laterally extensive. Intense silicification of the plagioclase-phyric flow (LOCATION 1) is concordant and extends at least 800 m to the west (Fig. 28). The intensity of silicification decreases upwards through the sequence of flows in a step-wise fashion, with each flow displaying a different and characteristic intensity of alteration. Silicification has affected flows over a stratigraphic thickness of 20 to 100 metres. Patchy epidotization, which is characterized by domains of clinozoisite-quartz enveloped by silicic rock, forms a more or less concordant zone that disappears less than 300 m to the west. This type of alteration occurs mainly in one massive 20 m thick flow (LOCATION 4).

**Geochemistry**

Pillows that have been silicified are strongly zoned, generally with an outer 1-2 cm wide selvage of hornblende-oligoclase-quartz, a 10-20 cm thick silicified

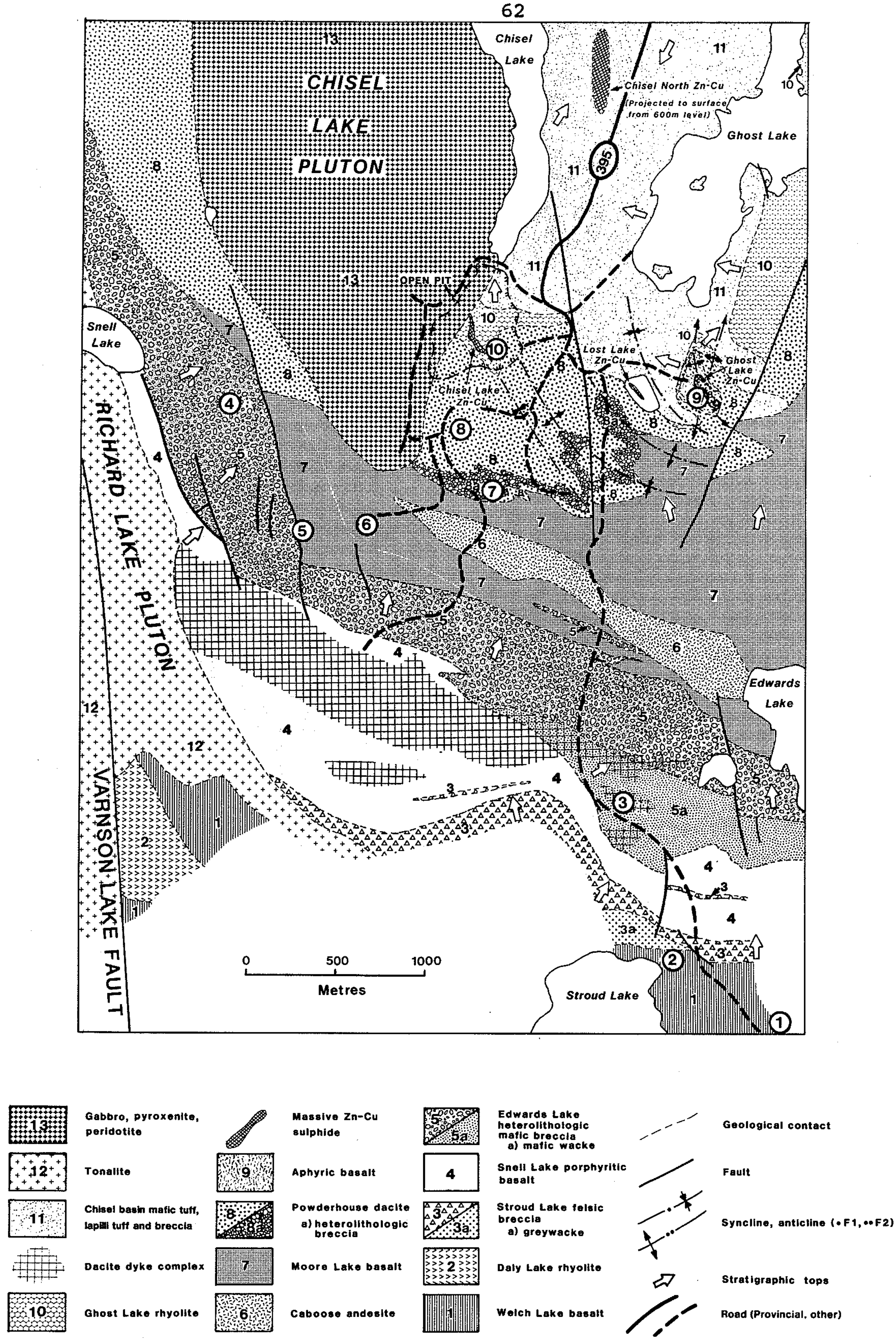


Figure 26: General geology, Chisel Lake area

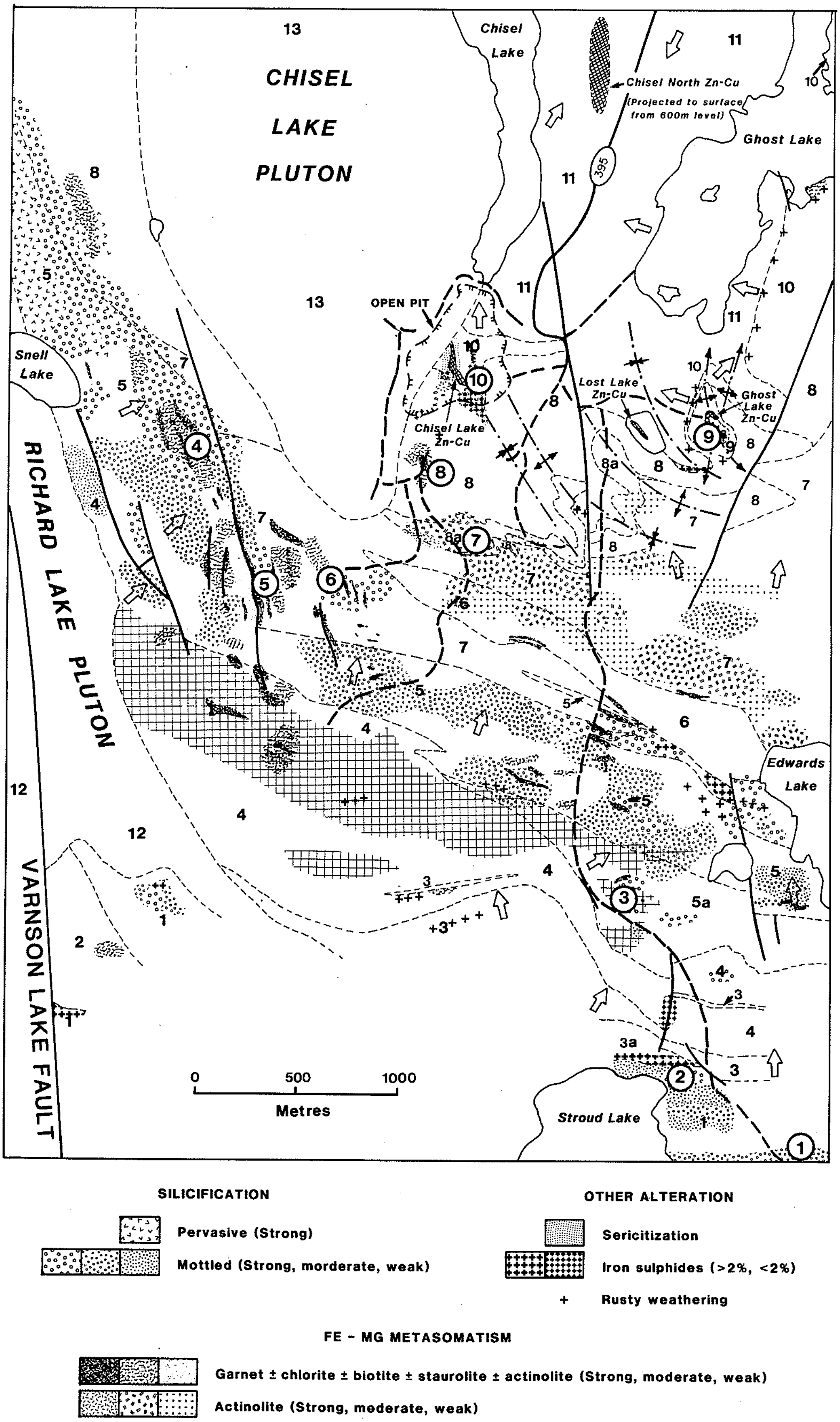


Figure 27: Hydrothermally altered rocks, Chisel Lake area

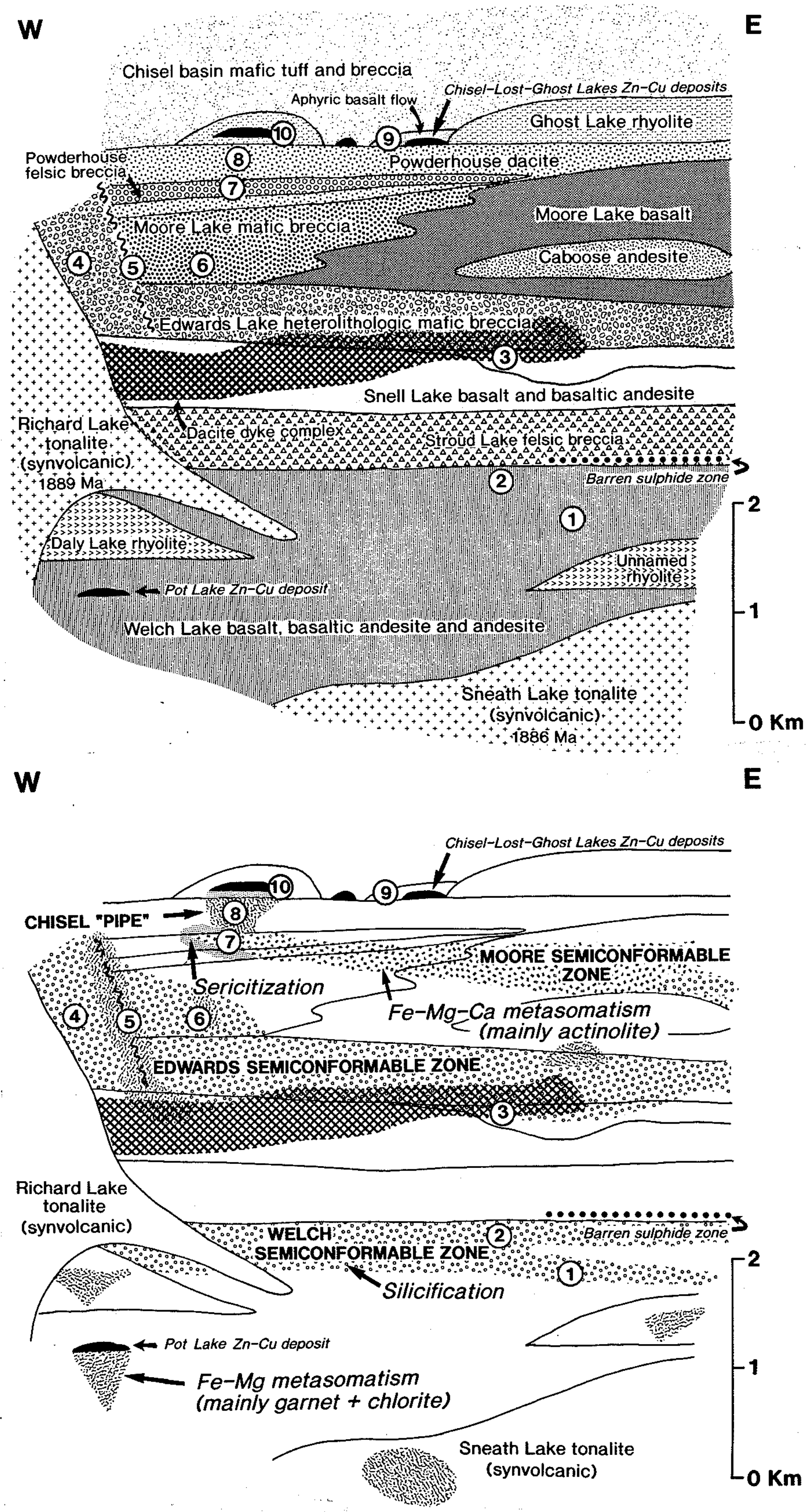


Figure 28: Schematic representation of simplified stratigraphic sequence (a) and alteration zones (b), Chisel Lake area

| | Gains | Losses | Immobile | Inconsistent |
|---|---|---|---|---|
| Selvage | $Fe_2O_3T$,MgO,Zn | $SiO_2$,$Na_2O$ | $TiO_2$,Zr | CaO,$K_2O$,Y, Cu,V |
| Margin (silicified) | $SiO_2$,$Na_2O$,Y, Zn,Cu? | $F_2O_3T$,MgO,V, CaO | $TiO_2$, Zr $Al_2O_3$ | $K_2O$ |
| Core (epidotized) | CaO,$Fe_2O_3$, $SiO_2$(small),Y ? | $Na_2O$,FeO,Zn | Zr,$Al_2O_3$, | MgO,$TiO_2$, $Fe_2O_3T$ |

margin, and an interior zone with 10-30 cm diametre domains of yellow-green clinozoisite and quartz. Elemental gains and losses during alteration of pillows, calculated using the method of Grant (1986), are summarized above:

Pillow margins show gains in $SiO_2$ that cannot be accounted for by redistribution of $SiO_2$ within a particular pillow; therefore, a source of $SiO_2$ external to the pillow is indicated. An overall small loss of $Fe_2O_3T$ and MgO from altered pillows is likely.

Epidotization of pillow cores involves large gains of CaO, oxidation of ferrous to ferric iron and large losses of $Na_2O$. Chemical changes in zones of patchy epidotization are similar to that displayed in epidotized pillow cores.

**Interpretation**

Silicification of pillows at this stop is interpreted by Skirrow (1987) to have occurred very close to, or at, the seafloor, probably while flows were still hot. According to Skirrow the early timing of alteration is evidenced by the presence of previously silicified fragments of plagioclase-phyric pillows (identical to the flow at Location 1) in the directly overlying breccia (LOCATION 2), and by overall concordance of alteration.

Skirrow (1987) envisaged the alteration process to have occurred in the following manner. The outermost parts of the lava pillows were rapidly cooled against cold seawater producing a glassy selvage and establishing a large temperature gradient between the selvage and the hot pillow margin and core. Silica, derived locally from alteration of glassy pillow selvages and interpillow hyaloclastite, or from lower parts of the volcanic pile, was precipitated in the pillow margins as the temperature of the invading silica-rich fluid was raised to greater than about 350°C (Kennedy, 1950). Fe, Ca and possibly Mg were leached from the pillow margins almost simultaneously with silica precipitation, promoted by high temperature and initially low pH (Seyfried & Bischoff, 1977). Tops and bottoms of pillows were most intensely altered because heat retention near these relatively flat surfaces would have been greater than at their sides where the radius of curvature of the pillow surface is smaller. Silicification of the pillow margin probably sealed the hotter interior from further interaction with the externally-derived $SiO_2$-rich fluids, but redistribution of elements internal to the margin may have led to epidotization of the pillow core. Not all flows are silicified - the alteration is most intense in pillows with abundant thermal contraction cracks, and it appears that these flows also contained slightly greater amounts of Al, Zr and REEs.

Zoned silicification-epidotization patches, which will be observed in the massive flow at LOCATION 4, may have also formed soon after lava extrusion by interaction of a $SiO_2$-rich, low-pH fluid with the hot flow. Here fluids may have gained access to the interior of the flow via thermal contraction cracks.

**LOCATION 1: Intensely silicified pillows, plagioclase-phyric mafic flow**

At this location the upper 15 m of a strongly silicified plagioclase-phyric mafic flow, overlain to the north by heterolithologic breccia (Location 2), is exposed. Pillows in this flow are relatively large (up to 2 x 3 m in diameter), contain 5-10% plagioclase phenocrysts (up to 2 mm long), and exhibit quartz-filled concentric thermal contraction cracks (up to 2 mm wide). Vesicles increase slightly in abundance towards the top of the flow (northwards) and are filled with quartz or quartz-epidote. Some of the features accompanying silicification of a pillowed mafic flow are well displayed at this outcrop.

Altered pillows at this outcrop show a characteristic zonation from margin to core, as follows: a) a 1-2 cm wide medium grey selvage composed of hornblende + oligoclase + quartz and, in places, garnet + chlorite + biotite; b) a 10-20 cm silicified light grey margin containing quartz + oligoclase + hornblende + magnetite + garnet; c) and a core with 10-30 cm diameter yellowish-green, epidotized domains composed mainly of clinozoisite and quartz. The silicified margin typically includes white weathering intensely silicified 5 to 20 cm wide domains composed of quartz + oligoclase (+ magnetite + hornblende), generally localized near the top and bottom of pillows. In strongly altered pillows these white weathering zones of intense silicification continue completely around the pillow forming "doughnut structures".

Patches of yellow-green epidozite on this outcrop are surrounded by light grey to white domains of silicification similar to those at the margin of altered pillows. Thermal contraction cracks pass through both the silicified and epidotized domains without deviation indicating alteration was a constant volume exchange of elements.

**LOCATION 2: Fragments of silicified pillows in a heterolithologic breccia bed**

A normally graded, heterolithologic breccia bed overlies and fills depressions in the plagioclase-phyric pillowed mafic flow of location 1. The breccia bed has a massive base and indistinctly stratified top, contains angular to subangular clasts up to 40 cm in diameter, grades upwards into granule-sized detritus, and is framework-supported. Many of the clasts are texturally and mineralogically identical to the underlying flow, and several of these clasts appear to be broken fragments of previously silicified pillows. According to Skirrow (1987) the implication is that silicification of the underlying flow preceded deposition of this overlying heterolitologic breccia bed. Other fragments in the bed include fine-grained dark grey hornblendic mafic volcanic rocks and white quartz-phyric felsic volcanic rocks.

**LOCATION 3: Silicified pillows in aphyric mafic flow**

A less intensely silicified pillowed mafic flow than that at location 1 is exposed here. The zonation of alteration within the pillows is almost identical to that at LOCATION 1. However, here pillows are smaller, selvages are more hornblendic, and intensely silicified patches (and associated thermal contraction cracks) occur closer to the selvages.

**LOCATION 4: Patches of silicification and epidotization in a massive aphyric flow.**

A massive mafic flow with distinctive patches of silicification and epidotization overlies and is separated from the silicified flow at Location 3 by several massive and pillowed flows, including a pillow fragment breccia. Alteration patches at LOCATION 4 are sinuous, typically 0.3 to 1.5 m long, and elongate parallel to thermal contraction cracks (i.e. they are subparallel to lower contact of the flow). Most are concentrically zoned from an outer dark green hornblende-rich periphery, to a middle light grey quartz, plagioclase, hornblende and magnetite-bearing silicic zone, to an interior light yellowish green core composed of clinozoisite, quartz and minor sphene and carbonate. Some alteration patches are connected and appear to form an anatomizing network. Thermal contraction cracks in this flow are typically filled by hornblende, but where they pass through the silicic peripheries of alteration patches they are filled with quartz and plagioclase.

**STOP 2: SILICIFIED PILLOWED MAFIC FLOWS IN THE WELCH SEMICONFORMABLE ALTERATION ZONE**

This stop is located at the top of the thick aphyric mafic flow sequence that forms the base of the Chisel Lake section (Fig. 26, 27 and 28). A spectacular example of a silicified pillowed aphyric basaltic andesite flow will be examined here. This alteration is part of a zone of silicification that occupies the upper 50 to 60 m of the aphyric basaltic andesite sequence at this locality (Fig. 27). Overlying felsic breccias are unaffected by silicification suggesting that this alteration was synvolcanic.

Proceeding west (along strike) from the road, weakly to moderately silicified pillows are crossed on route to the intensely altered pillows. At the stop, white weathering zones of intense silicification form a complete ring or "doughnut" around the inner margin of pillows, and enclose less altered or epidotized pillow cores. The form and chemical composition of the alteration is very similar to that at LOCATIONS 1 and 3 of STOP 1. The origin of the alteration is considered to be the same as that previously described for the rocks at STOP 1.

**STOP 3: PERVASIVE SILICIFICATION ASSOCIATED WITH DACITE DYKES IN THE EDWARDS SEMICONFORMABLE ALTERATION ZONE**

A wide array of mafic to felsic sills, dykes and plugs intrude the Edwards Lake heterolithologic mafic wacke/breccia and the underlying Snell Lake basalts. These intrusions are syn-Amisk as they are intruded by the Amisk-age Richard Lake pluton (Bailes and Galley, 1989). Most prominent among the synvolcanic intrusions is a large swarm of aphyric and plagioclase phyric dacite dykes (Fig. 26). The dacite dykes are identical in texture and chemistry to the Powderhouse dacite tuff, the unit that directly underlies the Chisel-Lost-Ghost-North Chisel Zn-Cu sulphide deposits (Bailes, 1988); these dykes are not present in post-Powderhouse units.

Skirrow (1987), Skirrow and Franklin (1989) and Bailes and Galley (1989) have all noted a close spatial association of pervasive silicification, in the Edwards zone, with individual dacite dykes and with the dyke swarm in general. This, combined with lack of silicification of the dykes themselves, suggests that silicification occurred in response to dyke emplacement. Mass balance calculations of elemental gains and losses by Skirrow (1987) indicate that leaching of Fe and Mg accompanied addition of $SiO_2$ during silicification.

$SiO_2$ solubility decreases with rising temperature between 350°C and 420°C at pressures of 800 bars (Kennedy, 1950), and leaching of Fe and other transition metals from basalt by seawater is most significant at temperatures greater than 380oC in experimental systems (Mottl et al., 1979). Based on these experimental results Skirrow (1987) has suggested that the felsic dykes at this outcrop were emplaced into a hydrothermal system heated by earlier mafic intrusions and the subvolcanic Sneath Lake pluton. He further suggests that dyke emplacement locally heated $SiO_2$-rich hydrothermal fluids to greater than 350°C causing silicification. The implication is that although the dykes are not likely to have been responsible for raising the overall geothermal gradient they may have been responsible for focussing hydrothermal activity. Absence of significant silicification of felsic dykes themselves could be due to self-sealing by silicified aureoles around the dykes.

Two widely spaced locations will be examined that illustrate the relationships between pervasive silicification and the dacite dykes.

**LOCATION 1: Dacite dykes and an associated zone of pervasive silicification**

Field distinction between dacite dyke rocks and silicified varieties of the host Edwards Lake mafic volcanic wacke is commonly difficult in the Edwards Lake area. At this location it is possible to discriminate between the two. The dacite intrusions are sheet-like bodies, cross-cut bedding, and have sharp, commonly flow-banded margins. They are creamy white in colour and are plagioclase-phyric with a fine grained groundmass of quartz, plagioclase and minor biotite. Plagioclase phenocrysts are commonly enveloped or partially replaced by biotite giving dykes a spotted appearance.

Adjacent to dacite dykes the host mafic volcanic wacke is weakly to intensely silicified. Silicified rocks are mottled shades of grey in colour, are composed of plagioclase, quartz and hornblende, and are slightly darker in colour than the adjacent dacite dykes.

Immobile element distributions confirm field distinctions between silicified mafic volcanic wacke and similar-looking dacite dyke rocks. $TiO_2$ and Zr abundances in a sample of massive, silicified mafic volcanic wacke taken 40 m north of this location are similar to those of a mafic rocks (i.e. low $Zr/TiO_2$ ratio). In contrast, dacite dyke rocks here and throughout the Edwards Lake area have, as one would expect, much higher $Zr/TiO_2$ ratios.

Silicification at this outcrop is part of large subconcordant zone. The zone coincides with an areally extensive swarm of dacite dykes and sills. In this zone mafic dykes are also abundant, locally forming up to 50 to 60% of outcrops.

**LOCATION 2: Dacite dyke with prominent silicified aureole**

A small-scale but representative example of silicification adjacent to a dacite dyke will be examined at this location. The dacite dyke is flow banded, is hosted by plagioclase phenocryst-rich mafic volcanic wacke, and has a narrow distinctive zone of silicification on its upper (north) contact. The alteration, which extends approximately 15 cm from the dyke contact, comprises patches of light grey weathering rock composed of plagioclase, quartz and hornblende. The dyke itself is not pervasively silicified, a feature typical of most dykes in the dacite swarm.

**STOP 4: SILICIFICATION IN MAFIC HETEROLITHOLOGIC BRECCIA, EDWARDS SEMICONFORMABLE ALTERATION ZONE**

An estimated 30 to 40% of the mafic volcaniclastic rocks in the Edwards Lake formation have been silicified (Fig. 28b and 29), with the silicification involving replacement of the mafic detritus by varying amounts of fine grained quartz and feldspar to produce a white or grey weathering rock. The silicification is more or less restricted to the Edwards Lake formation and has not significantly effected overlying and underlying formations, with the exception of some of the Moore Lake mafic breccias, suggesting that alteration was probably controlled by high primary permeability of this volcaniclastic unit, and that hydrothermal fluids probably moved laterally.

The Edwards Lake formation consists of up to 1200 m of mafic volcaniclastic wacke and breccia. The lower 550 m consists of fine grained mafic volcaniclastic sediments

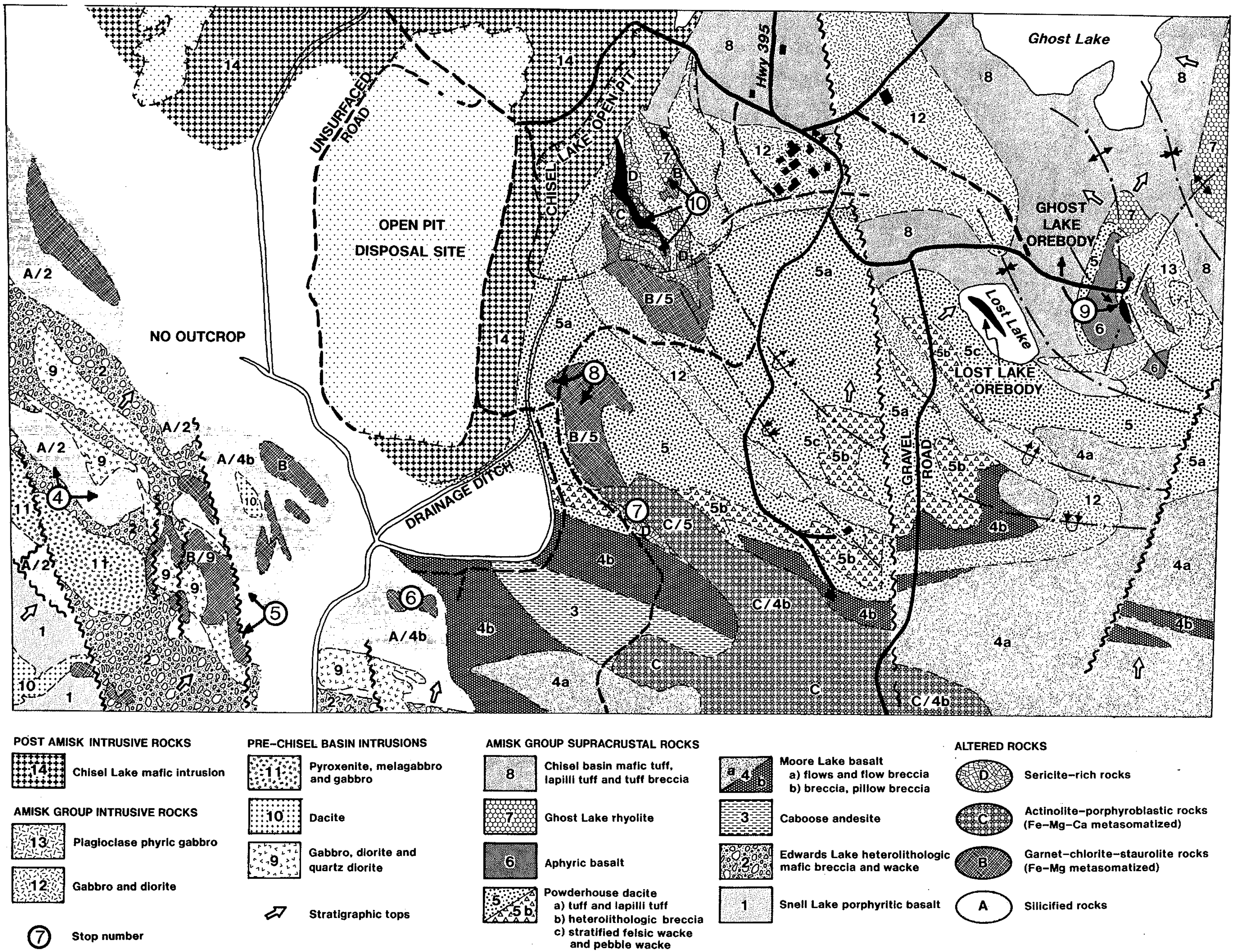


Figure 29: Geology of the Chisel Lake mine area, STOPS 4 to 10

(observed at STOP 3). The mafic wackes are overlain by heterolithologic mafic breccias (this stop) that are composed mainly of plagioclase-pyroxene-phyric mafic lava fragments and fine grained mafic and felsic volcanic clasts. Most breccia beds in the Edwards Lake formation are 1-20 m thick; Skirrow (1987) reports one 60 m bed. Organization of breccia beds is consistent with deposition by subaqueous debris flows (Bailes, 1986; Skirrow, 1987).

Silicification in the Edwards zone has a number of different forms. One is the selective alteration of clast margins and, in some instances, the entire fragment. This type of silicification of mafic fragments is easily recognized because of the contrast between dark less altered cores and light coloured quartz-plagioclase rich silicified margins; some of these silicified fragments also display an inner core of epidozite. A second type of silicification, referred to as mottled silicification, consists of millimetre-to centimetre-size oval to irregular domains composed of fine grainedquartz-plagioclase-(epidote). Typically the oval silicification domains are distributed randomly throughout both matrix and fragments, indicating that silicification postdated deposition of the volcaniclastic rocks. Other less prominent types of silicification include selective alteration of interfragment matrix, silicification of wallrock adjacent to fractures , and silicification of volcaniclastics adjacent to dykes.

The large outcrop at this stop displays many different types of silicification, with good examples of both mottled silicification and silicification of clast margins. In addition, the silicification is irregularly developed so that comparisons can be made along strike between relatively unaltered volcaniclastics and more strongly altered equivalents. A few examples have been identified in order to illustrate the character of the alteration, but there is no reason to restrict your attention to these examples.

**LOCATION 1: Coarse breccia with selective silicification of fragment margins**

Margins of fragments in a thick bed of heterolithologic mafic breccia at this location are variably but generally prominently silicified. The silicified rims are one to several centimetres wide, with local complete silicification of some fragments. Silicified rims are composed of fine grained quartz, plagioclase and minor epidote. Fragment cores generally consist of a mixture of quartz, plagioclase, actinolite and garnet, but some fragments display zoning that includes a core composed of yellow green epidosite and, in some examples, surrounding zones composed of quartz-plagioclase and/or amphibole-garnet.

**LOCATION 2: Large block displaying silicified rim and internal mottled silicification**

A pillow-shaped, 0.4 by 1.3 metre block at this location has a 2 to 3 cm white to light grey altered rim composed of fine grained quartz and plagioclase. Patchy 1 to 2 cm oval domains of silicification occur throughout the fragment, but are best developed near the outer margin.

**LOCATION 3: Mottled silicification spatially associated with a mafic dyke**

A narrow mafic dyke intruding well bedded mafic wacke has an adjacent 1 to 3 cm zone of pervasive silicification. In addition the adjacent mafic wackes are characterized by numerous 0.5 to 3 cm oval domains of fine grained quartz and plagioclase for a distance of 50 cm from the dyke margin.

Silicification adjacent to the mafic dyke is interpreted to be due to decreased silica solubility caused by rising temperature generated by dyke intrusion, identical to the mechanism described for silicification adjacent to dacite dykes at STOP 3.

**LOCATION 4: Orbicular domains of silicification overgrowing both matrix and fragments**

Orbicular quartz-plagioclase alteration structures overgrow both fragments and interfragment areas at this location indicating that alteration took place after deposition of the breccia. The orbicular alteration structures occur in two size ranges, 0.2 to 0.4 cm and 1 to 4 cm, but are otherwise identical. The small and large alteration structures, which occur together, are developed in irregular domains that cut across fragment boundaries; this is well displayed in an angular 35 by 20 cm block and surrounding detrital matrix at this location. Silicification of fragment margins is also well displayed at this location.

**STOP 5: ALTERATION ASSOCIATED WITH A SYNVOLCANIC FAULT IN THE EDWARDS ZONE**

At this stop a north-northwest-trending fault truncates a diorite intrusion and juxtaposes it against highly altered mafic breccias to the east (Fig. 27,28 and 28). For 30 m west of the fault the diorite intrusion is characterized by 10-15% garnet porphyroblasts (Fe-Mg metasomatism), and close to the fault the diorite contains local 10-50 cm wide north-trending linear zones composed entirely of chlorite and garnet.

East of the fault the mafic breccias are strongly altered for over 50 m, but the true extent of alteration to the east is not known as rocks are covered by swamp. Alteration is zoned from east to west (i.e. going towards the fault) as follows:

-35 m of mottled "silification" that increases in intensity to the west.

-10 m of uniformly "silicified" white weathering rocks of intermediate composition.

-3-4 m of staurolite-porphyroblastic rocks directly adjacent to the fault that are composed of 5-10%, 5-20 mm staurolite porphyroblasts, 5% garnet, 5% chlorite, 5% biotite, 50-60% quartz and 20-25% feldspar.

The altered fault at this stop is one of several that cut across the diorite intrusion and mafic breccias in this area. The faults coincide with an overall increase in level of alteration in the Edwards zone and are interpreted to be synvolcanic and to have focussed the flow of hydrothermal fluids in the Edwards alteration zone.

Strong alteration at this stop does not permit unequivocal identification of the mafic breccias east of the fault but their trace and REE contents are similar to those displayed by the Moore Lake basalt formation and are quite different than those characteristic of the Edwards Lake formation. The diorite west of the fault is emplaced in Edwards Lake heterolithologic mafic breccias and this suggests that their is at least 500 m of apparent right lateral offset on the fault at this location.

**LOCATION 1: Mottled silicification 35 m east of fault**

The altered rock at this location is characterized by 15 to 25% 1 to 3 cm orbicular domains of fine grained quartz and plagioclase in a recrystallized intermediate rock composed of 15% 0.5 to 2 mm garnet, 35% 0.2 to 4 mm actinolite, 3% 0.2 to 0.5 mm magnetite, and 37% fine grained plagioclase and quartz. The orbicular quartz-plagioclase domains occur both randomly and localized along planar structures. The overall composition of the rock, including quartz-plagioclase domains, is intermediate.

**LOCATION 2: Uniformly "silicified" rock 10 m east of fault**

The altered rock at this location contains no orbicular quartz-plagioclase domains and is texturally uniform. It is composed of 15% 0.5 to 2 mm garnet, 15% 0.5 to 2 mm actinolite, 2% chlorite, 1% biotite, and 67% fine grained quartz and plagioclase. The contact between this zone and the previous zone of mottled "silicification" is gradational over 3-4 m.

Despite the different appearance of rocks at this location and those at location 1 they are only slightly different in bulk chemical composition. The rock at this location contains 4% more $SiO_2$, 2% less $Fe_2O_3(T)$, 2% less CaO and 0.5% less $Na_2O$ than the rock at location 1; trace element and REE contents are virtually identical.

**LOCATION 3: Staurolite porphyroblastic rocks adjacent to fault**

Within 3 to 4 m of the fault the rocks display an abrupt increase in staurolite, chlorite, garnet and biotite content. Two samples analyzed from this zone display wide variations in major and trace element contents in comparison to each other and to less altered rocks further from the fault. Normally immobile elements, such as $TiO_2$, $P_2O_5$ and Zr, vary irregularly in content and this suggests that all elements have been mobilized during alteration close to the fault. The only consistent variation is a depletion in $Na_2O$ and an increase in $K_2O$. Chlorite-rich rocks at this location display significant increases in $FeO_T$ and MgO.

**STOP 6: HIGHLY ALTERED MAFIC BRECCIAS IN THE EDWARDS SEMICONFORMABLE ALTERATION ZONE**

At this outcrop (Fig. 27,28 and 29) an east-trending unit of variably silicified and garnet-chlorite-rich altered monolithologic mafic volcanic breccia (LOCATION 1) is cross-cut at a high angle by a zone of intensely Fe-Mg metasomatized rocks characterized by abundant porphyroblasts of staurolite and garnet in a chlorite-biotite-rich groundmass (LOCATION 2). The crosscutting zone of staurolite-garnet-chlorite-biotite-rich altered rocks at this stop are possibly related to a synvolcanic fault, similar to the zone at STOP 5; however the fault, if it exists, is not exposed. Least altered breccias at this stop include complete pillows as fragments and broken pillow pieces, and are interpreted to be pillow fragment breccias derived from cold fragmentation and slumping of Moore Lake basalt flows. Chemical analyses of pillow fragments from this breccia support derivation of these fragments from Moore Lake basalt flows.

At this stop we will first examine the least altered breccias in the centre of the outcrop (LOCATION 1) and then proceed to the most altered portion at the east end of the outcrop (LOCATION 2).

**LOCATION 1: Silicified and garnet-chlorite-bearing altered mafic monolithologic breccia**

The breccia at this location is coarse with many fragments to 40 cm in diameter and rare blocks up to 1 m in size. It is composed of medium grey, light grey and white weathering blocks which appear to be a heterolithologic mixture of mafic to felsic fragments but which are actually variably silicified aphyric mafic fragments. The primary mafic composition of fragments is attested to by their morphology; most are broken pieces of pillows, some are complete pillows, and one large block comprises a piece composed of several intact pillows. Many fragments contain up to 15% 1 to 10 mm quartz amygdales. Rare slabby fragments of altered laminated mafic tuff are present which must have been lithified prior to incorporation into the breccia.

Pillow fragment pieces vary from relatively unaltered medium grey blocks to white weathering silicified clasts composed almost entirely of quartz and feldspar. Many fragments are zoned with a less altered core composed of 30% black amphibole (1-2 mm), 10 to 15% anhedral garnet (0.5-4 mm), 10% quartz, and 50 to 55% fine grained plagioclase and a 1 to 3 cm wide white weathering rim composed of quartz, feldspar, minor amphibole and 2 to 3% magnetite. Rare multiple-zoned fragments with siliceous cores and rims and a median amphibole-rich band are present. Fragments with pale yellow-green epidote-rich cores occur locally. Inter-fragment matrix is a completely recrystallized mixture of 40 to 60% black amphibole (1-4 mm), 5 to 15% anhedral garnet (to 1 cm), 35% plagioclase, 5% quartz and 0 to 5% euhedral magnetite (0.5 - 1.5 mm).

Proceeding to the east, towards the cross-cutting zone of intensely Fe-Mg metasomatized rocks at LOCATION 2, the breccia becomes increasingly rich in Fe-Mg-bearing minerals such as garnet, chlorite and amphibole. Initially, the garnet-chlorite-amphibole alteration-assemblage is confined to the interfragment domains (i.e. zones of high permeability) but towards the east the fragments themselves are also affected.

The alteration of breccias at location 1 occurred in two stages. The early stage consisted of silicification during which Fe and Mg were removed and $SiO_2$ added. This stage of alteration is represented by the silicified, originally mafic, pillow fragments in the breccia. Zones of silicification completely rim margins of broken pillow pieces indicating that silicification postdated deposition of the breccia. The second stage of alteration consisted of addition of Fe and Mg and is represented by garnet, amphibole and chlorite-rich rocks. This alteration began by altering the permeable interfragment domains and then proceeded to alter the previously silicified pillow fragments. The zone of Fe-Mg metasomatism cuts across the east-trending unit of pervasively silicified pillow fragment breccia as can be observed at LOCATION 2.

**LOCATION 2: Staurolite-garnet-chlorite-biotite-rich altered rocks**

Staurolite-rich strongly altered rocks are exposed here. They form a cross-cutting north-trending zone (Fig. 29). The contact of this zone of alteration is gradational to the west into the less altered equivalents exposed at LOCATION 1. The most strongly altered rocks are characterized by subhedral to euhedral honey brown to dark brown staurolite porphyroblast (up to 2 cm in size).

The altered breccia west of the staurolite-bearing zone is a garnet-amphibole-biotite-rich rock with numerous white quartzofeldspathic fragments. The interfragment domains are composed of 25 to 30% amphibole plus biotite, 15% garnet, and 50 to 60% plagioclase. The fragments contain up to 5% garnet but virtually no other ferromagnesian minerals.

In the staurolite-bearing zone, to the east, the fragments are less conspicuous and where preserved are composed of quartz and feldspar with up to 50% anhedral garnet. The remainder of this zone is composed of 20% subhedral to euhedral staurolite (up to 2 cm), 15 to 20% anhedral to euhedral garnet (to 5 mm), 15% biotite, 10% chlorite, and 50% fine grained quartz and plagioclase.

**STOP 7: ALTERED POWDERHOUSE BRECCIA, MOORE SEMICONFORMABLE ALTERATION ZONE**

The strongly altered rocks at this location represent the western extremity of the semiconformable Moore alteration zone (Fig. 27,28 and 29). This outcrop is less than 500 m stratigraphically below the main Chisel Lake mine Zn-Cu massive sulphide ore zone, and there is a distinct possibility that the disconformable Chisel Lake mine footwall "pipe" is connected to the semiconformable Moore zone at this locality. Drill holes by HBED into deep parts of this zone have intersected significant volumes of sericite-, kyanite, and staurolite-bearing rocks, with subordinate areas of stringer pyrrhotite-spalerite-chalcopyrite, similar to altered rocks found in close proximity to massive sulphides in the Chisel open pit (Galley and Bailes, 1989).

Extensive alteration of the rocks at this locality preclude positive identification of the protolith, but along strike to the east-northeast these rocks can be traced into a heterolithologic felsic breccia belonging to the Powderhouse dacite. The most strongly altered rocks, which occur at the base of the outcrop adjacent to the small pond, consist of black weathering, locally gossaned actinolite-rich strata and minor, leucocratic zones of sericite-rich schist. The amphibole-rich rocks are composed of 35 to 50% 1-6 mm actinolite, 15% 1 mm biotite, 1 to 4% pyrite, 5 to 10% quartz and 25 to 40% plagioclase; they trace to the ENE into a breccia consisting mainly of felsic fragments with an interfragment matrix rich in coarse grained actinolite.

**STOP 8: DISTAL PART OF THE DISCONFORMABLE CHISEL MINE FOOTWALL PIPE (IN POWDERHOUSE DACITE)**

A 100-250 m thick unit of plagioclase phyric dacite tuff and lapilli tuff forms the stratigraphic footwall to the Chisel Lake, Lost Lake and Ghost Lake Zn-Cu massive sulphide deposits. The dacite tuff is typically a massive, pale buff weathering unbedded rock with 5-15% 0.5 to 2 mm tablet shaped plagioclase phenocrysts and glomerophenocrysts. It locally contains angular white weathering plagioclase phyric lithic felsic fragments and is occasionally well bedded. The dacite tuff is identical in texture and chemical composition to the dacite dyke complex observed previously at STOP 3. At this stop (Fig. 29) relatively unaltered dacite tuff (LOCATION 1) is compared to altered equivalents (LOCATION 2). The altered rocks at LOCATION 2 can be traced to the north (with a minor break) into the footwall alteration zone below the main Chisel Mine orebody.

**LOCATION 1: Relatively unaltered Powderhouse dacite**

Massive, homogeneous dacite tuff typical of the Powderhouse unit occurs at this outcrop located just west of the road. The characteristic plagioclase phenocyrsts and small white lithic felsic fragments of the Powderhouse formation are present. Minor alteration of the dacite has occurred and this is indicated by the presence of minor, small porphyroblasts of garnet and actinolite.

**LOCATION 2: Altered Powderhouse dacite**

One hundred and fifty metres east of LOCATION 1 the same rocks are intensely altered; the alteration is patchy in development and comprises 30 to 35% garnet, 25 to 30% quartz, 15 to 20% biotite, 10 to 15% staurolite and 2 to 5% sericite. Textures of the original rock are generally obliterated. Whole rock analyses indicate a depletion of CaO and Na2O and an increase in total iron content relative to the rock at LOCATION 1.

**STOP 9: SURFACE EXPRESSION OF THE CHISEL-LOST-GHOST MINERALIZED HORIZON (AT THE GHOST MINE VENT RAISE)**

Outcrops in the immediate vicinity of the Ghost Lake mine vent raise (Fig. 29) display the surface expression of Ghost Lake mine horizon and a directly overlying basaltic flow (Location 1) and hanging wall Chisel basin mafic tuff (LOCATION 2). This outcrop area has been intruded by a porphyritic gabbro which considerably complicates recognition of the original volcanic stratigraphy.

**LOCATION 1:**

Surface expression of the Ghost Lake mine horizon is a coarse felsic fragmental unit 30-60 cm thick, underlain to the east by graded intermediate sediments and overlain to the west by 1 m of mafic sediments and a 100 metre thick mafic flow (Fig. 29). The felsic fragmental unit is up to 10 m thick in Ghost Lake Mine, where it commonly occurs at the top of the massive sulphide zone. A similar unit also occurs in Chisel Lake mine. The Ghost Lake orebody is within 100 m of surface at this location and gossaned material here contains anomalous Cu and Zn values (400-600 ppm). The Ghost Lake orebody has no footwall alteration zone and is interpreted to be an exhalative deposit downslope from its vent.

The felsic fragmental unit is matrix-supported and consists of quartz-feldspar phyric felsic fragments up to 45 by 18 cm enclosed in a fine-grained matrix. Fragments have angular to highly irregular or subrounded shapes; some have silicic margins up to 1 cm thick. Elsewhere this unit is locally mineralized.

The footwall mafic sediments are well layered and display many primary sedimentary structures. including grading, parallel lamination, convolute lamination, scours, and flame structures. Bed thickness is from 15 cm to 1.2 m; Bouma "B" and "AB" beds predominate.

The mafic flow which overlies the felsic breccia is pillowed but selvages are poorly defined. Quartz amygdales up to 1 cm in diameter occur in oval epidosite masses and in unepidotized basalt. The basal 2 m of the flow is intensely breccias with a quartzofeldspathic cement. Thirty metres to the north of this locality the breccia zone is 11 m thick and better exposed. The top several metres of this flow, exposed in small scattered outcrops in the low area to the SW comprises flow top amoeboid pillow breccia.

**LOCATION 2: Chisel Basin basaltic tuff and fine-grained volcaniclastic sedimentary rocks (along with basalt flows and coarse mafic breccias that are not present at this location) overlie the Chisel, Ghost and Lost orebodies.**

Primary features at this location include graded bedding, cross lamination, scours, flame structures, load casts, bomb sag with lee side cross bedding, and possible accretionary lapilli. High angle faults with minor offsets are common. Note the absence of alteration in the hangingwall rocks compared to that observed in the footwall at previous stops.

**STOP 10: GEOLOGICAL SETTING AND ALTERATION ASSOCIATED WITH THE MASSIVE SULPHIDE OREBODY IN THE CHISEL MINE OPEN PIT.**

The Chisel Lake orebody was discovered in 1956 by Hudson's Bay Mining and Smelting Co. Ltd. by drilling a weak ground EM conductor. The deposit went into underground production in 1960 with reserves of 3.57 million tonnes grading 11% Zn, 0..42% Cu, 56.3 g/t Ag and 2.17 g/t Au. Between 1987 and 1989 drilling delineated a further 2.457 million tonnes grading 9% Zn and 0.3% Cu that will be developed by a second shaft 1000m to the north of the original mine site (Fig. 26). In 1988 excavation began to expose the crown pillar composed of 1.14 tonnes grading 10% Zn, 0.23% Cu, 1.4% Pb, 2.54 g/t Au and 54.8 g/t Ag (Northern Miner, Nov. 1988) In the spring of 1989 underground development ceased and production began in the open pit.

At surface the deposit is a single lense over 40 m thick and 190 m long of dominantly sphalerite and pyrite (Fig. 30). Between the 250 and 650 levels of the mine this single lense becomes a series of anastomosing lenses characteristic of polyphase folding. Below the 650 Level the lense breaks up into a series of fold noses and detached fold limbs. The deposit has been traced for 1500 m down a northeast-trending plunge that changes from approximately 40° at surface to less than 20° near it's lower limit.

The beginning of the Chisel North Zone is 300 m north-northeast of the lower limit of the main Chisel mine deposit (Fig. 26). From drill intersection this zone is believed to comprise two, overlapping panels of massive sulphide, with a cumulate length of over 300 m.

The Chisel deposit is situated at the contact between felsic volcanic rocks and overlying Chisel Basin mafic volcaniclastic strata (Fig. 29). The stratigraphic footwall is over 200 m of pyroclastic feldspar phyric tuff, lapilli tuff and tuff breccia of the Powderhouse Dacite. Overlying the dacite are massive flows of the Ghost Lake rhyolite. In the vicinity of the open pit these flows form a small dome up to 50 m thick surrounded by an apron of autoclastic breccia (Fig. 31). The masssive sulphide unit flanks the Ghost Lake rhyolite, and extends over the dome as a thin

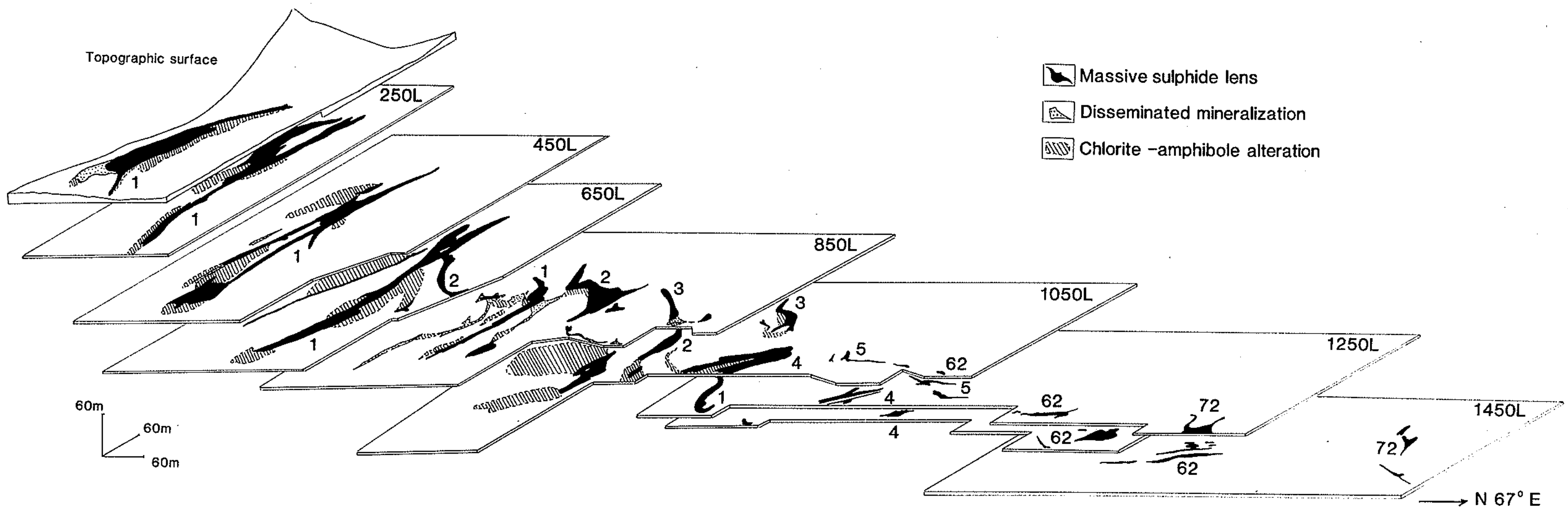


Figure 30: Morphology of the Chisel deposit (from Hudson's Bay Mining and Smelting, Snow Lake Mining Division).

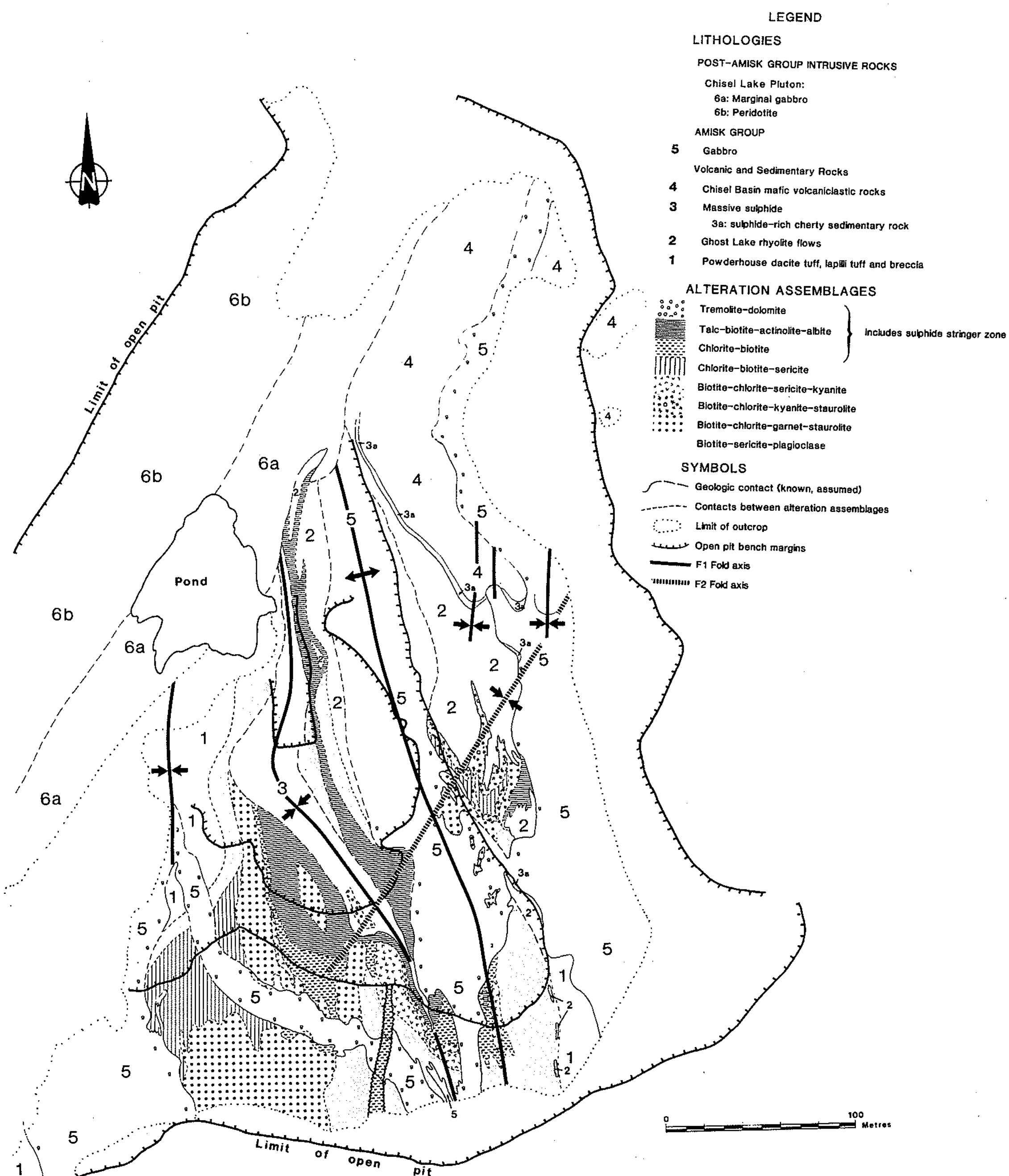


**Figure 31: Geology of the Chisel Lake open pit (STOP 10).**

sequence of interlayered chert and sulphide. The massive sulphide unit is overlain by well layered mafic epiclastic and pyroclastic rocks of the Chisel Basin.

The mine sequence is intruded by a series of aphyric, fine-grained gabbro dykes and sills up to tens of metres thick (Fig. 29 and 31). These are possibly feeders for basaltic flows higher in the volcanic sequence, and are infolded with the strongly deformed stratigraphy. The massive sulphide and associated strata are truncated by the undeformed, late-kinematic Chisel Lake Pluton, a zoned, mafic-ultramafic intrusion (Fig. 31).

The fossil hydrothermal system associated with the deposition of this VMS deposit has been recrystallized under lower almandine-amphibolite grade metamorphic conditions. Distinctive coare-grained metamorphic mineral assemblages allow a preliminary classification of alteration types based on their contained mineral assemblages. Nine distinct mineral assemblages, or zones, are recognized, eight of which are restricted to the statigraphic footwall of the deposit (Fig. 31). Contacts between the alteration zones are commonly diffuse over tens of centimetres, with contacts defined by the first appearence or disappearence of a characteristic metamorphic mineral. Crosscutting relationships between alteration zones are relatively consistent, and define an order of increasing intensity typified by a progressive loss in theoriginal textures of the footwall rocks. The original configuration of these alteration zones relative to the massive sulphide unit has been obsured by polyphase deformation, but preliminary reconstruction of the stratigraphy indicates that the alteration forms two discordant zones, the largest 200 m in diameter.

Internal zonation in the larger zone is crudely concentric, with a sericite-rich zone forming a halo about the others (Fig. 31). Within this halo, the staurolite-garnet-rich alteration is overprinted by a kyanite-rich zone that is in turn overprinted by chlorite-biotite and chlorite-talc-amphibole-sulphide-rich zones. The inner chlorite-talc-amphibole-sulphide zone is the host to the footwall sulphide stringer zone, which contains abundant, anastomosing veinlets of sphalerite-pyrite and chalcopyrite-pyrrhotite. The smaller zone is truncated by subsequent intrusion of the gabbro, and has a chlorite-talc-actinolite-sulphide rich core surrounded by a zone rich in kyanite and staurolite that grades outward into chlorite-biotite-garnet-staurolite and then a broad zone of quartz-sericite-pyrite.

Relative to unaltered Powderhouse dacite south of the pit, the following changes have occurred in whole-rock geochemistry in the discordant alteration zone:

1. Mg, Fe and S are elevated throughout the alteration zone, with a dramatic increase (up to 22% Mg) within the inner chlorite-talc-amphibole zone.

2. There is a gradual increase in K up to the edge of the chlorite-talc-amphibole-sulphide zone, where it drops sharply.

3. Within the chlorite-talc-amphibole-sulphide zone there is a sharp increase from background values of Zn, Cu, Pb, Cd, Au and Ag.

4. There is a strong depletion in Ca and Na throughout the alteration pipe.

A garnet-magnetite-chlorite mineral alteration assemblage occurs both in the stratigraphic footwall of the deposit and along the inside margins of the fine-grained, aphyric gabbro dykes that cross-cut the mine stratigraphy (Fig. 31). The alteration is typified by 20% garnet up to 7 mm in size, 1 to 2 mm sized magnetite grains and abundant, medium-grained chlorite. Zones of this alteration type are widest and most intense in the stratigraphic footwall to the deposit, but are also observed in gabbro dykes within the hangingwall Chisel basin sedimentary stata. The appearence of this distinctive mineral assemblage is accompanied by an increase in Mg, Cu and Pb, and a decrease in Ca and Na. The significance of this alteration within the post-ore gabbro dykes is not fully understood. One explanation is that they intruded the mine sequence while the hydrothermal system was still active, and that the dyke margins acted as conduits for the escape of hydrothermal fluids into the hangingwall Chisel Basin sequence.

**Structure**

Two fold phases have been recognized (Martin, 1966, Galley and Bailes, 1989) which can be related to the regional deformational history. F1 isoclinal folding has significantly shortened the stratigraphy and structurally thickened the massive sulphide lense (Fig. 31). The F1 isoclinal folds are refolded by NNE-striking, open to tight F2 folds. The second phase of folding is characterized by strong hinge-line extension that has rotated F1-flattened fragments and the plunge of the orebody into a moderatly northeast-plunging orientation. This polyphase deformation has segmented the orebody into a series of rootless folds (Fig. 32).

**LOCATION 1: Ghost Lake Rhyolite**

This exposure of the Ghost Lake rhyolite is within the structural hangingwall of the massive sulphide lense. The unit consists of massive, aphyric to feldspar-quartz phyric flow(s).The flows are composed of lobate tongues of massive rhyolite that are surrounded by rhyolite breccia and microbreccia. The rhyolite breccia and microbreccia are preferrentially altered, and have been recrystallized to staurolite-kyanite-biotite, staurolite-biotite-garnet, chlorite-biotite and chlorite-talc-amphibole-sulphide mineral assemblages; the latter contains sphalerite-chalcopyrite-pyrite stringers and elongate fragments of massive to semi-massive sphalerite. The alteration at this location is part of the smaller of the two discordant stringer zones recognized in the open pit.

**LOCATION 2: Sulphide-rich, cherty sedimentary rock**

At this location a 1 m thick unit of interlayered pyrite-sphalerite-chert lies along the contact between the Ghost Lake rhyolite and the Chisel Basin mafic volcaniclastic rocks; it is believed to be a stratigraphic equivalent of the massive sulphide unit. 1 to 3 cm wide bands of fine-grained pyrite, sphalerite, chlorite, biotite and garnet are interlayered with more siliceous, pyrite-rich bands. The phyllosilicate-rich bands appear to be normally graded. The hangingwall contact to the chert-sulphide unit is conformable with finely-laminated, siliceous sedimentary rocks of the Chisel Basin sequence.

This thin, sulphide-rich sedimentary unit may be comparable to the 'exhalite', or 'key tuffite' horizons that are associated with massive sulphide deposits in the Noranda (Simmons, 1973) and Mattagami (Roberts, 1975) base-metal camps. In the Noranda camp and Mattagami area these laminated, pyritic tuffaceous chert horizons commonly extend beyond the margins of the massive sulphide deposit and are used as key markers to denote metal-rich, hydrothermal activity along a particular horizon (Franklin et al, 1981).

The contact between the sulphide-chert and the overlying mafic volcaniclastic unit is gradational, with thin layers of sulphide continuing upwards into the laminated mafic sediments. Above this basal 1 to 2 m thick interval of finely laminated rock is a thick sequence of mafic volcaniclastic rock which contains thin layers of breccia, with both basalt and rhyolite clasts. At the north edge of the pit, sedimentation becomes noticeably cyclic, with highly vesicular and amygdaloidal basalt fragments suggesting a component of pyroclastic material.

**LOCATION 3: Footwall Alteration Zones**

Along the wall that marks the first production bench, a number of the footwall alteration zones can be

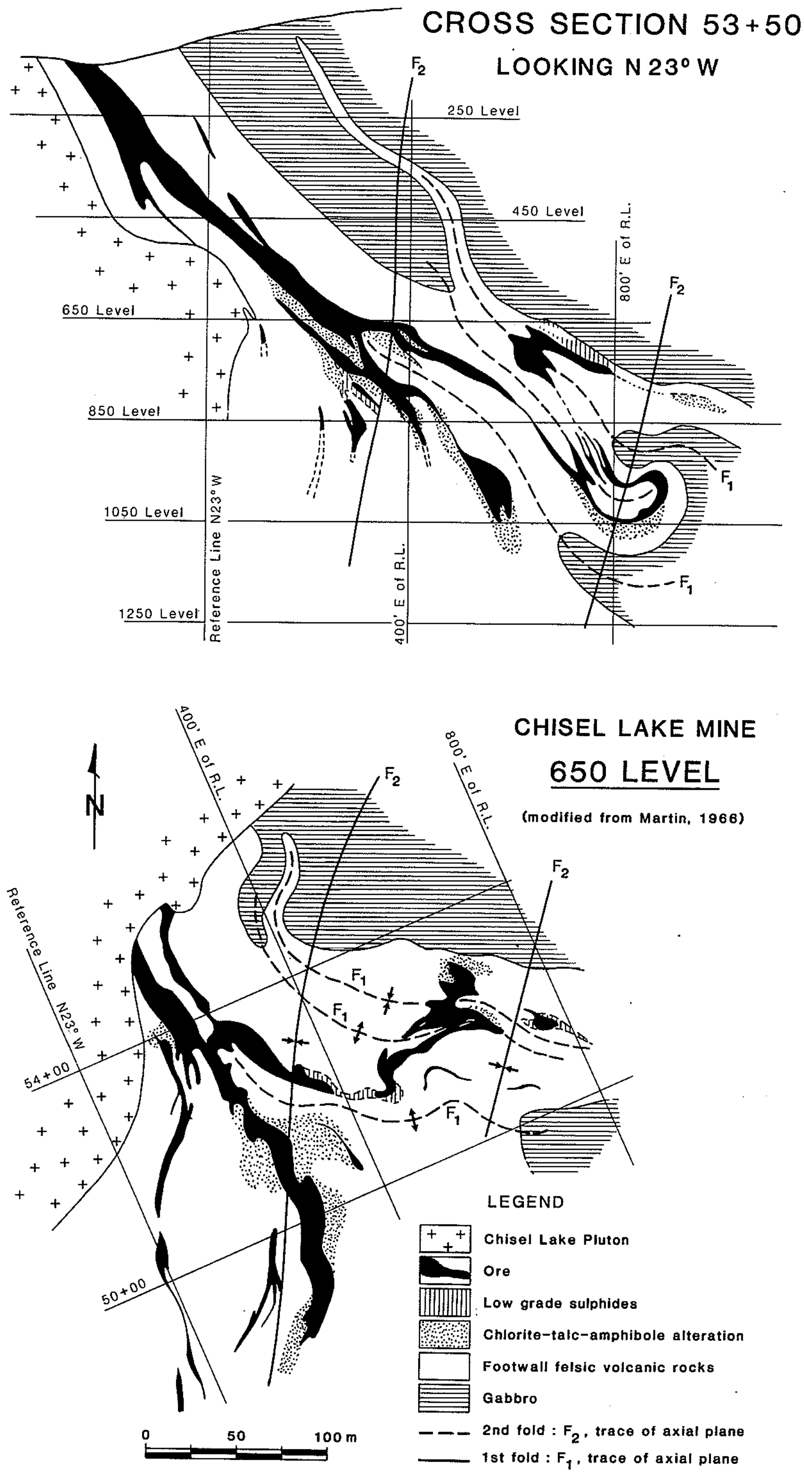


Figure 32: Geology of the Chisel Mine: a) cross section to the 1250 Level, and b) plan view of the 650 Level ( from Martin, 1966).

observed (Fig. 31). Furthest west is a zone of chlorite-biotite alteration in which 5 to 8 mm, euhedral flakes of biotite define a foliation in a finer-grained, homogenous matrix of oriented chlorite, sericite and pyrite and fine-grained polygonal quartz and Na-plagioclase.

This zone cross-cuts a 15 m wide zone of biotite-garnet-staurolite, in which the amount and size (up to 25 mm) of staurolite porphyroblasts increase towards the massive sulphide lense. This would suggest that within the zone of Fe-Mg alteration the rocks become more aluminous with proximity to the paleosurface.

Proceeding east along the bench there is a 2 m wide zone of kyanite-staurolite-sericite-chlorite and then a 30 m wide zone of widely-spaced sphalerite-pyrite stringers. The stringers have a halo of chlorite-actinolite-quartz within a host rock composed of quartz-biotite-chlorite-pyrite with minor talc. To the north, towards the second bench, the sphalerite-pyrite stringers increase in abundance and form a pseudo-breccia composed of siliceous rock in a sulphide matrix.

Within 1 to 2 m of the footwall contact with the massive sulphide the rock becomes a very Mg-rich talc-biotite-amphibole-sulphide rock with 40% $SiO_2$, 4% $Al_2O_3$ and 22% MgO. Porphyroblasts of gahnite have been observed within this zone.

## STOPS 11 TO 13: HYDROTHERMAL ALTERATION IN THE VICINITY OF THE ANDERSON LAKE AND STALL LAKE MINES

### Introduction

During this part of the field trip hydrothermally altered rocks in the stratigraphic footwall of the Anderson Lake and Stall Lake Cu-Zn massive sulphide deposits will be examined. Anderson Lake and Stall Lake are the largest of several Cu-Zn massive sulphide deposits that are spatially associated with a thick unit of quartz phyric felsic volcanic rocks (Lower Mine Felsics) located north and east of Anderson Lake (Fig. 21, 22 and 33). Other Cu-Zn massive sulphide deposits in this felsic unit include Rod, Linda, Ram and Joannie (Fig. 21). Descriptions of these Cu-Zn deposits are given by Walford and Franklin (1982, Anderson), Studer (1982, Stall), Coates et al. (1970, Rod) and Zaleski (1989, Linda)

At Anderson Lake approximately 3 km of north-facing Amisk Group subaqueous volcanic rocks are exposed below the McLeod Lake Thrust (Fig. 21 and 22). Walford and Franklin (1982) have subdivided, informally named and described Amisk rocks of the Anderson Lake area. Their stratigraphy and nomenclature is summarized in Table 4 and Fig. 22.

A rough correlation between the Chisel Lake and Anderson Lake sections (Fig. 22) is possible based on: 1) potential, but unproven, stratigraphic equivalence of the barren sulphide zone in the Chisel Lake section with a barren sulphide zone which occurs 10 m above the Anderson Cu-Zn sulphide deposit (Ziehlke, pers. comm., 1986) and 2) strong similarities between Chisel Basin tuff\lapilli tuff and mafic volcaniclastic rocks of the Threehouse mafic unit (Gale and Koo, 1977; Froese, pers. comm., 1986). Some of the implications of these correlations are:

1) The Lower Mine felsic unit (STOPS 11 and 12), which hosts the Anderson, Stall, Ram, Rod and Linda Cu-Zn massive sulphide deposits (Fig. 21 and 22), is probably a thicker, more proximal equivalent of the Stroud Lake felsic volcanic breccia and wacke unit that hosts the barren sulphide zone of the Chisel Lake area.

2) The Chisel, Lost and Ghost Zn-Cu massive sulphide deposits occur higher in the Amisk sequence than do the Anderson, Joannie, Stall, Ram, Rod and Linda Cu-Zn deposits. The base of the Threehouse unit at Anderson Lake is stratigraphically equivalent to the position of the Chisel-Ghost-Lost deposits in the section at Chisel Lake.

3) Between the time of deposition of the Anderson and Chisel Lake sulphide deposits 1400 to 1800 m of volcanic

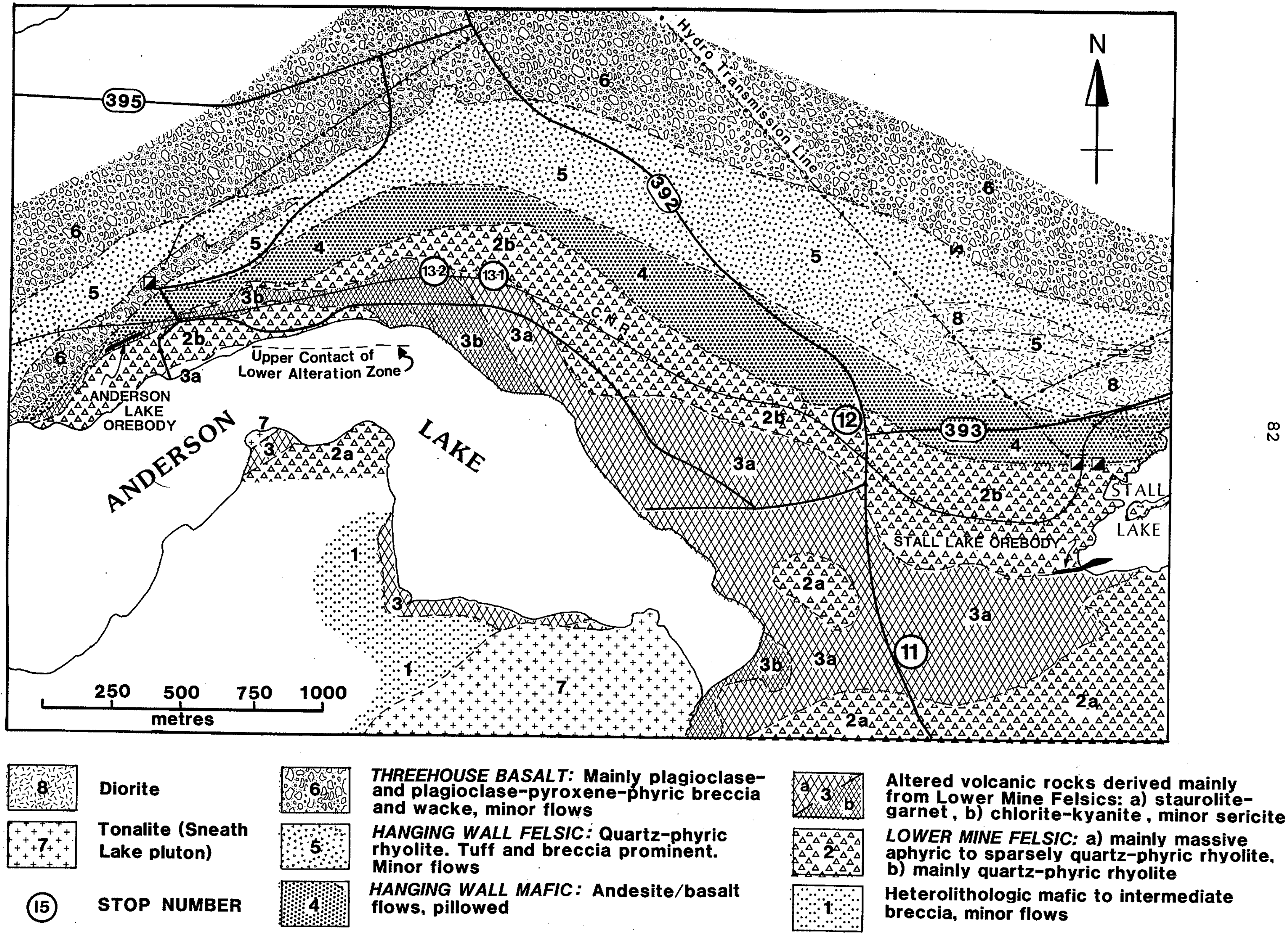


Figure 33: Geology of the Anderson Lake - Stall Lake area, STOPS 11 to 13

**Table 4: Stratigraphy of the Anderson Lake section (after Walford and Franklin, 1982)**

| Unit | Description |
|---|---|
| **Townsite mafic** | Pillowed to massive plagioclase and amphibole phyric basalt, amygdaloidal |
| **Townsite felsic** | Porphyritic rhyolite and felsic breccia, with minor mafic volcanic rocks |
| | *McLeod Road Thrust* |
| **Sedimentary** | Greywacke and shale turbidites |
| **Basalt and felsic breccia** | Aphyric pillowed to massive basalt and intercalated units of felsic breccia |
| **Threehouse mafic** | Plagioclase and amphibole phyric basalt flows and mafic epiclastic rocks |
| **Hanging Wall Felsic** | Porphyritic and aphyric rhyolite; includes lobate bodies of massive rhyolite and associated hyaloclastite, some tuff and breccia |
| **Hanging Wall Mafic** | Pillowed andesite near Stall Mine and mafic epiclastic rocks near Anderson Mine |
| **Lower Mine Felsic** | Aphyric massive felsic rocks (lower 600 m) and aphyric and quartz phyric felsic breccia (upper 300 m); upper 100 m is strongly quartz phyric and hosts the Stall and Anderson mines |
| **Mafic flows and breccia** | Aphyric basalt, mafic monolithologic and heterolithologic breccia |
| **Sneath Lake tonalite** | Equigranular and quartz phyric tonalite (synvolcanic) |

rocks (mainly the fractionated mafic to felsic Moore-Powderhouse-Ghost sequence) accumulated in the Chisel Lake section compared to only 100 to 250 m of strata in the Anderson Lake portion.

Walford and Franklin (1982), Studer (1982) and Trembath (1986) have described the Anderson Lake and Stall Lake deposits and associated alteration zones in detail. Their observations are partially summarized below.

The Anderson and Stall deposits, although not necessarily stratigraphically equivalent, occur within the uppermost, quartz-phyric 100 m (STOP 12) of the Lower Mine felsic unit (Fig. 22 and 33). They are overlain by basalt and andesite flows and breccia. Both deposits have extensive alteration zones: each has a pipe-like zone of intense alteration directly below the orebody which connects at depth with a lower, conformable zone of less intense alteration (Fig. 34). The alteration pipe below the Anderson deposit cuts across stratigraphy at an angle of 30o and has been traced for 1500 m to the southeast of the mine (Fig. 33). It consists of an inner zone of chlorite-biotite-kyanite schist (STOP 13-2), an irregular halo of biotite-muscovite-staurolite schist, and a staurolite porphyroblastic peripheral zone (STOP 13-1) with local fracture-controlled alteration (STOP 11) (Fig. 34 and 35). Quartz-chlorite-kyanite schist occurs about the central chlorite pipe away from the orebody; it displays gradational contacts up section with biotite-muscovite-staurolite schist and laterally with staurolite-porphyroblastic rocks. Disseminated pyrite, pyrrhotite and minor chalcopyrite and sphalerite are common in altered rocks near the orebody but magnetite is present instead in altered rocks more distal to the orebody (Fig. 35). Staurolite porphyroblasts show enrichment in zinc in altered rocks about the west end of the Anderson orebody and in its footwall chlorite pipe (Trembath, 1986).

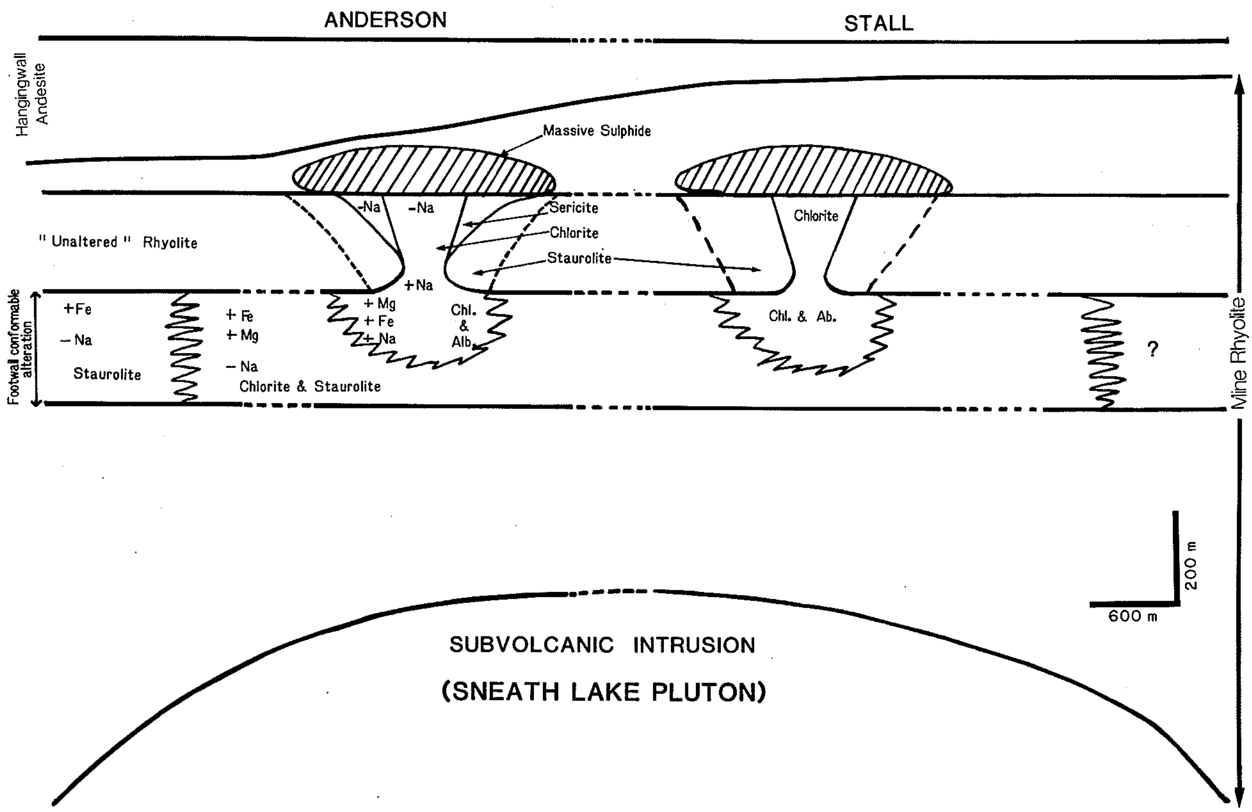


Figure 34: Simplified reconstruction of Anderson Lake - Stall Lake alteration zones, principle lithologic units and model characteristics (from Walford and Franklin, 1982)

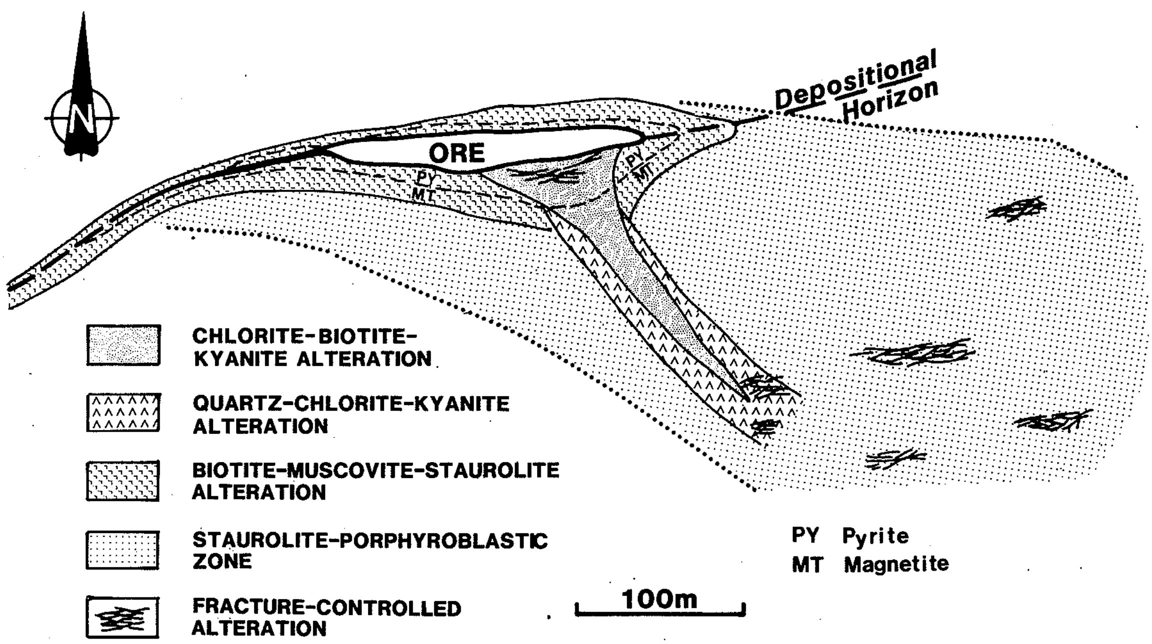


Figure 35: Distribution of alteration zones, Anderson Lake mine (from Trembath, 1986)

The lower conformable alteration zone occurs about 150 m stratigraphically below the orebody. This unit is zoned both vertically and along strike. Below the Anderson orebody it consists of 60 m of massive chlorite-biotite-kyanite schist with a zone of less intensely altered staurolitic rhyolite on its hanging wall side. It has been traced for 1500 m to the southwest and shows a decreasing chlorite content and increasing development of staurolite in that direction. Alteration pipes from the Stall and Ram deposits have been traced down through their footwall rocks where they join this lower conformable alteration zone (Fig. 34). The chemical changes attending the alteration, and the resultant metamorphic mineralogies, are also shown schematically on figure 34.

Walford and Franklin (1982) suggest that metal-rich fluids for the Anderson, Stall and Ram deposits probably formed by heating of intrastratal water in the lower felsic unit by the subvolcanic Sneath Lake tonalite intrusion. They suggest that these fluids may have been trapped in a conformable reservoir, with subsequent fluid movement through localized fractures permitting the fluids to be expelled on to the sea floor, forming the metal-rich sulphide deposits. The similar grade and isotopic characteristics of the Anderson and Stall sulphide deposits are consistent with a common fluid source.

Field trip stops will be made in the vicinity of the Anderson and-Stall Cu-Zn deposits where the effects of footwall hydrothermal alteration will be emphasized.

**STOP 11: ALTERATION IN THE LOWER MINE FELSIC UNIT BELOW THE STALL LAKE MINE (ON HIGHWAY 392, 600 m SOUTH OF INTERSECTION WITH HIGHWAY 393)**

Rhyolite at this outcrop is approximately 300 m stratigraphically below the Stall Lake orebody and was within the Stall Lake-Anderson Lake hydrothermal regime (Fig. 33). It displays a pervasive and characteristic alteration mineralogy.

Altered rhyolite has a "bleached" appearance and locally contains wavy, discontinuous, sub-parallel fractures which meet every 5-30 cm along strike and are spaced 1-5 cm apart. Origin of the fracture set, which parallels stratigraphy, is unknown but it is pre-metamorphic as the fractures are overgrown by porphyroblasts of staurolite, garnet, magnetite, chlorite and biotite. Bleached, silicified zones up to 3 cm wide occur adjacent to some fractures. Additional alteration phenomena away from the fractures include a patchy, coarse staurolite blastesis and "washed out", Na-poor, silicified zones containing amphibole or chlorite with magnetite. These latter alteration features are characteristic of the lower conformable alteration zone (Fig. 34).

Trembath (1986) has identified several small isolated zones of the wavy fracture-controlled alteration in the Anderson-Stall footwall alteration system (this is shown diagrammatically on Fig. 35). He interprets these fractures to be syn-hydrothermal as they display metamorphic mineral assemblages that are characteristic of hydrothermally altered rocks elsewhere in the Anderson-Stall alteration zone. He further suggests that these structures may have been a consequence of self-sealing of the venting hydrothermal system, with semi-horizontal fracturing occurring in the sealed cap rock due to reduced flow rate and consequent fluid over-pressuring. An alternative explanation put forward by Cees van Stall (pers. com., 1987) is that the fractures are a tectonic solution cleavage imposed on the altered rocks during pre-metamorphic F1 isoclinal folding.

**STOP 12: HOST RHYOLITE FRAGMENTALS OF THE STALL LAKE OREBODY, LOWER MINE FELSIC UNIT (INTERSECTION OF HIGHWAYS 392 AND 393)**

This rock is part of the extensive quartz-phyric rhyolite, the Lower Mine felsic unit, which hosts the Anderson Lake and Stall Lake ore deposits. The exact stratigraphic relationship of this outcrop to the ore bodies is uncertain but we are probably slightly within the hangingwall.

The fragmentals are crudely bedded with stratification defined by variation in fragment size. All the fragments are quartz-phyric rhyolite but there are subtle differences between fragments in the size and abundance of quartz phenocrysts. Most fragments are white-weathering, contain 10 to 15 per cent bluish quartz phenocrysts (1-4 mm) and are oval to lenticular in shape. There are also indistinct light grey fragments which are difficult to distinguish from the matrix. The matrix contains quartz phenocrysts similar in size and abundance to those in the fragments.

This outcrop is typical of the upper 100 m of the Lower Mine felsic unit. Walford and Franklin (1982) interpret this upper portion of the unit as a submarine pyroclastic ash flow.

**STOP 13: FOOTWALL ALTERATION PIPE OF THE ANDERSON LAKE OREBODY**

This stop emphasizes the footwall alteration zone of the Anderson Lake Mine. The most intensely altered zone consists of chlorite-kyanite schist and subsidiary sericite-kyanite schist. Less intensely altered rocks contain staurolite and magnetite.

The main alteration pipe cross-cuts the footwall rocks at approximately 30° to strike (Walford and Franklin, 1982) and can be traced in surface exposures over 1500 m east and east-southeast of the mine (Fig. 33). The best surface exposures of the alteration pipe are located 800 m east of the Anderson Lake mine headframe, along the abandoned CNR railway track. At this location the rocks are the more altered equivalents of the felsic fragmentals observed at STOP 11.

**LOCATION 1:**

The outcrop consists of felsic fragmental rocks that are part of a less-altered zone peripheral to the main Anderson alteration pipe. Mineralogical indicators of this peripheral alteration include garnet, staurolite and magnetite; these minerals typically occur in the matrix interstitial to the fragments. The fragments are flattened and lens-shaped. The clast population is all felsic but is heterolithologic as clasts display variations in the amount and size of contained quartz phenocrysts.

**LOCATION 2:**

The coarse, granoblastic quartz-kyanite-biotite-chlorite schist at this outcrop is part of the main 'pipe-type' alteration zone.

**STOPS 14 TO 17: GOLD OCCURRENCES IN THE SNOW LAKE AREA**

**Introduction**

Four stops will be made in and around the town of Snow Lake to illustrate some of the features that characterize gold occurrences in this region (Fig. 23 and 24). The Main Zone and Nor-Acme deposits (STOPS 14 and 16) are examples of economic gold mineralization that was localized by a combination of structural events. The Boundary and Bounter occurrences (STOPS 15 and 17) will illustrate how the absence of any one of these structural features results in sub-economic concentration of gold. If the timetable for underground development of the Nor-Acme deposit permits, an underground tour of this deposit will be made.

**STOP 14: SNOW LAKE MINES LTD. MAIN ZONE**

The surface excavation of this gold zone exposes an excellent example of a fault-hosted vein occurrence. The original occurrence was one of a half dozen in the area north of the town of Snow Lake that had attracted the attention of

Consolidated Goldfields Corp in 1983. After an extensive evaluation, the option was handed over to Hudson's Bay Exploration and Development, who continued drilling the occurrence. In 1987 Snow Lake Mines Ltd. took over the property and are presently holding the option. Accumulated drilling by the three companies has resulted in estimated reserves of 454,000 tonnes grading 10.28 g/t Au (Table 2).

The gold mineralization is contained within a 50 m wide fault zone that crosscuts a heterolithic mafic breccia unit near its northern contact with massive to pillowed basalt flows (Fig. 23 and 24). The gold zone is located at the point where the fault zone transects the nose of a D1 synform at a high angle. To the east of the fold axis the fault strikes west, dipping 50°, whereas to the west this structure curves northwards to merge with the McLeod Road Fault.

The gold zone is 100 m long, up to 10 m wide, and has been traced down-dip for 120 m, following the 45 to 50° dip of the fault. It plunges moderately to the northeast. The zone begins as a single, 30 cm wide vein to the west, with numerous, strongly buckled subsidiary veins striking almost perpendicular, with their fold axes plunging moderately to the northeast. For the easternmost 30 m a footwall vein appears, with the two attached by a series of northeast-striking ladder veins (Fig. 36).

The north-striking regional foliation is warped sinistrally as it is crossed by the shear foliation, and elongated breccia fragments plunge moderately to the northeast along the S1 foliation. The shear foliation is defined by the alignment of actinolite, biotite and chlorite. The veins contain angular fragments of wallrock which, along the vein margins, have extremely high aspect ratios parallel to the vein walls; this gives the veins a banded appearance. Slickensides along the vein walls plunge moderately to the northeast. The ladder veins are undeformed, their constant angle with the fault-parallel veins indicates their formation involved a component of sinistral movement (Fig. 36).

Coarse visible gold is contained within the quartz-albite-iron carbonate veins, and is associated with fine-grained, felted masses of asicular arsenopyrite within the wallrocks and wallrock fragments.

Localization of the gold zone at a D1 fold nose near the contact between two lithologies of contrasting competency, the xenolith-rich veins, the strong, reverse dip-slip component to host-fault movement and the consistent northeast plunge of all the linear elements is characteristic of gold occurrences in this area.

**STOP 15: BOUNDARY ZONE**

The Boundary Zone is an example of a vein breccia system that failed to fully develop. Mineralization is hosted by a fault that follows a contact between a mafic pebble breccia and tuff unit to the north and an aphyric to feldspar-quartz phyric dacite to the south, the contact defining the northeast limb of a D1 antiform (Fig. 24). The mineralization is localized where the fault truncates the nose of the fold. Where at the Snow Lake Mines Ltd Main Zone the fault-fold intersection appears to have been the focus for fault-parallel, vein breccia formation, at the Boundary Zone gold mineralization is within a series of thin, north-striking breccia zones that parallel the regional foliation within the footwall dacite (Fig. 37).

It would appear that rather than sustaining a fluid buildup of sufficient pressure to cause brecciation and vein formation within the fault, the fluids were bled off by reactivating the previously-formed regional foliation planes along the sole of the reverse fault within the brittle felsic rocks.

**STOP 16: NOR-ACME DEPOSIT**

The Nor-Acme deposit is the largest gold deposit within the Early Proterozoic Trans-Hudson Orogen, with a total production between 1949 and

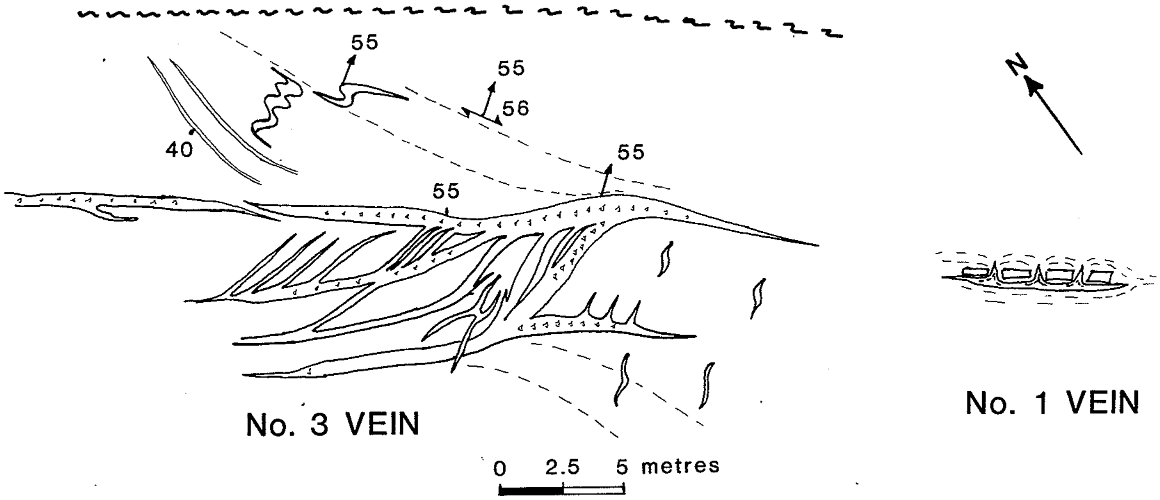


Figure 36: Schematic diagram of the configuration of the vein system at Snow Lake Mines Ltd. Main Zone.

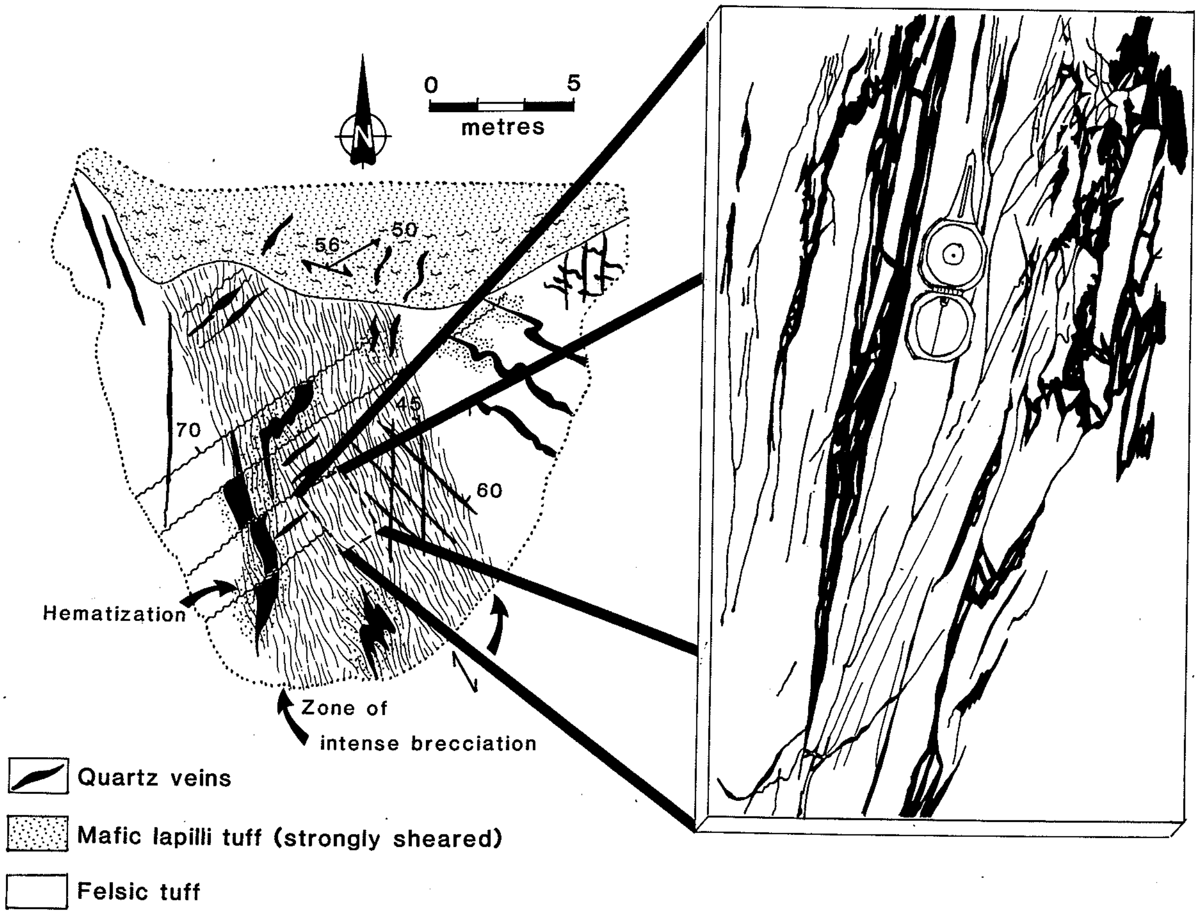


Figure 37: Surface exposure of the Boundary Zone (actual exposure known as the South Zone)

1958 of 4.91 million tonnes grading 5.14 g/t Au, and proven and probable reserves of 3.56 million tonnes grading 6.51 g/t Au (Northern Miner, December 4, 1989). The property is now under option to Inco Gold Corp. from High River Resources Ltd.

The deposit consists of four zones over a 2700 m interval along the arcuate Howe Sound Fault. The zones are localized along the portion of the fault that intersects, and offsets a D1 fold nose near the contact between dacite fragmental (footwall) and mafic fragmental rocks (hangingwall) (Fig. 23, 24 and 38). The fault also offsets a series of amphibolite dykes that intrude the volcanic sequence. The western-most gold zone (Toots) occupies the Howe Sound fault zone up to its intersection with the McLeod Road Fault. The former structure appears to offset the latter (Fig. 23 and 24).

The zones range from 3 to 30 m in width, the widest zone located at the point of maximum curvature along the fault trace. They are staggered en-echelon within the fault plane, with the western-most two zones (Toots and Dick) outcropping and the remaining two starting on the 1280 (foot) level of the mine (Fig. 38). The zones plunge northeast to north-northeast, between 40 to 80°, and are thickest along the shallower dipping parts of the fault (Ebbutt, 1941). The Toots zone extends for 900 m down plunge, while the eastern-most lenses are over 2000 m long.

**LOCATION 1: Toots Zone**

At this stop we will examine the surface exposure of the Toots Zone, the smaller of the two original ore bodies, the other being the Dick (Fig. 38). An east-trending mineralized fault breccia, cross-cutting north-striking units of quartz-phyric felsic rock, mafic heterolitologic tuff breccia and gabbro-pyroxenite dykes (Fig. 39), is exposed at this stop. Quartz-phyric felsic rocks are exposed on the northeast side of the outcrop, mafic volcanic rocks cross-cut by amphibolite dykes on its south side and biotite-altered gabbro on its northwest corner. The regional NNW-trending foliation, prominent in rocks south of the mineralized breccia, is overprinted by an east-trending shear foliation in the

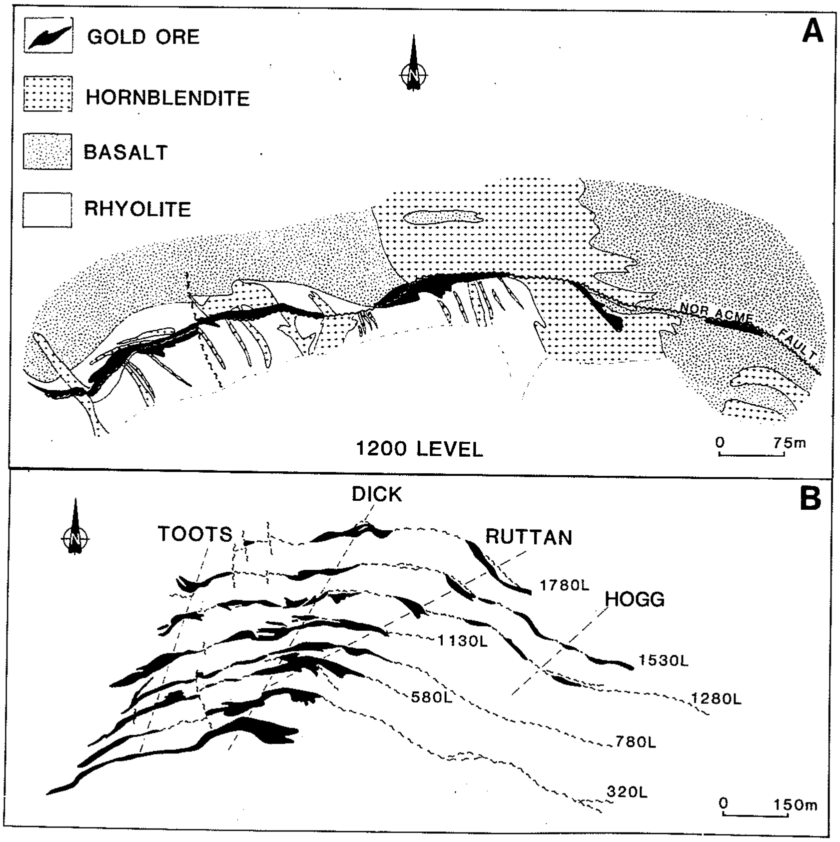


Figure 38: Geology of the Nor-Acme deposit: a) configuration of ore zone, and b) geology from the 1280 Level (from Zeihlke, 1982)

immediate hanging wall (north) of the breccia zone.

The mineralized fault breccia consists of 30-40% biotite-carbonate-albite-quartz-arsenopyrite-rich angular altered wallrock fragments in a matrix of aphanitic quartz, iron carbonate and albite. It is cross-cut by east-trending deformed and north-trending planar quartz veins. The mineralized breccia strikes parallel to the north-dipping Nor Acme Fault, with a small splay in the footwall to the main zone. Where the splay cross-cuts the structural footwall rocks, it changes from a fault breccia to a carbonate-rich intensely sheared zone. Underground at the Nor Acme Mine splay faults reportedly contained higher gold grades than the main zone.

Quartz-carbonate-tourmaline veins are commonly associated with the Nor-Acme deposit, and are observed for up to 400 m from the mineralized fault, as well as along strike from the breccia zones. An example of one of the quartz-carbonate-tourmaline veins is located 150 m to the east of the Toots Zone surface exposure.

**STOP 17: BOUNTER ZONE (HUDSONS BAY E XPLORATION AND DEVELOPMENT LTD.)**

The Bounter occurrence is an example of gold mineralization that is fault-controlled between lithologies of contrasting competency. The mineralization has not been localized by the intersection of the fault with a secondary structure, such as a D1

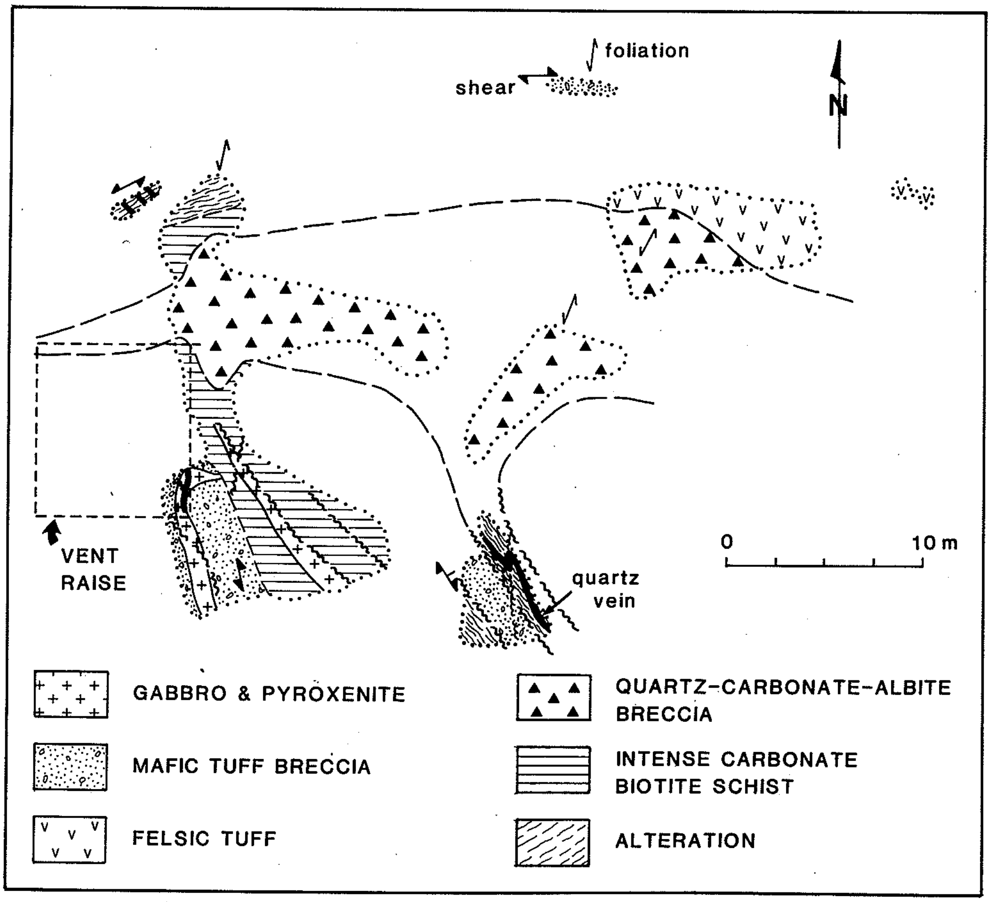


Figure 39: Surface geology of the Toots Zone

fold hinge, and is therefore diffuse, with the breccia veins characteristic of the Main Zone and Nor-Acme deposits being absent.

The Bounter Fault is a west-striking, moderately dipping structure which appears to splay off of, or be truncated by, the McLeod Road Fault at its western limit, has been traced for 3000 m to where it peters out into a number of anastomosing shears (Fig. 24). The fault forms a contact between mafic volcaniclastic rocks (footwall) and felsic volcaniclastic rocks (hangingwall) at its western end, and then cross-cuts the mafic volcaniclastic rocks for most of its strike length, The fault sinistrally offsets a large gabbro dyke.

Gold mineralization has been observed occurring sporadically along the entire length of the fault trace, with the Bounter occurrence forming a 530 m long zone along the central part of the structure defined by gold values exceeding 2000 ppb (Fig. 40). Drill results from this zone have been erratic to date, with one intersection of 10 metres of 14.9 g/tonne and another of 30 metres grading 1.362 g/tonne (Hudson's Bay Exploration and Development Ltd. data).

The mineralized zone is exposed in a trench where it is localized along the contact between a massive medium grained gabbro to the north (hangingwall), and a fine-grained immature mafic volcanic wacke to the south (Fig. 40). The zone consists of a cherty-textured rock composed of quartz, albite and iron carbonate, with 3-5% very fine grained acicular arsenopyrite and pyrite. The altered and mineralized rocks in the structural hangingwall locally retain their primary gabbroic textures. Note the lack of quartz veining and brecciation.

**Discussion**

A number of structural parameters are prerequisite for the deposition of desireable quantities of gold in this region; the lack of any one restricts the size and grade

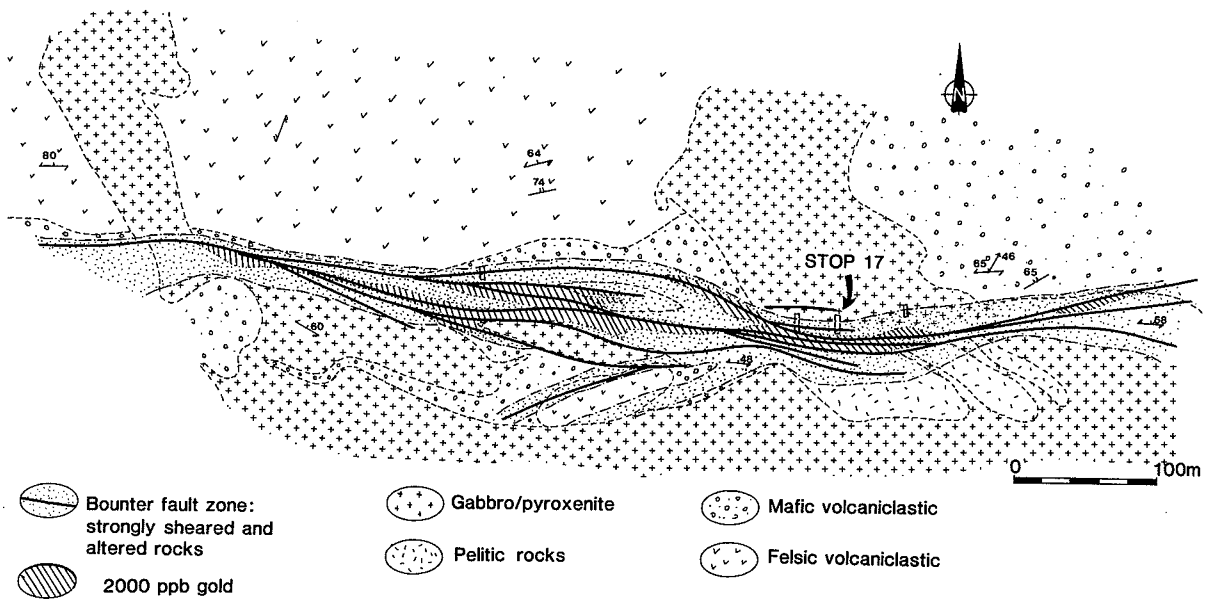


**Figure 40: Geology of the Bounter occurrence**

of the auriferous zone. The localization of any gold-bearing fluid along a fault system commonly requires the presence of a secondary structure which will alter the orientation of the internal strain regime of the fault sufficiently to cause a local buildup of fluid pressure. The sudden release of this pressure results in fracturing and vein formation. Local aberrations in the strain regime can be caused by the high-angle intersection of the fault with a previously formed anisotopic fabric such as lithological contacts and/or a fold structure. Sibson (1989) describe how the buildup and sudden release of fluid pressure results in the in-situ brecciation of the wallrocks and simultaneous infilling of the breccia zone with vein-forming fluids. The sudden offset of the D1 fold noses by the fluid-bearing faults in the Snow Lake area may have caused a similar phenomena to occur.

# THOMPSON AREA-GENERAL GEOLOGY AND ORE DEPOSITS

W. Bleeker
University of New Brunswick
Fredricton, New Brunswick

## Introduction

This part of the fieldtrip examines the geology of the Thompson Nickel Belt (TNB) and its nickel sulphide deposits. Focus is on the Thompson and Pipe II deposits and their settings. These deposits occur in the northern section of the TNB, which will be referred to as the Moak Lake-Pipe Lake area. This area, which also hosts the Moak, Mystery South, Pipe I and Birchtree deposits, is reasonably representative for the TNB as a whole.

## Geology of the Thompson Nickel Belt

### General Setting

The Thompson Nickel Belt (Zurbrigg, 1963; Bell, 1971; Coats and Brummer, 1971; Coats et al., 1972; Cranstone and Turek, 1976; Peredery et al., 1982; Green et al., 1985 and Bleeker, 1990) forms a 10 to 35 kilometre wide belt of variably reworked Archean basement gneisses and Early Proterozoic cover rocks along the northwestern margin of the Superior craton (Fig. 41). Strong gravity and magnetic expressions (Gibb, 1968; Kornik and MacLaren, 1966; Kornik, 1969) permit delineation of the TNB and its extension below platformal cover, as far south as South Dakota (Green et al., 1979). To the north-northeast, the TNB appears structurally coextensive with the Owl River shear zone (Bell, 1966), the aeromagnetic expression of which indicates a minimum sinistral displacement in the order of 100 km (Fig. 41). Lithotectonically, however, the TNB as part of the "Churchill-Superior Boundary Zone" (Weber and Scoates, 1978), swings to the east and has its extension in the Split Lake Block and the Fox River Belt (Fig. 41). Like the TNB, the Split Lake Block is dominated by variably reactivated basement gneisses, whereas the Fox River Belt consists of a homoclinal, steeply north-dipping sequence of Aphebian supracrustals and related intrusions (Baragar and Scoates, 1981).

Unreworked Archean crust to the southeast of the TNB includes low to medium grade granite-greenstone and gneiss terranes, and the high grade Pikwitonei granulite belt (Fig. 41). The latter shows sufficient similarities to the lower grade terranes to suggest that it represents deeper level exhumation of an overall gneiss and granite-greenstone crust (Roussel, 1965; Weber and Scoates, 1978; Hubregtse, 1980). The Pikwitonei granulite belt, which has an associated linear gravity high for much of its length (Gibb, 1968), parallels nearly the entire southeastern margin of the "Churchill-Superior Boundary Zone".

Archean crust of the northwestern Superior craton is further characterized by mafic to ultramafic dikes of the Molson swarm (Ermanovics and Fahrig, 1975; Scoates and Macek, 1978; Paktunc, 1987). This dike swarm, which has been dated at 1883 Ma (Heaman et al., 1986), can be followed into the TNB (Cranstone and Turek, 1976; Bleeker, in prep.), but is lacking from Aphebian crust to the northwest of the TNB.

On this side, the Churchill-Superior Boundary Zone is in fault contact with a collage of Early Proterozoic terranes (Lewry, 1981; Lewry et al., 1985 and 1987; Green et al., 1985; Hoffman, 1988a), of which the Kisseynew domain is in direct contact with the TNB. The Kisseynew domain probably represents the remnants of a back-arc or interarc basin (e.g. Hoffman, 1988a and references therein).

### Local Geology

Variably reworked Archean basement gneisses are volumetrically

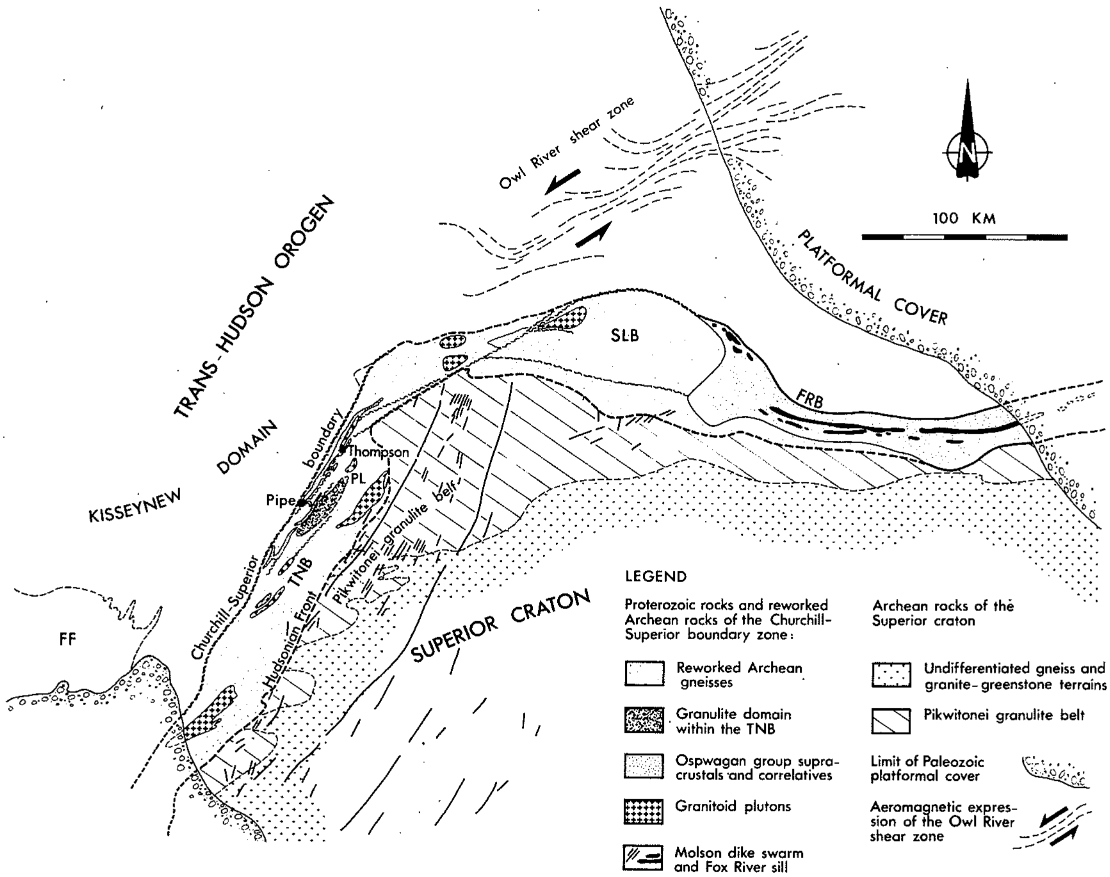


Figure 41: Simplified geological map of the northwest part of the Superior craton, "Churchill-Superior Boundary Zone" and adjacent internal zone of Trans-Hudson Orogen (Churchill Province). The "Churchill-Superior Boundary Zone" comprises the Thompson Nickel Belt (TNB), Split Lake Block (SLB) and Fox River Belt (FRB). Other abbreviations: FF (Flin Flon-Snow Lake volcanic belt) and PL (Paint Lake granulite domain). Modified after Manitoba Mineral Resources Division, 1979.

the dominant rock type in the TNB. These have been derived, at least partially, from Pikwitonei granulite facies protoliths. Along the eastern boundary of the Thompson Nickel Belt, the Hudsonian front, Pikwitonei granulites can be mapped into the TNB where they show progressive overprinting by Hudsonian ductile deformation and amphibolite facies metamorphism. Various gneisses along the western margin of the belt have been dated. Rb-Sr whole rock data (Cranstone and Turek, 1976) indicate an Archean origin, which has been confirmed recently by U-Pb zircon dating (Machado et al., 1987). Locally, the gneisses contain relics of granulite facies assemblages or pseudomorphs thereof. At one locality, such pseudomorphic textures have been recognized in gneisses that occur structurally just below the basement gneiss-cover sequence contact. Since this contact can be shown to represent an Early Proterozoic angular unconformity, granulite facies basement comparable to the Pikwitonei granulites must have been exposed prior to deposition of the Ospwagan Group cover sequence.

Remnants of the thin Early Proterozoic cover sequence, which is referred to as the Ospwagan Group (Scoates et al., 1977; Bleeker and

Macek 1988a; Macek and Bleeker, 1989; Bleeker and Macek in prep.), occur along the western margin of the belt, in deeply dissected fold interference patterns of regional scale. Although an empirical stratigraphy had been recognized by INCO geologists (Peredery et al., 1982), extreme deformation and poor exposure have obscured the fundamental relationships in this cover sequence. Detailed mapping of the new Thompson Open Pit (Bleeker, 1990), the Pipe Open Pit (Bleeker and Macek, 1988a and b) and remapping of other key areas (Macek and Bleeker, 1989) has revealed the existence of: 1) a rare sillimanite-rich meta-regolith just below the unconformity, 2) a basal pebbly conglomerate, 3) a lower transgressive sequence, which everywhere youngs away from the gneiss-metasediment interface, and in general 4) a detailed lithostratigraphy, which can be correlated throughout the TNB (Fig. 42). The lower fining-upward clastic sequence (Manasan Formation) is overlain by a package of rocks dominated by chemical and pelitic sediments (Thompson and Pipe Formations), after which there is a return to coarse clastic facies (Setting Formation), which is finally overlain by mafic to ultramafic volcanics (Ospwagan Formation). The volcanics are probably consanguinous with ultramafic sills which intruded the supracrustal sequence at various levels, most commonly near the base, and which generated the Ni sulphide deposits.

Unlike the polymetamorphic basement gneisses, Ospwagan group supracrustals record a single Hudsonian P,T-loop, with peak-metamorphic conditions ranging from lower to upper amphibolite facies, i.e. staurolite grade to garnet-sillimanite-K feldspar grade (Fig. 43). Metasediments are cut by Molson dikes bracketing their age between 2.4-1.88 Ga. Sr-isotope systematics suggest a narrower 2.1-1.88 Ga range (Brooks and Theyer, 1981).

Minor granitoid plutons, some with migmatitic envelopes, occur along the TNB. They are characterized by the occurrence of garnet and muscovite in addition to biotite; they appear anatectic in origin and are coeval with the Hudsonian thermal peak. Their intrusive relationships and single-phase upright fabrics ($S_3$) indicate that they postdate early collisional tectonism ($F_1$-$F_2$) but are overprinted by late upright structures ($F_3$). U-Pb zircon dating has been hindered by Archean inheritance, but one pluton yielded a concordant monazite age of 1822 ± 3 Ma (Machado et al., 1987).

<u>Significance of the Molson Dike Swarm</u>

Various workers have interpreted emplacement of the Molson dike swarm as an indication of initial rifting along the TNB segment of the Trans-Hudson orogen (Hubregtse, 1980; Green et al., 1985). Although a causal relationship is indeed suggested by spatial association and parallelism of the dike swarm with the TNB, the 1883 Ma age (Heaman et al., 1986) of the swarm is clearly too young for the initial rifting event (Bleeker, 1990). Along the western margin of the TNB, mafic dikes which can be correlated with the Molson swarm of the Archean foreland on the basis of their chemistry, orientation and habit, cross-cut not only basement gneisses but also the complete cover sequence and earliest Hudsonian fold structures ($F_1$). Rifting, subsidence, deposition of the Ospwagan Group and $F_1$ deformation thus all preceded 1883 Ma.

<u>Tectonostratigraphic Significance of the Ospwagan Group Cover Sequence</u>

The autochthonous nature and detailed lithostratigraphy of the Ospwagan Group cover sequence allow inferences to be made about the early tectonic evolution of the TNB (Fig. 42).

The lower clastic sequence of the Ospwagan Group (Manasan Formation) consists of a thin, locally developed quartz and feldspar pebble conglomerate, overlain by quartzites of arkosic to quartz-arenitic composition. These arenites fine upwards into quartz-rich siltstones which are overlain by wackes. The rather mature nature and

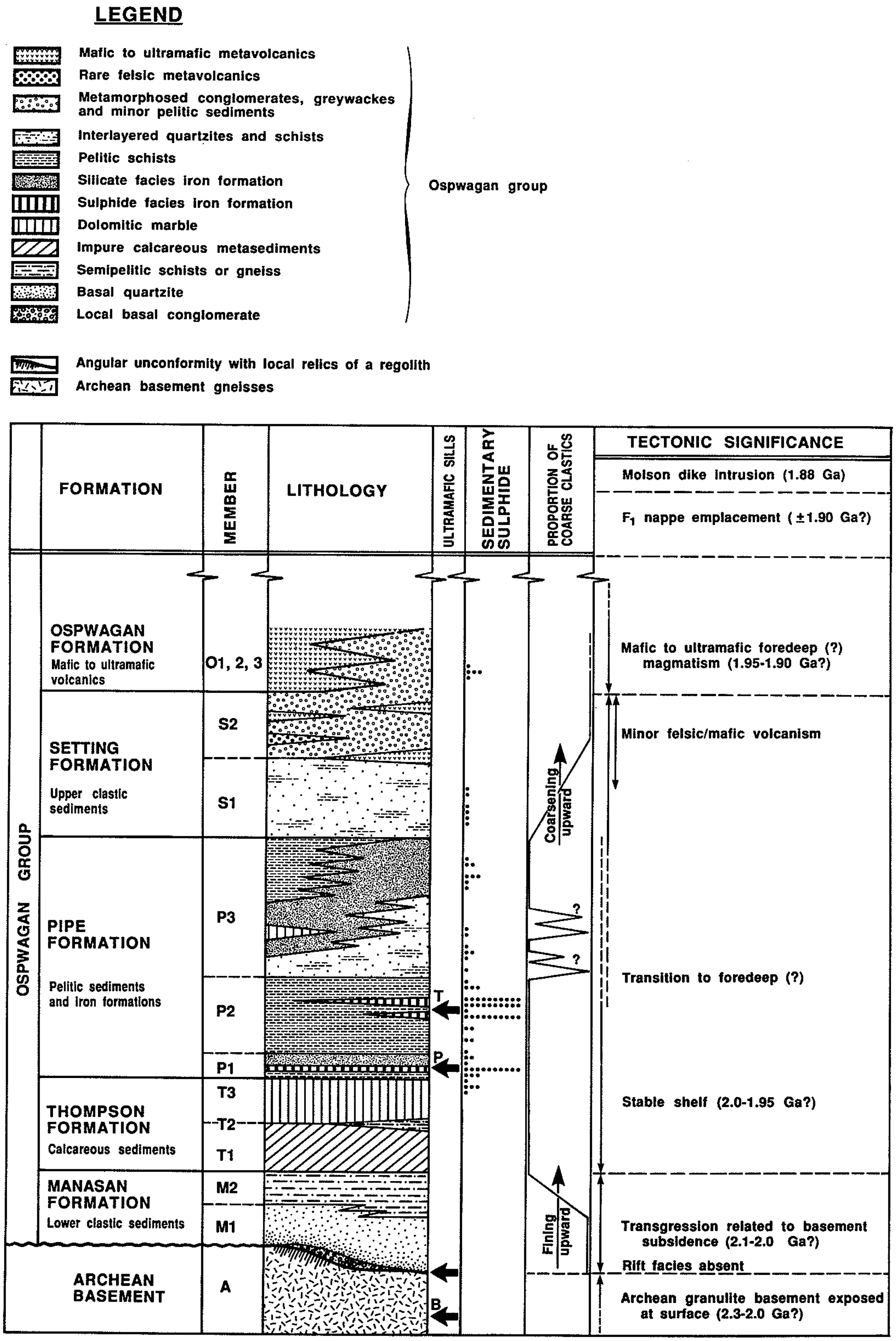


Figure 42: Stratigraphy of the Ospwagan Group and its tectonic significance for the early development of the Thompson Nickel Belt.

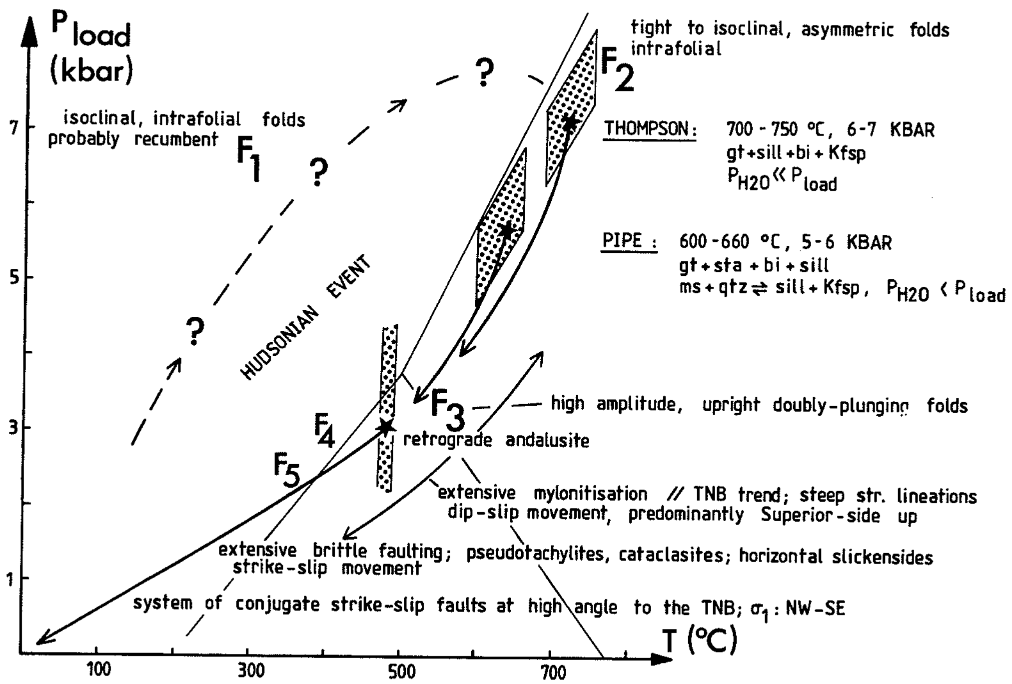


Figure 43: Generalized P,T,deformation-loop for the Thompson Nickel Belt (Bleeker, 1990).

uniform thickness of this lower clastic sequence, over strike lengths of many tens of kilometers, suggests its deposition was related to a transgression that swept throughout the area in response to passive margin subsidence, rather than to infill of localized rift basins. The TNB thus represents a domain somewhere on the subsided margin of the Superior plate, but it does not constrain the location of the rifted margin. Remnants of the Ospwagan Group are truncated by the fault-bounded western margin of the TNB, a relatively late structure known as the "Churchill-Superior boundary fault" (the Setting Lake lineament of Rance, 1966). The original extent of the Ospwagan Group and consequently the Superior plate must have reached much further west and probably still does so in the subsurface.

The clastic Manasan Formation is overlain by a sequence of chert, siliceous dolomite (Thompson Formation), graphitic sulphide facies iron formation, silicate facies iron formation, pelitic schists and again silicate facies iron formation (Pipe Formation). The lower part of this sequence (Thompson Formation) suggests establishment of a stable platform which evolved into an active tectonic environment-possibly a foredeep, with the recurrence of locally very immature, coarse clastic facies (Setting Formation; Fig. 42). Which lithostratigraphic horizon signifies exactly the platform to foredeep transition is not clear but following Hoffman (1988b), it is suggested that the transition took place prior to deposition of the second and main cycle of silicate facies iron formation (P3 member of Pipe Formation; Fig. 42).

Clastic foredeep sediments of the Setting Formation are associated with minor mafic and felsic volcanics and are overlain by the main sequence of mafic to ultramafic volcanics (Ospwagan Formation) at the top of the Ospwagan Group.

## Structural-Metamorphic History

Earliest structures due to compressional tectonism are isoclinal $F_1$ folds (Bleeker, 1990) which may be of regional extent, such as the nappe-like $F_1$ fold that dominates the Moak Lake-Pipe Lake region (Fig. 45, 46, 47 and 48). Intensely reworked basement forms the core of this

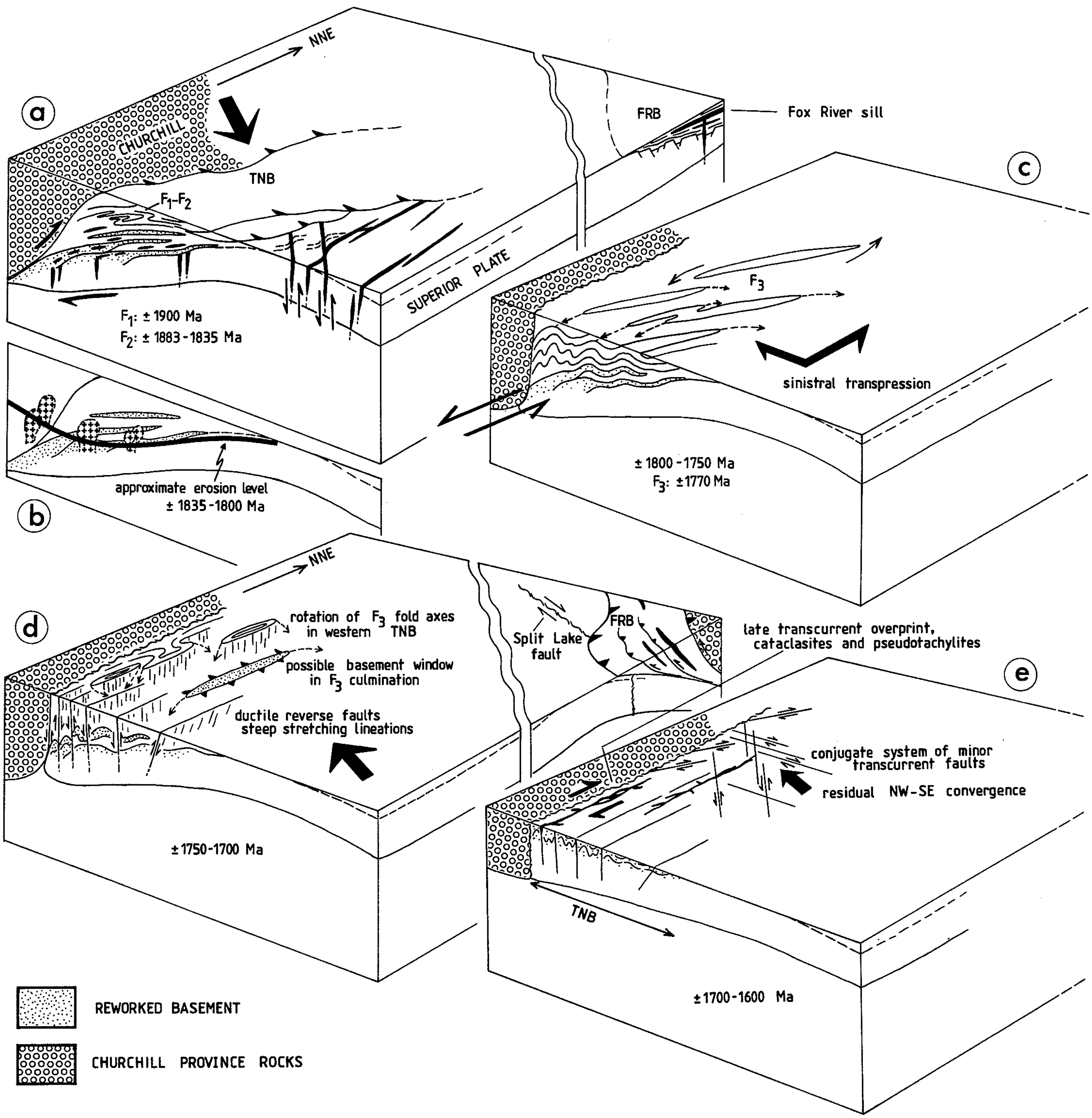


Figure 44: Time-sequential block diagrams, illustrating the tectonic evolution of the Thompson Nickel Belt (Bleeker 1990).

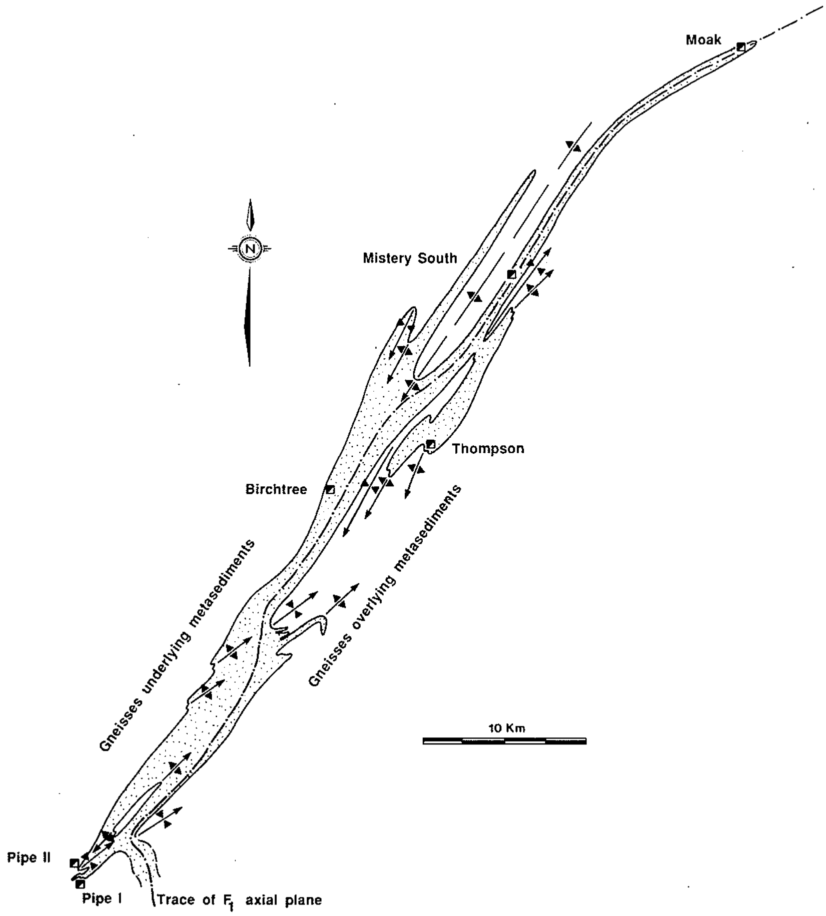


Figure 45: Simplified map of the Moak Lake-Pipe Lake area in the northern part of the Thompson Nickel Belt. Ospwagan Group metasediments (stippled pattern) occur within the deeply dissected remnant of a refolded nappe structure. Metasediments are completely enclosed by reworked basement gneisses and young away from the gneiss-metasediment contact, which represents a transposed angular unconformity. The trace of the $F_1$ axial plane and axes of major $F_3$ folds are indicated, as well as the localities of Ni sulphide deposits.

structure and thus locally overlies downward-facing supracrustals, such as at Thompson Mine. The metamorphic regime during $F_1$ is unknown (Fig. 43) but basement involvement in the nappe structure suggests at least lower amphibolite facies conditions. Timing of $F_1$ is uncertain but predated 1883 Ma since $F_1$ folds are cross-cut by mafic dikes which can be correlated with the Molson dike swarm. $F_1$ is overprinted by a second phase of tight to isoclinal folds ($F_2$), which developed under high temperature conditions. On a mesoscopic scale $F_2$ folds are prominent and fold Molson dikes. $F_2$ folds were probably recumbent and represent a second phase of ductile thrusting during which hot Kisseynew gneisses may have been emplaced onto the TNB.

The thermal peak of regional metamorphism overprinted $F_2$ and probably occurred around 1.82 Ga. The combined $F_1$-$F_2$ history can be interpreted as a phase of crustal thickening during which a SE tapering

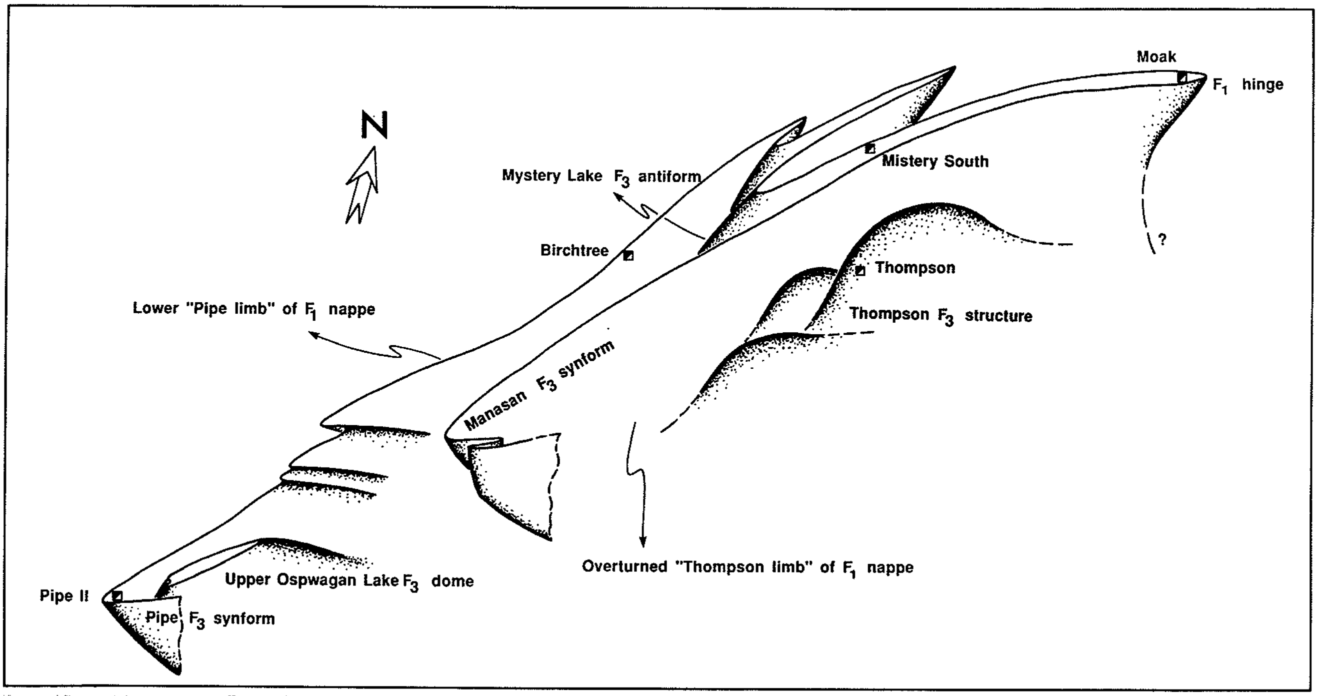


Figure 46: 3D sketch illustrating parts of the refolded nappe structure. The closure at Moak Mine represents an original $F_1$ hinge. The attitude of the $F_1$ axis and the overall vergence of the nappe are not well constrained.

wedge of recumbent folds and thrusts was emplaced on the margin of the Superior plate (Fig. 44a). Thermal relaxation of the thickened crust culminated in the generation of anatectic granites and the thermal peak of metamorphism (Fig. 44b). At least 30 Ma later and at much lower temperatures, intense sinistral transpression of the nappe/thrust pile produced high amplitude, nearly upright, doubly-plunging $F_3$ folds (Fig. 44c). These are the most obvious structures throughout the TNB, transposing the preexisting recumbent fold pile into a steep gneiss and schist belt. Axial planes of macroscopic $F_3$ folds dip steeply to the SE, trend N35-50E, and form a left-stepping en échelon pattern, with axial traces trending 0-15° clockwise of the N35E trend of the belt.

The main phase of mylonitization occurs late during or overprints $F_3$ and is confined to shear zones which tend to be parallel to steeply dipping limbs of the upright $F_3$ folds and thus conform to the en échelon structural trends of the belt. Obvious kinematic indicators in these shear zones reveal dip-slip (Fig. 44d). The ductile shear zones are overprinted by pseudotachylite generating brittle-ductile and brittle faults, which are steep and (sub)parallel to the belt. These faults are concentrated along the western margin of the belt, and are especially numerous along the "Churchill-Superior boundary fault". Earlier faults indicate sinistral strike-slip displacement, and are a late expression of the $F_3$ sinistral transpressive regime. Late movement on these faults is however dextral. A late system of conjugate, transcurrent brittle faults is pervasive throughout the belt (Fig. 44e) and developed in conjunction with dextral transpression on the main boundary fault.

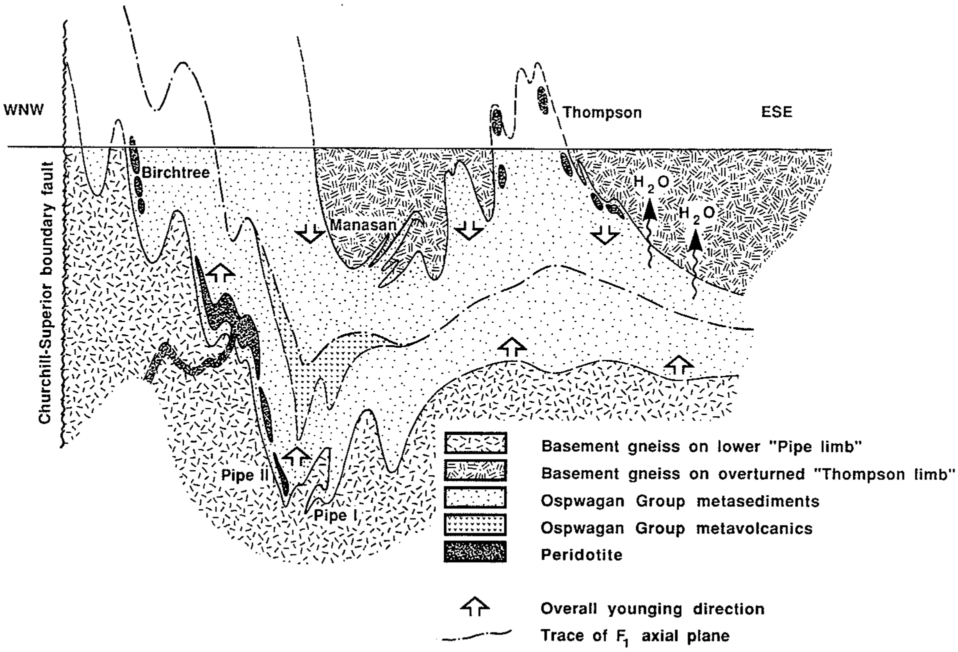


Figure 47: Schematic cross section through the refolded nappe structure. Note the overturned "Thompson Limb", the metasedimentary core and trace of the $F_1$ axial plane, and the lower "Pipe limb" of the nappe. Upright folds are $F_3$ structures. Ospwagan Group metavolcanics (Ospwagan Formation) occur on the lower "Pipe limb" of the structure.

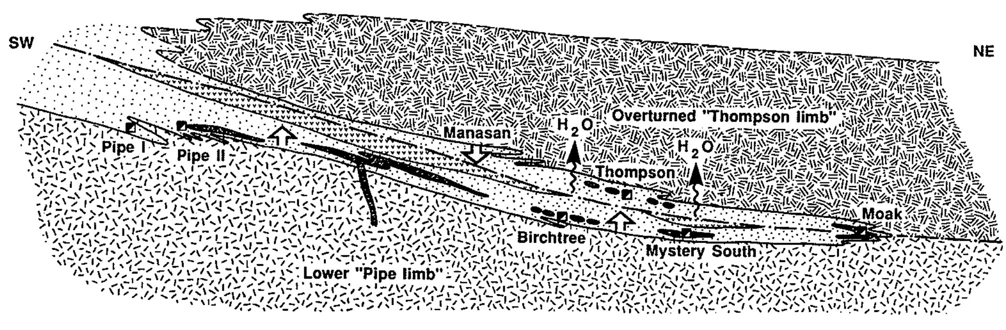


Figure 48: NE-SW "longitudinal" cross section through the refolded nappe structure. For legend refer to Figure 47. Upright $F_3$ folds are neglected in this schematic section to illustrate to original geometry of the $F_1$ nappe. Gneisses on the overturned "Thompson limb" show higher strain and were metasomatized by metamorphic fluids derived from the metasedimentary core of the nappe. Extreme stretching on the overturned limb has locally reduced the thickness of metasediments to just a few metres, such as along the east shore of Upper Ospwagan Lake. Subtle lithostratigraphic differences between "Thompson limb" and "Pipe limb" metasediments (cf. Figure 49a and b) reflect their large primary separation.

**Nickel Deposits in the Moak Lake-Pipe Lake Area**

Although many deposits are known from the southern part of the belt, some of which have been mined for some time such as the Falconbridge-owned Manibridge deposit (Coats and Brummer, 1971), the Moak Lake-Pipe Lake area in the northern part of the belt has been the most productive. All deposits in this area occur within the Early Proterozoic cover sequence which is preserved in the deeply dissected remnant of a complex fold interference pattern involving a $F_1$ nappe refolded by tight, upright, doubly plunging $F_3$ folds (Fig. 45). Figure 46 gives a simplified three dimensional sketch of parts of the structure, illustrating a lower upward facing "Pipe limb" and a downward facing, regionally overturned "Thompson limb". Upright $F_3$ folds are best illustrated in a transverse cross section (Fig. 47). Figure 48 shows a schematic cross section through the regional structure parallel to the $F_3$ axial planar trend. This allows the younger $F_3$ folds to be ignored and consequently this section provides the best picture of the $F_1$ nappe.

All deposits within the structure are associated with ultramafic sills which show variable degrees of disruption or boudinage (Fig. 48). The strain magnitude is extreme on the overturned "Thompson limb", but is much less on the lower upward facing "Pipe limb".

Another interesting consequence of the $F_1$ nappe structure is the metamorphic-metasomatic contrast between the lower "Pipe limb" and the overturned "Thompson limb". Reworked grey gneisses on the lower limb are still largely tonalitic in character, comparable to unreworked equivalents of the Archean foreland, whereas reworked gneisses on the overturned "Thompson limb" are often pink in colour, have a considerable K-feldspar content and show an abundance of pegmatitic sweats. The apparent addition of such components as potassium is attributed to upward migration of metamorphic fluids derived from the dehydrating metasediments in the synformal core of the nappe (Fig. 47 and 48).

Detailed lithostratigraphic analysis of the multiply transposed supracrustals shows that ultramafic sills intruded the cover sequence at various levels (Fig. 42). Sill or dike-like bodies occur also within the underlying basement. The Pipe II sill intruded low in the cover sequence, below the pelitic schists, along a graphitic sulphide facies iron formation (Fig. 49a). Other ultramafic bodies on the lower limb of the nappe occur in a similar lithostratigraphic position, e.g. those at Birchtree Mine. The Thompson sill intruded higher in the sequence, near the top of the pelitic schist unit (Fig. 49b). This horizon is also characterized by large concentrations of sedimentary sulphides in the form of disseminated, banded or massive pyrrhotite in a host of extremely graphitic schist or interlayered with chert. This second level of sulphide facies iron formation can also be identified at Pipe II Open Pit, where it forms a 10 to 50 centimetre thick band of pyrrhotite with inclusions of graphitic schist and chert.

All known deposits in the Moak Lake-Pipe Lake area are thus associated with major sedimentary sulphide concentrations. They combine the occurrence of an ultramafic sill with either the lower (Pipe II deposit) or the upper (Thompson deposit) sulphide facies iron formation. A classical problem of the Thompson Nickel Belt ore bodies has been the locally very high ratio of sulphide to ultramafic parent rocks (e.g. Table II in Peredery et al, 1982). Since the tonnage of sedimentary sulphides is in principal unlimited, it is thus attractive to involve the sedimentary sulphides in a genetic model for the origin of the Ni ore (Naldrett et al., 1979). Field observations, textural relationships and sulphide geochemistry, however, clearly indicate a magmatic origin for the bulk of the nickeliferous sulphides suggesting that assimilation in the intrusive stage has been the controlling factor in the genesis of voluminous Ni ore.

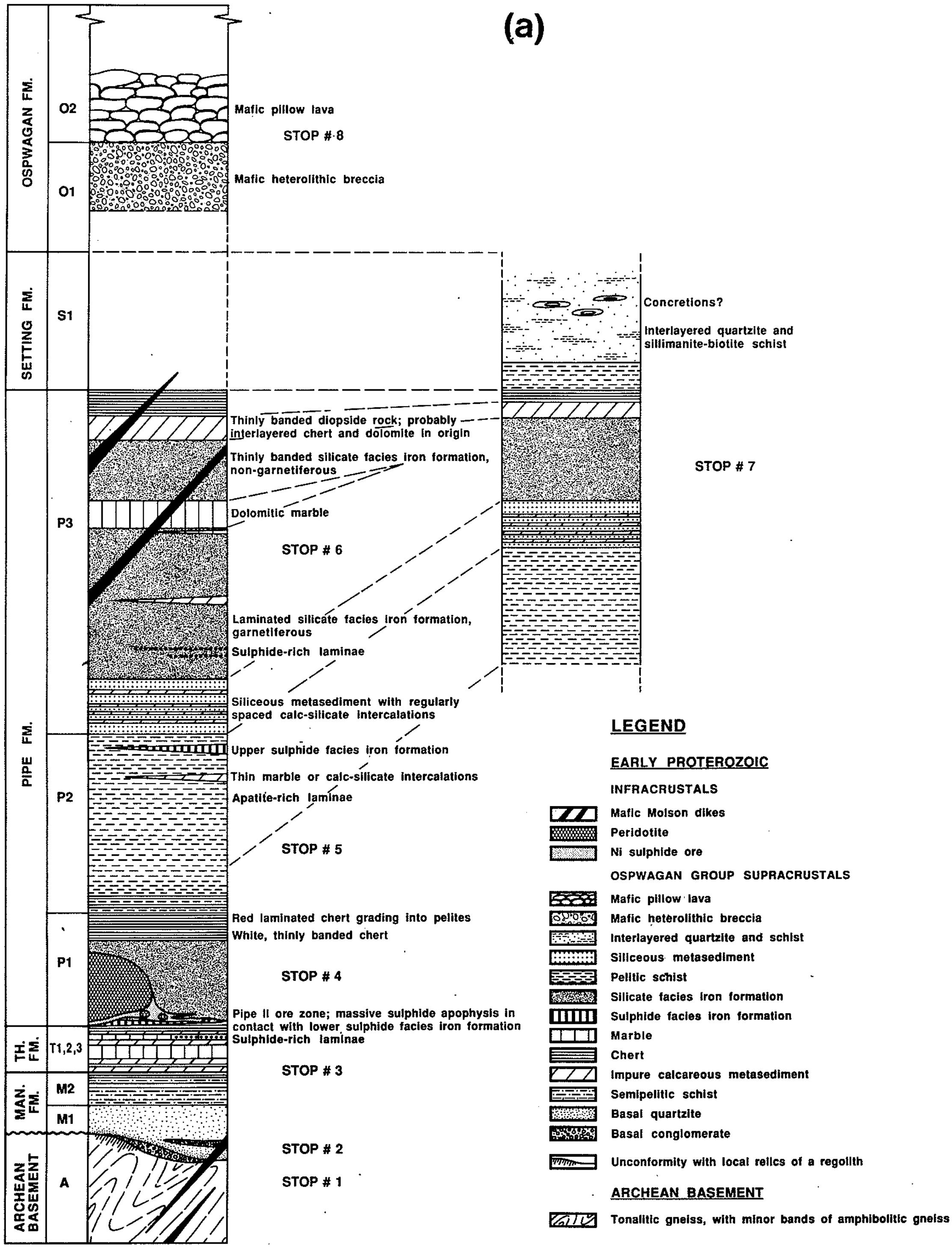


Figure 49: Reconstructed Ospwagan Group lithostratigraphy for Pipe II Open Pit (a) and Thompson Open Pit (b)(folllowing page). Note the different levels of the Pipe II and Thompson ore zones, both along thin sulphide facies iron formations. Excursion stops are indicated.

(b)

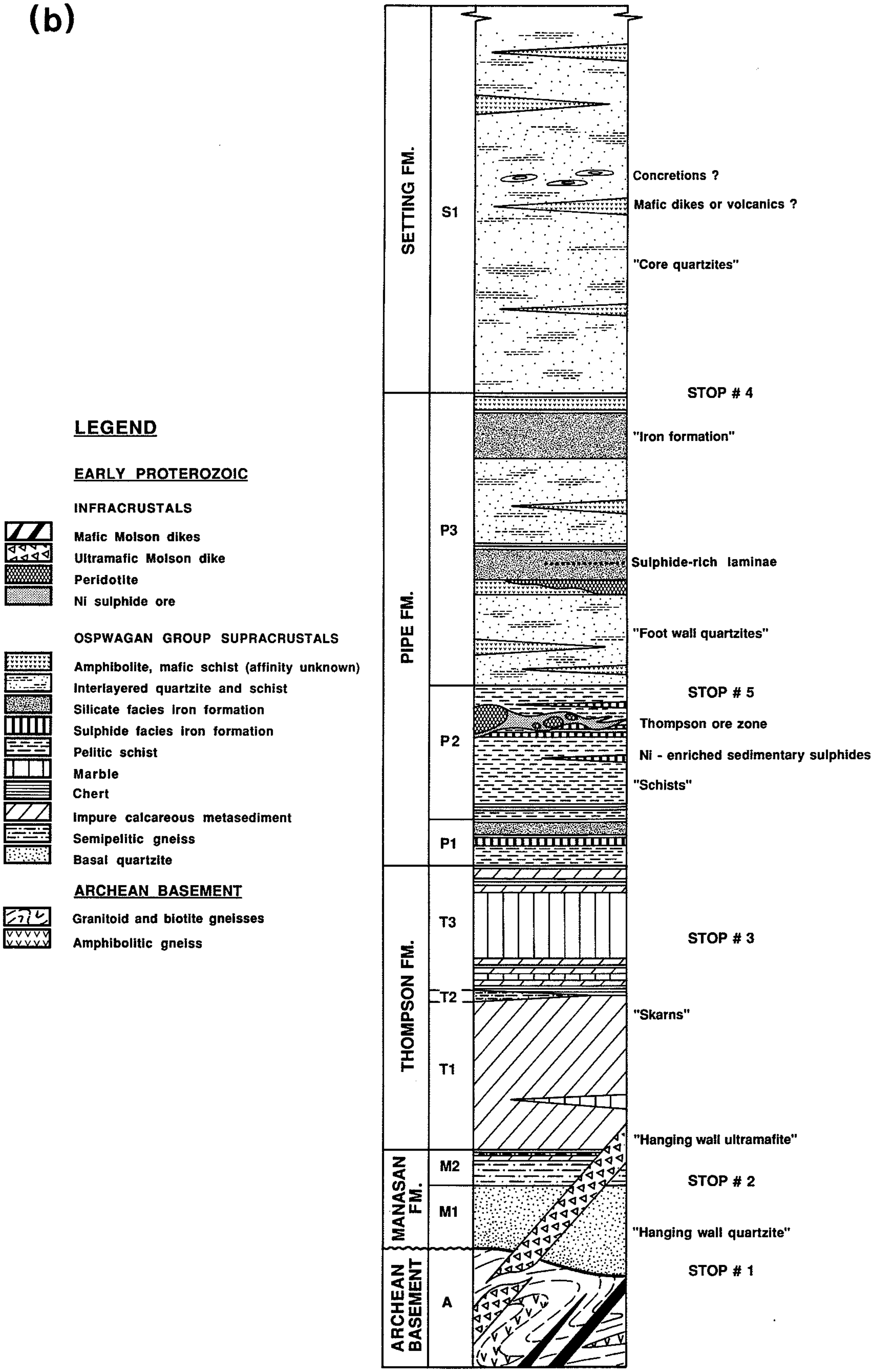
LEGEND
EARLY PROTEROZOIC
INFRACRUSTALS
Mafic Molson dikes
Ultramafic Molson dike
Peridotite
Ni sulphide ore
OSPWAGAN GROUP SUPRACRUSTALS
Amphibolite, mafic schist (affinity unknown)
Interlayered quartzite and schist
Silicate facies iron formation
Sulphide facies iron formation
Pelitic schist
Marble
Chert
Impure calcareous metasediment
Semipelitic gneiss
Basal quartzite
ARCHEAN BASEMENT
Granitoid and biotite gneisses
Amphibolitic gneiss
SETTING FM.
S1
Concretions ?
Mafic dikes or volcanics ?
"Core quartzites"
STOP # 4
PIPE FM.
P3
"Iron formation"
Sulphide-rich laminae
"Foot wall quartzites"
STOP # 5
P2
Thompson ore zone
Ni - enriched sedimentary sulphides
"Schists"
P1
THOMPSON FM.
T3
STOP # 3
T2
"Skarns"
T1
"Hanging wall ultramafite"
MANASAN FM.
M2
STOP # 2
M1
"Hanging wall quartzite"
ARCHEAN BASEMENT
A
STOP # 1

**Thompson Ni Sulphide Deposit**

History

After 10 years of intense exploration in the area, during which the low grade Moak and Mystery deposits were outlined, INCO discovered the Thompson ore body in 1956. A shaft had been sunk at Moak the previous year, for underground exploration and to prepare this deposit for production, but theseoperations were discontinued as soon as the Thompson discovery proved to be of sufficient tonnage (Fraser, 1985). At Thompson, production commenced in 1961 at which time 25 million tonnes of ore with 2.97% combined Ni-Cu had been intersected (Zurbrigg, 1963). A figure for the total tonnage has not been published but is estimated at 50 to 100 million tonnes at a similar grade (tonnages mentioned are rough estimates ment to give an order of magnitude). However, if dilution by wall rocks and redistribution of Ni to originally barren sedimentary sulphides is taken into account, the original tonnage of magmatic Ni sulphides must be much lower, possibly in the range of 20 to 40 million tonnes with approximately 10% Ni on a 100% sulphide basis.

Present production capacity of the Thompson facilities amounts to 50 million kilograms of refined Ni per year (Hopkins, 1986). Thompson underground operations provide approximately 6000 tonness of ore per day. During the seventies and early eighties additional ore supply came from Pipe Open Pit. Since 1986, the additional supply has come from the Thompson Open Pit and recently Birchtree Mine has been reopened.

The more than 1500 m long Thompson Open Pit was designed to mine 6.5 million tonnes of Ni sulphide ore (Hopkins, 1986) that remained as crown pillars between 400' level underground operations and surface. However, to get access to these near-surface ore reserves, extensive post-glacial overburden, consisting mainly of varved clays, had to be removed. This was accomplished by dredging during the period 1982-1986. Caprock drilling and first blasting of ore and wall rock commenced in late 1985.

A new open pit, called the South Pit and situated just southwest of the present pit, is currently being dredged and is planned to come on stream when the Thompson Open Pit is phasing out over the next two years.

Geology

The Thompson ore zone has a six km long surface trace, has been proven beyond 1500 m depths and is still partly open. The ore body is stratabound and occurs within and generally near the top of the pelitic schist unit (P2 member of the Pipe Formation; Fig. 49b, 50, 51 and 52). Despite the complex and protracted structural-metamorphic history of the ore body, involving six folding phases and sillimanite-garnet-K feldspar grade metamorphism, no significant remobilization of sulphides beyond the original host unit has been observed, except along late faults and as infilling of late stage tension gashes. Important remobilization occurred along the original host horizon, but is described as "passive" in response to folding and extension (Fig. 53b). Consequently, magmatic Ni sulphides do not extend beyond the range of ultramafic boudins which represent remnants of the original parent sill.

Sulphide Mineralization

Despite the complex history and overlap in some characteristics, sedimentary and magmatic sulphides can be recognized as two distinct sulphide populations, using field observations, structural, textural, mineralogical and chemical criteria (Table 5). However, relationships are complex due to interaction of sedimentary, magmatic, metamorphic and deformational processes.

**Sedimentary sulphides** consist of pyrrhotite, chalcopyrite, late pyrite and accessory phases and show: 1) a regional lithostratigraphic relationship, with the bulk of the sedimentary sulphides concentrated along two horizons (Fig. 42 and 49), 2) millimetre to decimetre scale interlayering with commonly extremely

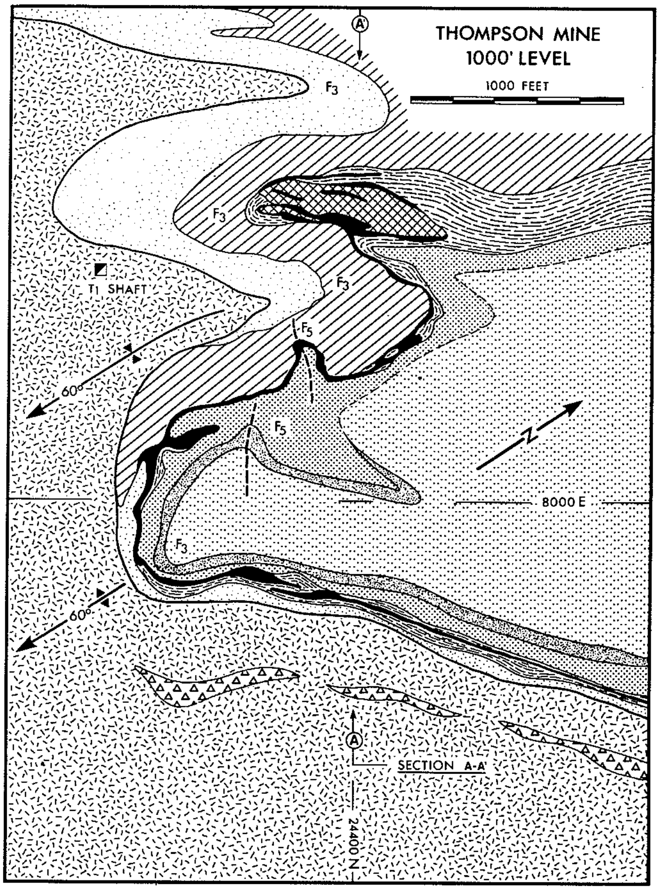


Figure 50: 1000 feet level map of Thompson Mine geology. For legend and section A-A', refer to Figure 11. Note the steeply south plunging $F_3$ hinges. The north-south trending, subvertical $F_3$ limb is refolded by vertically plunging $F_5$ folds. Modified after Zurbrigg, 1963.

graphitic schist, chert or silicate facies iron formation, 3) variable Cu concentrations which sometimes correlate with centimetre scale lithological banding, and 4) low Cr concentrations, e.g. 100 ppm. Cr correlates negatively with sulphide concentration and thus resides in the schist fraction of the samples. Commonly, the thicker sedimentary sulphide bands (> 5 cm) have been deformed into breccia sulphide, showing numerous schist, chert or other lithic inclusions "suspended" in a pyrrhotite matrix. All inclusions are however local and derived from the schist or chert intercalations or hosts. No "exotic" inclusions of ultramafic rock have been observed. Sedimentary sulphides are generally fine grained and impure, i.e. they contain numerous small inclusions of graphite and silicates such as quartz and biotite. Based on Ni concentrations, two types can be distinguished:

**Barren sedimentary sulphides:** have Ni concentrations below 500 ppm (1000 ppm on a 100% sulphide basis) and occur beyond the immediate vicinity of main Ni ore zones (Fig. 54 and 55).

**Ni-enriched sedimentary sulphides:** indistinguishable from barren sedimentary sulphides, except for elevated levels of Ni and Co. All occurrences of this sulphide type are in close proximity to main Ni sulphide ore zones. Ni concentration varies from slightly enriched (> 1000 ppm) up to 10 wt% and shows inverse correlation with distance to main Ni ore zones (Fig. 54 and 55). **"Mineralized schist"**, a minor but important ore type at Thompson, belongs to this sulphide type.

**Magmatic nickeliferous sulphides** consist of pyrrhotite, pentlandite, chalcopyrite, gersdorffite, chrome spinel and various accessory and secondary

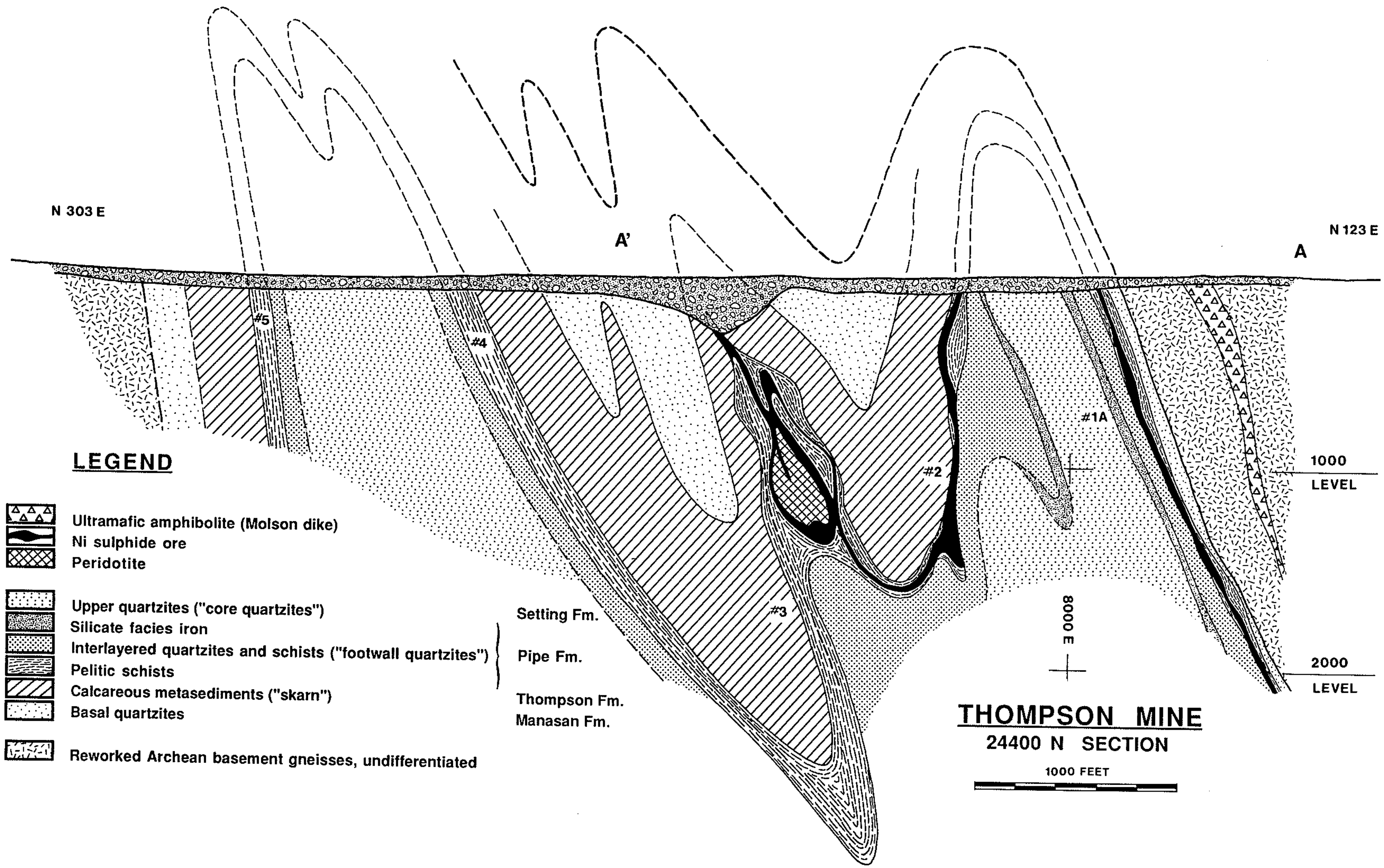


Figure 51: Cross section through the downward facing Thompson structure, looking NE. High amplitude, steeply southeasterly inclined folds belong all to the $F_3$ generation, which refold the overturned "Thompson limb" of the $F_1$ nappe. For reference, the Thompson Open Pit is situated on the overturned #1 limb of the structure.

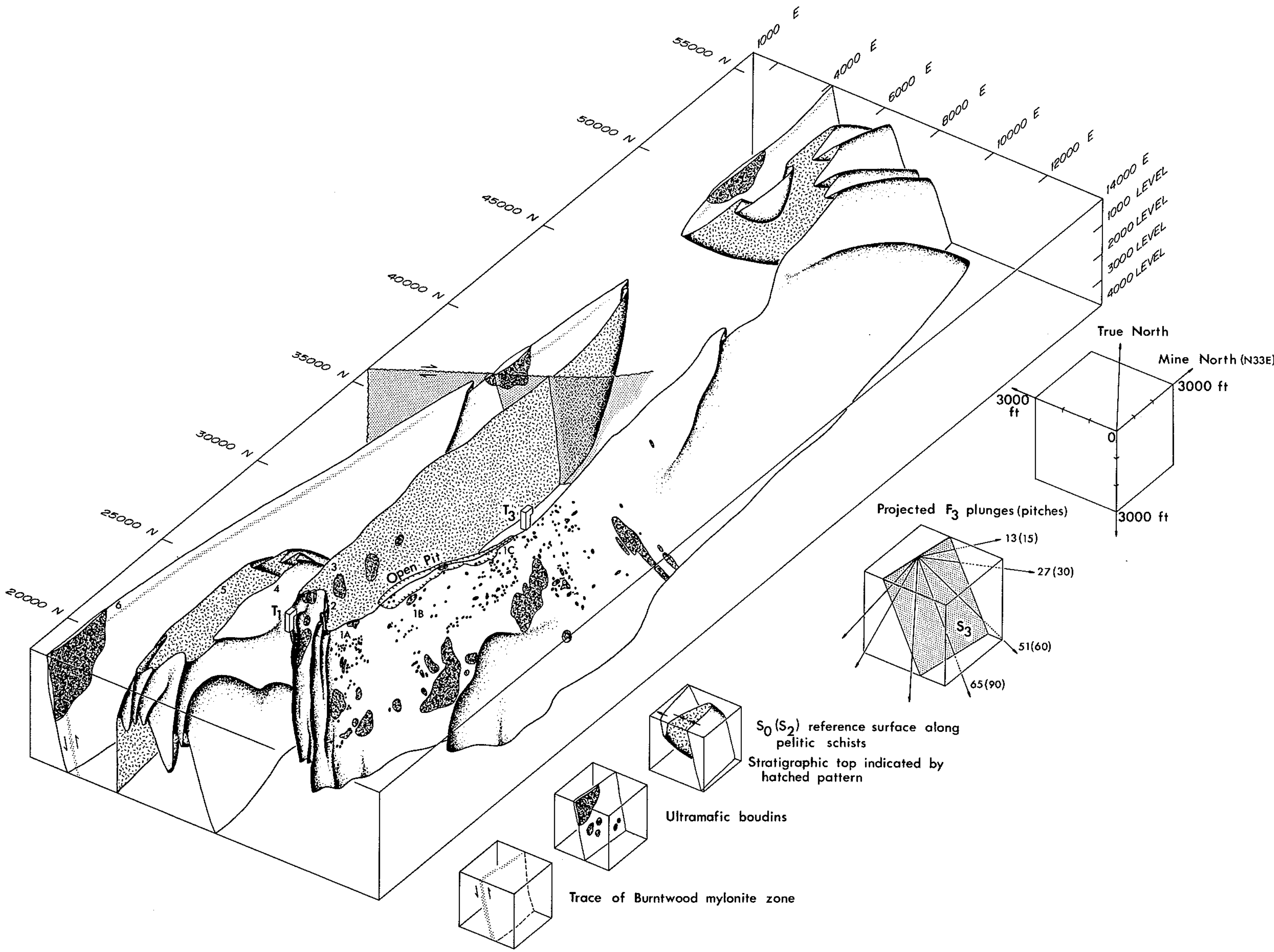


Figure 52: Orthographic block diagram of the Thompson structure. View towards N358°E, 35° down. Coordinates refer to Thompson Mine grid. Facing of the reference horizon indicated by patterned top. Note the extreme disruption of the ultramafic parent sill along the reference horizon. Extraparental magmatic sulphides occur stratabound along the reference horizon and do not extend beyond the range of ultramafic boudins.

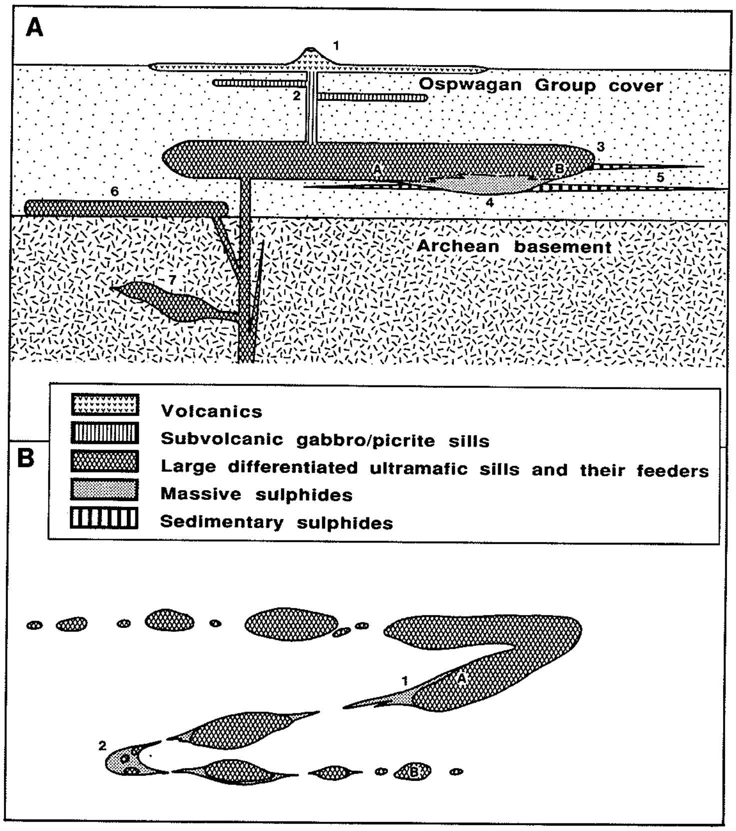


Figure 53: (a) Ultramafic magmatism near the end of Ospwagan Group deposition led to extrusion of mafic to ultramafic volcanics (1) and intrusion of subvolcanic gabbro/picrite sills (2). Large ultramafic sills deeper in the cover sequence and more irregular bodies within the basement (3, 6 and 7) are thought to be related to the volcanics. It is suggested that some of the sills may have acted as magma chambers to some of the volcanics. Locally, sills intruded along sulphide facies iron formations (5), giving rise to large concentrations of magmatic sulphides (4) through assimilation of sedimentary sulphide. (b) Stretching and folding of the parent sill, with its localized magmatic sulphide concentration between points A an B (cf. Figure a), is accompanied by "passive" remobilization of sulphides along the host horizon. Massive sulphide concentrations occur in boudin necks (1; e.g. Pipe II) and as completely separated lenses between larger boudins (2; such as some of the ore lenses at Thompson), but do not occur beyond the original boundaries A and B.

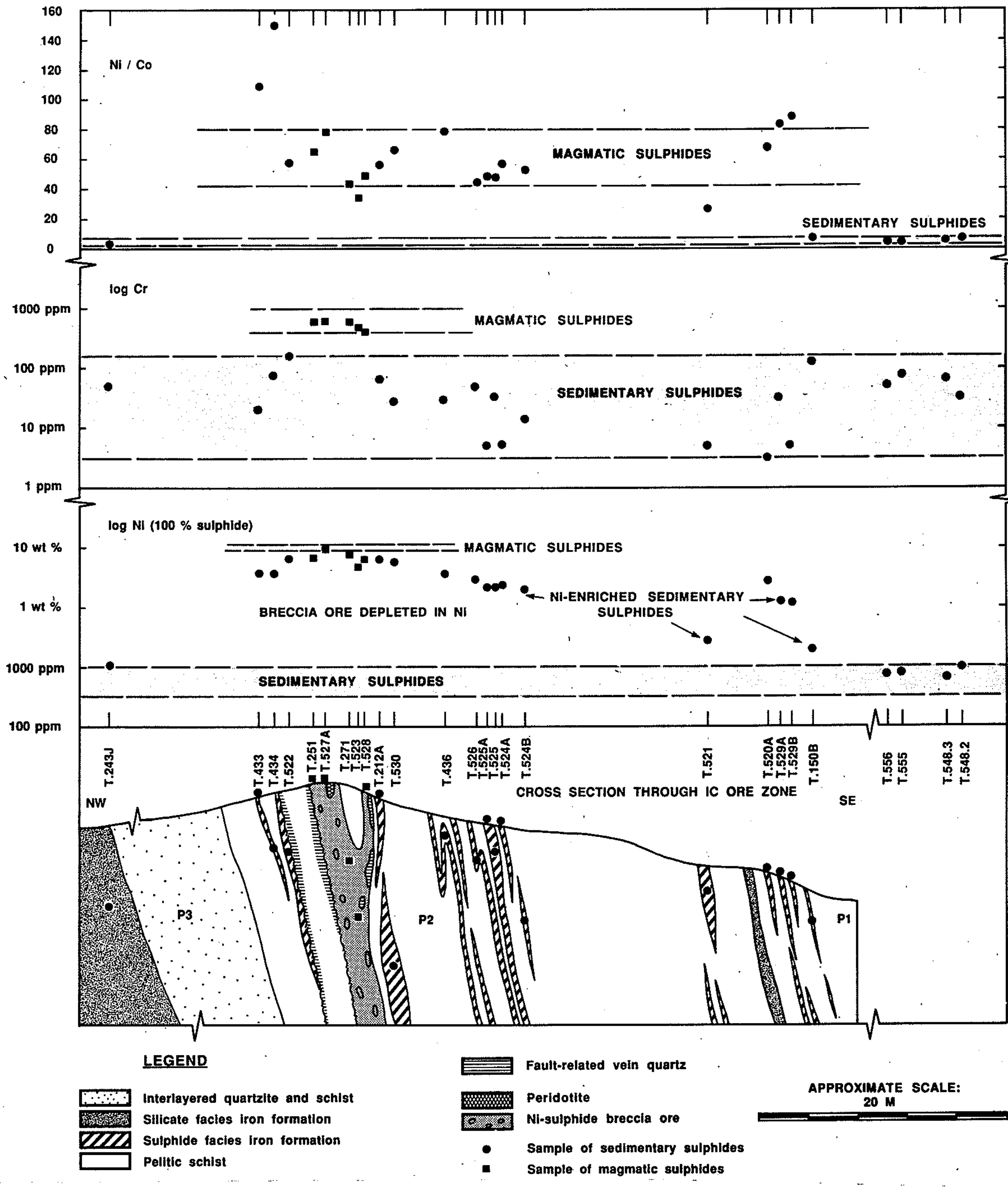


Figure 54: Ni, Cr and Ni/Co values for "whole rock" samples (n=22) across 1C ore zone at the north end of the Thompson Open Pit. Barren sedimentary sulphide samples (n=4) at the right side of the diagram were sampled at larger distances from the Thompson ore body. Sample locations of magmatic (solid squares) and sedimentary sulphides (solid dots) are indicated on the cross section. Note: 1) the extensive redistribution of Ni (and Co) from magmatic sulphides to adjacent sedimentary sulphides. 2) Inverse correlation of Ni-enrichment with distance to magmatic ore zone. 3) Magmatic sulphides are depleted in Ni relative to massive ore in the 1B zone. 4) Magmatic and sedimentary sulphides can still be distinguished on the basis of their Cr content. 5) Ni/Co ratios peak above the magmatic range in Ni-enriched sedimentary sulphides, suggesting greater mobility for Ni relative to Co.

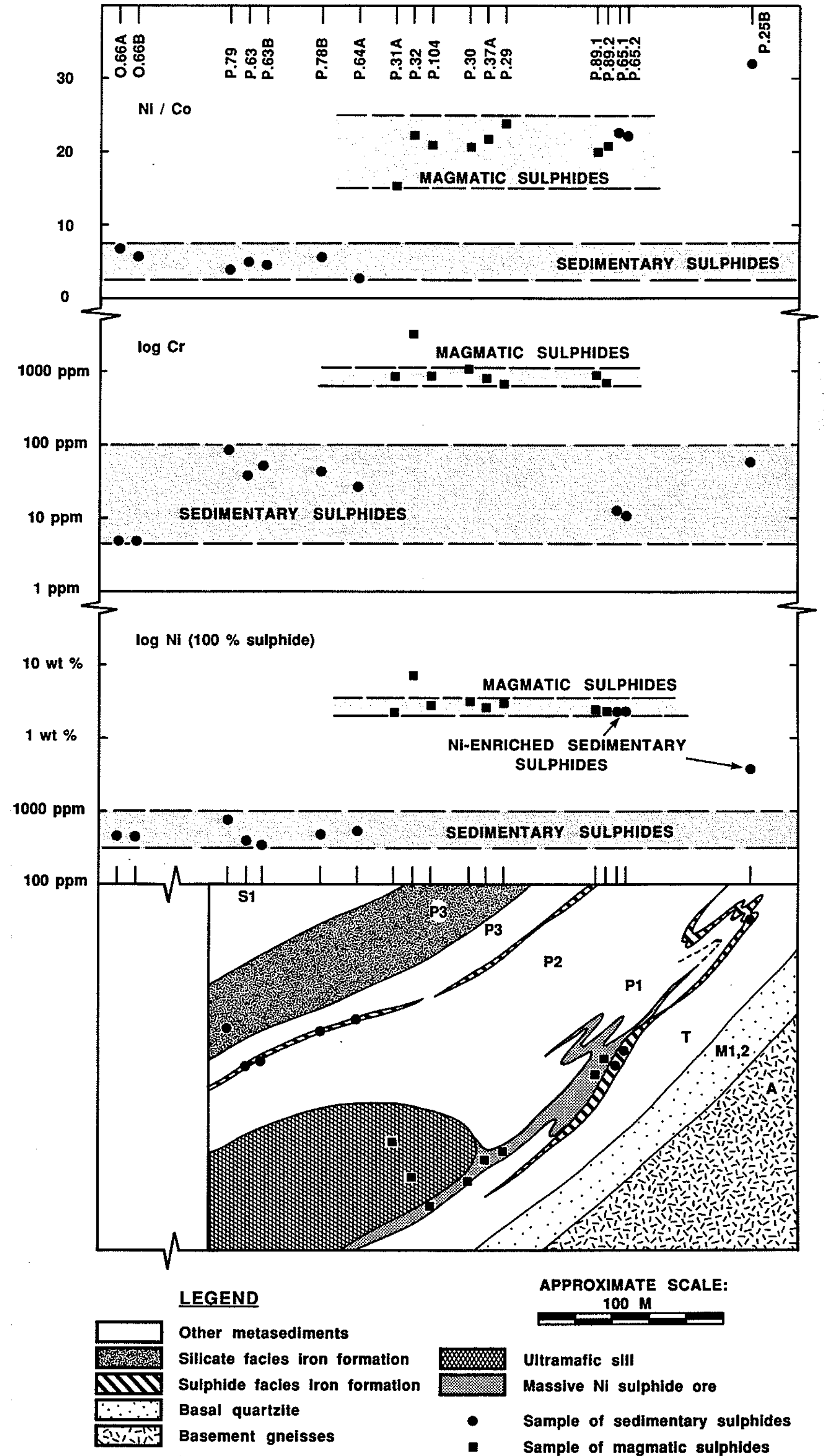


Figure 55: Ni, Cr and Ni/Co values for "whole rock" samples (n=16) across the Pipe II ore zone. Barren sedimentary sulphide samples from Ospwagan Lake (n=2) are included on the left side of the diagram. Comments as for Figure 54.

Table 5: Representative analyses of sulphide samples

| THOMPSON: | | | --- wt% --- | | ---------- ppm ---------- | | | | | ------- wt. ratios ------- | | | |
|---|---|---|---|---|---|---|---|---|---|---|---|---|---|
| sample | type(*) | | S | C | Ni | Cu | Co | Zn | Cr | Ni*/S | Ni/Cr | Ni/Cu | Ni/Co |
| T.372.1 | MI | I | 4.7 | 0.6 | 13000 | 270 | 270 | 280 | 590 | 0.278 | 22.0 | 48.1 | 48.1 |
| T.534 | ME | M | 35.7 | 0.1 | 98000 | 3700 | 1300 | 560 | 930 | 0.275 | 105.4 | 26.5 | 75.4 |
| T.512B | ME | M | 38.0 | 0.0 | 105000 | 5300 | 1500 | 550 | 560 | 0.276 | 187.5 | 19.8 | 70.0 |
| T.188C | ME | BR | 28.7 | 0.2 | 71000 | 3800 | 1100 | 360 | 530 | 0.247 | 134.0 | 18.7 | 64.5 |
| T.25 | ME | BR | 34.9 | 0.5 | 69000 | 310 | 1100 | 510 | 710 | 0.198 | 97.2 | 222.6 | 62.7 |
| T.512C | S | E | 27.6 | 5.6 | 66000 | 6000 | 1200 | 310 | 140 | 0.239 | 471.4 | 11.0 | 55.0 |
| T.425A | S | E | 32.9 | 1.9 | 52000 | 4000 | 660 | 280 | 5 | 0.158 | 10400.0 | 13.0 | 78.8 |
| T.436 | S | E | 19.9 | 4.0 | 18000 | 700 | 230 | 190 | 29 | 0.090 | 620.7 | 25.7 | 78.3 |
| T.521 | S | WE | 34.4 | 3.9 | 2500 | 900 | 93 | 63 | 5 | 0.007 | 500.0 | 2.8 | 26.9 |
| T.557 | S | WE | 15.5 | 0.1 | 1100 | 350 | 76 | 99 | 27 | 0.007 | 40.7 | 3.1 | 14.5 |
| T.556 | S | B | 16.1 | 1.9 | 300 | 440 | 65 | 82 | 51 | 0.002 | 5.9 | 0.7 | 4.6 |
| T.150B | S | B | 6.8 | 3.7 | 330 | 240 | 48 | 88 | 130 | 0.005 | 2.5 | 1.4 | 6.9 |
| T.548.3 | S | B | 19.0 | 14.0 | 330 | 1000 | 63 | 910 | 65 | 0.002 | 5.1 | 0.3 | 5.2 |
| T.243J | S,IF | B | 9.2 | 1.1 | 260 | 370 | 74 | 91 | 51 | 0.003 | 5.1 | 0.7 | 3.5 |
| T.558 | GN | B | 9.3 | 0.1 | 220 | 1200 | 170 | 93 | 34 | 0.002 | 6.5 | 0.2 | 1.3 |
| PIPE II: | | | | | | | | | | | | | |
| sample | type | | S | C | Ni | Cu | Co | Zn | Cr | Ni/S | Ni/Cr | Ni/Cu | Ni/Co |
| P.32 | MI | I | 2.8 | 0.1 | 5100 | 230 | 230 | 87 | 3200 | 0.183 | 1.6 | 22.2 | 22.2 |
| P.29 | MI | M | 39.8 | 0.2 | 31000 | 2500 | 1300 | 150 | 690 | 0.078 | 44.9 | 12.4 | 23.8 |
| P.89.1 | ME | M | 38.4 | 0.0 | 24000 | 2100 | 1200 | 200 | 870 | 0.063 | 27.6 | 11.4 | 20.0 |
| P.65.1 | S | E | 25.8 | 9.6 | 15000 | 1300 | 660 | 240 | 14 | 0.058 | 1071.4 | 11.5 | 22.7 |
| P.25B | S | WE | 15.0 | 9.7 | 1400 | 270 | 44 | 160 | 57 | 0.009 | 24.6 | 5.2 | 31.8 |
| P.63 | S | B | 19.6 | 3.9 | 200 | 330 | 40 | 1100 | 37 | 0.001 | 5.4 | 0.6 | 5.0 |
| O.66B | S | B | 30.8 | 3.6 | 360 | 400 | 62 | 580 | 5 | 0.001 | 72.0 | 0.9 | 5.8 |
| P.79 | S,IF | B | 6.0 | 2.0 | 120 | 140 | 32 | 160 | 85 | 0.002 | 1.4 | 0.9 | 3.8 |
| MOAK: | | | | | | | | | | | | | |
| sample | type | | S | C | Ni | Cu | Co | Zn | Cr | Ni/S | Ni/Cr | Ni/Cu | Ni/Co |
| MK.2 | MI | I | 8.2 | 0.0 | 11000 | 650 | 350 | 290 | 4400 | 0.133 | 2.5 | 16.9 | 31.4 |
| MK.3 | MI | SM | 16.4 | 0.1 | 19000 | 780 | 590 | 440 | 13000 | 0.116 | 1.5 | 24.4 | 32.2 |

*: Classification of sulphide samples:

first column:
MI : magmatic, intraparental
ME : magmatic, extraparental
S : sedimentary, pyrrhotite bands in graphitic schists or chert
S,IF: sedimentary, sulphide laminae in silicate facies iron formation
GN : pyrrhotite stringers in basement gneisses

second column:
I : interstitial, net-textured
SM: semimassive ore
M : massive ore
BR: breccia ore
E : Ni-enriched sedimentary sulphides, "mineralized schists"
WE: weakly Ni-enriched sedimentary sulphides
B : barren pyrrhotite

phases. They can be classified as "**intraparental**" or "**extraparental**" magmatic sulphides, depending on whether they occur within or external to the ultramafic parent rocks:

**Extraparental massive magmatic sulphides:** typical massive Ni sulphide ore at Thompson occurs as pods and lenses of variable size within the pelitic schist host rock. The extraparental magmatic nature of this main ore type is indicated by the following observations: 1) the occurrence adjacent to ultramafic boudins, 2) there is no known occurrence of this ore type beyond the range of ultramafic boudins, 3) the sulphides are often clean with little or no graphite, coarse grained, with few inclusions except for biotite flakes; if lithic inclusions are present, ultramafic inclusions are proportionally important, 4) the extraparental sulphides are chemically rather homogeneous with high Cr levels, e.g. 500 to 1500 ppm, and deposit-specific Ni/Cu, Ni/Co and Ni/S ratios, characteristics which they share with interstitial net-textured sulphides in the larger associated ultramafic boudins.

**Intraparental magmatic sulphides:** occur within ultramafic parent rocks as minor disseminations, net-textured interstitial sulphides, irregular interstitial sulphide specks or nests, and as semi-massive to massive concentrations in veins and breccias.

Other sulphide types can be recognized but are derived from the main types described above by operation of additional metamorphic or deformational processes:

**Mineralized pegmatite:** Ni-enriched sedimentary sulphides in which the schist component underwent pegmatitization; or locally pegmatites may have intruded sedimentary or magmatic sulphides.

**Breccia sulphide:** derived from preexisting sedimentary or magmatic sulphides by late ($F_3$ or post-$F_3$) deformation. The high ductility contrast between sulphides and country rock resulted in embrittlement of the wall rock and progressive incorporation of the fragments into the sulphide matrix ("Durchbewegung"). The abundance of inclusions correlates with progressive grain-size reduction of the sulphides. In the case of breccia ore derived from massive magmatic sulphides, it also correlates with progressive dilution of "primary" ultramafic inclusions with locally derived "secondary" inclusions of adjacent wall rocks.

**Pipe II Nickel Sulphide Deposit**

<u>History</u> (notes are taken from CIM Bulletin, May 1975, p. 120)

The Pipe II deposit was discovered in 1957. In 1961 INCO decided to mine the upper 720 feet of the orebody by open pit method and to sink a 1580 feet deep shaft to further explore the ore body underground. Dredging of silt and clay overburden began in 1967 and production from the open pit started in 1969. To facilitate mining of deeper parts of the ore body, the shaft was deepened to a depth of 3060 feet. However, unfavourable market conditions prevented the underground production from starting up. The open pit was mined out in 1984 at a depth of 800 feet. Currently, INCO is reassessing the Pipe II underground mine.

A total tonnage figure for the Pipe II deposit has not been published. Approximately 18 million tonnes of interstitial, breccia and massive sulphide ore has been mined from the pit.

<u>Geology</u>

The surface trace of the Pipe II ore zone is approximately one kilometre long and occurs for much of its length along the stratigraphic base of a more than two kilometre long, up to 150 m thick serpentinized ultramafic body (Fig. 56). The lens-like body, which is considered the boudinaged remnant of a larger sill, occurs on the western limb of the main mine structure-a tight, steeply northeast plunging $F_3$ synform with reworked basement gneisses on the limbs and highly deformed, staurolite

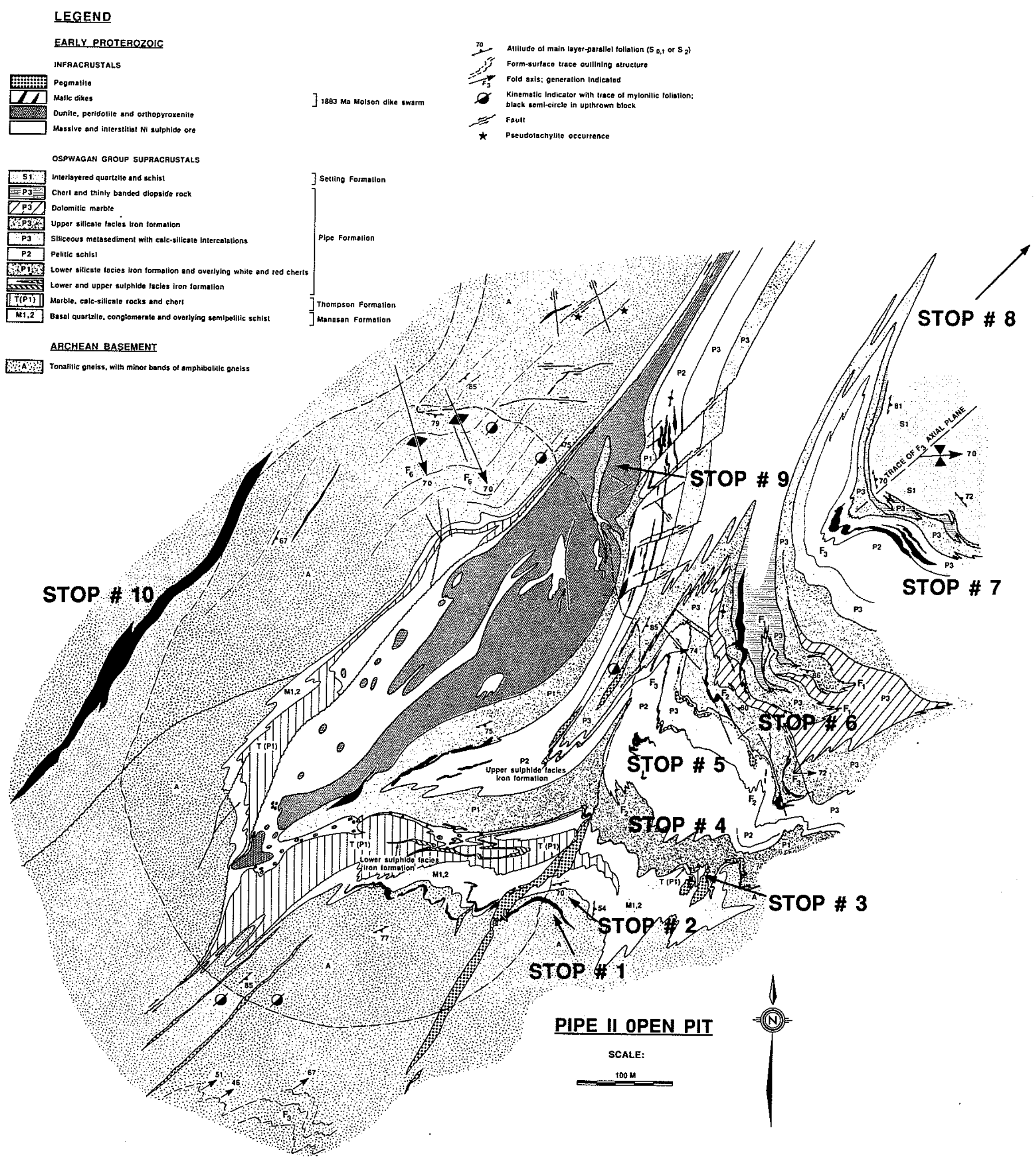


Figure 56: Geological map of Pipe II Open Pit (modified after Bleeker and Macek 1988b). Excursion stops are indicated.

grade Ospwagan Group cover rocks in the core. The ultramafic boudin dips 75° to the southeast and is conformable with the enveloping metasediments. Facing of the sill, based on its sulphide-->dunite-->peridotite-->orthopyroxenite differentiation profile, is towards the southeast and conforms to the overall younging direction of the enclosing metasediments on the western limb.

On a regional scale, the Pipe II ultramafic boudin is the southernmost member of a discontinuous array of ultramafic bodies which stretches from Pipe II Open Pit, along the west shore of Ospwagan Lake, to Birchtree Mine. Where the lithostratigraphic position of these bodies could be checked, they occur at exactly the same horizon within the Ospwagan Group cover sequence, i.e. above the carbonates and lower sulphide facies iron formation and below the first silicate facies iron formation (Fig. 49b). This intrusive level is well below the lithostratigraphic horizon of the Thompson ore zone.

Sulphide ore is concentrated near the abrupt southern termination of the Pipe II ultramafic boudin and extends beyond the parent body onto the eastern limb of the macroscopic $F_3$ fold, in the form of a complexly shaped, tapering apophysis-the so-called "hangingwall stringer" (Fig. 56). The more than 200 m long apophysis consists of extraparental massive sulphides carrying minor inclusions of serpentinized dunite right up to the point where it pinches out. Along its entire length it retains the same lithostratigraphic position as the parent sill on the western limb. The tapering apophysis is overprinted by $F_2$ and $F_3$ folds and is thus an early structural feature. This strongly suggests it formed during $F_1$ boudinage of the sill, by flow of basal massive sulphides towards a boudin neck. The local presence of sulphide mineralization in the sill possibly controlled location of the boudin neck. As at Thompson, the stratabound extraparental position of magmatic sulphides does not represent active remobilization but is due to passive remobilization accompanying boudinage of the parent sill in a stretching metasedimentary envelope (Fig. 53b). Further interesting conclusions can be drawn from a comparison of extraparental massive sulphide versus parent sill relationships at Pipe II and Thompson. In the lower strain Pipe II environment, the massive sulphide apophysis is still connected with its parent body and lithic inclusions are strongly dominated by dunite fragments. At Thompson, pods and lenses of extraparental massive sulphides may occur at distances of several hundred metres from large ultramafic boudins. The larger separation corresponds with an increase in wallrock inclusions.

The boudin-neck geometry suggest that a counterpart of the Pipe II deposit exists or did exist further along the intrusive horizon, possibly represented by the Pipe I deposit.

<u>Sill versus Flow</u>

The Pipe II ultramafic boudin is a remnant of a large conformable body. From an exploration and genetic point of view, it is very important to establish whether the body represents a flow or sill. The following observations have a bearing on this problem: 1) Ni-mineralized ultramafic bodies of similar nature occur within basement (e.g. the Bucko deposit) and at various levels within the cover sequence (e.g. along the basement cover interface, the Pipe II horizon, the Thompson horizon and at higher lithostratigraphic levels). 2) None of these bodies shows positive evidence for a flow origin. 3) Mafic to ultramafic volcanics do occur however, but stratigraphically overlie all ultramafic lenses within the underlying metasedimentary sequence. 4) No particular sedimentary rock is associated with the upper contacts of the ultramafic bodies. 5) The ultramafic bodies are well differentiated, medium to coarse grained, and as far as can be established, without a prominent upper chilled zone. One of the best contacts is exposed at Pipe II Open Pit and shows coarse orthopyroxenite grading into medium grained orthopyroxenite at the upper contact with silicate facies iron formation. The evidence clearly favours a sill origin.

It is suggested that the ultramafic sills may have acted as magma chambers to some of the overlying volcanics (Fig. 53a). Ultramafic magma which rose through the crust was denser than the sediment cover and would thus have had a tendency to spread laterally as soon as it ascended above the basement-cover interface. Progressive differentiation in the large sills extracted Fe-rich sulphide melt, olivine, chromite and orthopyroxene from the melt. Residual magma evolved towards lower densities which may have triggered further ascend to the surface. In this respect it is interesting to note that the localized occurrence of volcanics at the top of the Ospwagan Group correlates with relatively large ultramafic bodies in the footwall. This could also explain why evolved residual magma compositions appear to be lacking at the top of the ultramafic sills.

Sulphide Mineralization

The spectrum of sulphide mineralizations at Pipe II is essentially similar to Thompson with intraparental disseminated, net-textured interstitial, vein, breccia and massive magmatic sulphides, extraparental massive magmatic sulphides, Ni-enriched sedimentary sulphides and barren sedimentary sulphides. However, whereas at Thompson emphasis is on extraparental magmatic sulphides in the form of massive and breccia ore, and on Ni-enriched sedimentary sulphides, the bulk of Pipe II ore occurs within and at the base of the ultramafic parent sill.

Chemically, Pipe II ore is quite distinct with low Ni/S, Ni/Cu and Ni/Co ratios (Table 5). Chondrite-normalized PGE patterns of Pipe II ore samples are similar in shape but a factor 3 to 10 lower than those of typical Archean komatiite-related Ni sulphide ore (Naldrett et al., 1979; Fig. 57). Mineralogically, Pipe II ore consists of pyrrhotite, pentlandite, chalcopyrite, cubanite and locally abundant subhedral to euhedral spinel. Secondary phases are pyrite, marcasite, magnetite, violarite and mackinawite. Traces of galena have been observed in the sedimentary sulphides.

**Genesis of Ni Sulphide Mineralization in the Thompson Nickel Belt**

Chemical, textural and field observations indicate a magmatic origin for the bulk of Ni sulphides ores. Nevertheless the presence of an external sulfur source, like the two horizons of sulphide facies iron formation, appears to have been a controlling factor in the generation of voluminous magmatic sulphides.

A clear link between sedimentary sulphides and the nickeliferous magmatic sulphides is provided by Se/S ratios of the various sulphides (O.R. Eckstrand pers. comm.; Eckstrand et al., 1989). In terms of this ratio, Ni sulphide ores of the Thompson Nickel Belt show a mixing trend between mantle ratios and Se-depleted ratios of the sedimentary sulphides (Fig. 58), suggesting that on average as much as 80% of the ore sulphide was derived from the sedimentary sulphide source. Addition of sedimentary sulphide may also have caused a slight positive shift in $\delta^{34}S$ values.

Since sulphide addition must have occurred in the magmatic stage, and because the ultramafic sills are still in contact with the sedimentary sulphide source, bulk assimilation of country rocks by the ultramafic sills in their final intrusive position must have been the dominant process.

Highest values of Se/S ratios occur in the Bucko deposit (O.R. Eckstrand, pers. comm.). This Falconbridge-owned deposit in the southern part of the belt comprises disseminated sulphides within an ultramafic sill or dike hosted by basement gneisses. Relatively high Se/S ratios for this deposit indicate either less sulphide assimilation or that the assimilated sulphide was less Se-depleted. Since the country rocks for the Bucko deposit are

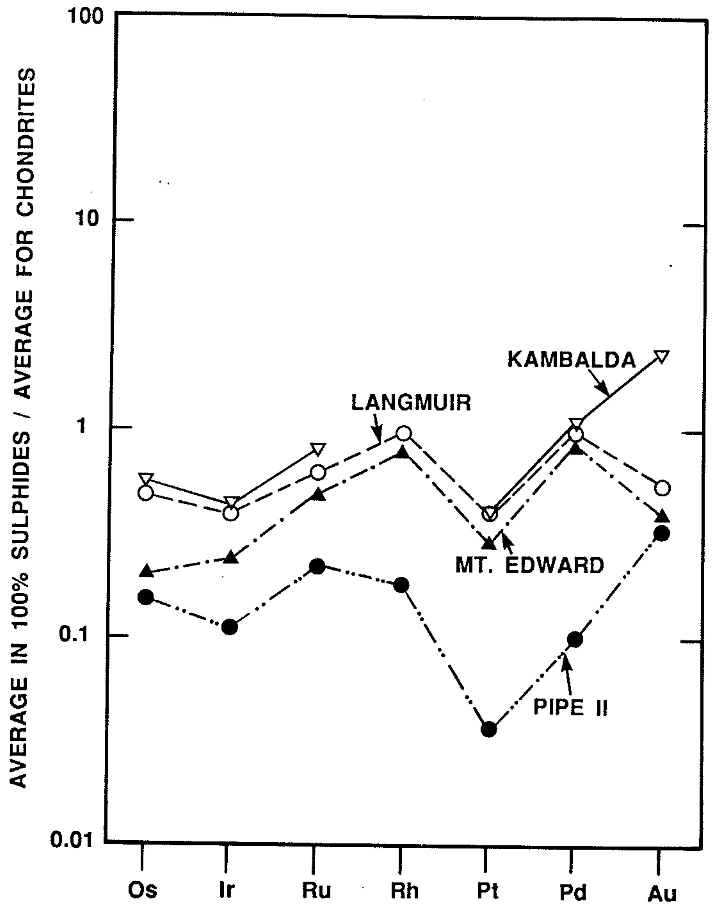


Figure 57: Chondrite-normalized PGE and Au data for Pipe II and other komatiite-related Ni sulphide deposits (taken from Naldrett et al., 1979).

intermediate to mafic Archean orthogneisses, the second explanation or a combination of both is favoured.

Assimilation being the major process raises the question to what extent other assimilants such as $SiO_2$ (and other components affecting melt structure) and C (affecting $fO_2$) may have contributed to generation of immiscible sulphide magma? Secondly, it raises the possibility that geochemical parameters, other than Se/S, may be successful in differentiating between mineralized ultramafic sills and barren sills.

A second important process, contributing to the complexity of the Ni sulphide ore bodies, is redistribution of Ni and to a lesser extent of other metals such as Co and Cu during medium to high grade metamorphism. Graphitic sedimentary sulphides, barren at relatively large distances from known Ni ore bodies (< 1000 ppm Ni), show elevated Ni concentrations in proximity to Ni ore bodies. Ni enrichment varies from slightly over 1000 ppm to 10 wt% and shows an inverse correlation with distance from the main ore zone. Schematic cross sections through the Thompson and Pipe II ore zones demonstrate the observed relationships (Fig. 54 and 55). Sedimentary sulphides in close proximity to magmatic sulphides are characterized by Ni and Ni/Co values which have completely equilibrated with the respective values in these magmatic sulphides. Cr concentrations, and probably other parameters such as PGE's, have remained distinct (Fig. 54 and 55). On approaching magmatic sulphide ore zones, Ni/Co increases from typical "barren" sedimentary values (2.5 to 7.0) to the deposit specific magmatic

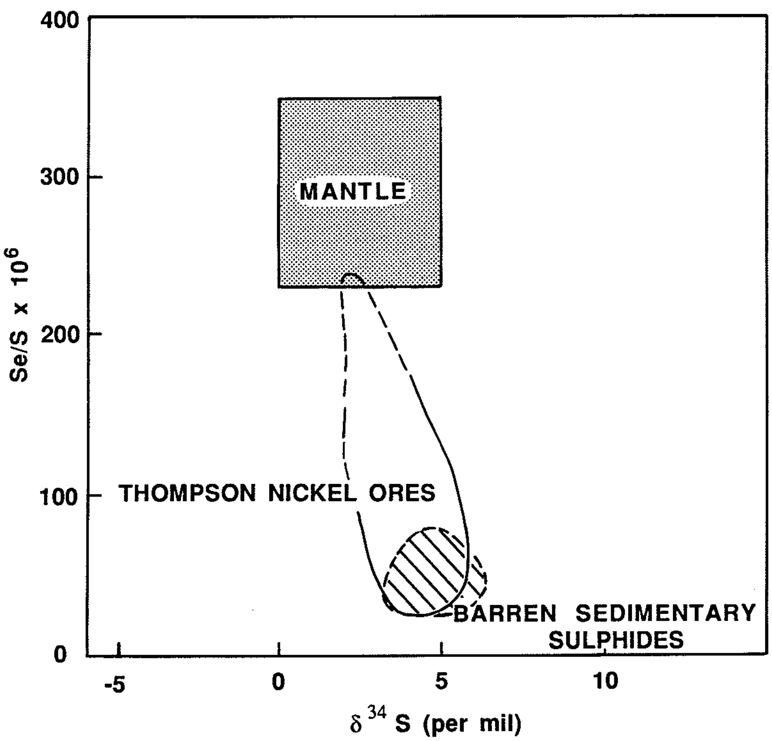


Figure 58: Se/S and $\delta^{34}$S data for nickel sulphide ore and barren sedimentary sulphides from the Thompson Nickel Belt (taken from Eckstrand et al., 1989).

ratios (e.g. Pipe II: 15-25, Thompson: 40-80) of adjacent magmatic sulphides. However, both at Thompson and at Pipe II, Ni/Co ratios peak above the magmatic ratios in moderately Ni-enriched sedimentary sulphides (Fig. 54 and 55). This suggests a slightly greater mobility of Ni relative to Co, a fact which may help to constrain the nature of the metamorphic redistribution process. Extensive Ni redistribution to originally barren sedimentary sulphides has locally led to significant Ni depletion of the magmatic sulphides, such as in breccia ore of the Thompson 1C zone (Fig. 54). Ni redistribution is much more extensive at Thompson than at Pipe II and thus correlates with metamorphic grade. Similar Ni redistribution to barren sedimentary sulphides has been documented in Ni deposits of the Kambalda district in Western Australia (Paterson et al., 1984).

## Stop Descriptions: Thompson Area

Introduction

The excursion concentrates on three localities: Thompson Open Pit, Pipe II Open Pit and Manasan Quarry. Current dredging of the South Pit at Thompson may have created fresh surface outcrops which will be included in the program if possible.

**STOPS 1-7: Thompson open pit**

### STOP 1: EASTERN GNEISS SHOULDER, NORTHWEST END OF THOMPSON OPEN PIT

The outcrop exposes a 30 meter section in the stratigraphic footwall of the Thompson ore zone, straddling the basement-cover contact (Fig. 59). Main features in this outcrop are: 1) completely reworked basement gneisses with abundant conformable pegmatite stringers. 2) Several tabular amphibolite bodies which are interpreted as Molson dikes. 3) Basement-cover contact and overlying basal quartzites. Parallelism of gneissic layering, basement-cover contact (i.e. originally an angular unconformity), and $S_{0,1,2}$ foliation in the quartzites qualitatively indicates the extremely high strains to which these rocks have been subjected. Transposition is attributed to F1 and to a lesser extent to $F_2$ folding. $F_3$ is responsible for reorientation of the downward facing metasediment-gneiss package into its present steeply southeast-dipping attitude.

### STOP 2: SOUTHEAST END OF 1C OPEN PIT, EASTERN SHOULDER AND EXPOSURES AROUND DRAINAGE SUMP

At this locality we will examine the "hanging wall ultramafic body" and the lower clastic sequence comprising basal quartzite and overlying semipelitic gneiss (Manasan Formation). The hangingwall ultramafic body is a well preserved dike-like body, post-$F_1$ in age, and chemically similar to pyroxenitic Molson dikes. In terms of its metamorphic character it is a forsterite-bronzite porphyroblastic ultramafic amphibolite. The semipelitic gneiss, probably a wacke in origin, forms the top of the fining-upward clastic sequence (M2 member of the Manasan Formation; Fig. 49b). It generally forms the metasedimentary unit with the strongest anatectic phenomena, but notice the lack of aluminous porphyroblasts. It has often been mistaken for basement gneiss, and has thus complicated or prevented meaningful structural and stratigraphic interpretations. We will observe this lithology at the other localities to be visited, demonstrating its usefulness as a regional marker. The semipelitic gneiss shows a gradational contact with overlying impure calcareous metasediments ("skarns") of the Thompson Formation, which can be observed in nearby outcrops and in the wall of the drainage sump.

### STOP 3: 1C THOMPSON OPEN PIT

The northern smaller pit of the Thompson Open Pit. Semipelitic gneiss and lower calcareous metasediments ("skarns") are visible in the southeast hangingwall of the pit. The late-kinematic pegmatite visible in this wall has been dated at 1768 ± 1.4 Ma (Bleeker and Roddick, in prep.). The wall at the NE end of the pit may provide a cross section through parts of the metasedimentary section including the ore zone. The northwest wall of the pit exposes an interlayered package of quartzite and biotite schist known as the "foot wall quartzites" (P3 member of Pipe Formation). The 1C ore body consists both of extraparental magmatic sulphides and Ni-enriched sedimentary sulphides. Much of the ore body comprises breccia ore in which both components may be intimately mixed.

To further illustrate the nature of the 1C ore zone and its wall rocks, polished hand samples and core from deeper portions of the 1C ore body will be shown.

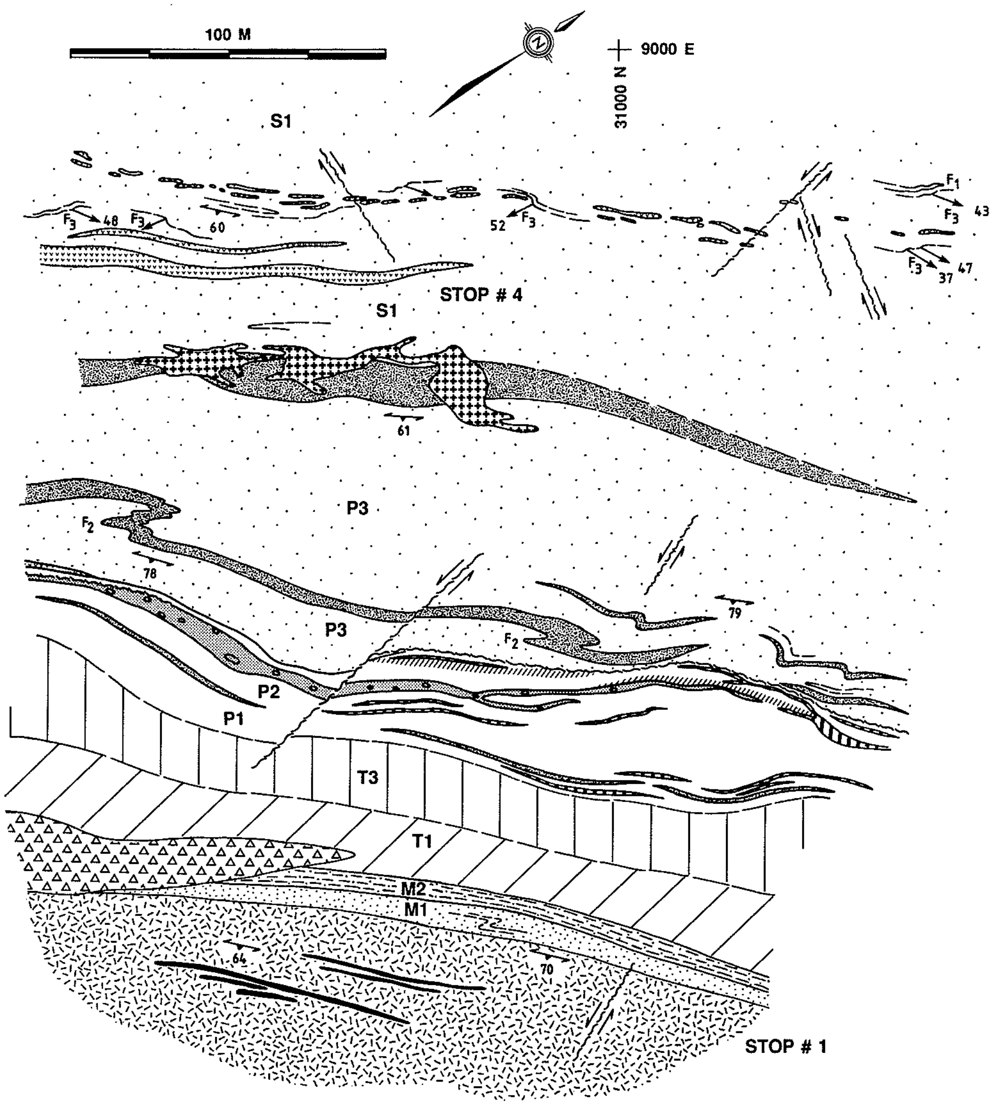


Figure 59: Geological map of the northern end of the 1C Thompson Pit and its shoulders. For legend, refer to Figure 60. Excursion STOPS #1 and #4 are indicated.

**STOP 4: NORTHWEST SHOULDER OF 1C PIT**

A walk up stratigraphy through the stratigraphic hanging wall of the Thompson ore zone (Fig. 59), from chert-banded silicate facies iron formation (P3 member of Pipe Formation) into a thick package of interlayered quartzites and biotite schists locally known as "core quartzites" (S1 member of Setting Formation). The latter rocks occupy the core of the antiformal Thompson structure (Fig. 52) and represent the highest lithostratigraphic level known in the Thompson Mine sequence. Stratigraphic and structural features will be discussed.

**STOP 5: 1B THOMPSON OPEN PIT, SW WALL ALONG RAMP**

This wall provides a good cross section from basement gneisses to "footwall quartzites" (Fig. 60).

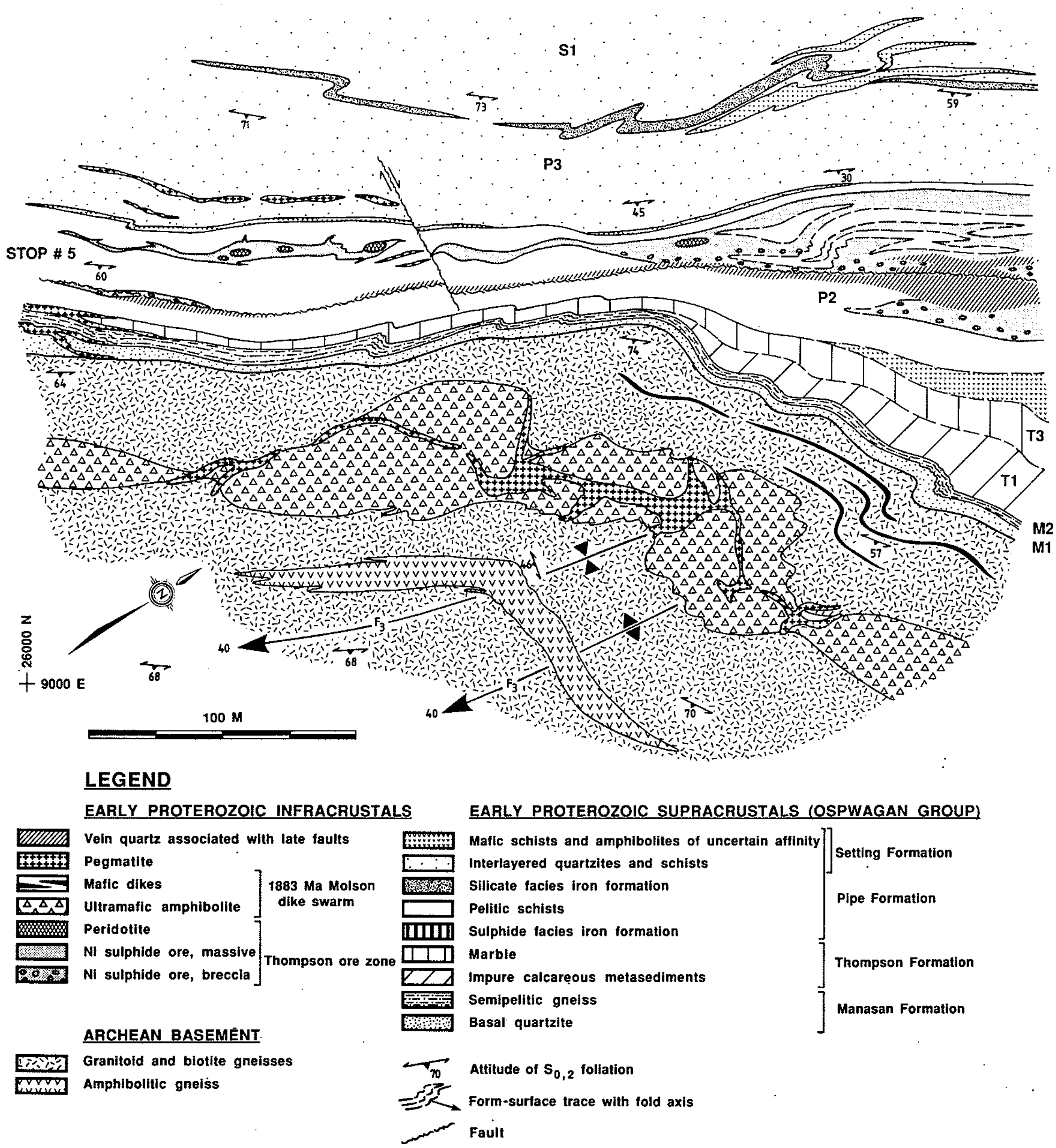


Figure 60: Geological map of the southern end of the 1B Thompson Pit. Excursion STOP #5 is indicated.

Although parts of the sequence have been greatly reduced structurally, such as the "skarn"-marble sequence, most units are present: 1) reworked basement gneisses with the ultramafic Molson dike, 2) well developed red to white basal quartzites, 3) semipelitic gneiss, 4) thin remnant of "skarn" and marble sequence, 5) pelitic schists and 6) stratigraphically overlying "footwall quartzites". The latter vary from interlayered quartzites and biotite schist to massive quartzites. Two sulphide bearing zones occur within the pelitic schists. The main ore zone occurs near the stratigraphic top of the schists, is two meter wide and consists of coarse grained magmatic sulphides. It pinches out higher up the wall.

**STOP 6: 1B THOMPSON OPEN PIT**

Depending on accessibility, we will descend into the 1B pit and examine the end walls, which display good cross sections through the ore zone and adjacent metasediments.

**STOP 7: SOUTH PIT**

Dredging of this new pit commenced at break up in 1989 and the pit is scheduled to come into operation as the present Thompson Open Pit is phased out. We will possibly examine parts of the new pit depending on what kind of outcrops are available, and their accessibility.

**STOPS 8-9: Manasan Quarry**

The remainder of the first day will be spend to visit Manasan Quarry. The quarry is situated 15 kilometre SSW of Thompson on the overturned "Thompson limb" of the $F_1$ nappe (Fig. 45 and 46) and exposes basement gneisses, a thick package of basal quartzites and stratigraphically overlying metasediments in a downward facing, NE plunging $F_3$ synform. The basal quartzite, with up to 90 wt% $SiO_2$, is used as a flux in smelting and converting processes at the Thompson plant (e.g. Boldt and Queneau, 1967).

**STOP 8: WESTERN LIMB OF MANASAN SYNFORM**

At the northwest end of the quarry, a section will be examined exposing from east to west: 1) reworked basement gneisses, 2) white, grey or pink basal quartzites with a few quartz pebble conglomerate layers near its base, 3) semipelitic schists and 4) a thick package of banded "skarns" and minor marble. Basement gneiss at this locality comprises orthogneiss of intermediate composition with mafic xenoliths. The thin basal conglomerate layers are not easily recognized due to stretching of the pebbles and green amphibole growth in the matrix. In general, the basal quartzite may contain considerable amounts of feldspar and mica, but locally grades into orthoquartzite. Semipelitic schists, the uppermost unit of the lower clastic transgressive sequence, form a thin band on this limb. Note however the characteristic color and presence of highly stretched microcline-rich sweats. Banded "skarns" at this locality are very similar to comparable rocks at Thompson, illustrating the original proximity of the two localities which are both situated on the overturned limb of the nappe. On the lower "Pipe limb" of the nappe, the skarn and marble sequence is quite different in character or lacking.

**STOP 9: EASTERN LIMB OF MANASAN SYNFORM**

The same sequence as in the previous stop is demonstrated. The basal conglomerate is better developed and preserved on this limb. The matrix of the conglomerate is rich in fine grained apatite, which is probably derived from a diagenetic apatite cement. $F_{1or2}$-$F_2$ interference is demonstrated in the semipelitic schists. Note that the $S_3$ axial plane trends N50°E, 15° clockwise of the trend of the Thompson Nickel Belt. This $F_3$ fold trend is typical and forms the en échelon pattern which dominates the late structure of the belt and is attributed to sinistral transpression.

**STOPS 10-17: Pipe II open pit lithostratigraphy**

Pipe II Open Pit (Fig. 56) is unique in that it exposes the most complete section through basement and cover sequence of the Thompson Nickel Belt. In spite of intense polyphase deformation many primary features are preserved allowing reconstruction of the lithostratigraphy and detailed setting of the Pipe II ore body. Better than average preservation of the Pipe II sequence is due to its location on or close to hinges of not only $F_3$, the main mine fold, but also $F_1$ and $F_2$. Secondly, metamorphic grade is not higher than staurolite grade, i.e. 50 to 100° lower than at Thompson.

After an introduction during which maps and polished hand samples will be examined, we will walk a traverse from basement gneisses to volcanics at the top of the Ospwagan Group. The second part of the day will focus on details of the ore body.

Stops are indicated on the Pipe II Open Pit map (Fig. 56) and the lithostratigraphic column (Fig. 49a).

**STOP 10: STRONGLY REWORKED BASEMENT GNEISSES INTRUDED BY MOLSON DIKE**

The grey gneisses show a Hudsonian transposition foliation. Although grain size is greatly reduced relative to Archean protoliths, a coarse relict texture is still visible locally. Note the reasonable preservation of the mafic dike in spite of the extreme strain in the basement gneisses. Mafic dikes like this occur throughout the western TNB and are chemically indistinguishable from Molson dikes (Fig. 61).

**STOP 11: GNEISS-BASAL QUARTZITE CONTACT AND MANASAN FORMATION**

Examination of lower transgressive sequence comprising: 1) a thin and local pebbly conglomerate, 2) quartzite with beds preserving grading, fining upwards through 3) finer grained and laminated quartzites into 4) semipelitic schists. Note again the characteristic purple colour and the microcline-rich sweats of the latter lithology. Exceptional preservation of the basal quartzite can be attributed to its location on a $F_2$ fold hinge.

**STOP 12: TRANSITION FROM SEMIPELITIC SCHIST, VIA CHERTY LAYERS, TO IMPURE CALCAREOUS METASEDIMENTS, MARBLE AND SULPHIDIC CHERT (THOMPSON FORMATION AND P1 MEMBER OF PIPE FORMATION)**

Two separate outcrops of this package (T(P1) on Fig. 56) will be visited, which directly underlies the intrusive horizon of the Pipe II ultramafic sill. The sulphidic chert,

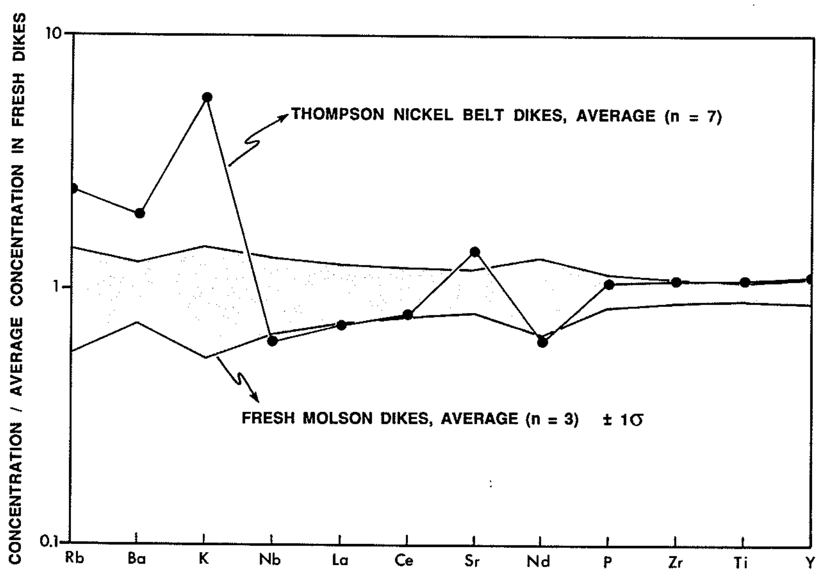


Figure 61: Comparison of incompatible element concentrations between fresh Molson dikes (n=3) from the Archean foreland and mafic dikes from the western Thompson Nickel Belt (n=7). High field strength incompatible element concentrations and their ratios are very similar for the two dike suites. Higher Rb, Ba and K concentrations reflect amphibolitization of the Thompson Nickel Belt dikes.

rather thin in these outcrops, are laterally continuous with nearly massive pyrrhotite. It is this horizon which must have supplied the bulk of assimilated sulphur to the sill. Note the strong difference between this carbonate-rich sequence and that of Thompson, reflecting the large original separation between the two localities.

**STOP 13: FIRST SILICATE FACIES IRON FORMATION**

This unit (remainder of P1 member of Pipe Formation) directly overlies the intrusive horizon of the Pipe II sill. Some members of this iron formation are highly magnetic, some show regular chert banding, others are massive. It is distinct from silicate facies iron formations higher up in the sequence and grades via white and red cherty units into pelitic schists.

**STOP 14: PELITIC SCHISTS AND UPPER SULPHIDE FACIES IRON FORMATION (P2 MEMBER OF PIPE FORMATION)**

The upper sulphide facies iron formation occurs near the top of the pelitic schists and can be correlated with sedimentary sulphides near the top of the schists at Thompson.

**STOP 15: SILICEOUS METASEDIMENTS AND MAIN CYCLE OF SILICATE FACIES IRON FORMATIONS (P3 MEMBER OF PIPE FORMATION)**

This package of rocks is extremely well preserved, as illustrated by the fact that many centimetre to decimetre wide layers can be followed throughout the entire eastern shoulder of the pit. Subtle differences allow a succession of chert-banded iron formations to be recognized which is interrupted by a clean dolomitic marble and capped by thinly-banded diopside rocks and chert. Note that the succession of iron formations shows a trend from laminated, garnetiferous varieties in the lower part to thinly banded, non-garnetiferous pyroxene-bearing varieties above the dolomitic marble. The same compositional trend appears to be present in Thompson, and probably reflects a progressive decrease of a residual Al-rich pelitic component.

The sequence of iron formations and dolomitic marble shows several large scale, tight to isoclinal $F_1$ folds, which are cross-cut by a dense swarm of Molson dikes. The post-F1 nature of these dikes will be demonstrated.

**STOP 16: FURTHER INTO THE CORE OF THE PIPE $F_3$ SYNFORM**

A large outcrop, isolated from previous localities, exposes a succession of clastic and chemical sediments which structurally repeats previously observed lithostratigraphy. The structurally highest part of the outcrop adds however a section of stratigraphy which correlates with the "core quartzites" at Thompson (S1 member of Setting Formation).

**STOP 17: OSPWAGAN GROUP VOLCANICS (O1 AND O2 MEMBERS OF THE OSPWAGAN FORMATION)**

Further into the core (300 metre) of the Pipe II synform, the local stratigraphic top of the Ospwagan Group comprises mafic heterolithic volcanic breccia overlain by basaltic pillow lavas.

<u>STOPS 18-19: Pipe II ore body</u>

**STOP 18: PIPE II ULTRAMAFIC SILL AND ITS UPPER CONTACT**

Exposures on the west limb show the upper part of the ultramafic sill and its contact with overlying silicate facies iron formation. In spite of serpentinization and tremolitization of the ultramafic rocks, primary textures are locally well preserved. Locally, a trend from dunite to orthopyroxenite can be observed. Relict textures in the orthopyroxenite show a decrease in grain size towards the upper contact, which is marked by a talc schist envelope. Metasediments overlying the sill will be examined, to demonstrate the stratigraphic position of the sill.

**STOP 19: EXAMINATION OF PIPE II OPEN PIT FROM OBSERVATION BOOTH**

This locality offers an excellent view of the geology in the pit walls, especially the massive sulphide apophysis in the southeastern wall. Note the tapering and conformable nature of the apophysis.

**END OF FIELD TRIP**

**ACKNOWLEDGEMENTS**

The authors would like to thank Hudson's Bay Mining and Smelting Co. Ltd., Inco Ltd., Inco Gold Ltd. and Snow Lake Mines Ltd. for allowing the use of company data, and access to their properties for the participants of this field trip. Hudson's Bay Mining and Smelting Co. Ltd. and Inco Ltd. are also thanked for their generous hospitality during the participants stay in Flin Flon and Thompson. We would also like to thank Alan Miller of the Mineral Resources Division, Geological Survey of Canada for critically reviewing the manuscript.

We hope that the content of the field guide will assist geologists in their understanding of Early Proterozoic deposit environments.

**REFERENCES**

Ashton, K.E., 1989, Kisseynew Lake-Florence Lake area: in Report of Activities 1989, Manitoba Energy and Mines, Min. Div., p.65-71.

Ayres, L.D. and Young, J., 1989. Characterization of mafic-ultramafic intrusive rocks in the Flin Flon-Snow Lake area, Manitoba; in Investigations by the Geological Survey of Canada in Manitoba and Saskatchewan during the 1984-1989 Mineral Development Agreements, edited by A. Galley, Geological Survey of Canada Open File 2133, pp. 64-48

Bailes, A.H., 1971, Preliminary compilation of the geology of the Snow Lake-Flin Flon Sherridon area: Manitoba Mines Branch, Geol. Paper 1/71, 27 p.

Bailes, A.H., 1975, Geology of the Guay-Wimapedi Lakes area: Manitoba Dept. of Mines, Res. and Environ. Manag., Min. Res, Div., Geol. Serv. Branch, Publ. 75-2, 104 p.

Bailes, A.H. and McRitchie, W.D., 1978, The transition from low to high grade metamorphism in the Kisseynew sedimentary gneiss belt, Manitoba: in Metamorphism in the Canadian Shield (A. Fraser and W.W. Heywood, eds.); Geological Survey of Canada, Paper 78-10, p. 155-177.

Bailes, A.H., 1980, Geology of the File Lake area: Manitoba Mineral Res. Div., Geol. Rep. 78-1, 134 p.

Bailes, A.H., 1985, Geology of the Saw Lake Area: Manitoba Energy and Mines, Geol. Serv., Geol. Rep. GR83-2, 47 p.

Bailes, A.H., 1986, Chisel-Morgan Lakes project in 1986 Report of Field Activities, Manitoba Energy and Mines, p. 70-76.

Bailes, A.H., 1987, Chisel-Morgan Lake Project: in 1987 Report of Field Activities, Manitoba Energy and Mines, p. 70-80.

Bailes, A.H,, 1988, Chisel-Morgan Lake Project: in 1988 Report of Field Activities, Manitoba Energy and Mines, p. 53-61.

Bailes, A.H., Hunt, P.A., and Gordon, T.M., 1990, U-Pb zircon dating of possible synvolcanic plutons in the Flin Flon belt at Snow Lake, Manitoba: in Radiogenic Age and Isotope Studies: Report 4, Geol. Surv. of Canada, Paper 90-2, in prep.

Bailes, A.H.,Syme,E.C., Galley, A.G. and Skirrow, R.G., 1987, Early Proterozoic volcanism ,hydrothermal activity, and associated ore deposits at Flin Flon and Snow Lake, Manitoba: Geol. Assoc. of Canada\Mineral. Assoc. of Canada, 1987 Annual Meeting, Field Trip Guidebook No. 1, 95 p.

Bailes, A.H., Gordon, T.M. and Hunt, P.A., 1988, U-Pb zircon geochronology of the Richard Lake tonalite, a possible synvolcanic pluton in the Flin Flon belt: in 1988 Report of Field Activities, Manitoba Energy and Mines, p. 63-65.

Bailes,A.H. and Galley, A.G., 1989, Geological setting of and hydrothermal alteration below the Chisel massive Zn-Cu sulphide deposit: in 1989 Report of Field Activities, Manitoba Energy and Mines, p. 31-37.

Bailes, A.H. and Syme, E.C., 1989, Geology of the Flin Flon-White Lake area: Manitoba Energy and Mines, Geol. Rep. GR 87-1, 313 p.

Baldwin, D.A., Syme, E.C., Zwanzig, H.V., Gordon, T.M., Hunt, P.A., and Stevens, R.D., 1987, U-Pb zircon ages from the Lynn Lake and Rusty Lake metavolcanic belts, Manitoba: two ages of Proterozoic magmatism: Can. Jour. Earth Sci., vol. 24, p. 1053-1063.

Baldwin, D.A., 1980, Porphyritic intrusions and related mineralization in the Flin Flon volcanic belt: Manitoba Energy and Mines, Econ. Geol. Rep. ER79-4, 23 p.

Baragar, W.R.A. and R.F.J. Scoates, 1981, The Circum-Superior belt: a Proterozoic plate margin?: **in** Kroner, A., ed., Prec. Plate Tect., Elsevier, Amsterdam, p. 297-330.

Bateman, J.D. and Harrison, J.M., 1945, Mikanagan Lake, Manitoba: Geol. Surv. of Canada, Map 832A, with descriptive notes.

Bell, C.K., 1966, Churchill-Superior boundary in northeastern Manitoba: Geol. Surv. Can., Paper 66-1, p. 3-136.

Bell, C.K., 1971, Boundary geology, upper Nelson River area, Manitoba and northwestern Ontario: **in**: Geoscience studies in Manitoba, Turnock, A.C., ed., Geol. Assoc. Can., Spec. Paper, no. 9, p. 11-39.

Bickford, M.E., Collerson, K.D., Lewry, J.F. Van Schmus, W.R. and Chiarenzelli, J.R., 1990, Proterozoic collisional tectonism in the Trans-Hudson orogen: Geology, vol. 18, p. 14-18.

Blair, B., Weber, W., Kornik, L.J. and Gordon, T.M., 1988, Project Cormorant: interpretations of sub-Paleozoic geology of the Cormorant Lake map area from geophysical and drill core data: Geoscience Canada, 15, p 98-100.

Bleeker, W. and J.J. Macek, 1988a, Thompson Nickel Belt Project: Pipe Pit Mine: **in** Report of Field Activities 1988, Manitoba Energy and Mines, p. 111-115.

Bleeker, W. and J.J. Macek, 1988b, Pipe Pit Mine (Sheets A,B,C,D,E,F,G and H): 1:400, Manitoba Energy and Mines, Geological Services, Preliminary Maps 1988T-1 to 1988T-8.

Bleeker, W., 1989, Litho-structural map of the Thompson Open Pit, Thompson Nickel Belt, Manitoba: scale 1:1200, with accompanying map description, Geol. Surv. of Canada, Open File 2089.

Bleeker, W., 1990, New structural-metamorphic constraints on Early Proterozoic oblique collision along the Thompson nickel belt, northern Manitoba, Canada: in The Early Proterozoic Trans-Hudson Orogen, edited by J.F. Lewry and M.R. Stauffer, Geol. Assoc. of Canada Special Paper.

Bleeker, W., in prep., Structural-metamorphic history of the Thompson Nickel Belt: Ph.D. thesis, University of New Brunswick.

Boldt, J.R. and P. Queneau, 1967, The winning of Nickel: Longmans Canada Limited, Toronto, 487 p.

Brooks, C. and P. Theyer, 1981, Rb/Sr geochronology in the Thompson Nickel Belt, Manitoba: implication for Aphebian crustal development and metallogenesis: Can. J. Earth Sci., vol. 18, p. 932-943.

Brun, J.P. and Burg, J.P., 1982, Combined thrusting and wrenching in the Ibero-American arc: a corner effect during continental collision: Earth Planet. Sci. Lett., vol. 61, p. 319-332.

Buckham, A.F., 1944, Athapapuskow Lake, Manitoba: Geol. Surv. of Canada, Map 807A, with descriptive notes.

Byers, A.R., Kirkland, S.J.T. and Pearson, W.J., 1965, Geology and mineral deposits of the Flin Flon area, Saskatchewan: Sask. Depart. of Mineral Res., Rep. No. 62, 95p.

Cerny, P., Trueman, D.L., Ziehlke, D.V., Goad, B.E. and Paul, B.J., 1981, The Cat Lake-Winnipeg River and Wekusko Lake Pegmatite Fields, Manitoba: Manitoba Mineral Res. Div., Econ. Geol.Rep. ER80-1.

Chandler, F.W. and R.R. Parrish, 1989, Age of the Richmond Gulf Group and implications for rifting in the Trans-Hudson Orogen, Canada: Precambrian Res., 44, p. 277-288.

Chauvel, C., N.T. Arndt, S. Kielinzcuk and A. Thom, 1987, Formation of 1.9 Ga old continental crust. I: Nd isotopic data: Can. J. Earth Sci., vol. 24, p. 396-406.

Coats, C.J.A., Clark, L.A., Buchan, R. and Brummer, J.J., 1970, Geology of the copper-zinc deposits of Stall Lake Mines Limited; Econ. Geol., vol. 65, p. 970-984.

Coats, C.J.A. and J.J. Brummer, 1971, Geology of the Manibridge nickel deposit, Wabowden, Manitoba: <u>in</u> Geoscience studies in Manitoba, Turnock, A.C., ed., Geol. Assoc. Can., Spec. Paper No. 9, p. 155-165.

Coats, C.J.A., T.T. Quirke, C.K. Bell, D.A. Cranstone and F.H.A. Campbell, 1972, Geology and mineral deposits of the Flin Flon, Lynn Lake and Thompson areas, Manitoba, and the Churchill-Superior front of the western Precambrian shield: Guidebook, field excursion A31-C31, Internat. Geol. Congress, XXIV Session, Canada.

Colvine, A.C., Andrews, A.J., Cherry, M.E, Durocher, M.E., Fyon, A.J., Lavigne Jr., M.J., Macdonald, A.J., Marmont, S., Poulsen, K.H., Springer, J.S. and Troop, D.G., 1984, An integrated model for the origin of Archean lode gold deposits: Ont. Geol. Surv. Open File Rep. 5524, 99 p.

Costa, U.R., Barnett, R.L. and Kerrich, R, 1983, The Mattagami Lake mine Archean Zn-Cu sulphide deposit, Quebec: hydrothermal coprecipitation of talc and sulphides in a seafloor brine-pool - evidence from geochemistry, $^{18}O/^{16}O$, and mineral chemistry: Econ. Geol., vol. 78, p. 1144-1203.

Cranstone, D.A. and A. Turek, 1976, Geological and geochronological relationships of the Thompson Nickel Belt, Manitoba: Can. J. Earth Sci., vol. 13, p. 1058-1069.

de Rosen-Spence, A.F., Provost, G., Dimroth, E., Gochnauer, K. and Owen, V., 1980, Archean subaqueous flows, Rouyn-Noranda, Quebec, Canada and their Quaternary equivalents: Precambrian Res., vol. 12, p. 43-77.

Delaney, G., Carr, S.D., and Parrish, R.R., 1988, Two U-Pb zircon ages from eastern Glennie Domain, Trans-Hudson Orogen, Saskatchewan: Geol. Surv. of Canada, Radiogenic age and isotope studies: Report 2, p. 51-58.

Ebbutt, F., 1944, The Nor-Acme property of the Howe Sound Exploration Company, Snow Lake, Herb Lake Mining Division, Manitoba: The Precambrian, vol. 17, no. 7, p. 6-11.

Eckstrand, O.R., L.N. Grinenko, H.R. Krouse, A.D. Paktunc, P.L. Schwann and R.F.J. Scoates, 1989, Preliminary data on sulphur isotopes and Se/S ratios, and the source of sulphur in magmatic sulphides from the Fox River Sill, Molson Dykes and Thompson nickel deposits, northern Manitoba: in Current Research, Part C, Geol. Surv. of Canada, Paper 89-1C, p. 235-242.

Ermanovics, I. and W.F. Fahrig, 1975, The petrochemistry and paleomagnetism of the Molson dikes, Manitoba: Can. J. Earth Sci., vol. 12, p. 1564-1575.

Esposito, B., 1986, Copper and Zinc in Manitoba: Manitoba Energy and Mines, Mineral Education Series, 24 p.

Fedikow, M.A.F., Ostry, G. Ferreira, K.J. and Galley, A.G., 1989, Mineral deposits and occurrences in the File Lake area, NTS 63K/16: Manitoba Energy and Mines, Min. Div., Min. Dep. Ser. Rep. 5, 277 p.

Fink, J.H., and Pollard, D.D., 1973, Structural evidence for dykes beneath silic domes, Medicine Lake Highland Volcano, California, Geology, vol. 11, p. 458-461.

Fogwill, W.D., 1983, Mining in Manitoba - past and present: Can. Inst. Mining and Metall., Directory 1983, p. 75-91.

Franklin,J.M., 1986, Volcanic-associated massive sulphide deposits - an update: in Geology and genesis of mineral deposits in Ireland, edited by C.J. Andrew et al., Irish Assoc. for Econ. Geol., p. 49-69.

Franklin, J.M., Sangster, D.F. and Lydon, J.W., 1981, Volcanic-hosted massive sulphide deposits: Econ. Geol., 75th Anniversary Volume, p 485-627.

Frarey, M.J., 1948, Crowduck Bay, Manitoba: Geol. Surv. of Canada, Paper 48-22.

Fraser, H.S., 1985, The Great Thompson Nickel Discovery: Inco Limited, Manitoba: 388 p.

Froese, E. and Moore, J.M., 1980, Metamorphism in the Snow Lake area, Manitoba: Geol. Surv. of Canada, Paper 78-27.

Furnes, H., Frideifsson, I.B., and Atkins, F.B., 1980, Subglacial volcanics - on the formation of acid hyaloclastites: J. of Volcan. and Geothermal Res., vol.8, p. 95-110.

Gale, G.H. and Koo, J., 1977, Evaluation of massive sulphide environments: Manitoba Mineral Res. Div., Non-renewable Resource Evaluation Program, 2nd Annual Report 1976-1977, p. 43-62.

Galley, A.G., Ziehlke, D.V., Ames, D.E. and Gordon, T.M., 1986, Gold mineralization in the Snow Lake-Wekusko Lake Region, Manitoba: in Gold in the Western Shield (L.A. Clark, Ed.), The Can. Inst. of Mining and Metall., Spec. Vol. 38, p. 379-398.

Galley, A.G. and Franklin, J.M., 1989, Setting of gold in the Phantom Lake region, Saskatchewan: in Investigations by the Geological Survey of Canada in Manitoba and Sakatchewan during the 1984-89 Mineral Development Agreements, Geol. Surv. of Canada, Open File 2133, p. 33-42.

Galley, A.G., Ames, D.E. and Franklin, J.M., 1989, Results of studies on the gold metallogeny of the Flin Flon belt: in Investigations by the Geological Survey of Canada in Manitoba and Saskatchewan during the 1984-89 Mineral Development Agreements, compiled by A.G. Galley, Geol. Surv. of Canada, Open File 2133, p.25-32.

Galley, A.G., and Bailes, A.H., 1989, Geological setting and associated alteration of the Chisel Lake massive sulphide deposit, Snow Lake, Manitoba: in Report of Actvities 1989, Manitoba Energy and Mines, Minerals Division, p. 145-151.

Gibb, R.A., 1968, A geological interpretation of the Bouguer anomalies adjacent to the Churchill-Superior boundary in northern Manitoba: Can. J. of Earth Sci., vol. 5, p. 439-453.

Gibson, H.L., Watkinson, D.H. and Comba, C.D.A., 1983, Silicification: Hydrothermal alteration in an Archean rhyolite formation , Noranda, Quebec: Econ. Geol., vol. 78, p. 954-971.

Gilbert, H.P., 1986, Geological investigations in the Tartan Lake - Lac Aimee area: in Report of Field Activities 1986, Manitoba Energy and Mines, Minerals Division, p. 43-48.

Gilbert, H.P., 1987, Geological investigations in the Tartan Lake - Lac Aimee area: in Report of Field Activities, 1987, Manitoba Energy and Mines, Minerals Division, p. 41-50.

Gilbert, H.P., 1988, Geological investigations in the Tartan Lake - Embury Lake area: in Report of Field Activities, 1988, Manitoba Energy and Mines, Minerals Division, p. 35-42.

Gilbert, H.P., 1989, Geological investigations in the Tartan Lake - Embury Lake area: in Report of Field Activities, 1989, Manitoba Energy and Mines, Minerals Division, p. 19-30.

Gill, J.B., 1981, Orogenic andesites and plate tectonics: Springer-Verlag, Berlin, Heilelberg, New York, 390p.

Gordon, T.M. and Gall, Q., 1982, Metamorphism in the Crowduck Bay area, Manitoba: Geol. Surv. of Canada, Paper 82-1A, p. 197-201.

Gordon, T.M., 1989, Thermal evolution of the Kisseynew sedimentary gneiss belt, Manitoba: metamorphism at an early Proterozoic accretionary margin: in Evolution of Metamorphic Belts, edited by J.S. Daly, R.A. Cliff and B.W.D. Yardley, Geol. Soc. Spec. Publ. No. 43, p. 233-243.

Gordon, T.M., Hunt, P.A., Bailes, A.H. and Syme, E.C., 1990, U-Pb zircon ages from the Flin Flon and Kisseynew belts, Manitoba: Chronology of Early Proterozoic accretionary margin: in The Early Proterozoic Trans-Hudson Orogen : lithotectonic correlations and evolution: J. R. Lewry and M.R. Stauffer (eds.), Geol. Assoc. of Canada, Spec. Paper.

Grant, J.A., 1986, The iscon diagram - A simple solution to Gresens' equation for metasomatic alteration: Econ. Geol., vol. 81.

Green, A.G., Cumming, G.L. and Cedarwell, 1979, Extension of the Superior-Churchill boundary zone into southern Canada: Can. Jour. Earth Sci., vol 16, p. 1691-1701.

Green, A.G., Hajnal, Z. and Weber, 1985, An evolutionary model of the western Churchill province and western margin of the Superior province in Canada and the north-central United States: Tectonophysics, vol. 116, p. 281-322.

Hannington, M.D. and Scott, S.D., 1989, Gold mineralization in volcanogenic massive sulphides: implications of data from active hydrothermal vents on the modern sea floor: Econ. Geol., Mono. 6. p. 491-507.

Harrison, J.M., 1949, Geology and mineral deposits of the File-Tramping Lakes area, Manitoba: Geol. Surv. of Canada, Memoir 250.

Harrison, J.M., 1951, Possible major structural control of ore deposits, Flin Flon-Snow Lake mineral belt, Manitoba: Can. Inst. of Mining and Metall., Trans., vol. 54, p. 4-8.

Heaman, L.M., N. Machado, T. Krogh and W. Weber, 1986, Precise U-Pb zircon ages for the Molson dyke swarm and the Fox River sill: implications for Early Proterozoic crustal evolution in NE Manitoba: Can. Contr. Mineral. Petrol., 94, p. 89.

Heiken, G., 1972, Morphology and petrography of volcanic ashes: Geol. Soc. of America Bull., vol.83, p. 1961-1988.

Heinrichs, T., 1984, The Umsoli chert, turbidite testament for a major phreatoplinian event at the Onverwacht/Fig Tree transition (Swaziland Supergroup, Archean, South Africa): Prec. Research, vol. 24, p. 237-283.

Hoffman, P.F., 1988a, United Plates of America, The Birth of A Craton: Early Proterozoic Assembly and Growth of Laurentia: Ann. Rev. Earth Planet. Sci., vol. 16, p. 543-603.

Hoffman, P.F., 1988b, Proterozoic foredeeps, foredeep magmatism and Superior-type iron formations in the Canadian shield: in Kroner, A., ed., Proterozoic Lithospheric Evolution, Geodynamics Series, Amer. Geophys. Union, vol. 17, p. 85-98.

Hopkins, J.L., 1986, Live at twenty-five: Canadian Mining Journal, July 1986, p. 29-31.

Hosain, I., 1988, Mineral producers, past producers and significant deposits in Manitoba: Manitoba Energy and Mines, internal circulation.

Howkins, J.B. and Martin, P.L., 1970, A comparison between the Flin Flon and Snow Lake orebodies of Hudson Bay Mining and Smelting Co. Ltd: Paper presented at Annual Convention, Can. Inst. of Mining and Metall. (unpubl.), April 1970.

Hubregtse, J.J.M.W., 1980, The Archean Pikwitonei granulite domain and its position at the margin of the northwestern Superior Province, central Manitoba: Manitoba Mines Branch, Geol. Paper 80-3, 16 p.

Hutcheon, I., 1977, The metamorphism of sulphide-bearing pelitic rocks from Snow Lake, Manitoba: Unpubl. Ph.D. Thesis, Carleton University, Ottawa.

Jackson, S.L., 1988, Metamorphism and structure of the Laurie Lake area, northern Manitoba: PhD thesis, Queen's University, Kingston.

Kappel, E.S. and Franklin, J.M., 1989, Relationship between geologic development of ridge crests and sulphide deposits in the Northwest Pacific Ocean: Econ. Geol., vol.84, p.485-505.

Kennedy, G.C., 1950, A portion of the system silica-water: Econ. Geol., vol. 45, p.629-653.

Ko, C.B., 1986, Geology of the Trout Lake copper-zinc sulphide deposit: Hudson Bay Mining and Smelting Company report (unpubl.), 33 p.

Koo, J. and Mossman, D.J., 1975, Origin and metamorphism of the Flin Flon stratabound Cu-Zn sulphide deposit, Saskatchewan and Manitoba: Econ. Geol., vol. 70, p. 48-62.

Kornik, L.J., 1969, An aeromagnetic study of the Moak Lake-Setting Lake structure in northern Manitoba: Can Jour. Earth Sci., vol. 6, 373-381.

Kornik, L.J., and MacLaren, A.S., 1966, Aeromagnetic study of the Churchill-Superior boundary in northern Manitoba: Can. Jour. Earth Sci., vol 3, p. 547-557.

Lewry, J.F. and Sibbald, T.I.I., 1980, Thermotectonic evolution of the Churchill province in northern Saskatchewan: Tectonophysics, vol. 68, p. 45-82.

Lewry, J.F., 1981, Lower Proterozoic arc-microcontinent collisional tectonics in the western Churchill Province: Nature, vol. 294, p. 69-72.

Lewry, J.F., T.I.I. Sibbald and D.C.P. Schledewitz, 1985, Variation in character of Archean rocks in the western Churchill Province and its significance: in Ayres, L.D., P.C. Thurston, K.D. Card and W. Weber, eds., Evolution of Archean Supracrustal Sequences: Geol. Assoc. of Canada, Spec. Paper 28, p. 239-261.

Lewry, J.F., R. Macdonald, C. Livesey, M. Meyer, R. Van Schmus and M.E. Bickford, 1987, U-Pb geochronology of accreted terranes in the Trans-Hudson Orogen, northern Saskatchewan, Canada: in Pharaoh, T.C., R.D. Beckinsale and D. Rickard, eds., Geochemistry and Mineralization of Proterozoic Volcanic Suites: Geol. Soc. Special Publ. No 33, p. 147-166.

Lydon, J.W., 1984, Ore deposit models-8. Volcanogenic massive sulphide deposits Part 1: A descriptive model: Geoscience Canada, vol. 11, p. 195-202.

Lydon, J.W., 1988, Volcanogenic massive sulphide deposits Part 2: Genetic models: Geoscience Canada, vol15, p. 43-65.

Macek, J.J, and Bleeker, W., 1989, Thompson nickel belt project - Pipe Pit Mine, Setting and Ospwagan Lakes: in Report of Field Activities 1989, Manitoba Energy and Mines, Minerals Division, p. 73-87.

Macek, J.J. and W. Bleeker, in press, Thompson Nickel Belt Project: Geological Investigations at Pipe Mine, Setting Lake and Ospwagan Lake: in Report of Field Activities 1989, Manitoba Energy and Mines.

MacGeehan, P.J., 1978, The geochemistry of altered volcanic rocks at Matagami, Quebec: A geothermal model for massive sulphide genesis; Can. J. of Earth Sci., vol. 15, p. 551-570.

MacQuarrie, R., 1980, Absolute age of the Flin Flon deposit: Bull. of the Can. Inst. of Mining and Metall., abstr., No. 4 District Meeting, vol. 73, p. 53.

Machado, N., L. Heaman, T.E. Krogh and W. Weber, 1987, U-Pb geochronology program: Thompson Belt Northern Superior Province: in Report of Field Activities 1987, Manitoba Energy and Mines.

Manitoba Mineral Resources Division, 1979, Geological map of Manitoba, scale 1:1000,000. Map 79-2.

Martin, P.L., 1966, Structural analysis of the Chisel orebody: Can. Inst. of Mining and Metall., Trans., vol. 64, p. 208-214.

Mottl, M.J., 1983, Metabasalts, axial hot springs, and the structure of hydrothermal systems at mid-ocean ridges: Geol. Soc. of America Bull., vol. 94, p. 161-180.

Mottl, M.J., Holland, H.D. and Carr, R.F., 1979, Chemical exchange during hydrothermal alteration of basalt by seawater-II. Experimental results for Fe, Mn and sulphur species: Geochemica et Cosmochemica Acta, vol3, p. 869-884.

Morton, R.L. and Franklin, J.M., 1987, Two-fold classification of Archean volcanic-associated massive sulphide deposits: Econ. Geol., vol. 82, p. 1057-1063.

Naldrett, A.J., E.L. Hoffman, A.H. Green, Chen-Lin Chou and S.R. Naldrett, 1979, The composition of Ni-sulphide ores, with particular reference to their content of PGE and Au: Canadian Mineralogist, vol. 17, p. 403-415.

Paterson, H.L., M.J. Donaldson, R.N. Smith, M.F. Lenard, J.J. Gresham, D.J. Boyack and R.R. Keays, 1984, Nickeliferous sediments and sediment-associated nickel ores at Kambalda, Western Australia: in Sulphide deposits in mafic and ultramafic rocks, D.L. Buchanan and M.L. Jones (eds), The Inst. of Mining and Metall., p. 81-94.

Paktunc, A.D., 1987, Differentiation of the Cuthbert Lake ultramafic dikes and related mafic dikes: Contrib. Mineral. Petrol., 97, p. 405-416.

Peredery, W.V. and Geological Staff, 1982, Geology and nickel sulphide deposits of the Thompson belt, Manitoba: in Precambrian sulphide deposits, H.S. Robinson memorial volume. Hutchinson R.W., C.D. Spence and J.M. Franklin (eds), Geol. Assoc. Can., Spec. Paper 25, p. 165-209.

Poulsen, K.H. and Robert, F., 1989, Shear zones and gold: practical examples from the southern Canadian Shield: in Mineralization in Shear Zones, edited by J.T. Bursnell, Geol. Assoc. of Canada Short Course #6, p. 239-266.

Price, D.P., 1977, Geology and economic potential of the Flin Flon-Snow Lake area: Centre for Precambrian Studies, University of Manitoba, 1977 Annual Report, p. 52-83.

Provins, N.M., 1980, Geology of the Centennial copper-zinc deposit, Flin Flon, Manitoba: Can. Inst. of Mining and Metall., 5th Annual District Four Meeting, Flin Flon, Manitoba, September, 1980.

Rance, H., 1966, Superior-Churchill structural boundary, Wabowden, Manitoba: Ph.D. thesis (unpubl.), Univ. of Western Ontario.

Ray, G.E. and Wanless, R.K., 1980, The age and geological history of the Wollaston, Peter Lake, and Rottenstone domains in northern Saskatchewan: Can. J. Earth Sci., vol. 17. p. 333-346.

Richardson, D.J. and Ostry, G, 1987, Gold deposits of Manitoba: Manitoba Energy and Mines, Econ. Geol. Rep. ER86-1, p.47.

Roberts, R.G., 1975, The geological setting of the Mattagami Lake mine, Quebec: A volcanogenic massive sulphide deposit: Econ. Geol., vol. 70, p. 115-129.

Roberts. R.G., 1987, Ore deposit models #11. Archean lode gold deposits: Geosc. Canada, vol. 14, no. 1, p. 37-52.

Rona, P.A., 1988, Hydrothermal alterationat oceanic ridges: Canadian Mineralogist, vol. 26, p. 431-465.

Roussel, D.H., 1965, Geology of Cross Lake area: Department of Mines and Natural Resources, Province of Manitoba, Publication 62-4, 69 p.

Russell, G.A., 1957, Structural studies of the Snow Lake-Herb Lake area, Herb Lake Mining Division, Manitoba: Manitoba Mines Branch Publication 55-3.

Sanderson, D.J. and Marchini, W.R.D., 1984, Transpression: J. of Struct. Geol., vol. 6, p. 449-458.

Sangster, D.F., 1972, Precambrian volcanogenic massive sulphide deposits in Canada: a review: Geol. Surv. of Canada, Paper 72-22.

Saunders, A.D., Tarney, J. and Weaver, S.D., 1980, Tranverse geochemical variations across the Antartic Peninsula: implications for the genesis of calc-alkaline magmas: Earth and Planet. Sci. Letters, vol. 46, p. 344-360.

Scoates, R.F.J., J.J. Macek and J.K. Russel, 1977, Thompson Nickel Belt project: in Report of Field Activities. Manitoba, Min. Res. Div., p. 47-53.

Scoates, R.F.J. and J.J. Macek, 1978, Molson Dyke Swarm: Manitoba Mines Branch, Geol. Paper 78-1, 53 p.

Sherman, G.R., Samson, I.M. and Holm, P.E., 1989, Deformation, veining and gold mineralization along part of the Johnson Shear Zone, Lynn Lake greestone belt, Manitoba: in Report of Field Activities 1989, Manitoba Energy and Mines, Min. Div., p. 16-18.

Seyfried, W.E. and Bischoff, J.L., 1977, Hydrothermal transport of heavy metals by seawater: the role of seawater/basalt ratio. Earth and Planet. Sci. Letters, vol. 34, p. 71-77.

Sibson, R.H., 1989, Earthquake faulting as a structural process: Jour. of Struct. Geol., vol. 11, No. 1/2, p. 1-14.

Simmons, B.D., 1973, Geology of the Millenbach massive sulphide deposit, Noranda, Quebec: Can. Inst. of Mining and Metall. Bull., vol. 166, no. 739, p. 67-78.

Skirrow, R.G., 1987, Silicification in a lower semiconformable alteration zone near the Chisel Lake Zn-Cu massive sulphide deposit, Manitoba: M.Sc. thesis, Carleton University, Ottawa

Skirrow, R.G. and Franklin, J.M., 1989, Semiconformable Hydrothermal alteration below the Chisel Lake massive sulphide deposit, Snow Lake Manitoba: Geol. Surv.of Canada, Open File 1986, 2 maps (1:2 000).

Stauffer, M.R. and Mukherjee, A., 1971, Superimposed deformations in the Missi metasedimentary rocks near Flin Flon, Manitoba: Can.J. of Earth Sci., vol. 8, p. 217-242.

Stauffer, M.R., 1984, Manikewan: An Early Proterozoic ocean in central Canada, its igneous history and orogenic closure: Precambrian. Res., vol. 25, p. 257-281.

Stauffer, M.R. and Lewry, J.R., 1988, Kinematic investigation of part of the Needle Falls Shear Zone: in Summary of Investigations 1988, Sask. Geol. Surv., Sask. Energy and Mines, Misc. Rep. 88-4, p. 156-160.

Stockwell, C.H., 1960, Flin Flon-Mandy area, Manitoba and Saskatchewan: Geol. Surv. of Canada, Map 1078A, with descriptive notes.

Studer, R.D., 1982, Geology of the Stall Lake copper deposit, Snow Lake, Manitoba: Can. Inst. of Mining and Metall. Bull., vol. 75, no. 837, p. 66-72.

Syme, E.C. and Forester, R.W., 1977, Petrogenesis of the Boundary intrusions in the Flin Flon area of Saskatchewan and Manitoba: Can. J. of Earth Sci., vol. 14, p. 444-455.

Syme, E.C., 1985, Athapapuskow Lake Project: in Report of Field Activities, 1985, Manitoba Energy and Mines, Geological Services, Mines Branch, p. 44-47.

Syme, E.C., 1986, Schist Lake area (Athapapuskow Project): in Report of Field Activities, 1986, Manitoba Energy and Mines, Minerals Division, p. 36-42.

Syme, E.C., 1987, Athapapuskow Lake Project: **in** Report of Field Activities, 1987, Manitoba Energy and Mines, Minerals Division, p. 30-39.

Syme, E.C., Bailes, A.H., Gordon, T.M. and Hunt, P.A., 1987, U-Pb zircon geochronology in the Flin Flon belt: Age of Amisk volcanism: **in** Report of Field Activities 1987, Manitoba Energy and Mines, Minerals Division, p. 105-107.

Syme, E.C., 1988, Athapapuskow Lake Project: **in** Report of Field Activities, 1988, Manitoba Energy and Mines, Minerals Division, p. 20-34.

Syme, E.C., 1990, Stratigraphy and geochemistry of the Lynn Lake and Flin Flon metavolcanic belts, Manitoba: **in** The Early Proterozoic Trans-Hudson Orogen: lithotectonic correlations and evolution; J.F. Lewry and M.R. Stauffer (eds.), Geol. Assoc. of Canada, Spec. Paper.

Tanton, T.L., 1941b, Schist Lake, Saskatchewan and Manitoba: Geol. Surv. of Canada, Map 633A, with descriptive notes.

Tanton, T.L., 1941a, Flin Flon: Geol. Surv. of Canada, Map 632A, with descriptive notes.

Tanton, T.L., 1941b, Schist Lake, Saskatchewan and Manitoba: Geol. Surv. of Canada, Map 633A, with descriptive notes.

Tarney, J. Saunders, A.D., Mattley, P.P., Wood, D.A. and Marsh, N.G., 1981, Geochemical aspects of back-arc spreading in the Scotia Sea and Western Pacific: Philos. Trans. of the Royal Soc. of London, A300, p. 263-285.

Thomas, D.J., 1989, Geology of the Douglas Lake-Phantom Lake area (Part of NTS 63K-12 and -13): **in** Summary of Investigations 1989, Sask. Geol. Surv; Sask. Energy and Mines, Misc. Rep. 89-4, p. 44-54.

Trembath, G.D., 1986, The compositional variation of staurolite in the area of Anderson Lake Mine, Snow Lake, Manitoba, Canada: Unpubl. M.Sc. Thesis, Univ. of Manitoba, Winnipeg, 187 p.

Walford, P.C. and Franklin, J.M., 1982, The Anderson Lake Mine, Snow Lake, Manitoba: Geol. Assoc. of Canada, Robinson Symposium Volume, p. 481-523.

Watkins, D.H., and Gibson, H.L., 1990, Noranda massive sulphide deposits: a guide to exploration and seafloor sulphide research: in Minerals Colloquium, Program with Abstracts, Geol. Surv. of Canada.

Weber, W. and R.F.J. Scoates, 1978, Archean and Proterozoic metamorphism in the northwestern Superior province and along the Churchill-Superior boundary, Manitoba: in Metamorphism in the Canadian Shield. Geol. Surv. Can., Paper 78-10, p. 5-16.

Williams, H., 1966, Geology and mineral deposits of the Chisel Lake map area, Manitoba: Geol. Surv.of Canada, Memoir 342.

Zaleski,E., 1989, Metamorphism, structure and petrogenesis of the Linda volcanogenic massive sulphide deposit, Snow Lake, Manitoba: Unpubl. PhD thesis, Univ. of Manitoba, Winnipeg, Manitoba, 344 p.

Zurbrigg, H.F., 1963, Thompson Mine geology: Can. Inst. Mining Met. Bull., vol.56, p. 451-460.